Role of the delta subunit of RNA polymerase in *Streptococcus mutans*

Von der Fakultät für Lebenswissenschaften

der Technischen Universität Carolo-Wilhelmina

zu Braunschweig

zur Erlangung des Grades einer

Doktorin der Naturwissenschaften

(Dr. rer. nat.)

genehmigte

D i s s e r t a t i o n

von Xiaoli Xue
aus Guangdong / China

1. Referentin: Prof. Dr. Irene Wagner-Döbler
2. Referent: Prof. Dr. Dieter Jahn
eingereicht am: 10.01.2011
mündliche Prüfung (Disputation) am: 21.02.2011

Druckjahr 2011

Vorveröffentlichungen der Dissertation

Teilergebnisse aus dieser Arbeit wurden mit Genehmigung der Fakultät für Lebenswissenschaften, vertreten durch die Mentorin der Arbeit, in folgenden Beiträgen vorab veröffentlicht:

Publikationen

Xiaoli Xue, Jinshan Li, Wei Wang, Helena Sztajer, Irene Wagner-Döbler. *Streptococcus mutans* proteome changes under various stresses, and the role of the delta subunit RpoE of the RNA polymerase.
Zur Veröffentlichung eingereicht

Xiaoli Xue, Helena Sztajer, Nora Buddruhs, Jörn Petersen, Manfred Rohde, Susanne R. Talay, Irene Wagner-Döbler. Lack of the Delta Subunit of RNA Polymerase Increases Virulence Related Traits of *Streptococcus mutans*.
Zur Veröffentlichung eingereicht

Xiaoli Xue, Jürgen Tomasch, Helena Sztajer, Irene Wagner-Döbler. The delta subunit of RNA polymerase, RpoE, is a global modulator of *Streptococcus mutans* environmental adaptation. Journal of Bacteriology. 2010. 192(19):5081-5092.

Tagungsbeiträge

Xiaoli Xue, Helena Sztajer, Irene Wagner-Doebler. ‘‘Function of AI-2 regulated genes in *Strepotococcus mutans*’’. ‘‘Summer School Signaling and Immunity’’. Goslar, Germany, 2008. (Poster)

Xiaoli Xue, Helena Sztajer, Ramiro Vilchez, André Lemme, Irene Wagner-Doebler. ‘‘Function of AI-2 regulated genes in *Strepotococcus mutans*’’. ‘‘Joint Annual Conference of the Association for VAAM and GBM 2008’’. Frankfurt/Main, Germany, 2008. (Poster)

1 Chapter 1 - General Introduction

1.1 The delta (δ) subunit of RNA polymerase, RpoE

1.1.1 Bacterial RNA polymerase

DNA-dependent RNA polymerase (RNAP) is a multi-subunit enzyme responsible for the RNA synthesis from DNA templates, a process termed transcription. The core RNAP (a complex of five subunits: α_2, β, β', and ω) is evolutionarily conserved in all living organisms, from bacteria to humans (Ebright, 2000;Werner, 2008). The DNA binding and RNA synthesis function of RNAP are carried out by two large subunits β' and β, and the α-dimer (α_2) assembles the enzyme and binds to the regulatory factors, and the ω subunit maintains the conformation of β' (Severinov, 2000). Although the core RNAP is capable of RNA synthesis, the holoenzyme requires one of the σ factors for directing the recognition of promoter DNA and initiation of the transcription (Borukhov & Nudler, 2003;Murakami & Darst, 2003). The majority of σ factors are closely related to the primary σ (σ^{70}) of *Escherichia coli*, and belong to the σ^{70}-family, which comprises four flexibly linked domains $\sigma_{1.1}$, σ_2, σ_3, and σ_4 that bind to the core RNAP (Campbell *et al.*, 2002;Campbell *et al.*, 2008;Murakami & Darst, 2003). The X-ray structure of *Thermus aquaticus* RNAP holoenzyme and fork-junction DNA complex shed light on the protein-DNA interaction (Fig. 1.1). The σ_2 , σ_3, and σ_4 domains bind to the promoter DNA -10, extended -10, and -35 elements, respectively (Campbell *et al.*, 2002;Murakami & Darst, 2003). Upon binding to a specific promoter site, the RNAP holoenzyme undergoes a structural transition, bends and unwinds the DNA fragment, and forms the open promoter complex. Subsequently, the RNA synthesis starts, and the σ factor is released when a stable transcription elongation complex is formed. After the transcription, the core RNAP is released from DNA and RNA to start a next cycle, thus transcription can be reprogrammed by using different σ subunits with different promoter activities (Mooney *et al.*, 2005;Mooney *et al.*, 2009).

Bacterial cells have one housekeeping σ for gene transcription in the exponential growth phase, and several alternative σ factors for activation of different sets of genes in response to environmental changes (Gruber & Gross, 2003). For example, *E. coli* contains 6 σ factors,

among which σ^S is the master regulator of stress responses (Hengge, 2009;Hengge-Aronis, 2002); and *Bacillus subtilis* contains 18 σ factors (Gruber & Gross, 2003) and σ^B is acting as a stress response regulator (Hecker *et al.*, 2007). By contrast, *S. mutans* contains only one alternative σ factor, ComX, besides the housekeeping σ factor (Ajdic *et al.*, 2002). Indeed, ComX is the only known alternative σ factor in streptococci (Luo & Morrison, 2003;Opdyke *et al.*, 2001) and it is a competence-specific regulator instead of a stress regulator (Luo *et al.*, 2003). Thus, it is very interesting to study how streptococci cope with stress without a global stress regulator.

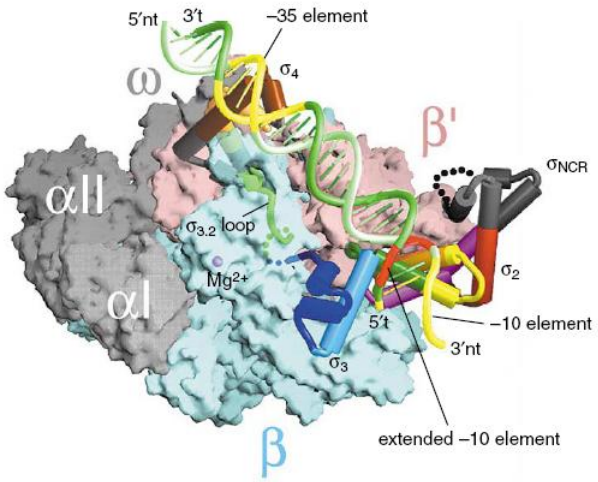

Fig. 1.1 Structure of the complex between the RNAP holoenzyme and fork-junction DNA. The core RNAP from *Thermus aquaticus* is shown as a molecular surface, with the αI, αII, and ω subunits shown in gray; the β subunit in cyan, and the β' subunit in pink. The σ factor is shown as a C σ backbone worm with its α helices shown as cylinders. The DNA phosphate backbone is shown as a worm, for the -35 and the -10 elements shown in yellow, and the extended -10 element in red (Murakami & Darst, 2003).

1.1.2 The δ subunit of RNA polymerase, RpoE, in Gram-positive bacteria

In Gram-positive bacteria, there is an additional delta (δ) subunit, RpoE, required for maintaining the transcriptional specificity. RpoE increases the transcriptional specificity by preferentially destabilizing weak promoter/RNAP complexes in *Bacillus subtilis* (Achberger *et al.*, 1982;Achberger & Whiteley, 1981). As shown in Fig. 1.2A, addition of RpoE (δ) greatly restricted the binding of non-promoter DNA fragments to RNAP (Achberger & Whiteley, 1981). Sequence alignment suggests that the primary σ factor (σ^A) and RpoE from *B. subtilis* may

together contain the activities found in the single primary σ factor (σ^{70}) of *E. coli* (Lopez de Saro *et al.*, 1995).

RpoE is a conserved protein in Gram-positive bacteria, with the most conserved region in 60-90 residues from the N-terminal domain (Jones *et al.*, 2003). The N-terminal domain from a truncated RpoE protein was stable and could be co-purified with RNAP in *B. subtilis*, thus was suggested to contain a function of binding to core RNAP (Lopez de Saro *et al.*, 1995). The N-terminal domain displays an ordered structure as judged by circular dichroism (CD) spectroscopy (Lopez de Saro *et al.*, 1995), and its structure has been clarified recently by nuclear magnetic resonance (NMR) (Fig. 1.3) (Motackova *et al.*, 2010).

By contrast, the C-terminal region of RpoE is highly unstructured and acidic, and is predicted to displace nucleic acids from RNAP (Lopez de Saro *et al.*, 1995). Adding of RpoE (δ) or its C-terminal domain (δC) together with core RNAP (E) greatly reduced the amount of RNA (Fig. 1.2B) and DNA (Fig. 1.2C) bound with RNAP.

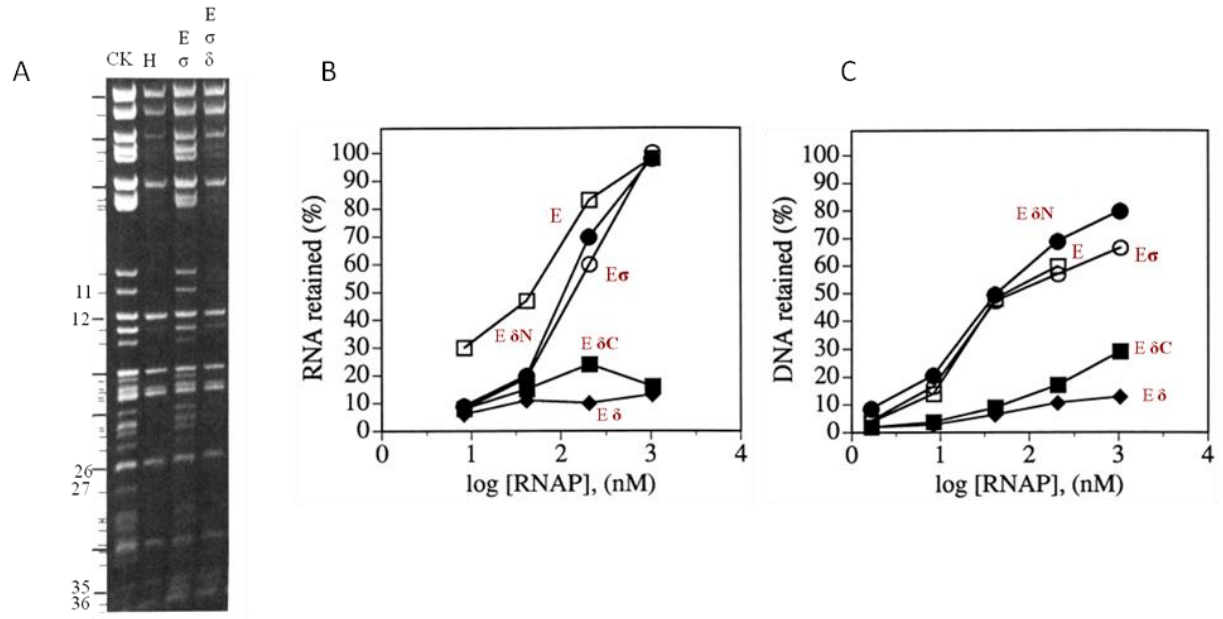

Fig. 1.2 The δ subunit increases the transcriptional specificity. (A) RpoE enhanced promoter selection (Achberger & Whiteley, 1981). Bands 11, 27, 36 contained no promoter DNA, while bands 12, 26, 35 contained promoter DNA. The first lane shows total DNA fragments as a control (CK); the next lanes show DNA fragments that bound to the purified holoenzyme RNAP (H), to core RNAP together with the σ subunit (E σ), and to core RNAP together with the σ and RpoE (δ) (E σ δ), respectively. The affinity of RNAP for RNA (B) and DNA (C) (Lopez de Saro *et al.*, 1995). Reduced amount of bound RNA and DNA was seen with the presence of δ (E δ) or the C-terminal part of RpoE (E σC) compared to core RNAP (E), while adding σ subunit (E σ) or the N-terminal part of RpoE (E σN) had no effect on the destabilization of RNAP and nuclear acids.

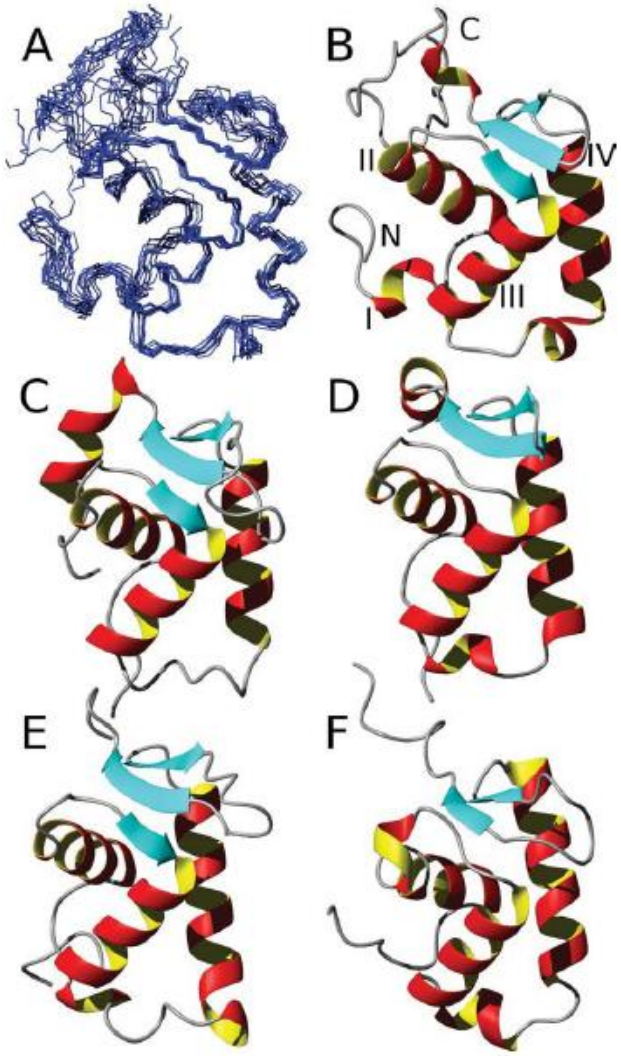

Fig. 1.3 Structure of the N-terminal domain of RpoE in *Bacillus subtilis*.
Superimposed backbone traces of 10 N-terminal structures with the lowest energy (A). The representative (lowest energy) structure of N δ (B) compared to its closest structure homologs Forkhead Box Protein K2, 2C6Y.PDB (C); Forkhead Box Protein P2, 2A07.PDB (D); Forkhead Box Protein 01, 3CO6.PDB (E); and Yeast linker Histone Hho1p, 1YQA.PDB (F). The N and C termini and the helices I to IV are labeled in Panel B (Motackova *et al.*, 2010).

Despite the inhibitory effect of RpoE on promoter binding, RpoE stimulated the RNA synthesis (Juang & Helmann, 1994), probably due to its ability to dissociate the binding of RNAP and nucleic acids, thus accelerating the RNAP recycling rate (Lopez de Saro *et al.*, 1995).

1.1.3 Function of RpoE in *vivo*

Although RpoE is a conserved protein in Gram-positive bacteria, and its biochemical functions in *vitro* have been well studied, its physiological role had been studied only in three species (*B. subtilis*, *Staphylococcus aureus*, and *Streptococcus agalactiae*) before our studies of RpoE in *Streptococcus mutans*. The effect of RpoE varies in these species. Knocking out *rpoE* caused mild effects in *B. subtilis*, e.g. altered cell morphology and an extended lag phase during growth (Lopez de Saro *et al.*, 1999). However, disruption of the *rpoE* homologgene in *S. aureus* resulted in a survival defect under amino acid starvation and acid stress conditions (Watson *et al.*, 1998). The Δ*rpoE* mutant in *S. agalactiae* also displayed growth delay, and more importantly, it had attenuated virulence in the neonatal rat sepsis model, and had increased sensitivity to killing in whole-blood bactericidal assays (Jones *et al.*, 2003;Seepersaud *et al.*, 2006). Since RpoE is suggested to partially have the role of σ^{70}, it could be more important in the bacterial species with less alternative σ factors for gene regulation. Thus, lack of RpoE could cause stronger effects in *S. auerus* which has two alternative σ factors: σB and σH (Tao *et al.*, 2010) and in *S. agalactiae* which has only one alternative σ factor ComX, than in *B. subtilis* which contains 17 alternative σ factors (Gruber & Gross, 2003).

1.2 Phylogeny and taxonomy of *Streptococcus mutans*

1.2.1 Phylogeny

Streptococci are a genus within the phylum Firmicutes (formerly known as Low GC Gram-positive bacteria). There are now over 100 *Streptococcus* species known, and they are categorized into six groups based on 16S rRNA sequences as shown in Fig. 1.4 (Nobbs *et al.*, 2009). The pyogenic group includes mainly pathogens from humans and other mammals, and they can cause serious inflammation and sequelae such as glomerulonephritis (*S. pyogenes*) and neonatal sepsis (*S. agalactiae*). The microbes from the anginosus, salivarius, mutans, mitis, and bovis groups are mainly isolated from the oral cavity of human and other animals. The mutans group comprises the microbes colonizing oral surfaces and is associated with the development of

tooth decay, ranging from human pathogens (*S. mutans* and *S. sorbrinus*) to macaques (*S. downei*) and other species (Nobbs *et al.*, 2009).

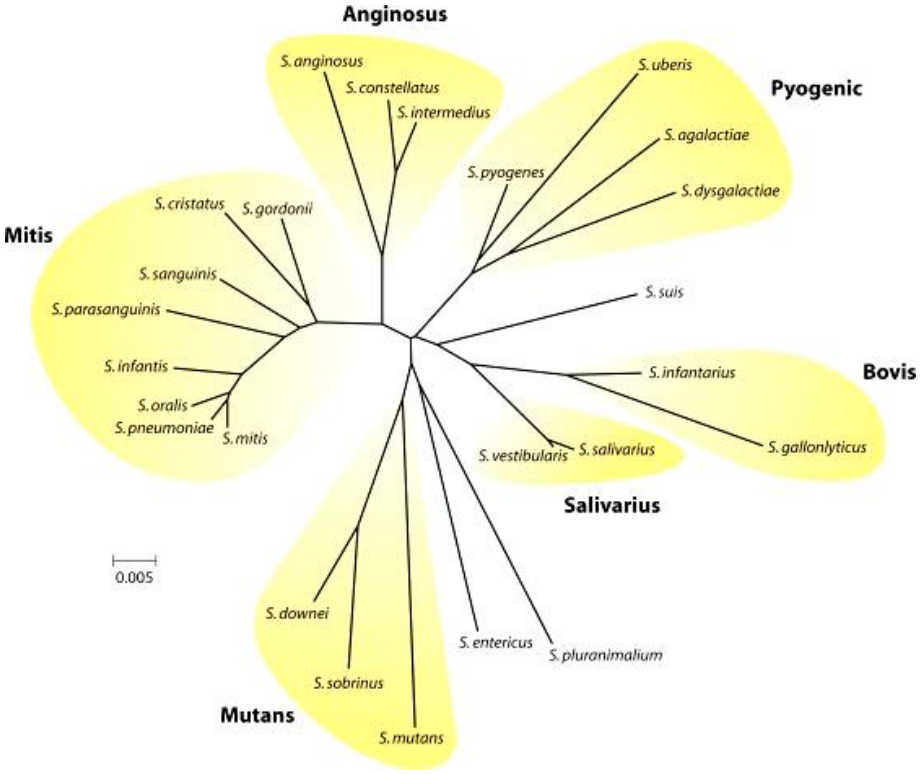

Fig. 1.4 Phylogenetic tree for streptococci based on 16S rRNA gene sequence comparisons. A number of species are not shown to simplify the figure. Streptococci are organized into six groups: pyogenic, bovis, salivarius, mutans, mitis, and anginosus (Nobbs *et al.*, 2009).

1.2.2 Traditional taxonomy

Traditional taxonomic approaches, such as haemolytic classification and serogrouping, are important in the medical application since these reactions have close connection with virulence. Streptococci causing complete lysis of red blood cells and giving clear areas around bacterial colonies on the blood agar plates belong to β-hemolytic Streptococci, while those with partial hemolysis and producing greenish colour due to the oxidation of iron in haemoglobin are classified into α-hemolytic (Coykendall, 1989;Facklam, 2002). *S. mutans* is characterized as α-

hemolytic (Facklam, 2002). Indeed, the majority of *S. mutans* isolated from dental plaque exhibits α-hemolysis, and only 6% of them has β-hemolysis (Wolff & Liljemark, 1978); while up to 30% of *S. mutans* isolated from blood displays β-hemolysis (Perch *et al.*, 1974). Thus, the occurrence of strains with β-hemolysis activity may suggest a role of this trait in the spread of infection.

The streptococci can also be classified using serotyping based on specific carbohydrate composition of cell wall antigens (Lancefield, 1933). *S. mutans* strains found in the oral cavity are classified into four serotypes (c, e, f, and k) according to the types of rhamnose-glucose polysaccharides on the cell wall, with the most prevalent (70-80%) serotype type c, and the serotype e about 20%, while serotype f and k comprise only 5% (Nakano & Ooshima, 2009). *S. mutans* is not highly invasive, but the serotypes k and f have higher detection rates in human blood and infective endocarditis samples, and are reported to be more virulent (Abranches *et al.*, 2009;Nakano *et al.*, 2010).

1.2.3 *S. mutans*

S. mutans inhabits the human oral cavity and is strongly correlated with dental caries. Fig. 1.5 shows the cell morphology of *S. mutans* and its characteristic grouping in chains or pairs under the microscope. It has a number of interesting features that contribute to its niche adaptation and pathogenesis, including facultative anaerobic organism, fermentation of a large spectrum of carbohydrates and production of acid byproducts, producing extracellular polysaccharides and forming biofilms, communication and competition with other species by physical and genetic interactions (e.g. producing competence-stimulating peptides as signalling molecules) and bacteriocins (e.g. mutacins), tolerance to environmental stresses, and its potential virulence to host tissues and cells.

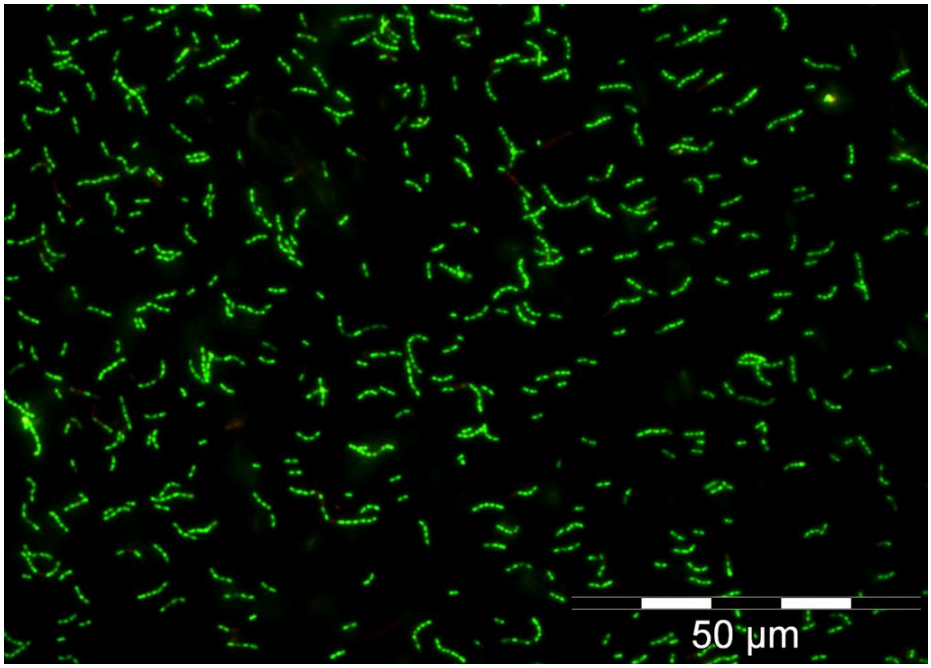

Fig. 1.5 *S. mutans* cell morphology. *S. mutans* UA159 strain was grown in Todd Hewitt broth supplemented with 1% yeast extract (THBY) at 37 ℃ enriched with 5% CO_2 overnight and stained with Live/Dead BacLight stain working solution in the dark for 15 min (L7012, Invitrogen). Image was taken under a fluorescence microscope (Olympus BX60). Majority of *S. mutans* cells remained alive and had intact cell membrane as indicated by the green colour (green-fluorescent SYTO 9 stain). The cells formed chains with various lengths.

1.2.4 *S. mutans* genome

The genome of *S. mutans* was first sequenced in 2002 using the strain UA159 which belongs to the most common serotype c and has since become a model for genetic studies of *S. mutans* (Fig. 1.6). It is composed of 2 Mbp with an average GC content of 36.8%, and contains 1963 ORFs, as shown in Fig. 1.6, circles A and B (Ajdic *et al.*, 2002). *S. mutans* has more than 280 genes (about 15% of the genome) for various transporter systems, which are important for nutrient acquisition and niche adaptation (Ajdic *et al.*, 2002). One of the most important features of *S. mutans* is its ability to ferment a wide spectrum of carbohydrates (Coykendall, 1989;Facklam, 1977). Accordingly, genes for transport and metabolism of many sugars and several sugar-alcohols were identified in the genome, as shown in circle C of Fig. 1.6 (Ajdic *et al.*, 2002).
The genome of another *S. mutans* serotype cNN2025 strain has been completely sequenced recently (Maruyama et al. 2009). The comparison of these two strains revealed a highly

conversed core-genome, while large genetic rearrangements were also observed (Maruyama *et al.*, 2009). Different from some streptococci, e.g. *S. pyogenes*, that tolerate phage integration to acquire genomic diversity (Ferretti *et al.*, 2004), *S. mutans* acquires new genetic traits by using natural transformation (Ferretti *et al.*, 2004), as well as by insertion sequence elements and transposons that contain restriction/modification systems, bacitracin synthesis systems, and transporters (Maruyama *et al.*, 2009).

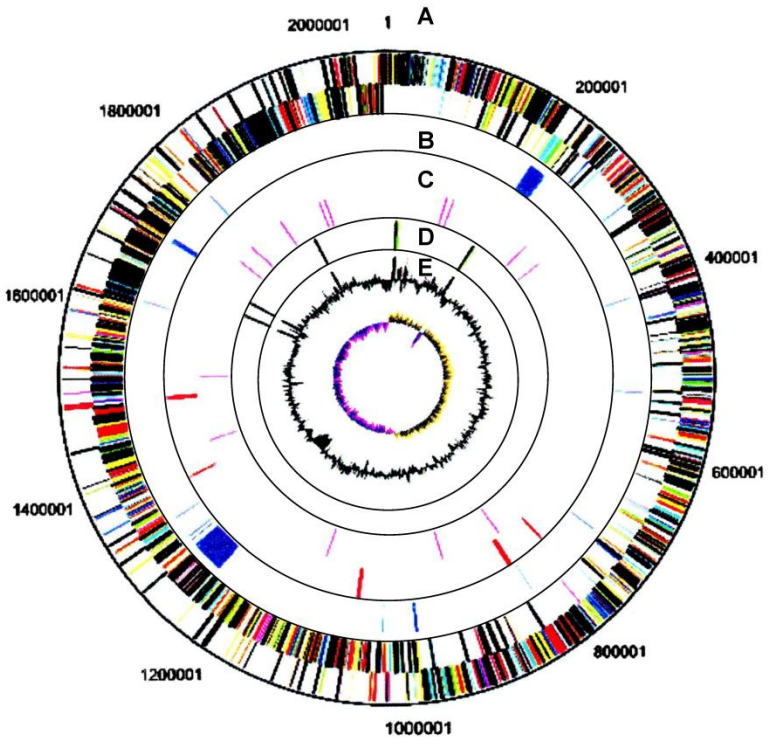

Color	Functional categories	ORFs
Dark gray	Amino acid transport and metabolism	170
Red	Carbohydrate transport and metabolism	99
Green	Cell division and chromosome portioning	18
Blue	Cell envelope biogenesis, outer membrane	68
Cyan	Cell secretion	24
Magenta	Coenzyme metabolism	35
Yellow	DNA replication, recombination and repair	101
Pale green	Energy production and conversion	60
Light blue	No database homology or function unknown	98
Orange	General function prediction only	238
Brown	Inorganic ion transport and metabolism	56
Ochre	Lipid metabolism	43
Light gray	Nucleotide transport and metabolism	64
Black	Posttranslational modification, protein turnover, chaperones	54
Purple	Signal transduction mechanisms	40
Salmon	Transcription	103
Pink	Translation, ribosomal structure and biogenesis	133

Fig. 1.6 Circular representation of the *S. mutans* UA159 genome. The outer two circles (A) show the position of the predicted ORFs on the complementary DNA strands. The ORFs have been color coded by functional category (the color legend is presented in the table on the right panel). The remaining circles are, proceeding inward: the location of the mobile genetic elements (B), the ABC transporters involved in the sugar metabolism, the PTS transporters and PTS Enzyme I (C), the position of the ribosomal RNA and tRNA genes (D), the %G+C content of the sequence, and the %G+C deviation by strand (E). Figure modified from (Ajdic *et al.*, 2002).

1.3 *S. mutans* and dental caries

Human dental caries is one of the most prevailing infectious diseases worldwide and places a significant burden on healthcare systems. Dental caries is an ecological disease in which the diet, the host and the oral microbes are interacting to promote its initiation and progression (Beighton, 2009;Moynihan & Petersen, 2004).

1.3.1 Dental biofilm

The oral cavity contains more than 700 different bacterial species (Aas *et al.*, 2005), as well as other microorganisms, e.g. *Candida albicans* (Zijnge et al., 2010). To avoid being cleared by saliva and to survive in the highly fluctuating oral cavity, oral microoragnisms need to adhere to the surface, and the best way is forming biofilms. Fig. 1.7 shows the *in situ* biofilms on natural teeth using phylogenetic probes (Zijnge *et al.*, 2010).

A model of dental biofilms initiation and progression has been developed based on several decades of laboratory work on isolated oral strains. Dental biofilms start with the adherence of initial colonizers, e.g. *S. oralis*, *S. sanguinis*, *S. mitis*, *S. gordonii*, and *Actinomyces naeslundii*, *A. oris* to the exposed salivary pellicle via specific surface adhesins (Kolenbrander *et al.*, 2010). Then genetically distinct microorganisms interact with these pioneer species through specific adherence termed coadhesion and coaggregation (Kolenbrander *et al.*, 2006). Inter/intra-species coaggregation, as well as the crosskingdom interaction with the yeast *Candida albicans* take places in oral biofilms, which is important for building a spatially organized community (Shirtliff *et al.*, 2009). The polymicrobial community within the biofilms profits from metabolic and genetic communication and is protected against external stress factors (Hojo *et al.*, 2009). The sophisticated communication mechanisms (inter-bacterial and bacterial–host) are shown in Fig. 1.8.

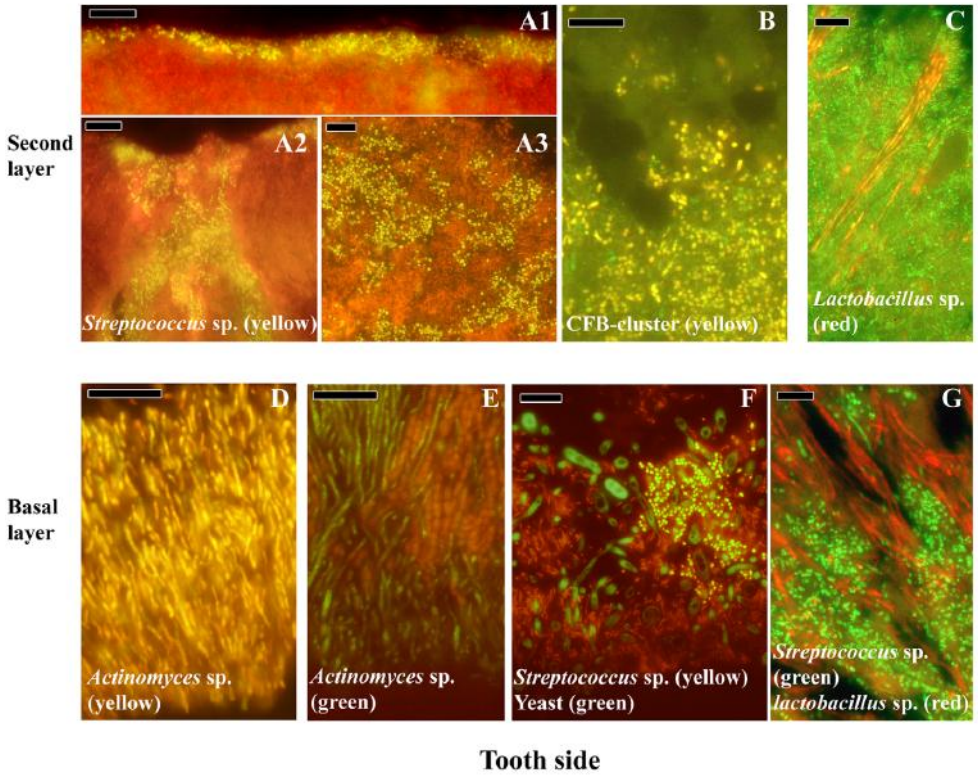

Fig. 1.7 Localization of the most abundant species in supragingival biofilms. The top layer contains *Streptococcus* sp. (yellow) with different organization, e.g. aligned as a thin coat on top of biofilm (panel A1), or colonized as cracks in the biofilm (panel A2), or without any apparent organization (panel A3). Also, there is a heterogeneous scattering of bacterial cells belonging to the *Cytophaga-Flavobacterium-Bacteroides* cluster (CFB-cluster), which appear filamentous, rod-shaped or even coccoid (panel B). *Lactobacillus* sp. (red) that are surrounded by cells with different morphologies are also identified (panel C). The basal layer of the tooth surface contains four different biofilm types: rod shaped *Actinomyces* sp. (yellow) dominated (panel D); a mixture of *Actinomyces* sp. (green) and chains of cocci, not identified as streptococci (panel E); streptococci (yellow) and yeasts (green) and bacteria unidentified (red), streptococci form a distinct colony around yeast cells (panel F); streptococci (green) growing in close proximity to *Lactobacillus* sp. (red) (panel G). Panels A, B, C, E, F are double stained with probe EUB338 (targets most bacteria) labeled with FITC or Cy3. Bars are 10 μm (Zijnge *et al.*, 2010).

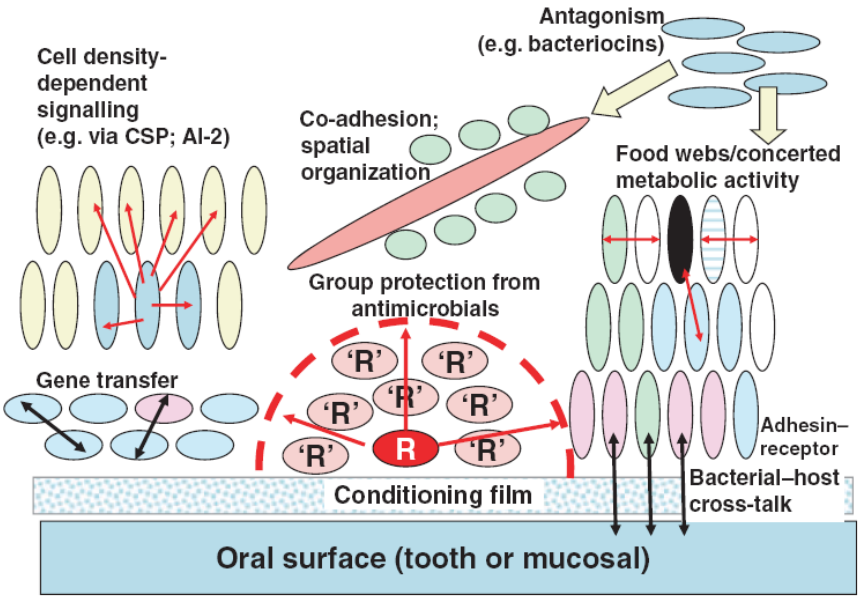

Fig. 1.8 Schematic representation of the types of interaction in dental plaque. The inter-bacterial and bacterial–host interactions that occur in a microbial community include the following: Bacteria adhere via adhesin–receptor interactions either to the conditioning film (derived either from saliva or gingival crevicular fluid) or to already attached cells. Bacteria communicate with each other in a cell density dependent manner via diffusible signalling molecules, with fungi, and with host cells. Cells are more tolerant of antimicrobial agents either because of the physical attributes of the biofilm and also because of the starvation growth mode of bacterial cells in the mature biofilms without cell division and little protein synthesis, both of which are major targets of most antibiotics, by spread of resistance genes via gene transfer, or through protection by neighbouring cells that produce neutralizing enzymes. Bacterial cells can also adhere on and have a cross-talk with host cells (Marsh *et al.*, 2011).

S. mutans has active communication with the oral microbes by both physical interactions and signalling mechanisms. It produces extracellular polysaccharides and surface adhesins that mediate its direct adherence and interaction with other microorganisms in the oral cavity (Kreth *et al.*, 2008;Zhu *et al.*, 2009). *S. mutans* produces, secretes, and senses the competence-stimulating peptide (CSP) to control its genetic competence (Li *et al.*, 2001), biofilm formation (Senadheera & Cvitkovitch, 2008), and bacteriocin production (Perry *et al.*, 2009), which make it more competitive in the oral community. *S. mutans* also secretes and uses fatty acids as well as CSP as signaling moleculars in the crosskingdom interaction, e.g. with the yeast *Candida albicans* (Jarosz *et al.*, 2009;Vilchez *et al.*, 2010).

1.3.2 Role of dental biofilm in caries development

Dental biofilm is implicated in caries, because shifts in the microbial balance of the community caused by a high sugar diet, low saliva flow rate, or impaired immune system, result in increased proportions of acid generating and aciduric bacteria, thus causing longer exposition of the tooth surface to low pH, eventually causing demineralization of the tooth enamel and thus the initiation of caries (Marsh, 2006). The critical pH of dental enamel demineralization is generally considered to be about 5.5 (Dawes, 2003), while the dental biofilm is estimated to lower the pH to about 4-5 quickly (about 7 minutes) after the sucrose consumption (Dawes & Dibdin, 1986). With a healthy diet, the sugar uptake is limited, and the acid products can be neutralized by saliva. The predominant genera in the normal mature plaque belong to *Actinomyces* and non-mutans streptococci, which are not aciduric, but have metabolic advantages in using salivary glycoproteins and can neutralize the intra- and extra-cellular pH through the arginine deiminase system (Takahashi & Nyvad, 2010). When the sugar uptake is frequent, the pH decrease in the plaque becomes more severe. Low pH causes phenotypic (acid adaptation) and genotypic (selection of aciduric microbes) changes of the microflora. Finally the highly aciduric mutans streptocci (e.g. *S. mutans*) and *Lactobacillus* become dominant, leading to a pronounced demineralization (Takahashi & Nyvad, 2010).

1.3.3 Cariogenicity of *S. mutans*

1.3.3.1 Carbohydrate metabolism and acidogenicity

The key factor contributing most to *S. mutans* cariogenicity is its strong acidogenicity from sugar fermentation (Takahashi & Nyvad, 2010). *S. mutans* is able to metabolize almost all sugars used by streptococci, and carbohydrate metabolism is the major source of energy production required for its survival, since it possesses an incomplete tricarboxylic acid (TCA) cycle (Ajdic *et al.*, 2002). *S. mutans* has a complete glycolytic pathway, and pyruvate is an important intermediate in glycolysis, which is then converted to the highly acidic product lactate (acidity pKa 3.86) as the main fermentation product. Under certain conditions (e.g. with limited glucose), *S. mutans*

can produce acid mixtures, e.g. acetate (pKa 4.76), and formate (pKa 3.77), together with ethanol, which is suggested to be important for energy production and acid tolerance under growth limiting conditions (Korithoski *et al.*, 2008). The acidic end products from carbohydrate metabolism can lower the pH down to 4 and cause demineralization of tooth enamel (Garcia-Godoy & Hicks, 2008), and also inhibit growth of many non-aciduric bacterial speices, allowing *S. mutans* to be more competitive in the oral bacterial community (Takahashi & Nyvad, 2010).

1.3.3.2 Biofilm formation

S. mutans can use sucrose to produce glucans that provide scaffolding support for its adhesion to smooth surfaces and promote biofilm formation. Fig. 1.9 shows the *S. mutans* biofilm under the scanning electron microscope. The glucosyltransferases GtfBCD (Kreth *et al.*, 2008;Terao *et al.*, 2009) and glucan-binding proteins GbpABCD have been shown to participate in the adherence to the tooth surface and affect the cariogenicity (Matsumoto-Nakano *et al.*, 2007). Besides the adherence mediated by glucan polysaccharides, *S. mutans* also contains surface antigen I/II SpaP to promote its adherence and biofilm formation (Zhu *et al.*, 2009). The signaling molecule CSP is reported to cause cell death of a subpopulation via a bacteriocin-like peptide and the released chromosomal DNA contributes to *S. mutans* biofilm formation (Perry *et al.*, 2009).

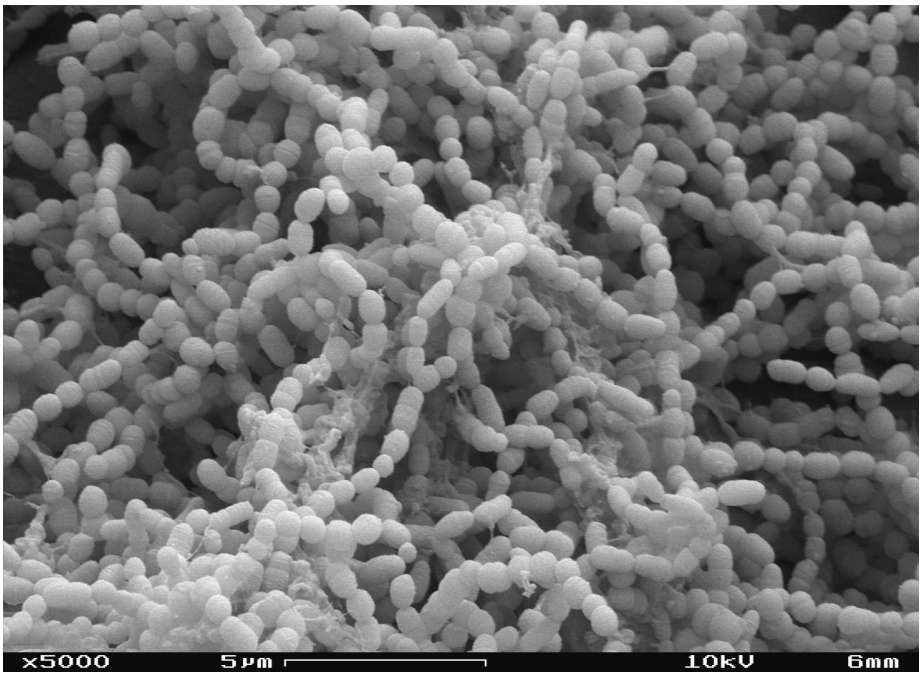

Fig. 1.9 Scanning electron microscope image of *S. mutans* biofilm. Biofilm was grown on the polystyrene surface for 16 h at 37 ℃ under anaerobic conditions (80% N_2, 10% H_2, 10% CO_2) in BM medium supplied with 0.5% sucrose.

1.3.3.3 *S. mutans* stress tolerance

To survive in the oral cavity, *S. mutans* has complex protective mechanisms that allow its tolerance to acid and oxidative stresses (Higuchi *et al.*, 2000;Lemos & Burne, 2008), two of the common stresses in the oral environment.

Acid tolerance

S. mutans has a well equipped acid defense system (Lemos & Burne, 2008), thus it has growth advantages compared to other non-aciduric bacteria and becomes dominant in the acidic stage of the caries process (Takahashi & Nyvad, 2010). The acid defense system includes the F_1F_0-ATPase which pumps protons out of the cell (Lemos *et al.*, 2005); the malolactic fermentation (MLF) which transforms malate to the weaker acid lactic acid and CO_2 to raise the intracellular pH (Lemme *et al.*, 2010;Sheng & Marquis, 2007). Moreover, the agmatine deiminase system (Griswold *et al.*, 2006) and branched-chain amino acid (BCAA) biosynthesis (Len *et al.*, 2004a)

produces ammonia and ATP to alkalinize the cytoplasmic pH. Fig. 1.10 summarizes the acid adaptation mechanisms in *S. mutans*.

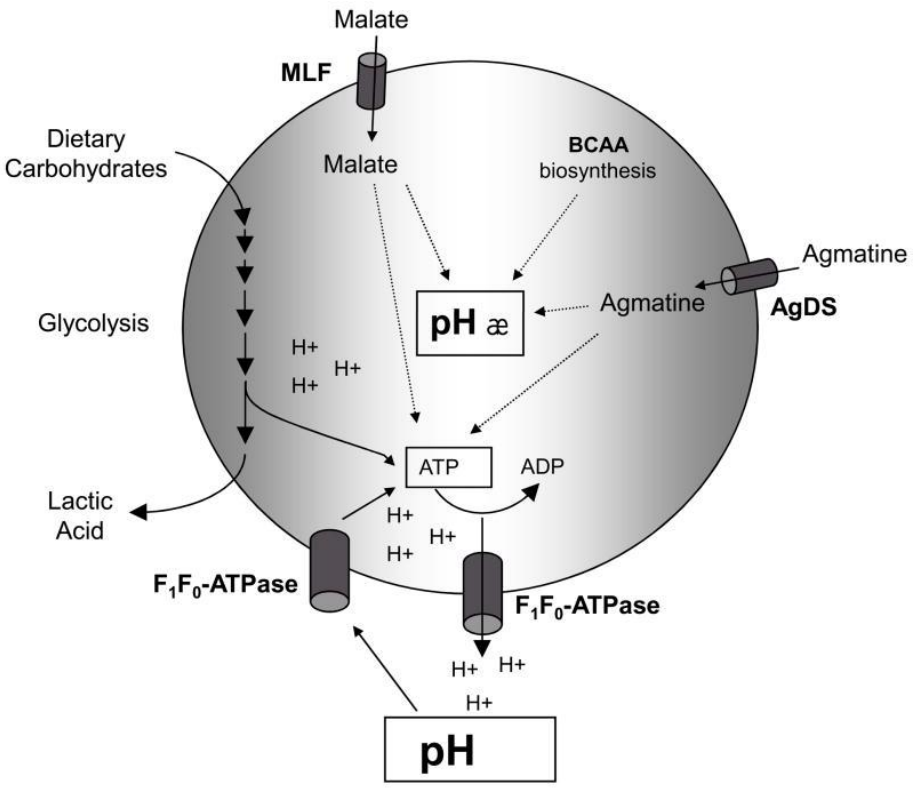

Fig. 1.10 Metabolic pathways that contribute to acid tolerance. The known acid protection mechanisms are as follows: increasing the cytoplasmic pH; generating ATP; AgDS, agmatine deiminase system; BCAA, branched-chain amino acid; MLF, malolactic fermentation (Lemos & Burne, 2008).

Oxidative stress tolerance

The reactive oxygen species (ROS), including superoxide anion (O_2^-), hydrogen peroxide (H_2O_2), and hydroxyl radical ($HO^{\cdot}$), are generated from incomplete reduction of oxygen (O_2) or released by other species in the oral cavity (Marquis, 2004). *S. mutans* does not contain catalase (the heme-containing peroxidase), a key enzyme required for oxidative stress protection (Higuchi *et al.*, 2000), and there is no such highly equipped defense system for oxidative stress as for acid stress. However, a number of oxidative defense enzymes have been identified in *S. mutans*: the superoxide dismutase (Sod) detoxifies O_2^- by converting it to O_2 and H_2O_2 (Nakayama, 1992;Poyart *et al.*, 2001;Thomas & Pera, 1983); the H_2O_2 - forming NADH oxidase Nox-1

functions together with the peroxidase AhpC, while the H_2O-forming NADH oxidase Nox-2 catalyzes directly the reduction of O_2 to H_2O (Higuchi *et al.*, 2000;Poole *et al.*, 2000); the iron-binding enzyme Dpr regulates the intracellular iron level to reduce the generation of ROS through the Fenton Reaction (Higuchi *et al.*, 2000); glutathione reductase GshR and thioredoxin reductase TrxB are important enzymes that repair oxidative damage in proteins (Carmel-Harel & Storz, 2000;De Angelis & Gobbetti, 2004;Jansch *et al.*, 2007). Moreover, the serine protease ClpP (Deng *et al.*, 2007b), the trigger factor RopA (Wen *et al.*, 2005), a putative oxidoreductase (SMU.2115) (Abranches *et al.*, 2006), a putative surface-associated protein BrpA (Wen *et al.*, 2006), and a putative phosphatase (SMU.1297) (Zhang & Biswas, 2009a) were also indicated to be involved in the oxidative stress tolerance.

Little is known about the regulation of oxidative stress reactions in *S. mutans*. The two-component systems (TCSs) VicRK and ScnRK, and the response regulator rr11 (SMU.1547c) of TCS hk11/rr11 were shown to be required to induce resistance of *S. mutans* against oxidative stress (Chen *et al.*, 2008;Deng *et al.*, 2007a;Perry *et al.*, 2008), but it is not known which signal they actually detect.

1.4 *S. mutans* infection of the host tissues and cells

Compared to other streptococci, *S. mutans* is not highly invasive, but it is frequently detected in heart valve and atheromatous plaque specimens (Nakano *et al.*, 2006a), and has been isolated from infective endocarditis (IE) (Nomura *et al.*, 2006), suggesting that it is a possible causative agent of IE. The streptococci pathogenesis (Mitchell, 2003) includes:

(1) Adherence to the tissue surface, mainly through binding to the human extracellular matrix (ECM) components, e.g. fibronectin, via the surface antigens and other surface structures. Several ECM binding proteins have been identified in *S. mutans* (Nobbs *et al.*, 2009). Fig. 1.11 shows the adherence of *S. mutans* to human epithelial cells HEp-2.

(2) Invasion into and survival in the host cells by acquiring nutrients and avoiding the host immune system activated by the invading bacteria. For example, a newly isolated *S. mutans* strain was shown to have lower cariogenicity but higher virulence to the blood due to loss of important antigens that allows to escape host phagocytosis (Nakano *et al.*, 2010).

(3) Cause damage to the host by releasing toxins or modulating host inflammatory response. *S. mutans* can effectively stimulate inflammatory cytokines production by mononuclear cells (Jiang & Schilder, 2002) and endothelial cells (Shun *et al.*, 2005).

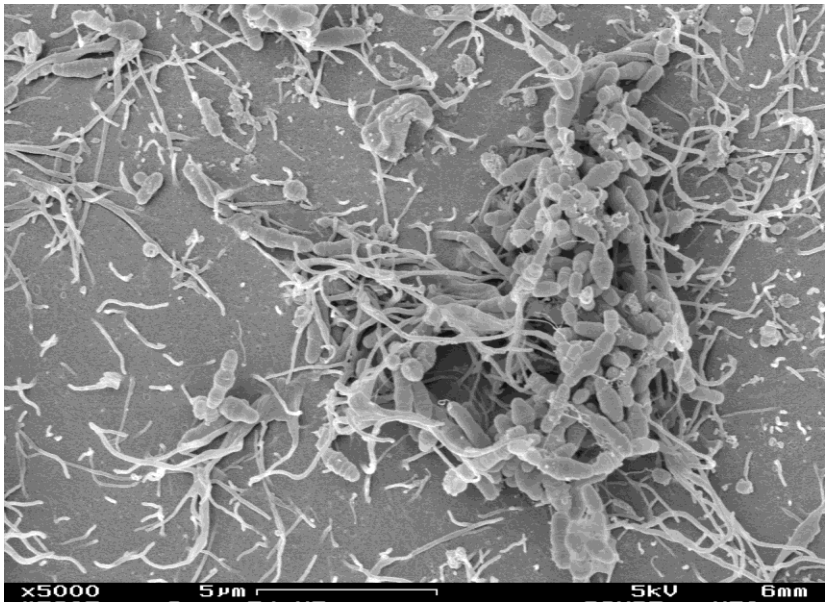

Fig. 1.11 Scanning electron microscope image of *S. mutans* adherence to human epithelial cells HEp-2. The sample was washed and fixed after 4-hour incubation of *S. mutans* from stationary growth phase together with the HEp-2 cell monolayer at 37 ℃ enriched with 5% CO_2.

1.5 Multiple 'omics' analyses in *S. mutans*

1.5.1 The ''omics'' technologies

The development of large scale profiling technologies allows identification and quantification of biological molecules (DNA, mRNA, proteins, metabolites) in a high-throughput manner, and thus allows determination of their variation between different biological states systematically (Fischer, 2005). These technologies are referred to as 'omics' technologies (Fig. 1.12). The newly developed Phenotype Microarray technique can record and compare the functional changes with 1920 phenotypic traits (Bochner, 2009), thus it belongs to the filed of the phenome. The arrows in Fig. 12 show the three levels (transcriptome, proteome, and phenome) used in this

study for investigating the function of RpoE in *S. mutans*. The advantages and limitations of these techniques, and some examples of their applications in *S. mutans* will be briefly discussed below.

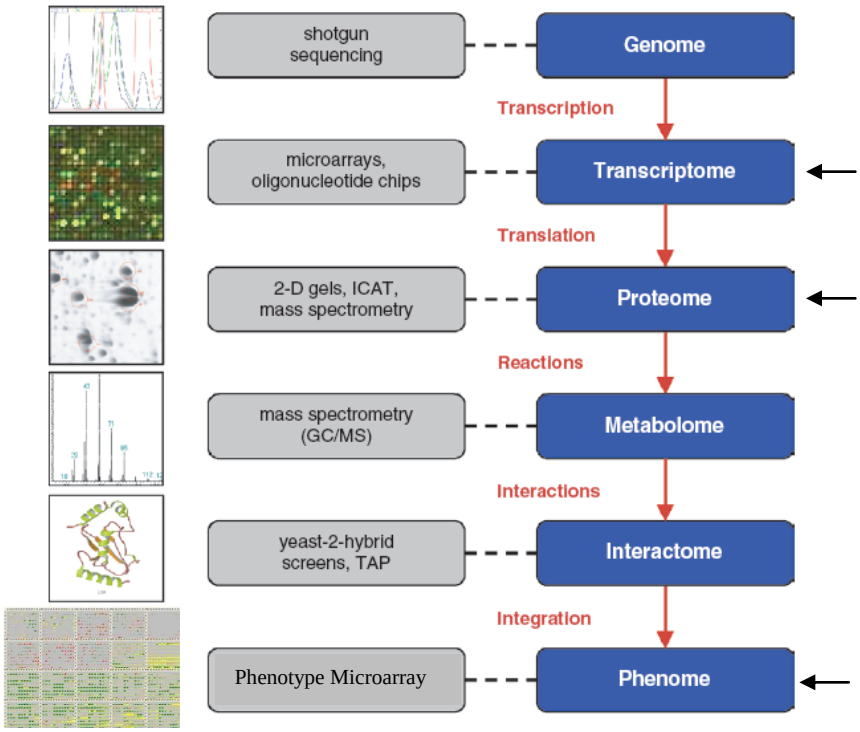

Fig. 1.12 The basic molecular levels of a cell, together with the biological processes communicating between these levels. The boxes to the left indicate representatives of newly developed ‘‘-omics’’ technologies (gray) that can quantitatively monitor the respective biological levels in a highly automated fashion. Image is modified from Fisher (Fischer, 2005).

1.5.2 Transcriptomics

Transcriptomics determines the types and amounts of mRNA molecules of the whole cell, thus provides information on the expression of all genes. Microarray-based technology involves specific binding of the RNA or cDNA samples labelled with fluorescent dyes to the high-density sense or antisense arrays comprised of oligonucleotides probes, thus it quantifies gene expression according to the light intensity bound on the arrays. Microarray technology is extremely sensitive and generates large data sets from different samples or samples obtained from different

treatments to be compared with each other and analysed together. There are also limitations in microarray-based technology, for example, only those organisms with available genome sequence can be used in microarray studies. This problem has been solved by new developed technologies, e.g. the high-throughput sequencing (van Vliet, 2010).
Nevertheless, transcriptome analysis is still very powerful in systematic studies of model organisms. Using ‘‘*Streptococcus mutans*’’ combined with ‘‘transcriptome’’ to search in Pubmed from NCBI results in 43 results, and the studies vary from stress tolerance, biofilm, competence, to virulence. Transcriptome studies in *S. mutans* under stress revealed that this bacterium is extremely sensitive to and can quickly adapt to environmental changes. For example, the adaptation of *S. mutans* to pH 5.5 caused differential expression of 169 upregulated and 108 downregulated genes (fold of change>=2, $p<0.01$). Interestingly, besides the known acid defense systems, multiple two component systems (TCSs) (e.g. VicRK, LiaSR, CiaHR, and ScnKR) were induced under acid stress, suggesting that signaling regulation is important in quick sensing and responding to acid fluctuations (Gong *et al.*, 2009). The growth under oxygen stress caused upregulation of 83 genes, and downregulation of 23 genes ($p<0.001$), and particularly, the bacteriocin-encoding genes were highly induced, which may reflect a defense mechanism of *S. mutans* to inhibit the competitors (Ahn *et al.*, 2007). Moreover, among the upregulated 83 genes 25 belonged to carbohydrate uptake and metabolism and energy production (Ahn *et al.*, 2007). For instance, the genes encoding the partial tricarboxylic acid cycle were induced, suggesting a requirement for energy to cope with the oxygen stress (Ahn *et al.*, 2007).

1.5.3 Proteomics

Proteomic seeks to identify and quantify all expressed proteins in a cell in a specific physiological condition. Two-dimensional gel electrophoresis (2-DE) is widely applied in proteomics due to its simplicity, relative inexpensiveness, and its ability to separate up to several thousand protein spots according to their isoelectric point and protein mass (Patterson & Aebersold, 2003). The limitations in 2-DE methods, such as difficulties in extraction of protein spots from gels, large time-consumption and difficulty to automate require the development of new technologies, e.g. reversed-phase (RP) HPLC (Reschiglian & Moon, 2008), and nongel-

based two-dimensional protein separations using isoelectric focusing and asymmetrical flow field-flow fractionation (Kim & Moon, 2009).

Using the conventional 2-DE based proteome analysis, Svensäter et al. demonstrated that *S. mutans* responded to diverse stresses, including oxidative, acid, starvation, salt and heat stresses, as shown by 40-69 protein spots with altered expression (Svensater *et al.*, 2000). Unfortunately, these protein spots were not identified probably due to technical limitations. Later, Len et al. reported that *S. mutans* grown at steady state (continuous culture, glucose limitation) at pH 5.0 in comparison to pH 7.0 resulted in 61 differentially expressed protein spots (representing 30 different proteins, of which 25 were induced under acid stress) that were associated with regulation or stress response pathways (Len *et al.*, 2004b); moreover, 70 protein spots (representing 33 different proteins) involved in metabolic pathways also had altered expression (fold of change > 1.5), the majority of which were associated with glycolysis, alternative acid production and branched chained amino acids (BCAAs) biosynthesis (Len *et al.*, 2004a). BCAAs biosynthesis was suggested here for the first time to be an acid protection mechanism since it reduced the H^+ concentration by consuming the strong acid formate and NADPH, and producing NH_3 (Len *et al.*, 2004a).

1.5.4 Phenotype microarray (PM) and its application in *S. mutans*

Phenotype microarray (PM) technology allows for high throughput phenotyping with 1,920 testable physiological traits (Bochner *et al.*, 2001). The system detects the conversion of carbon, nitrogen, phosphate and sulfate sources, but it also monitors the sensitivity for osmotic stress, various heavy metal ions, the pH and inhibitory chemicals. PM assays are performed in microtiter plate format and record the respiration of living cells through the NADH-dependent reduction of a tetrazolium redox dye. The formation of the purple color reflects both the import as well as the metabolic conversion of a specific substrate (Fig. 1.13). The absence of enzymes, e.g. induced by gene knock-outs, results in lack of color formation. The assay is more sensitive than traditional phenotypic growth tests on minimal medium because it also allows to monitor the usage of substrates that are not sufficient for growth (Bochner, 2009).

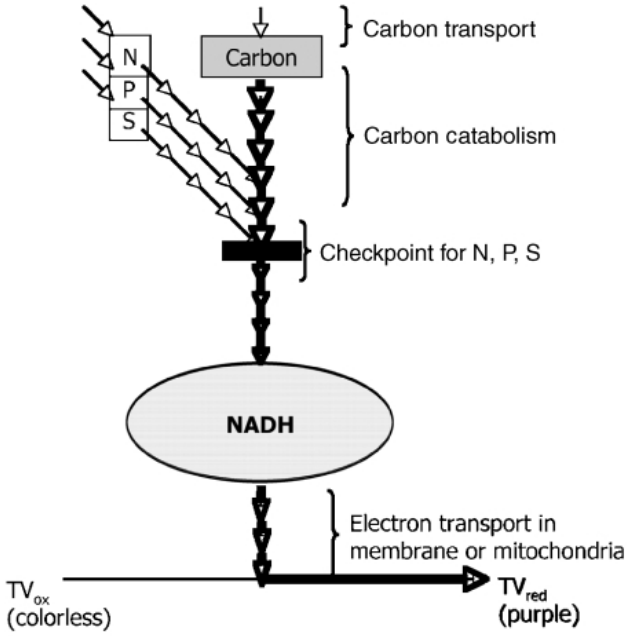

Fig. 1.13 The coordinated linkage of metabolic pathways. Schematic diagram of major metabolic pathways in bacteria and how their activities are converted to a colorimetric readout. A C-source that can be transported into a cell and metabolized to produce NADH will generate a redox potential and flow of electrons to reduce a redox dye such as tetrazolium violet (TV), thereby producing purple color. The more rapid this metabolic flow, the more quickly purple color is formed. However, many cells exhibit a phenomenon of checkpoint control, where the catabolism of the C-source is restricted if the cell does not also have sufficient levels of N, P, and S. This enables assays where one can also measure these N, P, and S catabolic pathways. The more active they are, the more rapid the catabolism of the C-source and the more quickly purple color is formed (Bochner, 2009).

PM analysis of the *htrA* (trypsin like serine protease) mutation in *S. mutans* resulted in loss of activity in salt and osmotic tolerance assays, which perfectly fitted with the osmotic stress results from other experiments (Biswas & Biswas, 2005) Moreover, the weaker metabolic activity of the mutant for two carbon sources was observed, which would otherwise not have been noticed (Biswas & Biswas, 2005). Using PM assays, the deletion mutatant of *liaS* (histidine kinase related to cell-envelope stress-sensing) in *S. mutans* caused resistance to a large spectrum of inhibitory compounds besides resistance to antibiotics that are targeting cell-wall biosynthesis, e.g. protein synthesis inhibitors, DNA synthesis inhibitors, and toxic compounds, which was unexpected since there were no direct connections of these functions (Zhang & Biswas, 2009b).

1.6 Objective of the thesis

The aim of the project is to systematically analyze the function of RpoE in *S. mutans*. Since complex regulation of gene expression is required for performance of all the biological functions of *S. mutans* described above, and the primary mechanism of RpoE is assuring transcriptional specificity, the ΔrpoE mutant was analysed first on the level of the transcriptome, followed by proteome and phenome analyses.

Transcriptome analysis of RpoE function

A *S. mutans rpoE* knockout mutant and its genetically complemented strain were constructed in this study, and their phenotypes were characterized to determine some of the functions of RpoE *in vivo*. The expression of *rpoE* during growth and under acid and oxidative stresses was studied using a luciferase reporter strain. The transcriptome comparison of the wild type and the Δ*rpoE* mutant under five conditions - log and stationary growth phases, acid (pH 5), oxidative (2 mM H_2O_2) and combined acid/oxidative (pH 5/2 mM H_2O_2) stresses - was conducted to investigate the role of RpoE on gene expression that is independent of environmental conditions.

Proteome analysis of *S. mutans* stress response and the role of RpoE

The proteome study was performed under identical experiment conditions as for the transcriptome study. The proteome changes of *S. mutans* under nutrient starvation (stationary growth phase), acid stress, oxidative stress, and acid and oxidative combined stress, were investigated. The influence of RpoE on these stress responses was evaluated by analyzing the proteome changes of the Δ*rpoE* mutant. Since the proteome and transcriptome studies used the same experimental conditions, a comparison of transcriptome and proteome changes was also performed to evaluate direct and indirect effects of RpoE on the proteome level.

Influence of RpoE on virulence related traits of *S. mutans*, and a global phenotypic comparison

The effect of RpoE on self- and co-aggregation, biofilm formation and biofilm structure, extracellular proteins, adherence to human extracellular matrix (ECM) components, and attachment to and invasion of human epithelial cells was investigated. Moreover, a global phenotypic characterization of the metabolic capabilities of the Δ*rpoE* mutant was performed.

Chapter 2

The delta subunit of RNA polymerase, RpoE, is a global modulator of gene expression in *Streptococcus mutans*

Xiaoli Xue, Jürgen Tomasch, Helena Sztajer, Irene Wagner-Döbler

Research Group Microbial Communication, Division of Cell Biology, Helmholtz Centre for Infection Research, Inhoffenstr. 7, D-38124 Braunschweig, Germany

2 Chapter 2 - The delta subunit of RNA polymerase, RpoE, is a global modulator of gene expression in *Streptococcus mutans*

2.1 Abstract

The delta subunit of RNA polymerase, RpoE, is wide spread in low G+C Gram-positive bacteria and is thought to play a role in enhancing transcriptional specificity by blocking RNA polymerase binding at weak-promoter sites and stimulating RNA synthesis by accelerating core enzyme recycling. Despite the well-studied biochemical properties of RpoE, a role for this protein *in vivo* has not been defined in depth. In this study, we show that inactivation of *rpoE* in the human dental caries pathogen *Streptococcus mutans* causes impaired growth, and loss of important virulence traits, including biofilm formation, resistance to antibiotics, and tolerance to environmental stresses. Complementation of the mutant with *rpoE* expressed in *trans* restored its phenotype to wild type. The luciferase fusion reporter showed that *rpoE* was highly transcribed throughout growth, and that acid and hydrogen peroxide stresses repressed *rpoE* expression. Transcriptome profiling of wild type and Δ*rpoE* cells in the exponential and early stationary phase of growth, under acid and hydrogen peroxide stress and under both stresses combined revealed that genes involved in histidine synthesis, malolactic fermentation, biofilm formation, and antibiotic resistance were down-regulated in the Δ*rpoE* mutant in all conditions. Moreover, the loss of RpoE resulted in dramatic changes in transport and metabolism of carbohydrates and amino acids. Interestingly, differential expression, mostly up-regulation, of 330 non-coding regions was found. In conclusion, this study demonstrates that RpoE is an important global modulator of gene expression in *S. mutans*, which is required for optimal growth and environmental adaptation.

2.2 Introduction

RNA polymerase from bacteria consists of the core (α_2 ββ' ω) enzyme and the σ factor, the main target for gene regulation. In Gram-negative bacteria, e.g. *Escherichia coli*, the σ subunit is required for specific promoter recognition and transcription initiation and also for reducing unspecific binding (Chamberlin, 1974). In Gram-positive bacteria, there is an additional delta (δ)

subunit RpoE, required for specificity of the enzyme. In *Bacillus subtilis*, promoter recognition and transcription initiation are determined by the σ subunit, but the dissociation of RNA polymerase from weak promoter sites is mediated by RpoE, which was demonstrated by biochemical studies (Achberger *et al.*, 1982;Achberger & Whiteley, 1981;Juang & Helmann, 1994). Sequence alignment suggests that the σ^A and RpoE subunits from *B. subtilis* may together contain the activities found in the single 70 kDa σ factor of *E. coli* (Jones *et al.*, 2003;Lopez de Saro *et al.*, 1995).

RpoE is suggested to be an abundant protein in *B. subtilis*; the expression of *rpoE* reaches a maximum value at the transition between logarithmic and stationary phase, and then the activity goes down at the stationary phase (Lopez de Saro *et al.*, 1999). The *rpoE* mutant of *B. subtilis* exhibited an extended lag phase and altered morphology (Lopez de Saro *et al.*, 1999). Recent studies in *Streptococcus agalactiae* demonstrated a link between RpoE amount and virulence, and reduced virulence of the *rpoE* mutant (Jones *et al.*, 2003;Seepersaud *et al.*, 2006). However, no further molecular mechanisms of RpoE function *in vivo* with regard to these phenotypic changes have been reported.

The Gram-positive bacterium *Streptococcus mutans* is a major pathogen responsible for human dental caries. Its ability to form a biofilm on the tooth surface, conversion of various carbohydrates to organic acids through glycolysis, and tolerance of environmental stresses are important properties for the progression of the disease, and are considered as virulence traits (Biswas *et al.*, 2008;Lemos & Burne, 2008). In the oral environment *S. mutans* is exposed to rapid variations in sugar sources and concentrations, and to quick changes in environmental pH and redox potential (oxidation level). All these environmental alterations require a complex and sophisticated regulation of gene expression to allow the bacterium to adapt to the changing environment, and to maintain basic metabolic processes necessary for survival. The molecular mechanisms of the adaptation of *S. mutans* to various environmental stresses have been studied. Svensäter et al. demonstrated that adaptation to acid, salt, and starvation stresses protected the cells against subsequent acid challenge with pH 3.5 (Svensater *et al.*, 2000). The authors further analyzed the stress responses by a proteome approach, and found a significant number of protein spots with altered expression under different stresses. However, these protein spots were not finally identified. It has been reported that nearly 14% of the genes in the genome were differentially expressed in acidic pH (Gong *et al.*, 2009). Two component systems (TCSs),

comprised of a sensor kinase and a response regulator protein, are one of the primary mechanisms used by *S. mutans* to quickly sense and respond to environmental acid fluctuations for optimal growth (Biswas *et al.*, 2008;Gong *et al.*, 2009;Senadheera *et al.*, 2009;Tremblay *et al.*, 2009). *S. mutans* has well adapted acid defense systems, including the F_1F_0-ATPases that pump protons out of the cell, and the malolactic fermentation and agmatine deiminase systems that contribute to alkalization of the cytoplasmic pH and generation of ATP as energy (Lemos & Burne, 2008). Because it lacks catalase (the heme-containing peroxidase) that degrades hydrogen peroxide (H_2O_2), *S. mutans* depends mainly on the NADH oxidase, superoxide dismutase, and glutathione reductase activity for protection against reactive oxygen species (Baldeck & Marquis, 2008;Higuchi *et al.*, 2000). Both transcriptomic (Ahn & Burne, 2007) and phenotypic (Ahn *et al.*, 2009) studies proved that oxygen caused not only altered sugar transport activity and rate of glycolysis, but also affected virulence-related traits, particularly by reducing bioflim formation.

The delta subunit RpoE of *S. mutans* is predicted to be a 194-amino-acid protein with a pI of 3.7 and a molecular mass of 22 kDa. The amino acid sequence alignment of *S. mutans* RpoE with those of other organisms exhibits considerable homology (Supplementary Figure S2.1). The highest homology in the proteins is seen in the amino-terminal domain, which represents the core RNA polymerase binding region (Lopez de Saro *et al.*, 1995). The carboxy-terminal domain of RpoE is highly acidic because of the enriched aspartate (D) (n =25) and glutamate (E) residues (n =22), which is consistent with the expected function as an unstructured polyanionic polymer that mimics and displaces nucleic acids from RNA polymerase (Lopez de Saro *et al.*, 1995).

To enhance our understanding of how the changes in RNA polymerase activity might affect *S. mutans* biological functions on the cellular and molecular levels, we constructed a *S. mutans rpoE* knockout mutant, and characterized its phenotype under normal and stressed conditions. The effect of these conditions on the expression of *rpoE* was studied using a luciferase reporter strain. We then conducted a transcriptome analysis under a range of conditions which revealed significant and coordinated changes of gene expression in the mutant, clearly accounting for its phenotype. The data show that RpoE functions as a global modulator of gene expression in *S. mutans*, affecting basic virulence related traits.

2.3 Results and discussion

2.3.1 Phenotypic characterization

2.3.1.1 The Δ*rpoE* mutant has a growth defect.

To access the function of the RpoE protein in *S. mutans*, a deletion of *rpoE* was created by replacing the coding sequence with an erythromycin antibiotic resistance cassette through homologous recombination. The *rpoE* mutation was complemented in *trans* with plasmid pDL-*rpoE*, which contained the promoter region and the entire *rpoE* coding sequence.
The Δ*rpoE* strain showed an extended lag-phase, slower growth, and failed to reach the same final optical density as the parent strain (Supplementary Figure S2.2). Moreover, the Δ*rpoE* strain had a strong tendency to clump when entering the late exponential phase and produced flocs which sedimented to the bottom of the culture vessel. Complementation of *rpoE* restored the growth phenotype of the wild-type strain with respect to growth rate, lack of clumping, and final OD_{600}, however, the lag-phase of the complemented strain was still longer than that of the wild type.
Interestingly, the Δ*rpoE* mutant had a similar cell morphology as the parent strain using Scanning Electron Microscopy (Supplementary Figure S2.3). Moreover, the Transmission Electron Microscopy analysis found no obvious defect in cell division or cell membrane of the Δ*rpoE* strain (data not shown). These observations indicate that the growth defect of Δ*rpoE* was due to other genetic and metabolic changes.

2.3.1.2 RpoE deficiency reduces resistance to antibiotics.

The ability of *S. mutans* to resist antibiotics, including kanamycin, tetracycline, rifampicin, and ampicillin, was tested. Compared to the wild type strain, the Δ*rpoE* mutant failed to grow at 1 μg/ml tetracycline and 100 μg/ml kanamycin. Thus, smaller concentrations from 0.1-1 μg/ml tetracycline or 10-100 μg/ml kanamycin were tested in a second experiment. The data show that Δ*rpoE* was more sensitive to these two antibiotics, and could not grow above 0.6 μg/ml tetracycline or 80 μg/ml kanamycin (Supplementary Table T2.1). The reduced tolerance of the mutant strain to both kanamycin and tetracycline, which interfere with translation by targeting

the 30S ribosomal subunit of the ribosome (Nishimura *et al.*, 2005;Thaker *et al.*, 2010), indicated a deficiency in ribosome function. For the antibiotic rifampicin that inhibits transcription by binding to the β subunit of the RNA polymerase (Floss & Yu, 2005), and the β-lactam antibiotic ampicillin that disrupts the crosslinking of peptidoglycan chains in the cell wall synthesis (Tipper, 1985), no obvious difference was found between the wild type and Δ*rpoE* strain (data not shown).

2.3.1.3 RpoE is required for stress tolerance.

The ability of the *rpoE* deletion strain of *S. mutans* to tolerate environmental stresses, particularly acid and H_2O_2 stresses, was determined. Cells in the exponential phase of growth were split into two parts; one was directly subjected to the killing stress without adapatation, while the other part was treated for two hours with sublethal adaptive stress before killing stress. As shown in Fig. 2.1, the pre-adaptation did protect both wild type and mutant strains from the more severe stress, indicated by the higher survival rate of 'adapted' cells. However, the survival rate of Δ*rpoE* was about 10 times lower in comparison to the parent strain, both with and without pre-adaptation. Genetic complementation could only partially restore the tolerance of the wild type strain. One possible reason for this might be the multiple copies (~20-30) of the plasmid carrying the *rpoE* gene in the complementation strain, which could cause global metabolic changes in the cells.

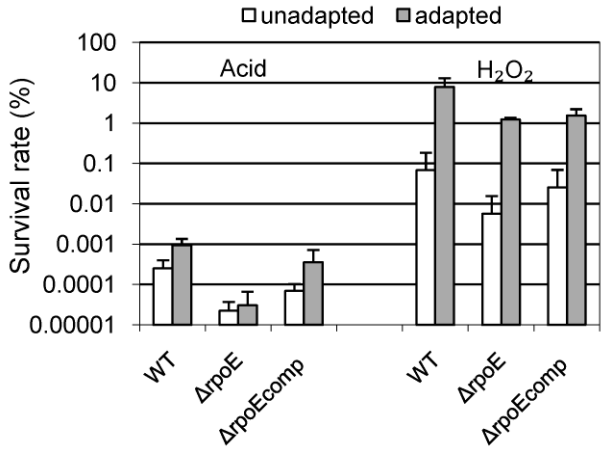

Fig. 2.1 Effect of pre-adaption to killing stress on the survival of *S. mutans*. The assay for 'unadapted' cells was carried out by directly transferring mid-exponential phase cells to challenge stresses at pH 3.0 (left pane) or 20 mM H_2O_2 (right pane) for 30 minutes. The assay for 'adapted' cells was carried out by incubating mid-exponential phase cells at pH 5.0 (left pane) or 2 mM H_2O_2 (right pane) for 2 h to induce an adaptation response, before exposing them to the challenging stresses. Survival was determined by plating 4-6 replicates on THBY agar plates. The results are expressed as the percentage of the cells surviving the challenge for 30 minutes in comparison to the total viable cells before treatment. Data are the average of three independent experiments. White columns: survival rate of 'unadapted' cells; black columns: survival rate of 'adapted' cells.

2.3.1.4 Inactivation of *rpoE* causes alterations in biofilm structure.

The capacity of the *rpoE* deletion strain of *S. mutans* to form biofims in the presence of 0.5% sucrose in both rich medium (THBYS) and minimal medium (BMS) was determined. Notably, Δ*rpoE* revealed a different biofilm architecture, especially in BMS medium (Fig. 2.2). The biofilm of Δ*rpoE* was inhomogeneous and comprised of large cell clusters. It appeared remarkably denser than the wild type biofilm in distinct areas. Moreover, we observed strong staining of the mutant biofilm with propidium iodide (red colour), indicating damaged membranes. Biomass quantification using crystal violet staining showed that Δ*rpoE* formed about 10 % more biofilm than the wild type in THBYS medium (Supplementary Figure S2.4), but there was no obvious change in biomass in BMS medium.

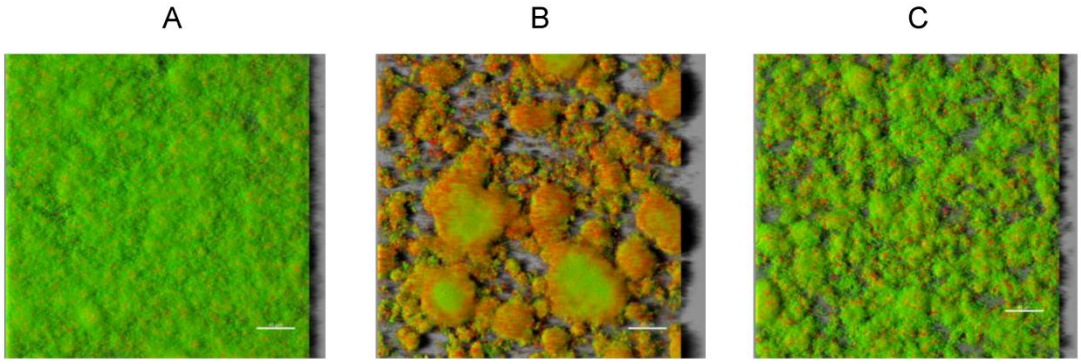

Fig. 2.2 Structures of *S. mutans* biofilms. *S. mutans* strains wild type (A), Δ*rpoE* (B), and Δ*rpoE*comp (C) were grown in a 96-well microtiter plate in BMS medium for 16 hours under anaerobic condition. The biofilms were stained with Live/Dead BacLight viability stain, and images of biofilms at various depth were taken by confocal laser scanning microscopy (CLSM). Three dimensional images were reconstituted by the software Imaris. The shadow at the right side of pictures indicated the biofilm height.

2.3.2 Expression of *rpoE* during growth and under stress.

A reporter strain WP-luc containing the promoter region of *rpoE* fused to a promoterless luciferase gene was constructed to characterize *rpoE* expression. The promoter of *rpoE* showed high activity, reaching a maximum at the late logarithmic phase of growth (Fig. 2.3A). Its expression declined in the stationary phase, but only in unbuffered medium. In buffered medium, *rpoE* expression remained constant at the maximum value in the stationary phase (Fig. 2.3A). In a previous study (Lopez de Saro *et al.*, 1999), a decline in *rpoE* expression in the stationary growth phase was reported. Since these experiments were performed in unbuffered medium, our data suggest that low pH rather than the growth phase may have caused the decline in *rpoE* expression. Indeed, the pH of the *S. mutans* culture in the stationary phase was below 5.0 in the medium without buffering, while in a buffered medium it remained at pH 6.5. Furthermore, we showed that the *rpoE* promoter activity was repressed under acid stress. A lower promoter activity was found at pH 5.0, and it went down quickly when the pH dropped to 4.0 (Fig. 2.3B). The *rpoE* promoter activity was also very sensitive to H_2O_2 stress, and it went down as the concentration increased from 2.0 to 2.4 mM. Interestingly, the repression of the *rpoE* promoter by H_2O_2 was relieved when weak acid and H_2O_2 stress were combined.

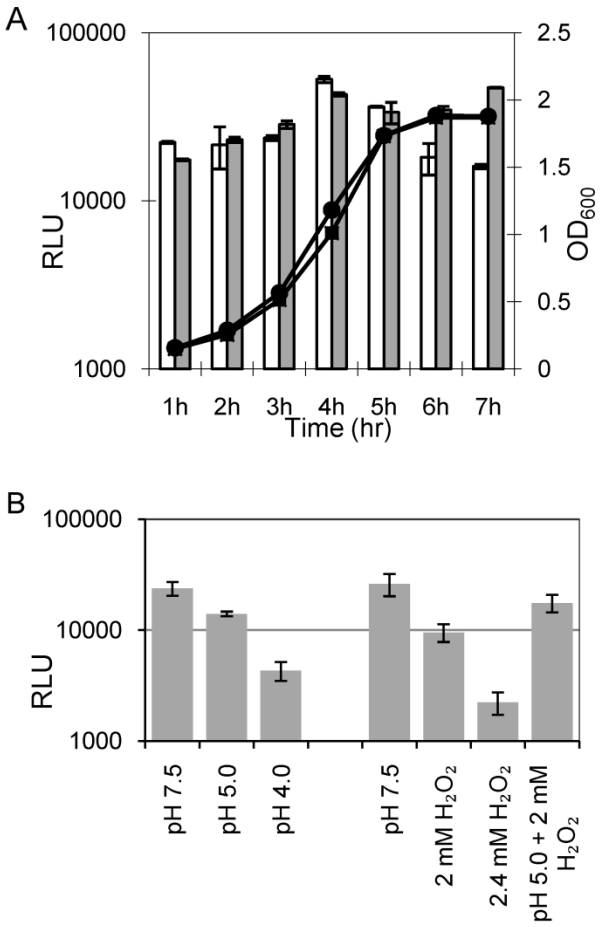

Fig. 2.3 Expression of the *rpoE* gene during growth and under stresses. Luciferase activity was measured in the reporter strain WP-luc carrying a *rpoE*::*luc* fusion in the wild type background. Relative light units were calculated by normalizing luminescence against optical density indicated at the right axis (OD_{600}). (A) Expression of the *rpoE* gene during growth. White bars, luciferase expression in unbuffered and grey bars, in phosphate buffered THBY medium. At least three independent experiments were carried out, and duplicate samples were measured each time. The representative result was shown above. • growth (OD_{600}) of the reporter strain in unbuffered, and ■ in buffered THBY. B: Expression of the *rpoE* gene under stresses. The luciferase activity was measured in log-phase WP-luc after a 2 h treatment with different types of stresses as following: acid stress; H_2O_2stress; both acid and H_2O_2 stresses were combined. Mean and standard deviation are shown for at least two independent experiments, each experiment contained four replicas.

2.3.3 Transcriptome profiling of the Δ*rpoE* mutant.

The Δ*rpoE* mutant showed less resistance to low pH and H_2O_2, and the adaptation conditions (pH 5.0 or 2 mM H_2O_2) were shown to provide protection against stronger stresses, therefore they were selected for microarray studies to further investigate the role of RpoE for stress

adaptation. The combination of both stresses was also studied, since the reporter strain analysis (Fig. 2.3B) had shown that both stresses together had less inhibitory effect on *rpoE* expression compared to H_2O_2 stress alone. Furthermore, cells from the logarithmic and early stationary phases of growth were studied to analyse the role of RpoE under normal growth conditions.
The raw data extracted from the Agilent microarray images were processed by the Bioconductor software packages. A principal component analysis was performed on the expression data of all samples to highlight their variability. As shown in Figure 2.4 biological replicates grouped closely together. The datasets of wild type and Δ*rpoE* mutant were clearly separated by the first two components explaining 48% of total variability. The datasets of acid and H_2O_2-stress were distant from all other samples when only the first two components were plotted, major differences between the log- and early stationary phase, acid or H_2O_2-stress became visible when the third component was plotted, too. In sum, these three components explain 61.1% of the variability in gene expression between the samples. The Linear Models for Microarray Data (LIMMA) package was used for the identification of differentially expressed genes. The transcription profiles of Δ*rpoE* compared to the wild type revealed a total of 550 genes that were differentially expressed (log2 fold change >= 1.0, $p < 0.05$) if all experimental conditions were combined (Supplementary Figure S2.5).

2.3.3.1 Non-coding regions.

A significant number of non-coding regions were found to be differentially expressed in the mutant. Under all experimental conditions, more than 50% of the total number of up-regulated transcripts were non-coding regions (Fig. 2.5). Among the down-regulated transcripts, non-coding regions represented about 20-30%. Since *rpoE* is postulated to reduce the specificity of binding of the RNA polymerase to DNA, lack of RpoE might offer the opportunity for transcription of DNA with weak promoters, especially since the majority of differentially expressed non-coding regions were up-regulated. Thus the global changes in gene expression observed in the *rpoE* mutant could indirectly be related to the massive changes in expression of intergenic regions, some of which might have regulatory functions.
It has been shown that small regulatory RNAs (sRNAs) have a broad effect on gene regulation in bacteria, and the majority of them are located inside the intergenic regions (Liu & Camilli,

2010;Waters & Storz, 2009). In streptococci species, sRNAs involved in the regulation of virulence factors have been reported (Romby & Charpentier, 2010). The sRNAs *fasX* and *pel* in *S. pyogenes* were shown to be growth phase-dependent, and regulated the expression of surface proteins and exotoxins (Kreikemeyer *et al.*, 2001;Mangold *et al.*, 2004). The sRNA *rivX* had been shown to be an effector of the virulence regulator CovR and Mga in *S. pyogenes* (Roberts & Scott, 2007). In *S. pneumoniae*, five highly similar sRNAs (*ccnABCDE*) that are under the direct control of CiaR of the CiaRH system were identified. Among them, *ccnDE* had been shown to be involved in stationary phase autolysis (Halfmann *et al.*, 2007), while *ccnA* expression reversed some phenotypes of a Δ*ciaR* mutant (Tsui *et al.*, 2010).

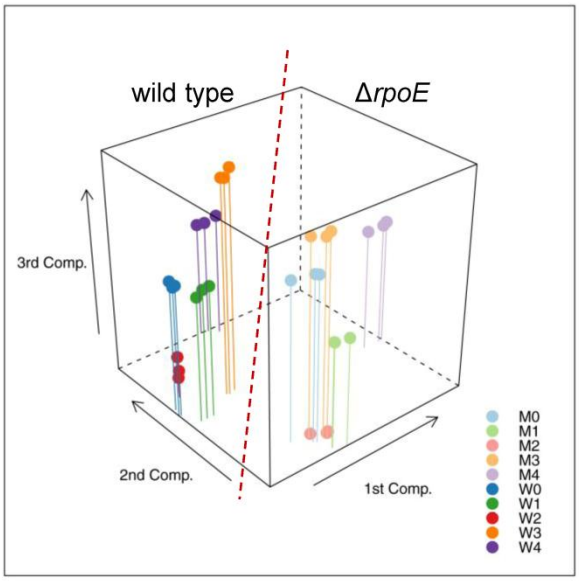

Fig. 2.4 Principal component analysis of microarray samples. The first three components explaining 61.1% of total sample variability in gene expression are plotted. The distance between samples on the plot is proportional to the variance between these samples by expression of genes clustered in the first three components. The samples of the Δ*rpoE* mutant are shown in a lighter colour. W: wild type; M: Δ*rpoE*; 0: Before treatment, log-phase cells; 1: Early stationary-phase; 2: Acid stressed cells; 3: H_2O_2 stressed cells; 4: Acid and H_2O_2 stressed cells.

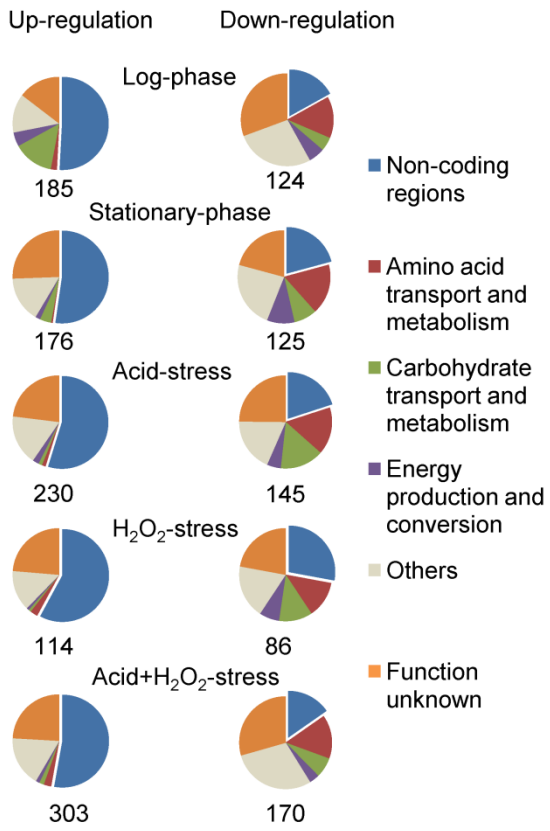

Fig. 2.5 Differentially expressed coding and non-coding regions in the Δ*rpoE* mutant compared to the wild type under five experimental conditions. For each condition, the percentage of up- and down-regulated coding regions and non-coding regions is shown in pie charts. Coding regions are further split into the various functional categories. The total number of differentially expressed genes is indicated below each pie chart.

Our microarray showed that 21 non-coding regions had a differential transcription level in the mutant (log2 fold change >= 1.0, $p < 0.05$) under all tested conditions, indicating a common mechanism dependent on RpoE function rather than experimental conditions. 16 of these 21 non-coding regions were kept for further analysis because they were present on the list of predicted small RNAs in *S. mutans* (http://www.oralgen.lanl.gov/oralgen/bacteria/analysis/srna_result/oralgen_srna_result_old/NC_004350/NC_004350.html). The expression patterns of all the coding genes and non-coding regions were analyzed by clustering using Genesis. 7 of these 16 non-coding regions had similar expression patterns as their up- or down-stream coding genes, thus they were considered as co-transcribed regions and ignored in further analyses. Interestingly, the remaining 9 non-coding

regions were all up-regulated in the mutant, independent of adjacent genes, suggesting they might represent regulatory RNAs (Supplementary Table T2.2). Despite the developing knowledge of the roles of small regulatory RNA (sRNA) in bacteria, the computational prediction of sRNAs remains a challenge due to the lack of conventional calculation modelling (Backofen & Hess, 2010). The prediction of sRNAs relies mainly on comparative genome analysis, in combination with thermodynamic stability or termination signals (Backofen & Hess, 2010). Thus the TransTermHP webservice (http://transterm.cbcb.umd.edu/query.php) was used for detection of Rho-independent transcription terminators, and 3 of these 9 transcripts were found to contain terminators. The first and second non-coding regions (smu-r1, smu-r2) contained putative promoters (Supplementary Figure S2.6, S2.7) predicted by SoftBerry webservice (http://linux1.softberry.com/berry.phtml?topic=bprom&group=programs&subgroup=gfindb), while the third one had too short sequence length (114 bp in total, however with only 45 bp before the putative terminator) to find a putative promoter. The secondary structures of smu-r1and smu-r2 (Supplementary Figure S2.6, S2.7) were predicted using RNAfold webservice (Gruber *et al.*, 2008). The potential targets of smu-r1and smu-r2 were predicted using TargetRNA webservice (Tjaden, 2008) (http://snowwhite.wellesley.edu/targetRNA/index.html) and sRNATarget (Zhao *et al.*, 2008) (http://ccb.bmi.ac.cn/starpecker/). The overlap from these two prediction services was considered as potential mRNA targets (Supplementary Figure S2.6, S2.7). However, the experimental confirmation of these 2 sRNAs and their interaction with target mRNAs will be needed for further conclusions.

2.3.3.2 Global changes caused by the lack of the *rpoE* gene.

Knock out of the *rpoE* gene resulted in significantly reduced expression of 24 genes (log2 fold change >= 1.0, $p < 0.05$) under all tested conditions. Table 2.1 lists these genes together with their fold change values. Several genes that had a strongly correlated function are also presented in the table despite a slightly lower cut-off value. Interestingly, the majority of these genes were down-regulated, suggesting a common regulatory mechanism independent of growth phase, pH, and H_2O_2 stress. Their physiological roles will be discussed below.

Table 2.1 Genes showing similar differential expression in the Δ*rpoE* mutant compared to the wild type strain under 5 experimental conditions, e.g. normal growth at log-phase or stationary-phase, acid stress, H_2O_2 stress, and a combination of both stresses.

Locus Tag	Gene symbol	Gene description	Log2 fold change (Δ*rpoE* /wild type) [a]				
			Log	Stationary	Acid	H_2O_2	Acid+ H_2O_2
SMU.96	***rpoE***	DNA-directed RNA polymerase subunit delta	-8.56	-7.62	-7.22	-7.30	-6.85
Malolactic fermentation							
SMU.137	*mleS*	malate dehydrogenase	-2.88	-3.45	-3.52	-2.18	-3.62
SMU.138	*mleP*	putative malate permease	-2.45	-2.82	-2.88	-1.60	-2.93
SMU.139	*oxdC*	Oxalate decarboxylase	-2.60	-3.06	-2.89	-1.85	-3.37
SMU.140	*gshR*	putative glutathione reductase	-2.46	-2.91	-2.72	-1.61	-2.85
SMU.141		hypothetical protein	-2.31	-2.72	-2.47	-1.35	-2.21
Histidine synthesis							
SMU.1260c	-	hypothetical protein	-1.43	-1.24	-0.95	-0.96	-1.29
SMU.1261c	-	putative phosphoribosyl-ATP pyrophosphohydrolase	-1.48	-1.20	-1.02	-0.90	-1.34
SMU.1262c		hypothetical protein	-1.55	-1.28	-1.08	-0.90	-1.80
SMU.1263	*hisI*	putative phosphoribosyl-ATP pyrophosphatase / phosphoribosyl-AMP cyclohydrolase	-1.78	-1.47	-1.55	-0.97	-2.11
SMU.1264	*hisF*	imidazole glycerol phosphate synthase subunit HisF	-1.82	-1.46	-1.57	-0.84	-2.07
SMU.1265	*hisA*	1-(5-phosphoribosyl)-5-[(5-phosphoribosylamino)methylideneamino] imidazole-4-carboxamide isomerase	-1.95	-1.59	-1.70	-1.07	-2.28
SMU.1266	*hisH*	imidazole glycerol phosphate synthase subunit HisH	-2.16	-1.83	-1.83	-1.22	-2.36
SMU.1267c		hypothetical protein	-2.20	-1.92	-1.87	-1.24	-2.36
SMU.1268	*hisB*	imidazoleglycerol-phosphate dehydratase	-2.22	-1.94	-1.93	-1.17	-2.67

SMU.1269	*serB*	putative phosphoserine phosphatase	-2.24	-1.91	-1.97	-1.12	-2.56
SMU.1270	*hisD*	histidinol dehydrogenase	-2.15	-1.99	-1.86	-1.04	-2.39
SMU.1271	*hisG*	ATP phosphoribosyltransferase catalytic subunit	-2.15	-2.14	-1.82	-1.07	-2.26
SMU.1272	*hisZ*	putative histidyl-tRNA synthetase	-1.96	-2.05	-1.59	-0.95	-2.09
SMU.1273	*hisC*	histidinol-phosphate aminotransferase	-2.01	-2.24	-1.69	-1.07	-2.27
Biofilm, adherence, virulence							
SMU.1004	*gtfB*	glucosyltransferase-I	-1.18	-0.90	-0.59	-1.17	-2.81
SMU.1005	*gtfC*	glucosyltransferase-Si	-1.39	-1.45	-1.32	-1.33	-1.89
SMU.1396	*gbpC*	glucan-binding protein C	-2.71	-1.79	-1.27	-1.28	-3.06
SMU.1397c	*irvA*	Transcriptional regulator	-1.40	-1.40	-1.26	-1.05	-1.38
SMU.610	*spaP*	cell surface antigen SpaP	-1.92	-0.99	-0.59	-1.41	-1.85
Antibiotic resistance							
SMU.440	-	hypothetical protein	-1.16	-1.23	-1.02	-0.35	-1.22
SMU.441	-	putative transcriptional regulator	-1.22	-1.24	-1.07	-0.49	-1.19
SMU.442	-	hypothetical protein	-1.12	-1.25	-1.00	-0.50	-1.10
Others							
SMU.1861c	-	hypothetical protein	-1.20	-1.35	-2.21	-1.82	-1.79
SMU.108	-	hypothetical SAM-dependent methyltransferases	1.69	2.54	2.15	1.19	2.33
SMU.109	-	lantibiotic related antibiotic efflux permease	1.17	1.10	1.25	1.10	1.16
SMU.1480	-	hypothetical protein	1.02	1.32	1.32	1.30	1.19
SMU.1642c	-	hypothetical protein	1.25	1.42	1.71	1.49	1.83
SMU.1643c	-	hypothetical protein	1.15	1.41	1.57	1.44	1.94
SMU.643	-	putative esterase	1.08	1.35	1.11	1.03	1.44

[a]: genes that were below the cutoff of 1.0 (log2 fold change) under some conditions, but had a strong correlation with other genes according to gene functional annotation or genomic location were also present in the table.

Malolactic fermentation.

One of the significant changes in the mutant was the down-regulation of genes for malolactic fermentation (MLF) (SMU.137-SMU.141). MLF protects the organism against acid stress by transforming L-malate to the weaker acid L-lactic acid and carbon dioxide. Products of this fermentation raise the cytoplasmic pH, and furthermore generate ATP as energy source for the extrusion of protons necessary for maintaining the intracellular pH more alkaline than the extracellular pH (Sheng & Marquis, 2007). Therefore, the strong reduction of these genes resulted in decreased acid tolerance, which was consistent with the phenotypic results in this study (Fig. 2.1). The expression of MLF genes is induced by low pH, by the substrate L-malate and to a lesser extent, by the positive regulator MleR (SMU.135) (Lemme *et al.*, 2010). However, despite the strong repression of the MLF structural genes in the Δ*rpoE* strain, the regulator gene *mleR* did not show a corresponding change. Furthermore, these genes were down-regulated in the Δ*rpoE* strain under every tested condition, regardless of growth phase or type of stress, indicating there should exist another regulatory mechanism directly related to the role of RpoE during transcription. Moreover, the overlap of the responses to acidic and oxidative stress is confirmed by the reduction of the putative glutathione reductase GshR in the same operon. GshR is an important antioxidant that reduces glutathione disulfide to the sulfhydryl form. Down-regulation of *gshR* might decrease the cellular oxidative protection and this might partly explain the sensitivity of the Δ*rpoE* mutant to H_2O_2.

Histidine metabolism.

All the genes for the histidine synthesis pathway (SMU.1260c-SMU.1273) were down-regulated in the Δ*rpoE* mutant. The pathway for histidine is interconnected with the purine synthetic pathway. The by-product of histidine biosynthesis, 5'-phosphoribosyl-4-carboxamide-5-aminoimidazole (AICAR) is an intermediate of purine biosynthesis that is rapidly recycled to ATP, which in turn is an important precursor of histidine biosynthesis (Nelson DL, 2004). Since RNA polymerase is essential for purine and pyrimidine synthesis, the loss of RpoE may decrease purine synthesis, and further affect histidine synthesis.

Using base composition analyses and BLAST taxonomy data, the histidine synthesis gene cluster has been suggested as a potential genomic island in the genome of *S. mutans* (http://www.oralgen.lanl.gov/). By comparative genomic analyses, Maruyama et al. showed that

genes for histidine metabolism are conserved among oral streptococci, and they speculated that the biogenesis of histidine may have physiological importance for the survival of streptococci in the oral environment (Maruyama *et al.*, 2009). The buffering capacity of the cytoplasm depends on the concentrations of proteins inside the cytoplasm and is one of the important pH homeostasis mechanisms (Baker-Austin & Dopson, 2007). Histidine has an ionizable side chain with a pKa near neutrality, thus proteins containing histidine residues buffer effectively near neutral pH.

Biofilm, adherence, and virulence.

Sucrose as a common dietary disaccharide is of particular interest because it is an important substrate for extracellular production of water-insoluble glucan which is mediated by the membrane bound glucosyltransferases (GtfB, GtfC). Glucan is important for adherence of *S. mutans* to the tooth surface and for forming the extracellular polysaccharide matrix of the biofilm (Kreth *et al.*, 2008). The cell surface glucan-binding protein (GbpC) has been shown to be involved in biofilm formation and architecture (Lynch *et al.*, 2007). In the Δ*rpoE* strain, these genes were all down-regulated, which may be the reason for the observed changes in its biofilm structure. Moreover, the expression of the cell wall-associated adhesin P1 (SpaP), which mediates the sucrose-independent adherence by binding to salivary pellicles formed on the tooth surface (Ahn *et al.*, 2008) was also depressed in the Δ*rpoE* strain. Furthermore, the transcriptional regulator gene *irvA*, located immediately adjacent to *gbpC*, promotes biofilm formation via inducing *gbpC* and *spaP* expression (Zhu *et al.*, 2009), and was repressed in the Δ*rpoE* strain. Since the adhesion, glucan-producing and binding enzymes are considered as conserved virulence factors of *S. mutans*, different virulence of the Δ*rpoE* strain can be expected.

Resistance to antibiotics.

Although the transcription levels of the 30S ribosomal proteins S1 RpsA (SMU.1200c) and S2 RpsB (SMU.2032) were similar in the microarray data, a lower transcription level of an operon related to polyketide antibiotic resistance SMU.440 - SMU.441 (Nan *et al.*, 2009) was observed in the Δ*rpoE* mutant under all conditions. The hypothetical protein (SMU.440) is conserved in some dental pathogenic bacteria and is associated with polyketide-like antibiotic resistance. The adjacent protein (SMU.441) belongs to the MarR protein family of transcriptional regulators,

which is involved in controlling multiple antibiotic resistances (Nan *et al.*, 2009). Moreover, the adjacent SMU.442 showed a similar expression pattern. Since proteins with related functions are often clustered into the same operon in bacteria, SMU.442 might also be involved in antibiotic resistance. Hence, the sensitivity of the Δ*rpoE* mutant to the polyketide antibiotic tetracycline might in part be due to the repression of SMU.440-SMU.442.

2.3.3.2 Significant changes in the Δ*rpoE* strain during growth.

In addition to the changes described above which occurred under all tested conditions, RpoE deficiency profoundly affected cellular physiology during growth and especially under acid and H_2O_2 stress, and had a major impact on the expression of genes for amino acid transport and metabolism, carbohydrate transport and metabolism, as well as energy production and conversion (Fig. 2.6, Supplementary Table T2.3).

Carbohydrate transport and metabolism, energy production and conversion.

Carbohydrate metabolism by fermentation is the principal source of energy production for *S. mutans*, which possesses an incomplete tricarboxylic acid (TCA) cycle (Ajdic *et al.*, 2002). Furthermore, the ability of *S. mutans* to catabolise a variety of carbohydrates plays an important role in pathogenesis, since its acidic end products, e.g. lactic acid, formate, and acetate, reduce the extracellular pH significantly and induce caries. The major uptake mechanism for sugars in *S. mutans* depends on the phosphoenolpyruvate-phosphotransferase system (PTS), which mediates the internalization and phosphorylation of various sugars. It consists of two nonspecific energy coupling components: enzyme I and histidine protein, and various substrate-specific multiprotein permeases (Gorke & Stulke, 2008).

The *rpoE* mutation caused dramatic changes in carbohydrate transport and metabolism (Fig. 2.6). The transcription of the PTS1 operon (SMU.871-872), the primary PTS for fructose uptake (Wen *et al.*, 2001), was reduced in the Δ*rpoE* mutant at the logarithmic phase of growth. Of note, the putative transcriptional repressor of the fructose operon SMU.870 had the same expression pattern as SMU.871 and SMU.872, indicating that the SMU.870 protein may function as a positive regulator. Thus, the Δ*rpoE* mutant failed to have this PTS; instead an alternative sugar uptake system, the multiple sugar-binding (MSM) ABC transporter genes including the

downstream operon (SMU.877-888) were highly induced. The MSM transporter is responsible for the uptake of a wide range of sugars that are structurally related to raffinose, including disaccharides (melibiose, sucrose) and monosaccharides (glucose, fructose, galactose) (Ajdic & Pham, 2007;Tao *et al.*, 1993). However, no obvious change was found in the transcription of the putative positive regulator of the MSM operon (SMU.876). Hence, there might be other regulatory mechanisms of MSM mediated sugar transport and metabolism.

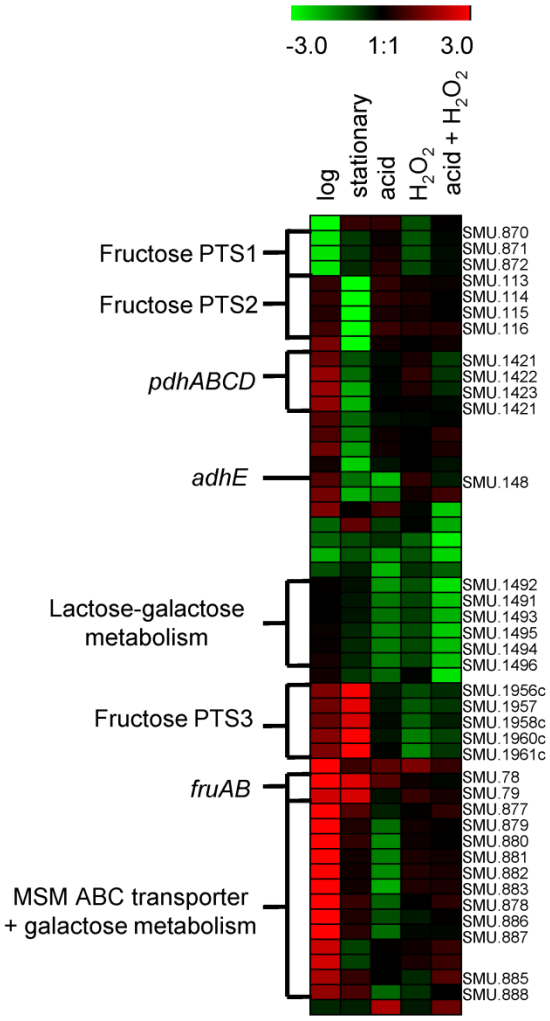

Fig. 2.6 Hierarchical clustering of differentially expressed genes involved in carbohydrate transport & metabolism and energy production & conversion. Gene expression ratios are calculated as log2 fold changes comparing the Δ*rpoE* mutant to the wild type strain. Red: up-regulated genes; green: down-regulated genes.

Wen et al. showed that genes in the fructose-specific PTS2 operon (SMU.113-116) were constitutively expressed at a basic level (Wen *et al.*, 2001), but no further report on the

regulation of this PTS was found. Our microarray results showed clear induction of this operon at the early stationary phase in the wild type, while deletion of *rpoE* abolished such induction. However, the transcription level of the fructose/mannose-specific PTS3 Lev (SMU.1956c-1961c) increased in the Δ*rpoE* mutant. Moreover, the up-regulation of fructan hydrolase genes *fruA* (SMU.78) and *fruB* (SMU.79) was observed. The expression of PTS3 Lev and FruA is repressed by fructose-specific PTS1 and PTS2 through carbon catabolite repression, which allows bacteria to metabolise the readily used sugars instead of non-preferred ones (Zeng *et al.*, 2006;Zeng & Burne, 2008;Zeng & Burne, 2010). Thus, the inhibitory effect of PTS3 Lev was relieved because of reduced repressor PTS1 and PTS2 in the Δ*rpoE* mutant. However, such changes might hamper efficient energy production, since the down-regulation of energy generation genes (*pdhABCD* and *adhE*) was observed in the early stationary phase. Since the optimization of carbohydrate utilization is crucial for oral streptococci, the inefficient sugar metabolism may be part of the reasons that contributed to the growth deficiency and reduced stress tolerance of the Δ*rpoE* mutant.

Amino acid transport.

Genes involved in amino acid transport and metabolism were significantly changed, the majority of which was down-regulated in the Δ*rpoE* mutant. Two osmoprotectant uptake ABC transporters OpuA (SMU.1062-1063) and OpuC (SMU.2116-2119) were down-regulated in the Δ*rpoE* mutant. Osmoprotectant molecules are soluble under physiological conditions and bear no net charge at neutral pH. Their accumulation in the cytosol is important for maintaining cell turgor and for stabilization of proteins, which is crucial for osmotic-stress adaptation of bacteria (Horn *et al.*, 2005). Thus, the reduced level of osmoprotectant ABC transporters in the Δ*rpoE* mutant could be a disadvantage for its survival in the fluctuating oral environment.

Iron transport.

Interestingly, the putative ferrichrome transporter genes (SMU.995-998) were induced in the Δ*rpoE* strain under every condition, except to a smaller degree under oxidative stress. Sufficient levels of iron are necessary for bacterial survival and growth, but the accumulation of iron can lead to the production of toxic oxygen radicals via Fenton chemistry (Clancy *et al.*, 2006;Zheng

et al., 1999). Thus its intracellular transport must be tightly controlled, and such induction might cause toxicity to the Δ*rpoE* strain.

2.3.3.3 Deficiency of the *rpoE* mutant in stress responses.

In addition to the changes of the Δ*rpoE* strain during growth, the loss of RpoE also caused deficiency in stress defense compared to the wild type strain. As an example, the lactose-galactose pathway, encoded by the *lac* operon (SMU.1491-1496), which generates the important substrate glucose 1-phosphate for glycolysis (Abranches *et al.*, 2004), was down-regulated in the Δ*rpoE* mutant compared to the wild type under all stress conditions (Fig. 2.6; Supplementary Figure S2.8). The high-affinity manganese and iron transporter operon *sloABCR* (SMU.182-186) was induced in the wild type under acid or H_2O_2 stresses, however the Δ*rpoE* strain did not have induction under H_2O_2 stress. The metal ions manganese and iron are cofactors for superoxide dismutase, the enzyme necessary for oxidative defense (Martin *et al.*, 1984;Rolerson *et al.*, 2006). Recent studies suggest a role of the SloABC transporter and its regulator SloR for the regulation of virulence in *S. mutans*, including adherence, biofilm formation, genetic competence, metal ion homeostasis, oxidative stress tolerance, and antibiotic resistance (Arirachakaran *et al.*, 2007;Paik *et al.*, 2003;Rolerson *et al.*, 2006).

2.3.3.4 Stress as an additional modulator of the transcriptome profile of *S. mutans*.

Both wild type and mutant strain had similar responses to specific stresses, which revealed that stresses act as additional modulators of gene regulation in *S. mutans*, and some of these responses are not dependent on RpoE. Gene expression changes corresponding to either acid or H_2O_2 stress could be found in the combined-stress condition. The copper transporting ATPase CopA (SMU.426), transcriptional regulator CopY (SMU.424) and chaperone CopZ (SMU.427), for instance, were up-regulated under acidic and combined-stress conditions in both wild type and mutant strains (Supplementary Figure S2.8). Interestingly, under H_2O_2 and combined-stress conditions, the strong induction of SMU.191c-SMU.217c was found in both strains. Within SMU.191c-SMU.217c, 5 genes (SMU.191c, SMU.198c, SMU.201c, SMU.207c, SMU.208c)

encode putative transposases and integrase, while SMU.194c encodes bacteriophage P2 associated and SMU.196c encodes immunogenic secreted protein. Transposases and integrases promote the movement of DNA segments to new locations, through a 'cut-and-paste' mechanism, without requirement of sequence homology (Hickman *et al.*, 2010). Transposases are the most abundant genes in both sequenced genomes and environmental metagenomes (Aziz *et al.*, 2010). Their mobile nature, on the one hand, may cause inactivation and mutation of structural genes in bacterial genome; however, on the other side, they diversify and enrich the genomes and offer a selective advantage to the bacteria (Hickman *et al.*, 2010;Hooper *et al.*, 2009). H_2O_2 has been reported to induce transposition activity in *Burkholderia cenocepacia* (Drevinek *et al.*, 2010), and increase transcription of transposases in *Porphyromonas gingivalis* (Diaz *et al.*, 2006). The increased transposase activity under oxidative stress was expected to contribute to the genomic rearrangement and diversity for better survival under environmental stress.
Interestingly, the combination of two stresses triggered new responses. The pyruvate dehydrogenase complex PdhABCD (SMU.1421-1424) that oxidizes pyruvate to acetyl-CoA and CO_2 (Carlsson *et al.*, 1985;Korithoski *et al.*, 2008), was strongly induced when acid and H_2O_2 stress were combined, while it was only weakly affected by single stress. Accordingly, the alcohol dehydrogenase AdhCD (SMU.129-130) that catabolises the conversion of acetyl-CoA to alcohol (Yamada & Carlsson, 1975), was derepressed under combined-stress conditions. These data suggest that *S. mutans* has sophisticate regulatory mechanisms, instead of simple combination, to protect itself against different stress sources.

2.3.4 Confirmation of gene expression by quantitative PCR.

The differential expression of 4 genes was confirmed by quantitative PCR in all samples using the same RNA sources as those used for the microarray analysis (Supplementary Table T2.4). The first gene in the histidine metabolism operon, *hisC* was down-regulated in the Δ*rpoE* mutant in every tested condition similar to the microarray result. More pronounced induction of the sugar transporter genes *levD* and *msmE* was found in the log-phase and early stationary phase of growth by quantitative PCR in comparison to the microarray data. The reduction of the expression of the transporter gene *fruC* at the early stationary phase in the mutant strain was also confirmed with both methods.

2.4 Summary of RpoE function in *S. mutans*.

The phenotypic and transcriptomic results allow to develop a concept of the global role of RpoE in *S. mutans*, likely caused by its modification of the transcriptional specificity of the RNA polymerase. As shown in Figure 2.7, *rpoE* transcription was inhibited by acid and H_2O_2. The lack of RpoE interfered with various biological functions, including growth, acid tolerance, biofilm formation, and resistance to antibiotics under all experimental conditions. Under normal growth conditions, RpoE had a significant effect on sugar transport and energy production, both of which affect cell growth. Under stress conditions, RpoE knock out caused deficiency in sugar metabolism and metal transport, resulting in reduced growth and survival of the mutant. Thus, RpoE acts as global modulator of gene expression. It is critical for optimal growth and quick adaptation to changing environmental conditions, and potentially increases the virulence of *S. mutans*.

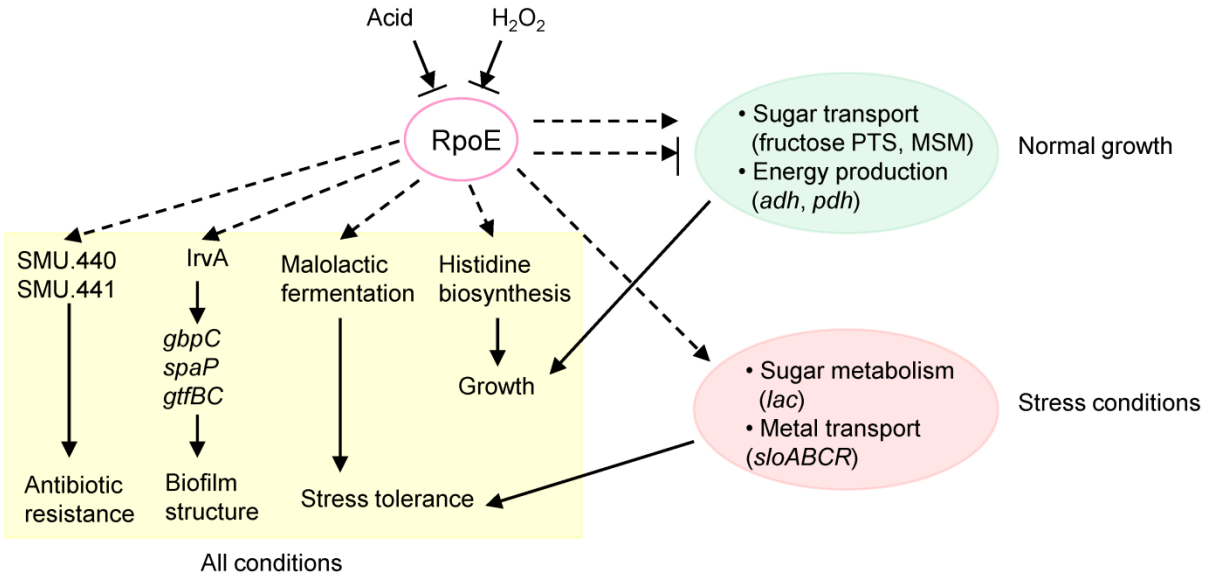

Fig. 2.7 Model of RpoE functions in *S. mutans*. The yellow shadow shows functions regulated by RpoE under all conditions, including the growth, acid tolerance, biofilm structure, and antibiotic resistance. The green part shows effect of RpoE on sugar transport and energy production under normal growth conditions, while the red part suggests function of RpoE on sugar metabolism and metal transport under stress conditions.

2.5 Acknowledgements

We thank Mathias Müsken for introduction to the CLSM. We gratefully acknowledge Robbert Geffers for the microarray technical support, and Michael Reck for the microarray design. X.L. Xue was supported by a CSC-Helmholtz Joint Fellowship.

2.6 Supplementary materials

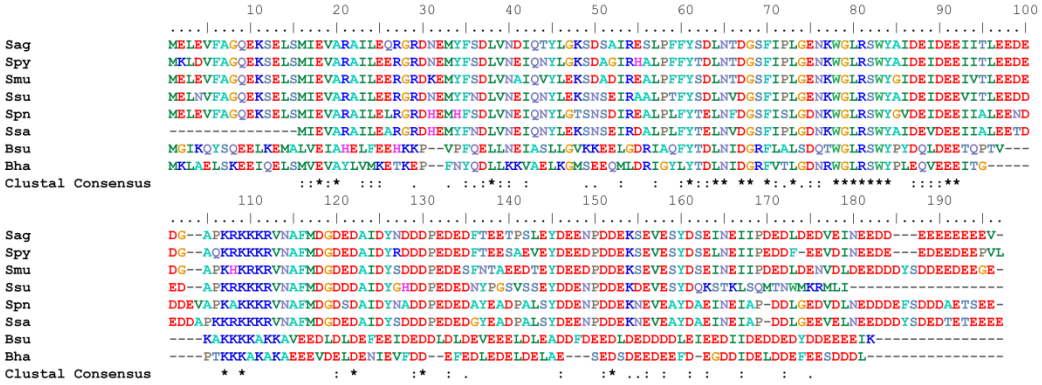

Figure S2.1 Amino acid sequence alignment of delta proteins using CLUSTAL W 2.0. Identical amino acid residues are marked with a star, strongly similar with two dots,and weakly similar with one dot. The default colourscheme is used for alignments. Species abbreviations: Sag, *S. agalactiae*; Spy: *S. pyogenes* M1 GAS; Smu, *S. mutans* UA159; Ssu, *S. suis* 98HAH33; Spn, *S. pneumoniae* G54; Ssa, *S. sanguinis* SK36; Bsu: *Bacillus subtilis* ; Bha: *B. halodurans* C-125.

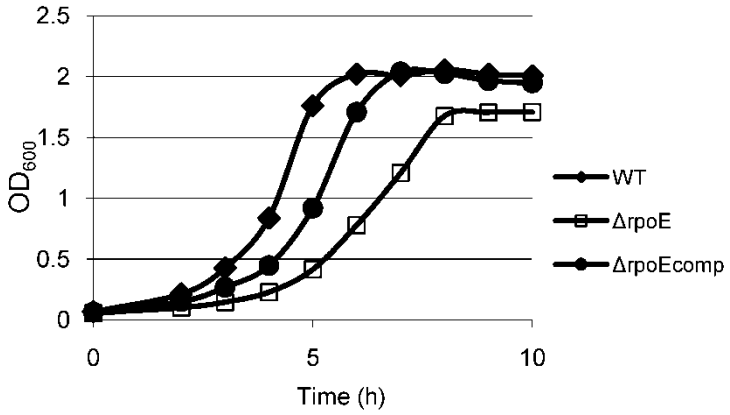

Figure S2.2 Growth defects of *S. mutans* Δ*rpoE* strain. The growth of *S. mutans* cultures in THBY medium pH7.5 at 37℃ in an atmosphere of 5% CO_2 were recorded every hour by measuring the absorbance (optical density) at 600nm. Strains: WT (wild type), Δ*rpoE*, Δ*rpoE*comp (Δ*rpoE* complementation). The data is a representative result from at least three independent experiments.

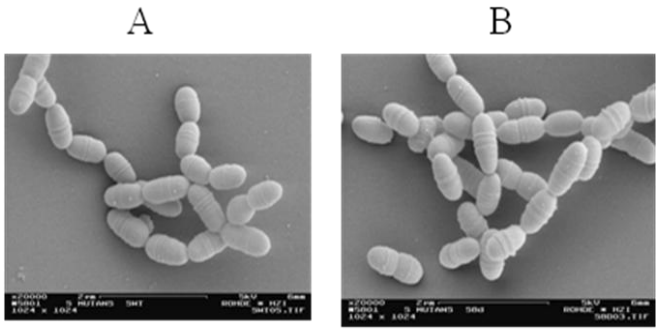

Figure S2.3 *S. mutans* wild type and Δ*rpoE* strains cell phenotype under scanning electron microscopy. A: wild type strain; B: Δ*rpoE* mutant.

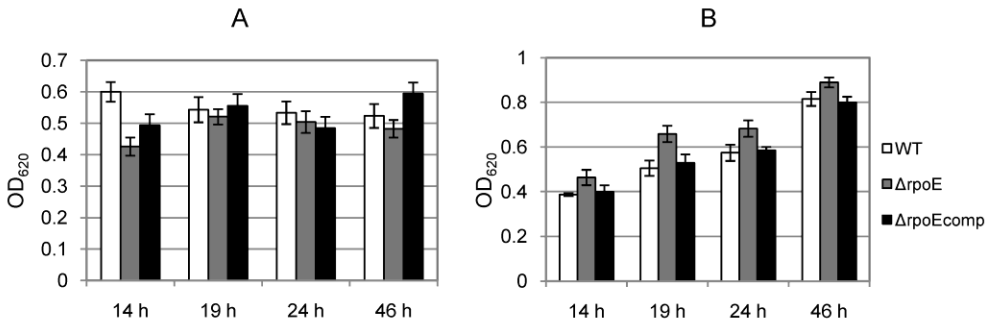

Figure S2.4 Biofilm quantification by crystal violet staining. Biofilm of *S. mutans* wild-type (blue columns), Δ*rpoE* (red columns), and Δ*rpoE*comp (green columns) grown in 96-well microtiter plates in THBYS (A) and BMS (B) medium were stained at different time points with 0.1% crystal violet and the absorbance of the extracted stain was measured at 620 nm. Data presented above is representative result from at least three independent experiments. Mean and standard deviation of twelve replicas of each sample are given.

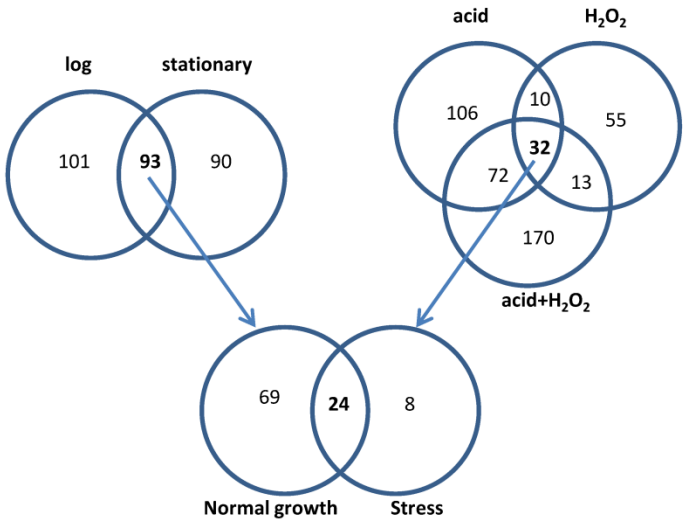

Figure S2.5 Venn diagram showing the number of differentially expressed genes in the Δ*rpoE* mutant compared to the wild type strain under 5 experimental conditions.
Sample collection was as following: Log, M0/W0; stationary, M1/W1; acid, M2/W2; H_2O_2, M3/W3; acid + H_2O_2, M4/W4.

smu-r1

A

>chromosome Streptococcus mutans UA159 (Nucleotides 530356 - 530591 Reverse Strand)

-35

GAGTTACTCCTCTAAAATGATATGACATATTATATTACAATTTGAATAAAAATACAAGTT

-10 Transcription start

ACCTTTTAACAATTTACAA**G**AGCAAAAGCAGACAAACAACAAGTCCCCTAAAAACTATTA

TTTAATCAACAACACCAAAAATAAAGCTCTTGTACTGAACTTTAAAAAGGAGTCCAGAAC

TGAACTGCACCCCAAAAGTTAGACAGAAAAAATCTAACTTTTGGGGTGTTTTTATT

Terminator

B

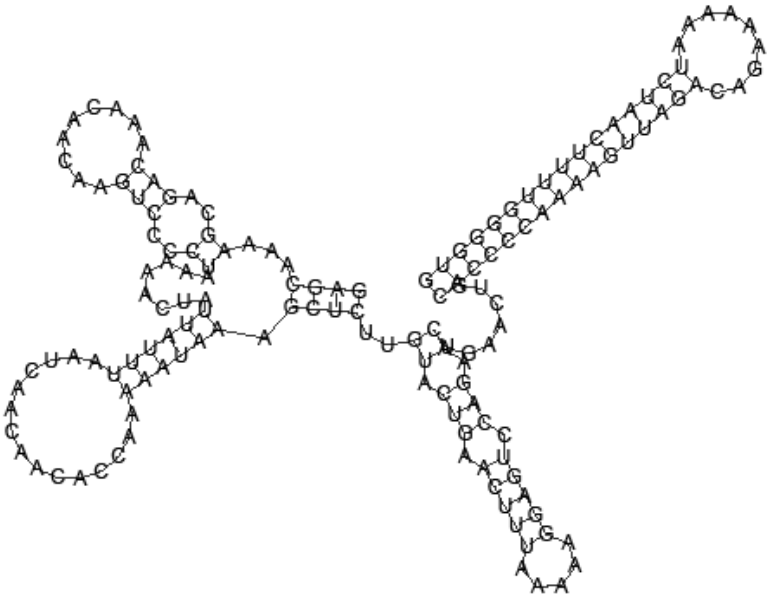

C

r1.1 **SMU.948** hypothetical protein

```
sRNA              2    AGCAAAAGCAGACAAACAACAAGUCCCC--UAAAAACUAUUAUUUAAUCAACAACACCAAAAAUA    64
                       || || |||| | |||  ||||:|| |   ||||||  | :| | |||     ||||||||||||
mRNA (SMU.948)   69    UCCUUGUCGUGUAUUUUAUGUUUAGUGUUUAUUUUU--UCGUCAUUUA-----UGUGGUUUUUAU    12
```

r1.2 **SMU.1025** putative transcriptional regulator

```
sRNA             100    ACUGAACUGCACCCCAAA    117
                        ||||||||||||||||||
```

```
mRNA (SMU.1025)          -89    UGACUUGACGUGGGGUUU    -106
```

r1.3 **SMU.2059c** putative integral membrane protein

```
sRNA                     1      GAGCAAA-AGCAGACAAACAACAAGUCCCCUAAAAACUAUU---AUUUAAUCAACA      52
                                ||||||  |: |:||| | |||||||||  | | || | ||   |||||| | |||
mRNA (SMU.2059c)         55     CUCGUUAAUUCUUUGUCUCUUGUUCAGG--ACUAUUAAAAACUUUAAAUUCGCUGU       2
```

r1.4 **SMU.327** DNA repair protein RadA

```
sRNA                     48     CAACAACACCAA-AAAUA--AAGCUCU-UGUACUGAACUUU       84
                                || ||||||||| ||||   ||:|||| ||:||:|  ||||
mRNA (SMU.327)           -119   GUAGUUGUGGUUAUUUAAGAUUUGAGAGACGUGGC--GAAA      -157
```

r1.5 **SMU.1507c** hypothetical protein

```
sRNA                     28     CCUAAAAACU-AUU----AUUUAAUCAACAACA       55
                                |||| ||||| ||:    |||| ||||||||||
mRNA (SMU.1507c)         71     GGAUAUUUGAGUAGCAGUUAAAAUAGUUGUUGU       39
```

Figure S2.6. Predicted smu-r1 promoter and terminator (A), secondary structure (B), and interaction with target mRNAs (C). A: The putative -35 and -10 regions were marked by green colour. The sequence of smu-r1 was underlined. The predicted transcription start was indicated by bold, while the putative terminator was marked by red colour.

smu-r2

A

>chromosome Streptococcus mutans UA159 (Nucleotides 739911 - 740429 Reverse Strand)
TTCATATCCTCCCCTAACATTCAATAATAATTTAAAGCAAACCAGATAATCTTATTTTAC
AGACAATCATACCTTATTACATTTTACTTCTCACTTCAAAGAATAGCTGCCAAAACAACA
GACTAATCACTCCGCTTATATTATAGCATAAAATATTATGCAGAAGTTAGGATTATATAA
TGTAGCGAAAGTCAAAGCTCAGCAATATTGCAGCATTCTATACTAACAACATAACTTGAG
-35 -10 Transcription start
AGTGACATTAACAATAAAAATTAAACGGCAACTTCCTAAAATTAGCTC**C**AATCACCTTTC
AGAACGAAAATTGAATGTGAGATAGCGCCGACTGACTAACAATCTGGATAAGGAAATCAC
AACCTTTCTAAATTTCAATTATTAAACTATCAAAAATAATCACTTTGGAGAACATATTAA
AACCGTATGGCGTATAGTTATACGGTTTTAATGCTCACTTTTACACTGCAAAAAGCCTTG
GTTTCAAGGCTTTTCATTGCTACGATTTGTCAAAGGTTT
Terminator

B

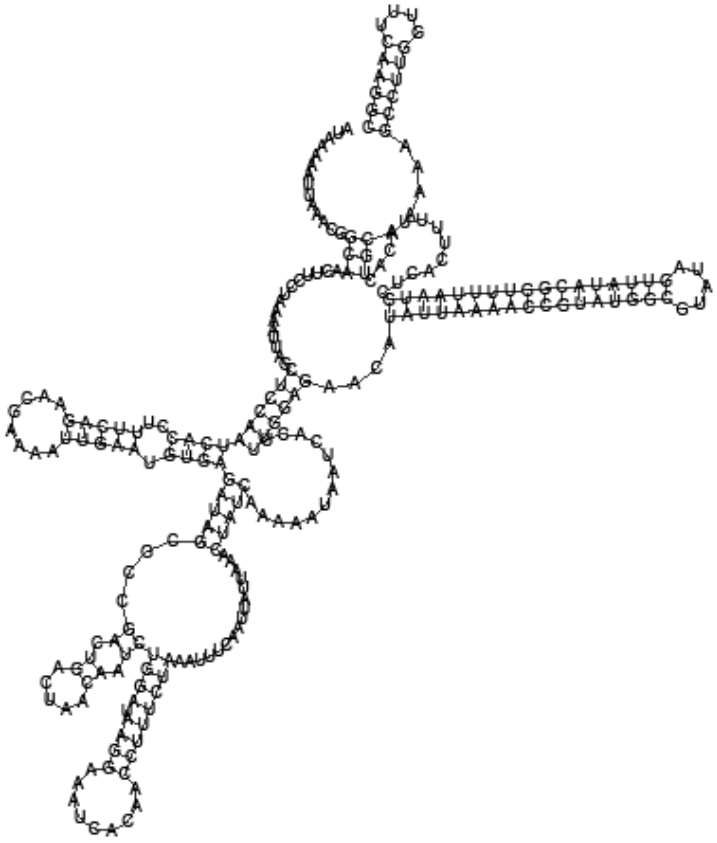

C

r2.1 **murB** UDP-N-acetylenolpyruvoylglucosamine reductase

```
sRNA          60 AUAAGGAAAUCACAAC-CUUUCUAAAUUU-----CAAUU-AUUAAACUAUCAAAAAUAAU--C---ACUUUGGAGAACAUAUUAAAACCGUAUGGCGUAUAGUUAUAC-GGUUUUA--AUGCUCACUUUUACACUGC 181
mRNA (murB)  50 UAUGCCUAUAG--UUGCGGAAGAUUUGAAAACAAGUAAAGUAAAUUG-UAGUAAUCGAUAAAGAGAUGAAAAA----GUAUAAUUUUU---UAGC-CAU-UUAAUUUGGCUAAAAUAAUAUAGUUUAAAAUG-GAUG -74
```

r2.2 **SMU.896** hypothetical protein

Score: -97 Pvalue: 0.000684607

```
sRNA                77 UUUCUAAAUUUCAAUUAUUAAA-CUAUCAAAA 107
mRNA (SMU.896)     -10 AGAGACUAAAGGUUAGUAGUUUUGAUAGUUUU -41
```

r2.3 **SMU.213c** hypothetical protein

Score: -88 Pvalue: 0.00236569

```
sRNA                75 CCUUUCUAAAUUUCAAUUAUUAAAC-UAUCAAAAAUAAUCACUUU 118
mRNA (SMU.213c)    -12 GGAAAGAUUUAA---UAUUAGUUUGUGCGGUUUAUAGU--UGAAA -51
```

r2.4 **SMU.1969c** putative transcriptional regulator

```
sRNA          17 CGAAAAUUGAAUGUGAGAUAGCGCCGACUGACU--AACAAUCUGGAUAAG--GAAAUCAC-A--ACCUUUCUAAAUUUCAAU-UA-UUAAACUAUCAAAAAUAAUCACUUUGGA--GAACAUAU--UAAAA 134
mRNA (SMU.1969c) 78 GCUUUUAACUGACA---------GGUAGA--GAACUCGUUAGAAUGAUUAGACUUUAGGGGUUCUUAGAAGAUU-AAAGUUAUAUUAGUGGGAAAGACU--AAUAGUCAA-CCUAACUGAUAUAUUGUUUU -38
```

r2.5 **cysK** putative cysteine synthetase A; O-acetylserine lyase

Score: -83 Pvalue: 0.00470788

```
sRNA                59 GAUAAGGAAAUCACAACCUUUCUAAAUUUCAAUUAUUAAACUAUCAAAAAUAAUCACUUUGGAG 122
mRNA (cysK)        -81 CUAUUCCUUUAGUAUAGUGCCC--UUGAAGUUAUUAAACUAAUGGUCGUUGU-ACCGAAAAUUC -141
```

r2.6 **SMU.375** hypothetical protein

Score: -82 Pvalue: 0.00540194

```
sRNA                25 GAAUGUGAGAUAGCGCCGACUGACUAACAAUCUGGAUAAGGAAAUCACAACCUUUCUA 82
```

```
                                  ||| | :|:|||| | |   ||||||||| |||  |  ||    |||||| |||:|||
mRNA (SMU.375)          -79       CUUCCUUUUUAUCACAG---ACUGAUUGU-AGAAGUUGUC----AGUGUUUGAAGGAU      -128
```

r2.7 **SMU.1392c** putative acetyltransferase

Score: -80 Pvalue: 0.00711096

```
sRNA                 8   CUUUCAGAAC--GAAAAUUGAAUGUGAGAUAGCGCCGACUGACUAACAAUCUGGAUAAGGAAAUCACAACCUUU--CUAAAUUUCAAUUAUU--AAACU----AUCAAAAA   108
                         ||||||||||  ||| ||:   |||:|  | | |||:| |  ||||     |:||:| :||| ||    |||||  ||   |||  ||: ||  |||||    ||||||||
mRNA (SMU.1392c)    46   GAAAGUCUUGUCCUUAUAG---ACAUUGAA-CACGGUU-A--GAUU-----AUCUGUAUCUUCAGA---GGAAAAAGA---AAAUAUAGAAAACUUUGAAUCAUAGUUUUU   -47
```

r2.8 **SMU.874** bifunctional homocysteine S-methyltransferase/5,10-methylenetetrahydrofolate reductase protein

Score: -80 Pvalue: 0.00711096

```
sRNA 48   CUAACAAUCUGGAUAAGGAAA-UCACAACCUUUCUAAA-UUUC--AAUUAUUAAACUAUCAAAAAUAAUCACUUUGGAGAACAUAUUAAAACCGU-AUGGC-GUA-UAGUUAUACGGUU-UUAAUGC-UCACUUUUACACUGCAA   183
          |:| |||||||||:| ||  | || |  ||||:||  | ||||  |||| || |     |||  |  | | || | ||  || |:|||||| | | :|| |:| | ||| |  |||||| |:|| |   ||||| ||::|||
mRNA
(SMU. 16  GGUCGUUAGACCUGUACCAGUGAGGG--GGAAGGAAAUCAAAGGAUUAAAAACU-----GCUUGAAGGAAUCAA-CGUC--GU-UGAUUUUGGAAGUUUCGUCGUUACCAA-AGACCAAGAACUGCGCA---AAAAUUUGGUGUU   -114
874)
```

r2.9 **SMU.564** hypothetical protein

Score: -78 Pvalue: 0.00935811

```
sRNA              21   AAUUGAAUGUGA--GAUAG-C-GCCGACUGACUAACAAUCUGGAUAAG-----GAAAUCACAACCUUUCUAAAUUUCAA-UUAUU   95
                       ||||||||||:|  |||   | |||   |||  || | ||||| || |     ||||| ||| | |:| | | |||||| || ||
mRNA (SMU.564)   -113   UUAACUUACAUUUGCUAAAAGACGGAGAACUUUUUAUCAGACCGAUACGAAAACUUUA-UGUCGUAGACAGU-AAAGUUCAAGAA   -195
```

Figure S2.7 Predicted smu-r2 promoter and terminator (A), secondary structure (B), and interaction with target mRNAs (C). A: The putative -35 and -10 regions were marked by green colour. The sequence of smu-r2 was underlined. The predicted transcription start was indicated by bold, while the putative terminator was marked by red colour.

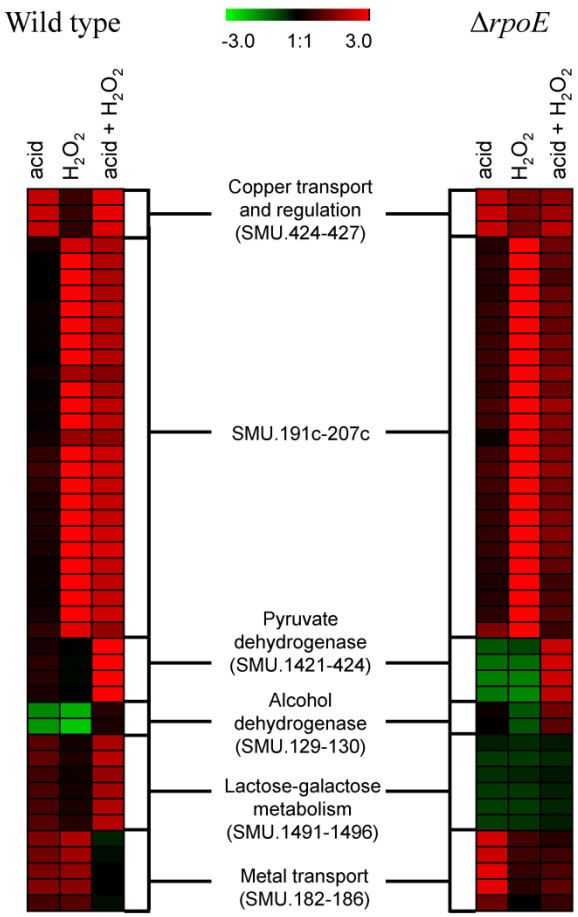

Figure S2.8. Hierarchical clustering of differentially expressed genes under stresses in *S. mutans* wild type and Δ*rpoE* mutant strains. Gene expression ratios are calculated as log2 fold changes under stresses comparing to the control (log-phase cells, before treatment). Red: up-regulated genes; green: down-regulated genes.

Table T2.1 Inhibition of growth of *S. mutans* wild type, Δ*rpoE*, and Δ*rpoE*comp strains by tetracycline and kanamycin.

A: Tetracycline (μg/ml) [a]

	1	0.8	0.6	0.4	0.2
WT	+	+	+	+	+
Δ*rpoE*	-	-	-	+[b]	+
Δ*rpoE*comp	+[c]	+	+	+	+

B: Kanamycin (μg/ml)

	100	80	60	40	20
WT	+	+	+	+	+
Δ*rpoE*	-	-	+	+	+
Δ*rpoE*comp	-	+[c]	+	+	+

[a] +: Visible growth; -: no visible growth.

[b] Δ*rpoE* mutant forms flocks at the presence of 0.4 μg/ml tetracycline.

[c] Δ*rpoE*comp strain showed weaker growth than the wild type strain.

Table T2.2 Differentially expressed non-coding regions in the Δ*rpoE* mutant compared to the wild type strain under 5 experimental conditions, including normal growth at log-phase or early stationary-phase, growth under acid stress, H_2O_2 stress, and acid+H_2O_2-stressed growth.

		Log2 fold change (Δ*rpoE* / wild type)						
#	non-coding regions_start_stop / upstream gene-function / down-stream gene-function	log-phase	stationary-phase	acid-stress	H_2O_2-stress	Acid+H_2O_2-stress	Gene Dir type	Terminator start_stop
1.	NC_004350__530356_530591	1.52	1.65	1.18	1.13	1.37	<-->	530364_530404
	SMU.566c-hypothetical protein	-0.30	-0.18	0.28	-0.51	-0.43		
	SMU.567-putative glutamine ABC transporter, permease	-0.50	-0.26	-0.48	-0.37	0.21		
2.	NC_004350__739911_740429	1.16	1.55	1.45	1.19	2.19	->->	739940_739955
	SMU.788-putative RNA methyltransferase	0.39	0.69	0.34	0.30	0.84		
	SMU.789-hypothetical protein	0.35	0.31	0.30	0.05	0.98		
3.	NC_004350__862809_862923	1.18	1.52	1.37	1.27	1.67	->->	862854_862874
	SMU.906-putative ABC transporter, ATP-binding protein	0.50	0.35	0.48	0.28	1.06		
	SMU.909-putative permease	0.40	0.54	0.39	0.36	0.36		
4.	NC_004350__1894335_1894524	1.25	1.58	1.82	1.17	1.66	<-->	-
	SMU.2027-putative transcriptional regulator	0.22	0.50	1.28	0.14	-0.51		
	SMU.2028-levansucrase precursor; beta-D-fructosyltransferase	0.25	0.12	-1.67	0.71	-1.12		
5.	NC_004350__1912245_1912417	1.93	1.16	1.69	1.13	1.68	<-->	-
	SMU.2038-putative PTS system, trehalose-specific IIABC component	-0.23	-0.96	-0.65	-1.16	0.91		
	SMU.2040-putative transcriptional regulator; repressor of the trehalose operon	-0.03	-0.24	0.14	0.24	0.13		
6.	NC_004350__1919190_1919336	1.53	1.71	1.42	1.29	2.25	<-<-	-
	SMU.2044-putative stringent response protein, ppGpp synthetase	-0.49	-0.15	-0.14	0.03	-0.86		
	SMU.2046c-hypothetical protein	1.51	0.26	0.87	-0.30	1.23		

7.	NC_004350__368829_368962	1.83	2.31	2.35	1.51	2.31	<-->	-
	SMU.392c-hypothetical protein	0.71	1.18	1.03	0.73	0.71		
	SMU.393-hypothetical protein	-0.30	0.13	1.25	-0.57	0.92		
8.	NC_004350__381368_381675	1.03	2.46	2.48	1.54	3.31	<-->	-
	SMU.406c-hypothetical protein	-0.18	0.02	0.23	-0.29	0.36		
	SMU.407-hypothetical protein	0.22	0.13	0.15	0.54	0.71		
9.	NC_004350__401703_402053	1.34	1.48	1.32	1.29	1.64	<-->	-
	SMU.429c-hypothetical protein	-0.24	-0.04	-0.23	-0.43	-0.39		
	SMU.431-putative ABC transporter, ATP-binding protein	0.60	0.41	0.52	0.53	-0.07		

-: no terminator was found.

Table T2.3 Differentially expressed genes in the Δ*rpoE* mutant compared to the wild type under log-phase or early stationary-phase growth conditions.

Locus Tag	Gene symbol	Gene description	Log2 fold change (Δ*rpoE* / wild type)	
			Log-phase	Stationary-phase
Carbohydrate transport and metabolism, energy production and conversion				
SMU.870	*fruR*	putative transcriptional regulator	-2.71	-0.7
SMU.871	*pfkB*	putative fructose-1-phosphate kinase	-2.7	-0.64
SMU.872	*fxpC*	putative fructose-PTS II ABC	-2.75	-0.51
SMU.877	*agaL*	alpha-galactosidase	3.6	0.96
SMU.878	*msmE*	multiple sugar-binding ABC transporter, sugar-binding protein	3.6	0.65
SMU.879	*msmF*	multiple sugar-binding ABC transporter, permease	3.25	0.36
SMU.880	*msmG*	multiple sugar-binding ABC transporter, permease	3.41	0.58
SMU.881	*gtfA*	sucrose phosphorylase	3.04	0.22
SMU.882	*msmK*	multiple sugar-binding ABC transporter, ATP-binding protein	3	0.21
SMU.883	*dexB*	dextran glucosidase DexB	3.1	0.23
SMU.885	*galR*	galactose operon repressor GalR	2	0.64
SMU.886	*galK*	galactokinase	3.86	0.37
SMU.887	*galT*	galactose-1-phosphate uridylyltransferase	3.76	0.48
SMU.888	*galE*	UDP-galactose 4-epimerase, GalE	1.72	0.88
SMU.113	*pfk*	putative fructose-1-phosphate kinase	0.59	-4.25
SMU.114	*fruC*	putative fructose-PTS IIBC	0.63	-4.17
SMU.115	*fruD*	putative fructose-PTS IIA	0.43	-3.05
SMU.116	*lacD2*	tagatose 1,6-diphosphate aldolase	0.79	-3.47
SMU.1956c	*levX*	hypothetical protein	1.49	2.91
SMU.1957	*levG*	putative frutose/mannose-PTS IID	1.34	2.71
SMU.1958c	*levF*	putative frutose/mannose-PTS IIC	1.18	2.55
SMU.1960c	*levE*	putative frutose/mannose-PTS IIB	1.58	3.13
SMU.1961c	*levD*	putative frutose/mannose-PTS IIA	1.5	3.17
SMU.78	*fruA*	fructan hydrolase	3.14	2.64
SMU.79	*fruB*	fructan hydrolase	2.46	2.56
SMU.1421	*pdhC*	branched-chain alpha-keto acid dehydrogenase subunit E2	1.18	-0.99
SMU.1422	*pdhB*	putative pyruvate dehydrogenase E1 component beta subunit	1.75	-1.29
SMU.1423	*pdhA*	putative pyruvate dehydrogenase	1.78	-2.04
SMU.1424	*pdhD*	putative dihydrolipoamide dehydrogenase	1.7	-2.15
SMU.148	*adhE*	bifunctional acetaldehyde-CoA/alcohol dehydrogenase	0.98	-1.35
Amino acid transport				

SMU.1062	*opuAb*	putative proline/glycine betaine ABC transporter, permease protein	-1.55	-1.84
SMU.1063	*opuAa*	putative proline/glycine betaine ABC transporter, ATP-binding	-1.54	-1.93
SMU.2116	*opuCa*	putative osmoprotectant amino acid ABC transporter, ATP-binding	-1.14	-0.95
SMU.2117	*opuCb*	putative osmoprotectant ABC transporter; permease	-1.19	-1.02
SMU.2118	*opuCc*	putative osmoprotectant-binding protein	-1.17	-1.04
SMU.2119	*opuCd*	putative osmoprotectant ABC transporter; permease protein	-1.2	-1.09
Iron transport				
SMU.995	-	ferrichrome ABC transporter, permease	0.89	0.88
SMU.996	-	ferrichrome ABC transporter, permease	0.95	1.12
SMU.997	-	ferrichrome ABC transporter, ATP-binding	1.09	1.35
SMU.998	-	ferrichrome ABC transporter, periplasmic ferrichrome-binding	1.06	1.27

Table T2.4 Confirmation of differential gene expression by quantitative PCR in comparison to the microarray results.

	Microarray Fold change (Δ*rpoE* / wild type)						Real-time PCR Fold change (Δ*rpoE* / wild type)				
	M0/W0	M1/W1	M2/W2	M3/W3	M4/W4	adjusted p value	M0/W0	M1/W1	M2/W2	M3/W3	M4/W4
levD	2.83	8.99	0.95	0.33	0.65	1.25E-08	6.88 ±0.06	19.76 ±0.08	0.38 ±0.48	0.25 ±0.04	0.17 ±0.52
msmE	12.15	1.57	0.44	0.99	1.44	1.35E-12	23.17 ±0.22	1.74 ±0.42	0.31 ±0.13	0.72 ±0.01	0.80 ±0.06
hisC	0.25	0.21	0.31	0.48	0.21	6.07E-15	0.24 ±0.02	0.21 ±0.07	0.29 ±0.04	0.39 ±0.01	0.20 ±0.02
fruC	1.55	0.06	1.47	1.28	0.99	1.92E-10	2.48 ±0.01	0.40 ±0.01	1.50 ±0.01	3.54 ±0.01	1.59 ±0.00

Chapter 3

Streptococcus mutans proteome changes under various stresses, and the role of the delta subunit RpoE of the RNA polymerase

Xiaoli Xue[1], Jinshan Li[2, 3], Wei Wang[2], Helena Sztajer[1], Irene Wagner-Döbler[1]

[1]Research Group Microbial Communication, Division of Cell Biology, Helmholtz Centre for Infection Research, Inhoffenstr. 7, D-38124 Braunschweig, Germany

[2] Institute of Bioprocess and Biosystems Engineering, Technical University Hamburg-Harburg, Denickestr.15, D - 21071 Hamburg, Germany

[3]Institute of Microbiology, Chinese Academy of Sciences, NO.1 West Beichen Road, Chaoyang District, 100101 Beijing, China

3 Chapter 3 - *Streptococcus mutans* proteome changes under various stresses, and the role of the delta subunit RpoE of the RNA polymerase

3.1 Abstract

Streptococcus mutans is a human dental pathogen which has complex regulatory networks for adaptation to its fluctuating oral environment. Here, we studied the proteome response of *S. mutans* under four stress conditions: (1) nutrient starvation, (2) oxidative stress, (3) acid stress, and (4) combined acid and oxidative stress. Transcriptional specificity in low G+C Gram positive bacteria is maintained by RpoE, the delta subunit of the RNA polymerase. Our previous study showed that *rpoE* mutation results in global changes in *S. mutans* transcriptome. To evaluate the role of RpoE in stress response, the proteome changes of the Δ*rpoE* mutant were studied under same conditions as the wild type.

A total of 280 cellular protein spots were reproducibly detected, of which 97 differentially expressed protein spots were identified by MALDI-TOF MS. The nutrient starvation (stationary growth phase) was characterized by upregulation of proteins for alternative carbohydrate metabolism. Oxidative stress (2 mM H_2O_2) caused very strong and specific responses, e.g. upregulation of the enzymes for oxidative stress defense, general stress response, and glycolysis, as well as downregulation of translation related proteins. The weak acid stress (pH 5) resulted in upregulation of acid as well as oxidative defense proteins, and changes in a number of additional enzymes. H_2O_2 in combination with low pH caused reduced changes in the amount of proteins related to oxidative stress defense in comparison to H_2O_2 stress alone, indicating a cross-protection between these two types of stresses.

Lack of RpoE revealed both increased and reduced proteins involved in acid tolerance responses, carbohydrate metabolism, protein synthesis, and general stress response at the log phase in the absence of stress. Under starvation and oxidative stress, the mutant had very similar but weaker responses than the wild type. Under acid stress, general stress proteins were more strongly induced than in the wild type. The cross-protection effect between acid and oxidative stress was less pronounced in the Δ*rpoE* mutant. Comparison of gene expression data suggested some of these proteomic responses were occurring on the transcriptome level, e.g. upregulation of glycolysis under oxidative stress; while some were regulated on the post-transcriptome level, e.g.

upregulation of alternative carbohydrate metabolism under starvation stress, thus they were affected by the reduced transcriptional specificity of the mutant RNA polymerase in both direct and indirect ways. The data demonstrate on the proteome level that H_2O_2 triggers a complex defense reaction for which low pH may function as a preadaption in *S. mutans*. Loss of RpoE affects its adaptive responses to starvation, acid and oxidative stresses.

3.2 Introduction

Streptococcus mutans, a facultative anaerobic bacterium, is considered as an important pathogen responsible for human dental caries (Ajdic *et al.*, 2002;Russell, 2008). It metabolises various carbohydrates to produce acidic products, and forms biofilms (plaque) on the tooth surface, which are the main reasons for tooth decay (Ajdic & Pham, 2007;Hojo *et al.*, 2009). *S. mutans* has developed complex regulatory mechanisms to survive in the oral environment, which is characterized by quick fluctuations of sources and concentrations of carbohydrates, as well as by changing pH and redox levels (Lemos *et al.*, 2005;Lemos & Burne, 2008).
Reactive oxygen species (ROS), including superoxide anion (O_2^-), hydrogen peroxide (H_2O_2), and hydroxyl radical ($HO^\cdot$), are generated from incomplete reduction of oxygen (O_2) or released by other species in the oral cavity (Marquis, 2004). Compared to acid stress, oxidative stress caused by ROS can be harsh for *S. mutans*, as it does not contain catalase, a key enzyme required for oxidative stress protection (Higuchi *et al.*, 2000). However, a large number of other ROS defense mechanisms have been found: the superoxide dismutase (SodA) detoxifies O_2^- by converting it to O_2 and H_2O_2 (Nakayama, 1992;Poyart *et al.*, 2001;Thomas & Pera, 1983); the H_2O_2-forming NADH oxidase Nox-1 functions together with the peroxidase AhpC, while the H_2O-forming NADH oxidase Nox-2 catalyzes directly the reduction of O_2 to H_2O (Higuchi *et al.*, 2000;Poole *et al.*, 2000); the iron-binding enzyme Dpr regulates the intracellular iron level to reduce the generation of ROS through the Fenton Reaction (Higuchi *et al.*, 2000); glutathione reductase GshR and thioredoxin reductase TrxB are important enzymes that repair oxidative damage in proteins (Carmel-Harel & Storz, 2000;De Angelis & Gobbetti, 2004;Jansch *et al.*, 2007). Besides the known antioxidant enzymes, the two component signal transduction systems (TCSs), VicRK and ScnRK, and the response regulator RR11 (SMU.1547c) of the TCS HK11/RR11 were shown to be required for protection of *S. mutans* from oxidative stress (Chen

et al., 2008;Deng *et al.*, 2007a;Perry *et al.*, 2008). Moreover, the serine protease ClpP (Deng *et al.*, 2007b), the trigger factor RopA (Wen *et al.*, 2005), a putative oxidoreductase (SMU.2115) (Abranches *et al.*, 2006), a putative surface-associated protein BrpA (Wen *et al.*, 2006), and a putative phosphatase (SMU.1297) (Zhang & Biswas, 2009a) were also shown to be involved in the oxidative stress tolerance.

To cope with fluctuating pH, *S. mutans* is well equipped with acid defense systems, which have been studied extensively: the F_1F_0-ATPase pumps protons out of the cell (Lemos *et al.*, 2005); the malolactic fermentation (MLF) transforms malate to the weaker acid lactic acid and CO_2 to raise the intracellular pH (Lemme *et al.*, 2010;Sheng & Marquis, 2007); and the agmatine deiminase system produces ammonia and ATP to alkalinize the cytoplasmic pH (Griswold *et al.*, 2006). Moreover, various TCSs, especially VicRK, LiaSR, and CiaHR, have been shown to be required for acid adaptation (Biswas *et al.*, 2008;Gong *et al.*, 2009).

Two-dimensional gel electrophoresis (2-DE) based proteome technology is a powerful tool in understanding the global response of oral bacteria to environmental challenges at the protein level (Len *et al.*, 2003;Macarthur & Jacques, 2003;Renzone *et al.*, 2005). Thus, the effect of pH on the proteome of *S. mutans* has been well studied. Changes in metabolic pathways, including glycolysis, alternative acid production and branched chained amino acids (BCAAs) biosynthesis, were identified in *S. mutans* during growth at low pH (Len *et al.*, 2004a;Renzone *et al.*, 2005). Moreover, proteins involved in DNA replication, transcription, translation, protein folding and cleavage were upregulated under acidic conditions (Len *et al.*, 2004b;Wilkins *et al.*, 2002).

Concerning the H_2O_2 stress, Svensäter et al. (Svensater *et al.*, 2000) demonstrated that *S. mutans* responded to diverse stresses, including oxidative, acid, starvation, salt and heat stresses, as shown by 40-69 protein spots with altered expression. Unfortunately, these protein spots were not identified.

Transcription is the first step in gene regulation, and bacterial cells normally have one housekeeping σ factor and several alternative σ factors to activate different sets of gene expression in responding to environmental changes (Gruber & Gross, 2003). In Gram-negative bacteria (e.g. *E. coli*), σ^S is the master regulators of stress responses (Hengge, 2009;Hengge-Aronis, 2002), while in Gram-positive bacteria (e.g. *Bacillus subtilis*), σ^B is acting as a global regulator of stress responses (Hecker *et al.*, 2007). However, *S. mutans* contains only the major σ factor (RpoD) and an alternative σ factor (ComX) (Ajdic *et al.*, 2002), which is the only known

secondary σ factor in streptococci (Luo & Morrison, 2003;Opdyke *et al.*, 2001) and is a competence-specific regulator (Luo *et al.*, 2003). It does not contain a global stress regulator as σ^B, instead, the TCSs play important roles in sensing environmental changes and regulating gene expression (Lemos & Burne, 2008).

The delta (δ) subunit of the RNA polymerase, RpoE, is a conserved protein in low G+C Gram positive bacteria (Firmicutes). RpoE is maintaining transcriptional specificity by reducing unspecific binding of RNA polymerase to DNA and by accelerating the core enzyme recycling (Achberger *et al.*, 1982;Achberger & Whiteley, 1981;Juang & Helmann, 1994). The physiological role of RpoE has been studied only in a few reports. The Δ*rpoE* mutant of *Bacillus subtilis* revealed an extended lag phase of growth and altered cell morphology (Lopez de Saro *et al.*, 1999). The cellular amount of the RpoE protein was demonstrated to affect the virulence in *S. agalactiae* (Jones *et al.*, 2003;Seepersaud *et al.*, 2006). To evaluate the role of RpoE in *S. mutans*, a Δ*rpoE* mutant was constructed in our previous work (Xue *et al.*, 2010). The mutant showed impaired growth, altered biofilm architecture, and reduced resistance to antibiotic and to acid and oxidative stresses. Large changes in gene expression were observed for a core set of genes which were differentially expressed under all tested conditions. Interestingly, the mutant showed not only downregualtion, but also upregulation of a large number of genes, including intergenic regions (Xue *et al.*, 2010). The aim of this study was to investigate the effect of stresses on *S. mutans* on the proteome level, i.e. starvation (stationary phase of growth), acid stress (pH 5) and oxidative stress (H_2O_2). Moreover, combined pH 5/H_2O_2 stress was studied to facilitate our understanding of the cross-protection of acidic and oxidative stresses. In addition, we studied the role of RpoE for these adaptive responses on the proteome and transcriptome levels.

3.3 Results and Discussion

3.3.1 Experimental set-up

The whole-cell protein extracts of *S. mutans* wild type and the Δ*rpoE* mutant from four adaptive conditions: (1) starvation (stationary phase); (2) oxidative stress (2 mM H_2O_2); (3) acid stress (pH 5); and (4) a combination of both stresses (pH 5 and 2 mM H_2O_2); as well as from the

control condition (log phase before stress treatment) were subjected to two-dimensional gel electrophoresis (2-DE). For each strain in each condition, 2-4 replicates comprised of 2 biological and 0-2 technical replicates were performed, resulting in a total of 24 gels. 280 protein spots were detected in the pH range of 4-7 and molecular weight between10 -100 kD. After spot detection, calibration of gel-gel variation and spot volume normalization, differences in protein amount and significance were calculated. The technical replicates for the wild type and the mutant under the control condition (log phase) revealed a correlation coefficient above 0.99. The correlation coefficient between biological replicates was above 0.99 for all datasets, except for M 2 (the Δ*rpoE* mutant at pH 5), thus the reproducibility was high. Because the M 2 biological replicates displayed a lower correlation coefficient (0.97), more replicates (two technical replicates of each biological replicate) were performed for both the wild type and the mutant.

3.3.2 Principal component analysis of the complete dataset

A principal component analysis was performed on the expression data of the total 280 protein spots for all analyzed samples to determine similarities and differences between the samples. As shown in Fig. 3.1, biological replicates grouped very closely together, as expected from the correlation analysis described above. The expression datasets of the wild type and the Δ*rpoE* mutant were separated by the first three components, which contributed to about 50% of the total variance. The expression patterns of the wild type at the log and stationary growth phase and under acid stress were similar, since *S. mutans* is an acid producer and therefore has a high acid tolerance (Lemos *et al.*, 2005;Lemos & Burne, 2008). In contrast, the H_2O_2 stress had a remarkable impact on the wild type, indicated by the large distance of the H_2O_2 dataset from the others. Surprisingly, the combined acid and oxidative (H_2O_2) stress clearly diminished the effect of the oxidative stress. This might be due to a cross-protection effect, which will be described later. By contrast, in the Δ*rpoE* mutant, the distance between the datasets of any of these adaptive conditions and the log phase was reduced, indicating that loss of RpoE resulted in an inability of the mutant to respond strongly and specifically to the environmental changes.
104 protein spots which had fold of change >=2, $p < 0.05$ in at least one comparison (under stress conditions compared to the log phase for wild type and the mutant or the comparison of two strains at the log phase) were excised and digested by trypsin, and 97 protein spots were

successful identified by MALDI-TOF (see supplementary table T3.1 for a complete list of identified proteins). For a comprehensive data analysis in each comparison, the expression data of all identified protein spots with fold of change >=1.3, p<0.05 are considered as significant changes.

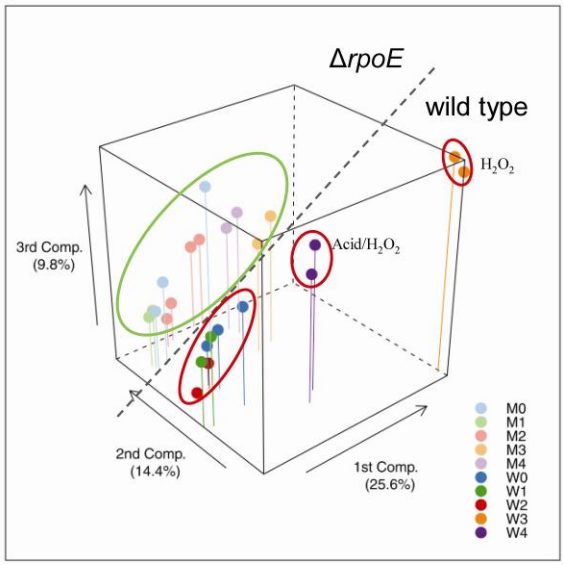

Fig. 3.1 Principal component analysis of the proteome data derived from 2-DE. The distance between samples on the plot is proportional to the variance in the expression of protein spots clustered in the first three components. Samples of the Δ*rpoE* mutant are shown in lighter colours. W: wild type; M: Δ*rpoE*; 0: log growth phase; 1: nutrient starvation (stationary growth phase); 2: acid stress (pH 5); 3: H_2O_2 stress (2 mM H_2O_2); 4: acid/H_2O_2 (pH 5/2 mM H_2O_2) stress.

3.3.3 Proteome changes in *S. mutans* under stress

3.3.3.1 Nutrient starvation (stationary growth phase)

While PCA analysis revealed a large similarity between the proteome profiles of log phase and stationary phase of growth based on the expression patterns of all 280 spots, a small subset of proteins was significantly changed in the stationary phase in comparison to the log phase. The complete data can be found in supplementary table T3.2. The upper panel of Fig. 3.2 shows the protein gels from one of the two biological replicates of each growth phase and indicates proteins with fold of changes >=2.0, and p<0.05. Most of these protein spots with increased expression are involved in carbohydrate metabolism.

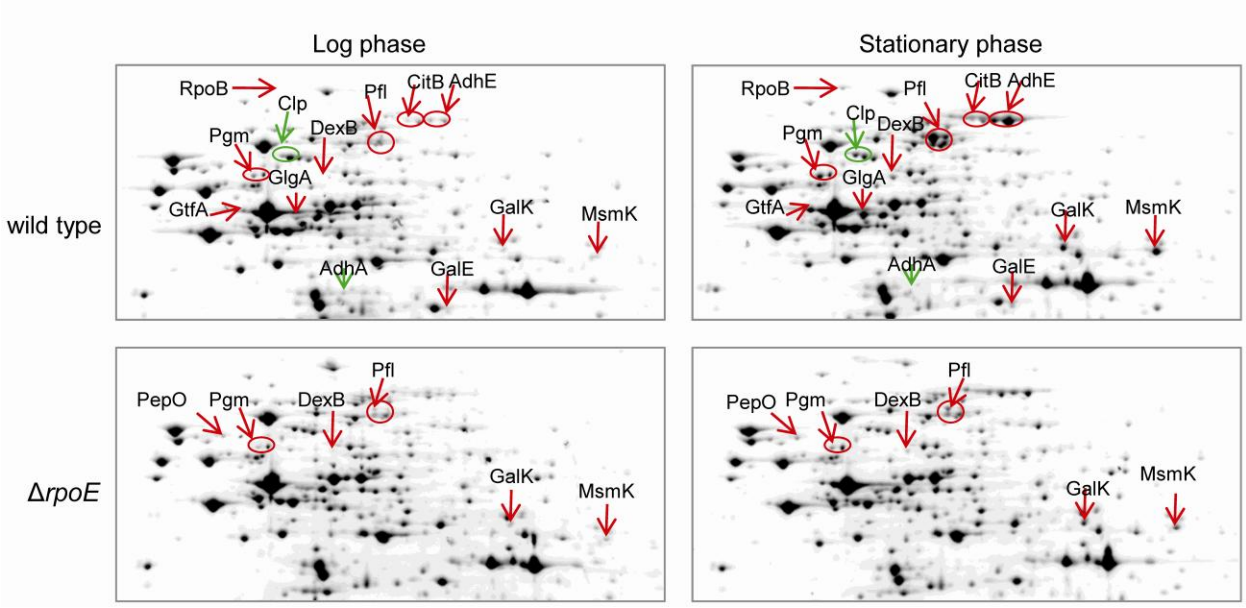

Fig. 3.2 2-DE images of *S. mutans* wild type and the Δ*rpoE* mutant proteome. Left: log phase; right: stationary phase. Upper and lower panels show the proteome of the wild type and the Δ*rpoE* mutant, respectively. Gels were stained with Sypro-RuBPS fluorescent dye, then imaged with a CCD based Fujifilm LAS-1000 image analyzer with light spots on the black background. Images were inverted by Progenesis SameSpots software. Only half of the gel images with major changes are shown. Red and green arrows highlight the up- and down-regulated protein at the stationary phase (fold of changes >=2, P<0.05). Majority of the upregulated proteins are involved in sugar metabolism. Similar but less pronounced response was observed in the mutant.

At the entry into the stationary growth phase, carbon sources are being depleted from the culture. The induction of alternative enzymes for sugar metabolism at the stationary phase is an important adaptive response of streptococci which allows metabolizing less favorite sugars that can be taken up from the environment after the primary substrates have been depleted. In *S. pyogenes* and *S. agalactiae*, enzymes functioning in glycolysis and pyruvate metabolism were upregulated at the stationary phase (Chaussee *et al.*, 2008;Sitkiewicz & Musser, 2009;Wood *et al.*, 2009). Similar results were found here and are summarized in Fig. 3.3 for *S. mutans*. The proteins functioning in the multiple sugar transport and metabolism (MSM) system were highly induced, including MsmK, GtfA, DexB, GalK and GalE. The MSM system is involved in uptake and metabolism of a wide range of sugars, including trisaccharides (raffinose), disaccharides (sucrose, melibiose), and monosaccharides (glucose, fructose, galactose) (Abranches *et al.*, 2004;Tao *et al.*, 1993). Thus, induction of the MSM system facilitates the metabolism of less

desirable sugars to continually provide carbon and energy sources required for survival. In addition, the glycogen synthase (GlgA) is induced. Glycogen is a carbon and energy storage compound which can be used when exogenous supplies are limited and therefore enables bacterial survival (Preiss, 1984;Wilson *et al.*, 2010). Furthermore, several enzymes of the pyruvate metabolism, e.g. Pfl, AdhE, and CitB, were induced. Pfl and AdhE are involved in the heterofermentation of pyruvate and generate the weaker acid products formate and ethanol (Korithoski *et al.*, 2008), which is important for balancing the intracellular pH at the stationary phase of growth.

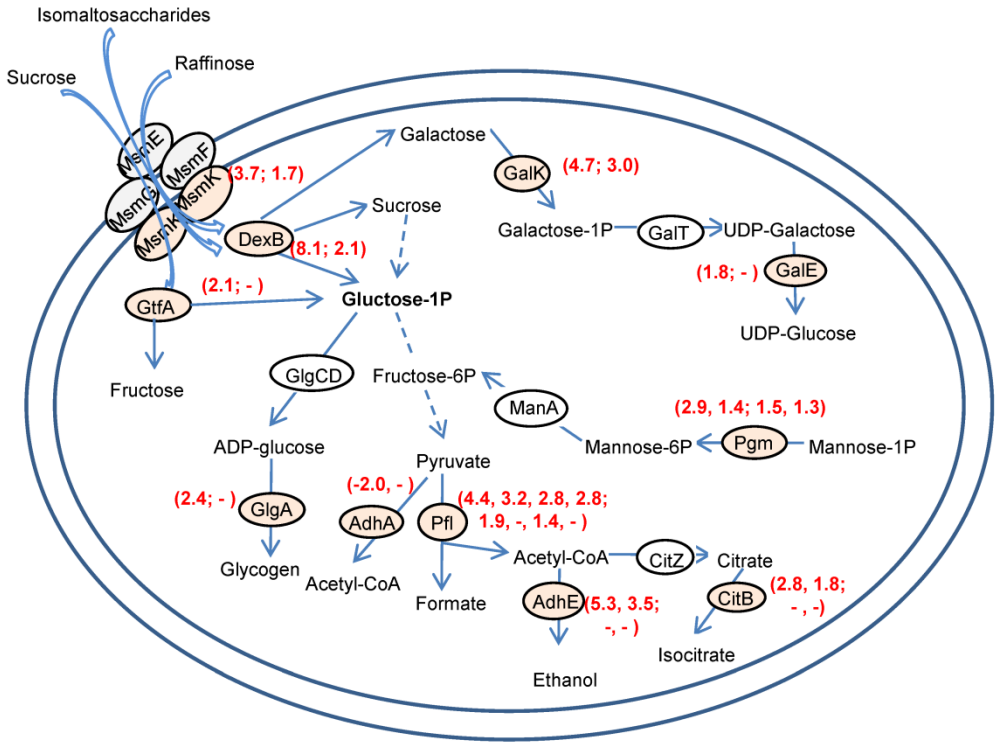

Fig. 3.3 Induction of an alternative carbohydrate metabolism at the stationary phase. Proteins involved in the multiple sugar transport and metabolism (MSM) system, glycogen biosynthesis, and pyruvate metabolism were upregulated at the stationary phase in the wild type and to a lesser extent, in the Δ*rpoE* mutant. The enzymes involved, but not identified in this study are enclosed in ovals filled with white color, while the identified enzymes are enclosed in ovals filled with light grey color. Folds of changes given in brackets were calculated by comparing the protein expression at the stationary phase to the log phase. The data of the wild type and the Δ*rpoE* mutant are separated with semicolon. The expression changes of proteins with different isoforms are separated with comma. ‘‘-’’ means no significant changes.

3.3.3.2 Oxidative stress (H_2O_2)

H_2O_2 is an effective disinfectant which causes oxidative damage of dental plaque, and is widely used in oral care products (Marquis, 2004). Accordingly, H_2O_2 stress was found to cause drastic changes of protein expression, including the upregulation of antioxidant enzymes, general stress proteins, and glycolysis proteins, and downregulation of translation related proteins and the regulator protein VicR (see table 3.1 for a complete list of significantly changed proteins). The enzymes known to be involved in the antioxidant defense of *S. mutans* were all upregulated, e.g. the superoxide dismutase SodA, the NADH oxidase Nox-1, the glutathione reductase GshR, and a predicted ATP binding protein of the iron/sulphur (Fe/S) assembly system Suf, YurY (SMU.247). The Suf system is important for biogenesis of Fe/S proteins, and is required for the oxidative defense in bacteria (Albrecht *et al.*, 2010;Py & Barras, 2010;Thibessard *et al.*, 2004). In addition, an increase in the chaperone GroEL, DnaK, the protease ClpE, and the peptidase PepO, as well as reduced expression of ClpP and changes in the cysteine aminopeptidase PepC were found under oxidative stress. It has previously been shown that GroEL and DnaK affect virulence traits of *S. mutans*, and their transcription was quickly induced by acid and oxidative stresses (Lemos *et al.*, 2001;Lemos *et al.*, 2007).

Table 3.1 Differentially expressed proteins under oxidative stress in comparison to the log phase in the *S. mutans* wild type and the Δ*rpoE* mutant, and the corresponding changes in gene expression.

Spot No.	Gene code	Gene name	Protein name	W3/W0*	P (anova)	W3/W0 t§	M3/M0	P (anova)	M3/M0 t
oxidative stress defense									
375	SMU.629	*sodA*	manganese-type superoxide dismutase, Fe/Mn-SOD	**26.6**	0.0001	-1.7	**3.6**	0.0260	ns
376	SMU.629	*sodA*	manganese-type superoxide dismutase, Fe/Mn-SOD	**1.6**	0.0030	-1.7	**1.9**	0.0210	ns
146	SMU.838	*gshR*	glutathione reductase	**6.9**	0.0001	-2.9	**3.4**	0.0011	-1.9
150	SMU.838	*gshR*	glutathione reductase	-1.1	0.6750	-2.9	**-1.3**	0.0220	-1.9
317	SMU.247	*yurY*	ABC transporter, ATP-binding protein	**6.9**	0.0003	-1.4	**4.0**	0.0160	ns
318	SMU.247	*yurY*	ABC transporter, ATP-binding protein	1.4	0.0640	-1.4	1.5	0.0710	ns
519	SMU.765	*nox-1*	alkyl hydroperoxidase reductase, subunit F (NADH oxidase)	**1.8**	0.0310	-2.4	**1.6**	0.0080	ns
general stress									
682	SMU.1954	*groEL*	chaperonin GroEL	**2.4**	0.0203	ns	**3.2**	0.0006	ns
57	SMU.82	*dnaK*	chaperone protein DnaK (HSP-70)	**2.0**	0.0150	-1.8	2.1	0.0720	1.2

44	SMU.562	*clpE*	ATP-dependent protease ClpE	**2.2**	0.0000	-1.6	**2.6**	0.0031	1.4
469	SMU.2036	*pepO*	endopeptidase O (peptidase)	**1.7**	0.0240	1.0	**1.4**	0.0040	1.3
389	SMU.1672	*clpP*	ATP-dependent Clp protease, proteolytic subunit	**-2.1**	0.0380	ns	1.4	0.1700	ns
149	SMU.466	*pepC*	cysteine aminopeptidase C	**2.6**	0.0067	1.2	**1.9**	0.0260	1.1
558	SMU.466	*pepC*	cysteine aminopeptidase C	-1.1	0.5590	1.2	**-2.4**	0.0008	1.1
carbohydrate metabolism									
622	SMU.1191	*pfkA*	6-phosphofructokinase	**4.8**	0.0004	ns	**1.7**	0.0010	ns
305	SMU.99	*fbaA*	fructose-1,6-biphosphate aldolase	**2.4**	0.0007	ns	1.1	0.6080	ns
231	SMU.360	*gapC*	glyceraldehyde-3-phosphate dehydrogenase	**4.3**	0.0028	ns	**2.3**	0.0021	ns
750	SMU.360	*gapC*	glyceraldehyde-3-phosphate dehydrogenase	**4.3**	0.0001	ns	**3.0**	0.0046	ns
440	SMU.360	*gapC*	glyceraldehyde-3-phosphate dehydrogenase	1.2	0.3810	ns	**-1.9**	0.0130	ns
665	SMU.676	*gapN*	glyceraldehyde-3-phosphate dehydrogenase	**4.5**	0.0009	ns	**2.7**	0.0073	ns
744	SMU.1247	*eno*	enolase	**5.8**	0.0010	ns	**3.4**	0.0010	ns
118	SMU.1190	*pykF*	pyruvate kinase	**6.4**	0.0000	ns	**2.1**	0.0109	ns
194	SMU.361	*pgk*	phosphoglycerate kinase	1.3	0.3280	ns	**1.8**	0.0060	ns
70	SMU.1077	*pgm*	phosphoglucomutase	**1.3**	0.0070	1.1	**-2.0**	0.0016	-3.2
703	SMU.882	*msmK*	multiple sugar-binding ABC transporter, ATP-binding protein	**-2.2**	0.0488	1.2	-1.4	0.1700	-4.9
677	SMU.1564	*glg*	glycogen phosphorylase	**-2.1**	0.0476	1.2	-1.1	0.6180	-2.6
252	SMU.1115	*ldh*	lactate dehydrogenase	**3.1**	0.0008	ns	1.4	0.1790	ns
458	SMU.402	*pfl*	pyruvate formate-lyase	-1.3	0.2780	1.0	**2.1**	0.0028	-1.5
459	SMU.402	*pfl*	pyruvate formate-lyase	1.3	0.2030	1.0	**2.1**	0.0098	-1.5
461	SMU.402	*pfl*	pyruvate formate-lyase	-1.5	0.0760	1.0	1.1	0.4270	-1.5
676	SMU.402	*pfl*	pyruvate formate-lyase	**-3.1**	0.0028	1.0	-1.4	0.0560	-1.5
235	SMU.127	*adhA*	acetoin dehydrogenase (TPP-dependent), E1 component alpha subunit	-1.1	0.5620	-3.6	**2.7**	0.0081	-2.0
272	SMU.1043c	*eutD*	phosphotransacetylase (phosphate acetyltransferase)	**-1.4**	0.0420	1.1	**-2.2**	0.0208	-1.7
577	SMU.1426c	*glmM*	phosphoglucosamine mutase (phosphoacetylglucosamine mutase)	**-1.3**	0.0170	-1.1	**-2.1**	0.0244	-1.1
183	SMU.1233	*deoB*	phosphopentomutase	**-1.7**	0.0230	1.0	-1.1	0.4160	1.3
492	SMU.2038	*pttB*	phosphotransferase system, trehalose-specific IIBC component (EIIBC-tre)	**-1.8**	0.0080	-1.5	-1.5	0.0580	-2.8
352	SMU.636	*nagB*	glucosamine-6-phosphate isomerase (N-acetylglucosamine-6-phosphate isomerase)	1.4	0.2280	-1.1	**2.7**	0.0020	2.2
translation									
719	SMU.1847	*elp*	translation elongation factor P	**-5.4**	0.0026	1.1	-1.2	0.5060	-1.1

92	SMU.2098	*argS*	arginyl-tRNA synthase	**-2.5**	0.0174	-1.0	-2.3	0.0560	1.1
147	SMU.2102	*hisS*	histidyl-tRNA synthetase (histidine--tRNA ligase)	**-2.0**	0.0070	-1.8	**-2.0**	0.0264	-1.4
501	SMU.773c	*lysS*	lysyl-tRNA synthetase	**-4.1**	0.0051	-1.2	**-2.3**	0.0004	-1.1
217	SMU.1512	*pheS*	phenylalanyl-tRNA synthetase alpha subunit	**-2.6**	0.0426	-1.2	-1.3	0.4470	-1.2
182	SMU.1085	*prfA*	peptide chain release factor 1	**-2.0**	0.0397	-1.1	**-2.1**	0.0126	-1.2
53	SMU.1586	*thrS*	threonyl-tRNA synthetase	**2.5**	0.0005	-2.1	**2.4**	0.0005	-1.9
268	SMU.496	*cysK*	cysteine synthetase A (O-acetylserine lyase)	**-2.5**	0.0235	-1.3	-1.0	0.9310	-2.1
628	SMU.2032	*rpsB*	30S ribosomal protein S2	-2.3	0.0940	-1.0	**-1.6**	0.0040	-1.1
277	SMU.445	*glyQ*	glycyl-tRNA synthetase alpha subunit	1.2	0.0750	-1.3	**-1.5**	0.0300	-1.0
lipid metabolism									
326	SMU.1746c	*fabM*	enoyl-CoA hydratase/trans-2, cis-3-decenoyl-ACP isomerase	**7.0**	0.0004	1.1	**2.3**	0.0080	1.1
638	SMU.1742c	*fabK*	trans-2-enoyl-ACP reductase II	**-1.8**	0.0350	1.0	**-2.9**	0.0012	1.0
198	SMU.1739	*fabF*	3-oxoacyl-(acyl-carrier-protein) synthase	**1.4**	0.0370	1.0	**-1.8**	0.0080	1.0
216	SMU.1309c	*gldA-2*	glycerol dehydrogenase	-1.2	0.0004	1.1	**1.3**	0.0030	1.1
transcription									
208	SMU.2001	*rpoA*	DNA-directed RNA polymerase, alpha subunit	**3.0**	0.0028	ns	**2.3**	0.0100	-1.0
444	SMU.1990	*rpoB*	DNA-dependent RNA polymerase, beta subunit	**8.9**	0.0008	ns	**6.1**	0.0271	1.1
6	SMU.1990	*rpoB*	DNA-dependent RNA polymerase, beta subunit	**-3.6**	0.0680	ns	**-3.5**	0.1182	1.1
48	SMU.751		putative transcriptional accessory protein	**-4.3**	0.0002	1.2	**-2.1**	0.0320	-1.0
108	SMU.2157	*guaB*	inosine monophosphate dehydrogenase	**2.2**	0.0013	1.1	**1.8**	0.0090	1.0
115	SMU.2157	*guaB*	inosine monophosphate dehydrogenase	**-1.5**	0.0040	1.1	**-2.3**	0.0068	1.0
cell division									
728	SMU.557	*divIVA*	cell division initiation protein DivIVA	**2.1**	0.0050	1.0	**1.8**	0.0350	-1.0
726	SMU.557	*divIVA*	cell division initiation protein DivIVA	**-3.6**	0.0006	1.0	-1.0	0.9040	-1.0
two-component response regulator									
330	SMU.1517	*vicR*	two-component response regulator	**-2.6**	0.0001	-1.2	-1.8	0.0580	1.1
acid stress defense									
237	SMU.233	*ilvC*	ketol-acid reductoisomerase	**2.4**	0.0010	1.1	-1.0	0.6190	1.1
215	SMU.1203	*ilvE*	branched-chain amino acid aminotransferase IlvE	**1.3**	0.0400	1.2	**-1.3**	0.0460	1.3
166	SMU.364	*glnA*	glutamine synthetase type 1 (glutamate--ammonia ligase)	-1.1	0.7660	1.5	**-2**	0.0250	ns
481	SMU.137	*mleS*	malolactic enzyme	1.4	0.0580	1.1	**2.4**	0.0130	1.8
others									

32	SMU.546	*typA*	putative GTP-binding protein, possible elongation factor	**2.6**	0.0012	-1.1	**2.6**	0.0038	-1.1
33	SMU.546	*typA*	putative GTP-binding protein, possible elongation factor	1.3	0.0900	-1.1	1.2	0.4760	-1.1
214	SMU.1653	*serA*	D-3-phosphoglycerate dehydrogenase	1.0	0.7930	1.2	**-2.1**	0.0264	-1.2
408	SMU.1859	*ssb*	single-stranded DNA-binding protein	**-1.6**	0.0170	ns	-1.0	0.9150	ns
116	SMU.1691	*dltA*	D-alanine-D-alanyl carrier protein ligase	**1.6**	0.0070	1.0	**1.5**	0.0380	-1.1
641	SMU.1348c	*psaA*	ABC transporter, ATP-binding protein	-1.5	0.0910	ns	**-1.9**	0.0020	1.0
388	SMU.554		conserved hypothetical protein	**-2.0**	0.0302	1.1	-1.8	0.0800	-1.0
400	SMU.961		conserved hypothetical protein	**4.7**	0.0013	10.9	2.9	0.0810	7.2
624	SMU.1760c		conserved hypothetical protein	**5.8**	0.0004	1.9	**4.2**	0.0009	1.5
748	SMU.1760c		conserved hypothetical protein	2.4	0.0620	1.9	**2.4**	0.0000	1.5
94	SMU.475		conserved hypothetical protein	-1.6	0.0750	-1.1	**2.7**	0.0220	-1.2

[*] Protein fold of changes under oxidative stress in the log phase of growth compared to the log phase of growth without oxidative stress in the wild type (W3/W0) and in the Δ*rpoE* mutant (M3/M0). Values in bold are significant ($p < 0.05$).

[§] t: transcriptome data. Changes in gene expression were determined under the same conditions as those for the proteome. Data show fold of change of gene expression under oxidative stress (log phase of growth) compared to gene expression in the log phase of growth without oxidative stress. All transcriptome data which were significant (with $p<0.005$) are shown. Those with $p>=0.005$ are indicated as ‘‘ns’’ (not significant). See methods for details on microarray methodology (Xue *et al.*, 2010).

Consistent with the increased demands on energy generation, the protein expression of the complete glycolysis pathway was strongly induced under oxidative stress as shown in Fig. 3.4 Glycolysis is a major mechanism for generation of NADH, which is important for elimination of H_2O_2 by NADH oxidases (Higuchi *et al.*, 2000). H_2O_2 has been reported to damage the glycolytic system of *S. mutans*, which was indicated by reduced glucose consumption and reduced levels of ATP and NADH (Baldeck & Marquis, 2008). Our data are not necessarily contradictory to the previous findings, since they reflect the absolute amount of proteins, but not protein activities. The increased protein amount could be a compensation for the reduced protein activity under oxidative stress. In addition, the reduced levels of ATP and NADH under oxidative stress described before (Baldeck & Marquis, 2008) could have been caused by the large demand for energy and NADH for oxidative defense rather than by a defect of the glycolysis enzymes. Ahn et al. reported enhanced expression of genes related to carbohydrate uptake and reduced glycolysis rate in aerobically grown *S. mutans* cells (Ahn *et al.*, 2009;Ahn & Burne, 2007), which confirms the proteome data reported here.

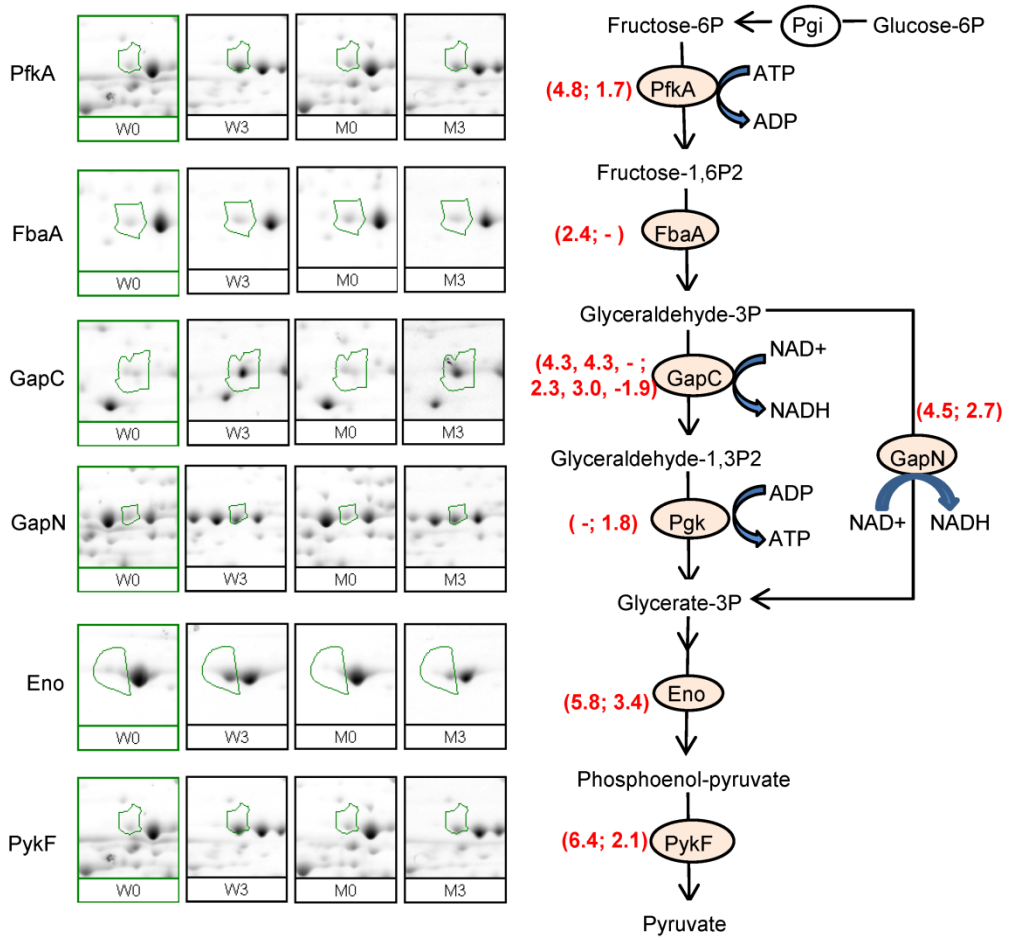

Fig. 3.4 Induction of glycolysis enzymes under oxidative stress. Glycolysis enzymes were upregulated under oxidative stress in the *S. mutans* Δ*rpoE* mutant and, especially, in the wild type. The images of representative protein spots are shown in on the left panel. On the right panel, enzymes involved in the glycolysis pathway are enclosed in ovals filled with light grey color. Folds of expression changes of these proteins under oxidative stress in comparison to the log phase are given in brackets on the right panel, the data for the wild type and the Δ*rpoE* mutant are separated with semicolon. The expression changes of proteins with different isoforms are separated with comma. ‘‘-’’ means no significant changes.

Oxidative stress has been previously reported to reduce the growth rate of *S. mutans* under oxidative stress (Ahn *et al.*, 2009;Baldeck & Marquis, 2008). In our experiment, no growth occurred during 2 h incubation under oxidative stress, however the cells remained alive as indicated by bacterial Live/Dead staining, suggesting they were in a resting state (data not shown). In the proteome data, significant changes of proteins involved in transcription and translation were seen, which are discussed below (see also Table 3.1). Translation related proteins, e.g. the 30S ribosomal protein S2 RpsB, the translation elongation factor Efp, the

peptide chain release factor PrfA, and four aminoacyl tRNA synthetases ArgS, HisS, LysS, and PheS, were downregulated (table 3.1). The only enzyme which showed increased expression was the threonyl-tRNA synthetase ThrS. Aminoacyl-tRNA synthetases are key enzymes for translation, and oxidative stress impairs the editing activity of ThrS, thus causing protein mistranslation and impairing the growth (Ling & Soll, 2010), which could justify the upregulation of ThrS. Interestingly, the putative transcriptional accessory protein (SMU.751) was reduced, while altered expression of subunits of the RNA polymerase occurred, e.g. an increased amount of the α subunit, and changed expression of two isoforms of the β subunit of RNA polymerase. Changes of two isoforms of the inosine monophosphate dehydrogenase GuaB, which converts inosine monophosphate, IMP, to xanthosine monophosphate, XMP, a precursor of guanosine derivatives and thus required for DNA and RNA synthesis, were also observed. The altered amount of enzymes for transcription and translation under oxidative stress might indicate the need to produce more stress responsive proteins at the expense of the normal activity for growth.

Interetingly, the response regulator VicR was downregulated. The TCS VicRK is a key regulatory system that is required for *S. mutans* biofilm formation, competence, and stress tolerance, including acid, oxidative and osmotic stresses (Deng *et al.*, 2007a;Liu *et al.*, 2006;Senadheera *et al.*, 2009;Senadheera *et al.*, 2005). A Δ*vicR* mutant is not viable, showing the importance of this regulator for *S. mutans* (Senadheera *et al.*, 2005). Thus, the reduced amount of VicR will amplify the stress damage. However, the connection between a reduced level of VicR and the other observed oxidative responses awaits further study.

Finally, changes in the amount of proteins responsible for fatty acid biosynthesis (FabF, FabK and FabM) were observed. In *S. pneumoniae*, the biosynthesis of unsaturated fatty acids is carried out by FabM, while saturated fatty acids are synthesized by FabK (Marrakchi *et al.*, 2002). In our proteome data, FabM was increased, while FabK was decreased, suggesting an increased synthesis of unsaturated fatty acids under oxidative stress. FabM has been shown to modulate the membrane fluidity in *S. mutans* and contributes to its survival at the extreme acidic pH (pH 2.5)(Altabe *et al.*, 2007;Fozo & Quivey, Jr., 2004). Out data show that FabM may also be required for the oxidative stress. We did not find any significant changes of these fatty acid biosynthesis proteins under acid stress here (supplementary table T3.3), most likely because we used a weak acid stress (pH of 5.0).

3.3.3.3 Acid stress (pH 5.0)

Of the known adaptive responses to low pH in *S. mutans* we found induction of the enzymes for branched chain amino acids (BCAAs) biosynthesis (IlvC, IlvD, IlvE) and the enzyme MleS for malolactic fermentation (MLF) (see supplementary table T3.3). The membrane proteins for the F_1F_0-ATPase were not found since only the intracellular proteome was analyzed in this study. Proteins of the agmatine deiminase system were also not found, which could be due to their relatively low level of expression (Griswold *et al.*, 2006). Only small changes in proteins related to translation, transcription, and carbohydrate and lipid metabolism were found, suggesting that a pH of 5.0 was not a strong stress factor for *S. mutans*. However, several enzymes for oxidative stress defense were induced (Nox-1, SodA, and YurY).This could be one of the mechanisms for the observed cross-protection between acid and oxidative stresses.

3.3.3.4 Combined acid and oxidative stress

The analysis of the proteome response under combined acid (pH 5) and oxidative (H_2O_2) stress in comparison to each of these stresses separately could help to understand the cross-protection between acid and oxidative stress in *S. mutans*, which has been reported previously but not been well understood. Svensäter et al. reported that pre-adaptation to starvation, salt or acid stresses protected *S. mutans* cells from further acid challenge at pH 3.5, but there was no mechanism reported (Svensater *et al.*, 2000). Another study showed that the antioxidant enzyme SodA and iron chelators were required for bacterial acid tolerance, and a cross-protection between acid and oxidative stress was proposed (Bruno-Barcena *et al.*, 2010;Sanders *et al.*, 1995). Here we provide a global view of cross-protection at the proteome level. A complete list of changed proteins under combined acid and oxidative stress can be found in supplementary table 4. Proteins which were differentially expressed under at least two of the three stress conditions analysed are shown in table 2. The drastic changes caused by H_2O_2 damage alone were partially reduced by the combination of acid and hydrogen peroxide stress, indicated by changes in expression of the same proteins, but to a smaller extent (table 3.2). As one example, the

induction of the antioxidant enzymes SodA and GshR, as well as the induction of enzymes for carbohydrate metabolism was reduced under combined acid/H_2O_2 treatment in comparison to H_2O_2 stress alone. Furthermore, the reduced expression of proteins related to translation and transcription under H_2O_2 stress was partially relieved under the combined acid/H_2O_2 condition. Thus, this study shows that a relatively low concentration of H_2O_2 (2 mM) is sufficient to cause extreme repression of major biological activities of *S. mutans*, however, a pH of 5.0 reduces the damage caused by H_2O_2. Since low pH occurs in dental plaque under physiological conditions, the data provide a rationale for the need to use high concentrations of H_2O_2 for oral hygiene.

Table 3.2. Proteins which were differentially expressed under at least two stress conditions: acid stress, oxidative stress, and combined acid and oxidative stress.

Spot No.	Gene code	Gene name	W2/W0*	P (anova)	W3/W0	P (anova)	W4/W0	P (anova)
oxidative stress defense								
375	SMU.629	*sodA*	**2.3**	0.0150	**26.6**	0.0001	**9.6**	0.0001
376	SMU.629	*sodA*	1.8	0.1040	**1.6**	0.0030	**1.5**	0.0130
146	SMU.838	*gshR*	1.2	0.5170	**6.9**	0.0001	**2.5**	0.0310
519	SMU.765	*nox-1*	**2.1**	0.0121	**1.8**	0.0310	-1.1	0.6990
general stress								
44	SMU.562	*clpE*	**-1.4**	0.0490	**2.2**	0.0000	**1.6**	0.0001
149	SMU.466	*pepC*	1.1	0.5240	**2.6**	0.0067	**3.1**	0.0090
carbohydrate metabolism								
305	SMU.99	*fbaA*	**1.6**	0.0100	**2.4**	0.0007	**2.9**	0.0098
231	SMU.360	*gapC*	-1.1	0.7000	**4.3**	0.0028	**4.8**	0.0003
750	SMU.360	*gapC*	1.1	0.6070	**4.3**	0.0001	**7.6**	0.0000
622	SMU.1191	*pfkA*	1.1	0.0160	**4.8**	0.0004	**1.8**	0.0002
665	SMU.676	*gapN*	1.4	0.1020	**4.5**	0.0009	**1.9**	0.0180
118	SMU.1190	*pykF*	1.3	0.3080	**6.4**	0.0000	**1.9**	0.0220
70	SMU.1077	*pgm*	**1.6**	0.0020	**1.3**	0.0070	**-1.5**	0.0005
71	SMU.1077	*pgm*	**-1.4**	0.020	1.3	0.1050	**1.6**	0.0060
252	SMU.1115	*ldh*	-1.4	0.2850	**3.1**	0.0008	**2.6**	0.0290
577	SMU.1426c	*glmM*	-1.2	0.0840	**-1.3**	0.0170	**-2.3**	0.0090
Translation								
719	SMU.1847	*elp*	1.0	0.9690	**-5.4**	0.0026	**-2.1**	0.0099
53	SMU.1586	*thrS*	**1.5**	0.0010	**2.5**	0.0005	**1.9**	0.0001
32	SMU.546	*typA*	-1.6	0.0520	**2.6**	0.0012	**1.6**	0.0350
147	SMU.2102	*hisS*	**-1.3**	0.0330	**-2.0**	0.0070	-1.6	0.0700
Transcription								

48	SMU.751		**-2.3**	0.0040	**-4.3**	0.0002	**-2.0**	0.0166
108	SMU.2157	*guaB*	**1.6**	0.0110	**2.2**	0.0013	**1.6**	0.0060
115	SMU.2157	*guaB*	**1.6**	0.0220	**-1.5**	0.0040	-1.2	0.1210
acid defense								
237	SMU.233	*ilvC*	**2.1**	0.0280	**2.4**	0.0010	**2.8**	0.0210
497	SMU.2128	*ilvD*	**1.5**	0.0050	1.1	0.3030	**2.1**	0.0001
215	SMU.1203	*ilvE*	**2.1**	0.0060	**1.3**	0.0400	-1.1	0.0450
Regulators								
330	SMU.1517	*vicR*	1.2	0.4070	**-2.6**	0.0001	**-1.4**	0.0030

* Protein fold of changes under acid stress (W2/W0), oxidative stress (W3/W0) and acid and oxidative stress combined (W4/W0) compared to the log phase in the wild type. Values in bold are significant (fold of change >=1.3, $p < 0.05$). Only protein spots which showed significant changes in at least two conditions were selected.

3.3.4 Effect of lack of RpoE on the proteome of *S. mutans* and its response to stress

The Δ*rpoE* mutant of *S. mutans* was constructed by replacing the coding sequence of the *rpoE* gene with an erythromycin resistance cassette (Xue *et al.*, 2010). Genetic complementation of the mutant with the *rpoE* gene in *trans* showed reversal to the wild type phenotype (e.g. growth, biofilm formation, and stress tolerance), indicating that secondary mutations were not present (Xue *et al.*, 2010). Lack of RpoE resulted in substantial changes in gene expression in *S. mtuans* (Xue *et al.*, 2010). Here, we analyzed the proteome changes caused by lack of RpoE, and whether corresponding changes can be seen in both transcriptome and proteome data. In addition, we studied the proteome changes of the Δ*rpoE* mutant under various stresses to evaluate the role of RpoE for adaptation responses in *S. mutans*. To be able to interpret the proteome data in more depth, the corresponding transcriptome data (GEO record GSE22333), some of which were not analyzed in our previous study, were used.

3.3.4.1 Comparison of the Δ*rpoE* mutant to the wild type at the log phase of growth

Comparison of the Δ*rpoE* mutant to the wild type revealed differences in proteins involved in acid tolerance responses, central carbohydrate metabolism, translation, and general stress

response (table 3.3). The Δ*rpoE* mutant had a reduced amount of the malate dehydrogenase MleS and the oxalate decarboxylase OxdC from the MLF acid defense system. The gene expression data also show a strong downregulation of these two enzymes. Previously we had shown that the whole operon of MLF (SMU.137 - SMU.141) belonged to the core set of changed genes in the mutant and was strongly downregulated under all conditions (Xue *et al.*, 2010). By contrast, the BCAAs biosynthesis enzymes (ketol-acid reductoisomerase IlvC, dihydroxy-acid dehydratase IlvD, and aminotransferase IlvE) together with the glutamine synthetase GlnA, suggested as an additional acid adaptation response in *S. mutans* (Len *et al.*, 2004a), were induced in the Δ*rpoE* mutant. Corresponding changes can be seen on the transcriptome level, but they were very small and thus were below the cut-off applied in the microarray study. Thus, one acid defense system was upregulated, while the other one was downregulated, and these changes occurred both on the transcriptional and translational level. 9 proteins in the carbohydrate metabolism were differentially expressed in the mutant (table 3.3). The pyruvate formate-lyase Pfl functioning in the conversion of pyruvate to formate, and the acetoin dehydrogenase AdhA, one of the subunits of the pyruvate dehydrogenase complex (PDH) that oxidizes pyruvate to acetyl-CoA and CO_2 were downregulated. Pyruvate is an important intermediate in glycolysis, and can be converted to diverse acid end products in *S. mutans* (Korithoski *et al.*, 2008). Interestingly, consistent with our previous finding that the histidine biosynthesis genes were downregulated in the Δ*rpoE* mutant (Xue *et al.*, 2010), the phosphopentomutase DeoB had a reduced expression. DeoB is involved in the pentose phosphate pathway, and it catalyzes the intramolecular transfer of the phosphate group between Ribose-1P and Ribose-5P. Ribose-5P is a direct precursor of phosphoribosyl pyrophosphate, which is an important intermediate for histidine and purine/pyrimidine biosynthesis (Tozzi *et al.*, 2006). Due to the central function of the RNA polymerase in purine/pyrimidine biosynthesis, loss of RpoE could interrupt the connection between the pentose phosphate pathway and the histidine and purine/pyrimidine biosynthesis pathways.

Upregulation of several tRNA synthetases was observed in the Δ*rpoE* mutant, including the aspartyl-tRNA synthetase AspS, the glycyl-tRNA synthetase GlyQ, the histidyl-tRNA synthetase HisS, and the lysyl-tRNA synthetase LysS, while the amount of the elongation factor Elp was reduced. Changes in the oxidative stress defense, general stress response, and fatty acid metabolism were also found. Thus, the *rpoE* mutation caused global changes in the proteome.

Table 3.3 Differentially expressed proteins in the *S. mutans* Δ*rpoE* mutant in comparison to the wild type at the log phase of growth and the corresponding changes in gene expression.

Spot No.	Gene code	Gene name	Protein name	M0/W0*	P (anova)	M0/W0 t§
acid stress defense						
481	SMU.137	*mleS*	malate dehydrogenase	**-2.1**	0.0059	-7.4
179	SMU.139	*oxdC*	oxalate decarboxylase	**-1.7**	0.0440	-6.1
237	SMU.233	*ilvC*	ketol-acid reductoisomerase	**1.7**	0.0010	ns
497	SMU.2128	*ilvD*	dihydroxy-acid dehydratase	**1.5**	0.0310	1.3
215	SMU.1203	*ilvE*	branched-chain amino acid aminotransferase	**2.0**	0.0012	1.2
166	SMU.364	*glnA*	glutamine synthetase type 1 (glutamate-ammonia ligase)	**2.6**	0.0087	1.1
carbohydrate metabolism						
235	SMU.127	*adhA*	acetoin dehydrogenase (TPP-ependent), E1 component alpha subunit	**-2.5**	0.0017	-3.6
458	SMU.402	*pfl*	pyruvate formate-lyase	**-1.7**	0.0250	1.1
676	SMU.402	*pfl*	pyruvate formate-lyase	**-1.3**	0.0130	1.1
183	SMU.1233	*deoB*	phosphopentomutase	**-1.9**	0.0009	-1.5
744	SMU.1247	*eno*	enolase	**-1.8**	0.0470	ns
71	SMU.1077	*pgm*	phosphoglucomutase	**-1.6**	0.0040	1.7
352	SMU.636	*nagB*	glucosamine-6-phosphate isomerase (N-acetylglucosamine-6-phosphate isomerase)	**-1.6**	0.0370	-2.2
492	SMU.2038	*pttB*	phosphotransferase system, trehalose-specific IIBC component (EIIBC-tre)	**1.4**	0.0250	-1.2
305	SMU.99	*fbaA*	fructose-1,6-biphosphate aldolase	**1.5**	0.0100	ns
272	SMU.1043c	*eutD*	phosphotransacetylase (phosphate acetyltransferase)	**2.0**	0.0077	1.5
translation						
63	SMU.2101	*aspS*	aspartyl-tRNA synthetase	**2.2**	0.0022	1.2
277	SMU.445	*glyQ*	glycyl-tRNA synthetase alpha subunit	**2.1**	0.0028	-2.1
147	SMU.2102	*hisS*	histidyl-tRNA synthetase (histidine--tRNA ligase)	**1.5**	0.0180	-1.4
501	SMU.773c	*lysS*	lysyl-tRNA synthetase	**1.3**	0.0260	-1.2
719	SMU.1847	*elp*	translation elongation factor P	**-1.5**	0.0420	-1.2
oxidative stress defense						
519	SMU.765	*nox-1*	alkyl hydroperoxidase reductase, subunit F (NADH oxidase)	**-1.7**	0.0170	-1.1
150	SMU.838	*gshR*	glutathione reductase	**1.8**	0.0090	1.0
general stress						
389	SMU.1672	*clpP*	ATP-dependent Clp protease, proteolytic subunit	**-2.3**	0.0166	-1.4
44	SMU.562	*clpE*	ATP-dependent protease ClpE	**-1.6**	0.0000	-1.7
469	SMU.2036	*pepO*	endopeptidase O (peptidase)	**-1.6**	0.0050	-1.0
558	SMU.466	*pepC*	cysteine aminopeptidase C	**1.4**	0.0090	-1.0

fatty acid metabolism						
198	SMU.1739	*fabF*	3-oxoacyl-(acyl-carrier-protein) synthase	**1.4**	0.0080	-1.0
638	SMU.1742c	*fabK*	trans-2-enoyl-ACP reductase II	**1.7**	0.0010	ns
others						
115	SMU.2157	*guaB*	inosine monophosphate dehydrogenase	**1.8**	0.0010	1.0
214	SMU.1653	*serA*	D-3-phosphoglycerate dehydrogenase	**1.7**	0.0090	1.3
408	SMU.1859	*ssb*	single-stranded DNA-binding protein	**-1.8**	0.0030	ns
72	SMU.1444c	*yqgA*	metallo-beta-lactamase superfamily protein hypothetical protein	**-1.4**	0.0160	ns
641	SMU.1348c	*psaA*	ABC transporter, ATP-binding protein	**1.5**	0.0040	ns
94	SMU.475		conserved hypothetical protein	**-3.4**	0.0091	-1.0
400	SMU.961		conserved hypothetical protein	**-2.1**	0.0320	-1.2
748	SMU.1760c		conserved hypothetical protein	**-1.7**	0.0000	1.2

[*] Protein fold of changes in the Δ*rpoE* mutant compared to the wild type at the log phase (M0/W0). Values in bold are significant ($p < 0.05$).
[§] t: transcriptome data. Changes in gene expression were determined under the same experimental conditions as for the proteome All fold of change values which were significant (with $p<0.005$) are shown. Those with $p>=0.005$ are indicated as ‘‘ns’’ (not significant). See table 1 for further explanations.

3.3.4.2 Proteome changes of the Δ*rpoE* mutant under stress

The *rpoE* mutation also had complex influence on *S. mutans* proteome under stress conditions. The mutant had very similar but weaker responses to starvation and oxidative stress than the wild type. For example, a weaker induction of enzymes for sugar metabolism was observed under starvation stress (Fig. 3.3). Similarly, glycolysis enzymes were weakly induced under oxidative stress (Fig. 3.4). For example, while the pyruvate kinase PykF was upregulated 6.4 fold in the wild type, it was only upregulated 2.1 fold in the mutant.

Although pH 5 is a weak acid for *S. mutans* indicated by the small changes in the proteome, the Δ*rpoE* mutant displayed some stronger changes under acid stress. 9 proteins necessary for translation were downregulated while 4 general stress proteins were upregulated (supplementary table T3.3). Moreover, the cross-protection between acid and oxidative stress as described above for the wild type was not observed in the Δ*rpoE* mutant due to its decreased response to oxidative stress.

3.3.5 Comparison of proteome and transcriptome analysis

The experimental setup for the proteome study here was identical with that of the transcriptome study reported previously (Xue *et al.*, 2010), allowing us to compare the data from both levels of regulation. In our previous study, the transcriptome data of the Δ*rpoE* mutant were directly compared to the wild type under the same condition. A total of 550 differentially expressed genes (fold of changes >= 2; $P < 0.005$) were found when all experimental conditions were combined. Among them, a core set of 24 genes was influenced by lack of RpoE under all investigated conditions. The complete operon for MLF, the histidine biosynthesis operon, and genes influencing biofilm formation and antibiotic resistance were among the core genes.
In the proteome study, only 2 proteins (MleS and OxdC which are part of MLF) from the core set of 24 genes were identified. Their downregulation was observed in the mutant only at the log phase of growth. This may be due to the lower sensitivity of the 2-DE based proteome analysis compared to the microarray analysis. However, the main reason for the lack of detection of most of these proteins may be due to differential regulation at the post-transcriptional level thus the protein amount of all these proteins is not necessarily be significantly changes, also some of them are extracellular or membrane proteins and thus were not the subject of this study. For example, the oxidative stress response (induction of known antioxidant and glycolysis pathway enzymes, downregulation of translation related proteins) were clearly observed on the proteome level, but no or only small changes were seen in the transcriptome data (table 3.1, out lined by red lines), suggesting a post-transcriptional regulation mechanism, e.g. changes in the rate of translation or degradation. Nevertheless, strong correlation between transcriptome and proteome data was observed for certain changes. For example, the induction of an alternative carbohydrate metabolism at the stationary phase in the wild type, while with weaker changes in the mutant, were revealed by both proteome and transcriptome data (outlined by red lines in the supplementary table T3.2). Thus, the relaxed transcriptional specificity caused by loss of RpoE may have influenced the proteome in direct and indirect ways.

3.4 Conclusions

The analysis of the proteome response of *S. mutans* was conducted for four types of stress: The transition to the stationary growth phase (nutrient starvation), which resulted in a shift to an alternative carbohydrate metabolism; oxidative stress (2 mM H_2O_2) which induced a very strong response, including changes in proteins for oxidative stress defense, general stress, glycolysis, translation and transcription; weak acid stress (pH 5) which induced MLF and BCAAs biosynthesis, two known acid defense systems of *S. mutans*, as well as proteins required for protection against oxidative stress. The damage of oxidative stress was reduced when combined with acid stress, indicating that *S. mutans* cells adapted to low pH may be prepared for the stronger stress caused H_2O_2, e.g. some of the enzymes required for oxidative defense are also induced at a pH of 5.

The delta subunit of the RNA polymerase affects gene expression in a global way by relaxing the specificity of transcription. Here we studied the effect of *rpoE* mutation on the proteome. Loss of RpoE caused changes in proteins responsible for the acid defense and carbohydrate metabolism, downregulation of general stress proteins and upregulation of several tRNA synthetases. Compared to the wild type, the Δ*rpoE* mutant was not able to respond discriminately to adaptive stresses. This was observed for the attenuated response at entry into the stationary growth phase, and for oxidative stress, and stronger effect of acid stress, as well as reduced acid and oxidative cross-protection. Some of the observed changes occurred also on the level of transcription, in accordance with the mechanistic model for RpoE functioning by directing the transcription specificity of the RNA polymerase; while some changes were apparently the results of post transcriptional changes of protein expression in the Δ*rpoE* mutant.

3.5 Acknowledgements

We greatly thank Jürgen Tomasch for his assistance with the principle component analysis. X. Xue was supported by a CSC-Helmholtz Joint Fellowship.

3.6 Supplementary materials

Table T3.1 MALDI-TOF identification of proteins in *S. mutans*.

Spot No.	Gene code	Gene name	GI No.	Protein name	Nominal mass (M_r)*	pI value	Matched peptides	Sequence coverage (%)	Score §	P value
6	SMU.1990	*rpoB*	24378350	DNA-dependent RNA polymerase, beta subunit	132805	5.04	28	39	237	3.9E-21
15	SMU.670	*citB*	24377048	aconitate hydratase, aconitase A	98278	5.32	7	14	65	6.4E-04
16	SMU.148	*adhE*	24376524	alcohol-acetaldehyde dehydrogenase	97331	5.49	24	43	217	3.9E-19
17	SMU.148	*adhE*	24376524	alcohol-acetaldehyde dehydrogenase	97331	5.49	16	35	193	9.8E-17
20	SMU.670	*citB*	24377048	aconitate hydratase, aconitase A	98278	5.32	21	32	193	9.8E-17
32	SMU.546	*typA*	24376921	GTP-binding protein (tyrosine phosphorylated protein A), possible elongation factor	68441	4.98	11	28	86	5.3E-06
33	SMU.546	*typA*	24376921	GTP-binding protein (tyrosine phosphorylated protein A), possible elongation factor	68441	4.98	13	33	141	1.6E-11
44	SMU.562	*clpE*	24376938	ATP-dependent protease ClpE	83910	5.27	14	29	116	4.9E-09
48	SMU.751		24377125	putative transcriptional accessory protein	79070	5.79	26	47	307	3.9E-28
53	SMU.1586	*thrS*	24377953	threonyl-tRNA synthetase	74825	5.26	16	37	140	2.0E-11
57	SMU.82	*dnaK*	24376461	chaperone protein (heat shock protein) DnaK (HSP-70)	65246	4.58	13	35	159	2.5E-13
63	SMU.2101	*asps*	24378460	aspartyl-tRNA synthetase	67096	5.29	17	41	181	1.6E-15
70	SMU.1077	*pgm*	24377454	phosphoglucomutase	63113	4.88	23	61	264	7.8E-24
71	SMU.1077	*pgm*	24377454	phosphoglucomutase	63113	4.88	26	66	327	3.9E-30
72	SMU.1444c	*yqgA*	24377815	metallo-beta-lactamase superfamily proteinhetical protein	61790	5.62	13	29	142	1.2E-11
74	SMU.883	*dexB*	24377261	glucan 1,6-alpha-glucosidase (dextran glucosidase DexB)	62105	5.04	10	31	105	6.2E-08
92	SMU.2098	*argS*	24378457	arginyl-tRNA synthase	63534	5.75	14	30	149	2.5E-12

94	SMU.475		24376850	conserved hypothetical protein	60306	5.58	13	29	125	6.2E-10
108	SMU.2157	*guaB*	24378516	inosine monophosphate dehydrogenase	53118	5.66	12	40	121	1.6E-09
115	SMU.2157	*guaB*	24378516	inosine monophosphate dehydrogenase	53118	5.66	21	67	235	6.2E-21
116	SMU.1691	*dltA*	24378060	D-alanine-D-alanyl carrier protein ligase	57580	5.26	13	39	101	1.6E-07
118	SMU.1190	*pykF*	24377568	pyruvate kinase	54390	5.09	16	45	163	9.8E-14
125	SMU.881	*gtfA*	24377259	sucrose phosphorylase GtfA	55766	4.82	20	69	258	3.1E-23
146	SMU.838	*gshR*	24377213	glutathione reductase	49119	5.46	6	34	58	2.9E-03
147	SMU.2102	*hisS*	24378462	histidyl-tRNA synthetase (histidine--tRNA ligase)	48980	5.7	8	25	80	2.2E-05
149	SMU.466	*pepC*	24376841	cysteine aminopeptidase C	50597	5.38	9	34	86	4.5E-06
150	SMU.838	*gshR*	24377213	glutathione reductase	49119	5.46	8	34	83	1.1E-05
166	SMU.364	*glnA*	24376739	glutamine synthetase type 1 (glutamate--ammonia ligase)	50094	5.12	14	48	137	3.9E-11
168	SMU.2085	*recA*	24378444	recombination protein RecA	41395	5.24	13	41	141	1.6E-11
179	SMU.139	*oxdC*	24376517	oxalate decarboxylase	44133	4.89	7	32	80	1.7E-05
182	SMU.1085	*prfA*	24377463	peptide chain release factor 1	40626	4.92	11	39	100	2.0E-07
183	SMU.1233	*deoB*	24377611	phosphopentomutase	44042	5.35	10	42	108	3.1E-08
187	SMU.886	*galK*	24377264	galactokinase GalK	43322	5.55	12	45	129	2.5E-10
194	SMU.361	*pgk*	24376736	phosphoglycerate kinase	42019	5.23	13	41	154	7.8E-13
198	SMU.1739	*fabF*	24378108	3-oxoacyl-(acyl-carrier-protein) synthase	43806	5.66	19	77	258	3.1E-23
208	SMU.2001	*rpoA*	24378361	DNA-directed RNA polymerase, alpha subunit	34606	4.76	12	45	150	2.0E-12
214	SMU.1653	*serA*	24378021	D-3-phosphoglycerate dehydrogenase	42828	5.56	17	60	219	2.5E-19
215	SMU.1203	*ilvE*	24377580	branched-chain amino acid aminotransferase	37822	5.03	14	57	149	2.5E-12
216	SMU.1309c	*gldA-2*	24377685	glycerol dehydrogenase	40330	5.16	8	34	72	1.3E-04
217	SMU.1512	*pheS*	24377880	phenylalanyl-tRNA synthetase alpha subunit	39499	5.87	8	28	94	8.6E-07
231	SMU.360	*gapC*	24376735	extracellular glyceraldehyde-3-	36160	5.71	11	45	110	2.0E-08

				phosphate dehydrogenase						
235	SMU.127	*adhA*	24376504	acetoin dehydrogenase (TPP-dependent), E1 component alpha subunit	36427	5.13	4	24	56	4.7E-03
237	SMU.233	*ilvC*	24376610	ketol-acid reductoisomerase	37319	5.01	12	43	131	1.6E-10
238	SMU.233	*ilvC*	24376610	ketol-acid reductoisomerase	37319	5.01	12	43	129	2.5E-10
252	SMU.1115	*ldh*	24377491	lactate dehydrogenase	35280	5.01	6	25	52	1.4E-02
268	SMU.496	*cysK*	24376870	cysteine synthetase A (O-acetylserine lyase)	32417	5.82	6	40	57	4.3E-03
272	SMU.1043c	*eutD*	24377419	phosphotransacetylase (phosphate acetyltransferase)	36416	4.92	9	48	135	6.2E-11
277	SMU.445	*glyQ*	24376819	glycyl-tRNA synthetase alpha subunit	35230	4.93	6	21	73	9.6E-05
305	SMU.99	*fbaA*	24376476	fructose-1,6-biphosphate aldolase	31577	4.96	7	28	100	2.0E-07
317	SMU.247	*yurY*	24376625	ABC transporter, ATP-binding protein	28262	4.61	5	30	47	3.7E-02
318	SMU.247	*yurY*	24376625	ABC transporter, ATP-binding protein	28262	4.61	8	37	81	1.4E-05
321	SMU.1322	*budC*	24377697	acetoin reductase (acetoin dehydrogenase)	26887	5.95	16	83	211	1.6E-18
326	SMU.1746c	*fabM*	24378116	enoyl-CoA hydratase/trans-2, cis-3-decenoyl-ACP isomerase	29080	5.81	9	37	85	5.8E-06
330	SMU.1517	*vicR*	24377886	two-component response regulator VicR	26898	5.08	7	36	105	6.2E-08
352	SMU.636	*nagB*	24377011	glucosamine-6-phosphate isomerase (N-acetylglucosamine-6-phosphate isomerase)	25457	5.33	12	74	153	9.8E-13
375	SMU.629	*sodA*	24377003	manganese-type superoxide dismutase, Fe/Mn-SOD	22611	4.99	6	38	73	9.6E-05
376	SMU.629	*sodA*	24377003	manganese-type superoxide dismutase, Fe/Mn-SOD	22611	4.99	4	31	51	1.4E-02
388	SMU.554		24376930	conserved hypothetical protein	21741	5.61	6	43	94	7.3E-07
389	SMU.1672	*clpP*	24378042	ATP-dependent Clp protease, proteolytic subunit	21656	5.47	5	58	68	2.8E-04
400	SMU.961		24377335	conserved hypothetical protein	20069	5.07	6	41	71	1.7E-04
408	SMU.1859	*ssb*	24378226	single-stranded DNA-binding protein	18321	4.98	8	48	111	1.6E-08

440	SMU.360	*gapC*	24376735	extracellular glyceraldehyde-3-phosphate dehydrogenase	36160	5.71	16	62	162	1.2E-13
444	SMU.1990	*rpoB*	24378350	DNA-dependent RNA polymerase, beta subunit	132805	5.04	15	20	103	9.8E-08
453	SMU.1510	*pheT*	24377878	phenylalanyl-tRNA synthetase beta subunit	87517	4.93	12	26	88	3.3E-06
455	SMU.1838	*secA*	24378205	preprotein translocase subunit SecA	95668	5.12	26	52	213	9.8E-19
458	SMU.402	*pfl*	24376777	pyruvate formate-lyase	87950	5.24	14	28	121	1.6E-09
459	SMU.402	*pfl*	24376777	pyruvate formate-lyase	87950	5.24	11	23	109	2.5E-08
461	SMU.402	*pfl*	24376777	pyruvate formate-lyase	87950	5.24	4	8	58	3.0E-03
466	SMU.956	*clp*	24377329	ATP-dependent Clp protease, ATP-binding subunit	77139	4.99	30	63	350	2.0E-32
467	SMU.956	*clp*	24377329	ATP-dependent Clp protease, ATP-binding subunit	77139	4.99	12	31	182	1.2E-15
469	SMU.2036	*pepO*	24378398	endopeptidase O (peptidase)	71780	4.73	12	32	108	3.1E-08
481	SMU.137	*mleS*	24376515	malolactic enzyme	59809	4.74	13	34	117	3.9E-09
492	SMU.2038	*pttB*	24378400	phosphotransferase system, trehalose-specific IIBC component (EIIBC-tre)	70912	5.83	4	17	46	4.5E-02
497	SMU.2128	*ilvd*	24378488	dihydroxy-acid dehydratase	61084	5.19	14	35	130	2.0E-10
501	SMU.773c	*lysS*	24377146	lysyl-tRNA synthetase	56344	5.18	20	46	171	1.6E-14
519	SMU.765	*nox-1*	24377137	alkyl hydroperoxidase reductase, subunit F (NADH oxidase)	55397	4.8	17	55	218	3.1E-19
533	SMU.1536	*glgA*	24377905	starch (bacterial glycogen) synthase	54391	4.99	16	49	163	9.8E-14
558	SMU.466	*pepC*	24376841	cysteine aminopeptidase C	50597	5.38	9	30	79	2.4E-05
577	SMU.1426c	*glmM*	24377799	phosphoglucosamine mutase (phosphoacetylglucosamine mutase)	48679	4.79	14	53	178	3.1E-15
581	SMU.1200	*rpsA*	24377577	ribosomal protein S1	43660	5	8	29	86	4.6E-06
622	SMU.1191	*pfkA*	24377570	6-phosphofructokinase	35805	5.4	10	36	111	1.6E-08
624	SMU.1760		24378127	conserved hypothetical	33119	5.12	14	50	133	9.8E-

	c			protein						11
626	SMU.888	*galE*	24377266	UDP-galactose 4-epimerase GalE	39170	5.44	15	65	211	1.6E-18
628	SMU.2032	*rpsB*	24378394	30S ribosomal protein S2	29075	5	14	56	168	3.1E-14
638	SMU.1742c	*fabK*	24378111	trans-2-enoyl-ACP reductase II	33571	5.74	9	45	96	4.9E-07
641	SMU.1348c	*psaA*	24377724	ABC transporter, ATP-binding protein	25924	5.78	8	52	97	4.3E-07
665	SMU.676	*gapN*	24377055	NADP-dependent non-phosphorylating glyceraldehyde-3-phosphate dehydrogenase	51276	5.12	18	69	208	3.1E-18
676	SMU.402	*pfl*	24376777	pyruvate formate-lyase	87950	5.24	26	52	257	3.9E-23
677	SMU.1564	*glg*	24377931	glycogen phosphorylase	86933	5.22	15	32	121	1.6E-09
682	SMU.1954	*groEL*	24378314	chaperonin GroEL	57066	4.68	22	52	246	4.9E-22
703	SMU.882	*msmK*	24377260	multiple sugar-binding ABC transporter, ATP-binding protein	41995	5.92	20	57	185	6.2E-16
719	SMU.1847	*elp*	24378214	translation elongation factor P	20768	4.89	6	56	73	9.0E-05
726	SMU.557	*divIVA*	24376933	cell division initiation protein DivIVA	30803	4.48	8	51	105	6.2E-08
728	SMU.557	*divIVA*	24376933	cell division initiation protein DivIVA	30803	4.48	11	56	133	9.8E-11
744	SMU.1247	*eno*	24377625	enolase	46886	4.67	13	45	125	6.2E-10
748	SMU.1760c		24378127	conserved hypothetical protein	33119	5.12	15	50	162	1.2E-13
750	SMU.360	*gapC*	24376735	extracellular glyceraldehyde-3-phosphate dehydrogenase	36160	5.71	16	60	185	6.2E-16

[*] The Mr and pI are calculated values.

[§] 104 protein spots with fold of change >2, P<0.05 in at least one group of comparison were excised, and digested by typsin for MALDI-TOF analysis. Protein score is -10*Log(p), where p is the probability that the observed match is a random event. Protein scores >45 are considered as positive results and shown in the table (p<0.05).

Table T3.2 Differentially expressed proteins at the stationary growth phase in comparison to the log phase in the *S. mutans* wild type and the Δ*rpoE* mutant, and the corresponding changes in gene expression.

Spot No.	Gene code	Gene name	Protein name	W1/ W0*	P (anova)	W1/ W0 t§	M1/ M0	P (anova)	M1/ M0 t
carbohydrate metabolism									
74	SMU.883	*dexB*	glucan 1,6-alpha-glucosidase (dextran glucosidase DexB)	**8.1**	0.0001	13.2	**2.1**	0.0076	1.8
17	SMU.148	*adhE*	alcohol-acetaldehyde dehydrogenase	**5.3**	0.0021	11.5	2.0	0.0680	2.3
16	SMU.148	*adhE*	alcohol-acetaldehyde dehydrogenase	**3.5**	0.0059	11.5	1.6	0.0600	2.3
187	SMU.886	*galK*	galactokinase GalK	**4.7**	0.0018	19.5	**3.0**	0.0001	1.7
703	SMU.882	*msmK*	multiple sugar-binding ABC transporter, ATP-binding protein MsmK	**3.7**	0.0125	12.1	**1.7**	0.0480	1.8
71	SMU.1077	*pgm*	phosphoglucomutase	**2.9**	0.0002	3.0	**1.5**	0.0130	1.2
70	SMU.1077	*pgm*	phosphoglucomutase	**1.4**	0.0130	3.0	**1.3**	0.0050	1.2
15	SMU.670	*citB*	aconitate hydratase, aconitase A	**2.8**	0.0015	2.7	1.6	0.1860	-1.1
20	SMU.670	*citB*	aconitate hydratase, aconitase A	**1.8**	0.0460	2.7	1.2	0.4420	-1.1
533	SMU.1536	*glgA*	starch (bacterial glycogen) synthase	**2.4**	0.0062	5.3	1.6	0.1050	1.5
125	SMU.881	*gtfA*	sucrose phosphorylase GtfA	**2.1**	0.0121	12.5	1.3	0.1950	1.8
626	SMU.888	*galE*	UDP-galactose 4-epimerase GalE	**1.8**	0.0000	3.0	1.2	0.3340	1.7
458	SMU.402	*pfl*	pyruvate formate-lyase	**4.4**	0.0004	1.5	**1.9**	0.0100	-1.0
459	SMU.402	*pfl*	pyruvate formate-lyase	**3.2**	0.0014	1.5	1.3	0.1790	-1.0
676	SMU.402	*pfl*	pyruvate formate-lyase	**2.8**	0.0008	1.5	**1.4**	0.0130	-1.0
461	SMU.402	*pfl*	pyruvate formate-lyase	**2.8**	0.0025	1.5	1.4	0.1180	-1.0
272	SMU.1043c	*eutD*	phosphotransacetylase (phosphate acetyltransferase)	**1.4**	0.0230	1.9	**-1.9**	0.0180	1.0
235	SMU.127	*adhA*	acetoin dehydrogenase (TPP-dependent), E1 component alpha subunit	**-2.0**	0.0420	-1.7	2.1	0.0550	-1.0
305	SMU.99	*fbaA*	fructose-1,6-biphosphate aldolase	-1.1	0.4700	ns	**-1.6**	0.0350	ns
231	SMU.360	*gapC*	extracellular glyceraldehyde-3-phosphate dehydrogenase, plasmin receptor	-1.0	0.9350	ns	**-1.5**	0.0130	ns
general stress									
466	SMU.956	*clp*	ATP-dependent Clp protease, ATP-binding subunit	**-2.2**	0.0214	-1.2	-1.7	0.0860	1.0
467	SMU.956	*clp*	ATP-dependent Clp protease, ATP-binding subunit	**-2.0**	0.0209	-1.2	-1.4	0.2360	1.0
57	SMU.82	*dnaK*	chaperone protein (heat shock protein) DnaK (HSP-70)	**-1.7**	0.0120	-1.2	-1.1	0.9190	-1.2
469	SMU.2036	*pepO*	endopeptidase O (peptidase)	**1.5**	0.0370	1.1	**2.0**	0.0255	-1.0
translation									
63	SMU.2101	*asps*	aspartyl-tRNA synthetase	**1.5**	0.0290	1.1	-1.2	0.2280	-1.0

277	SMU.445	*glyQ*	glycyl-tRNA synthetase alpha subunit	**1.8**	0.0040	1.5	-1.2	0.2800	1.2
501	SMU.773c	*lysS*	lysyl-tRNA synthetase	1.2	0.1850	-1.4	**-1.3**	0.0090	1.0
558	SMU.466	*pepC*	cysteine aminopeptidase C	-1.0	0.7860	-1.1	**-1.3**	0.0300	1.1
transcription									
444	SMU.1990	*rpoB*	DNA-dependent RNA polymerase, beta subunit	**2.1**	0.0357	ns	1.7	0.1600	-1.4
cell division									
726	SMU.557	*divIVA*	cell division initiation protein DivIVA	**-1.5**	0.0070	1.1	-1.2	0.1580	1.0
728	SMU.557	*divIVA*	cell division initiation protein DivIVA	**1.7**	0.0070	1.1	1.0	0.7810	1.0
acid stress defense									
497	SMU.2128	*ilvd*	dihydroxy-acid dehydratase	**1.6**	0.0070	1.6	-1.1	0.5360	1.0
166	SMU.364	*glnA*	glutamine synthetase type 1 (glutamate--ammonia ligase)	1.6	0.0590	1.5	**-1.6**	0.0500	ns
237	SMU.233	*ilvC*	ketol-acid reductoisomerase	1.0	0.7920	-1.0	**-1.4**	0.0060	-1.0
oxidative stress defense									
519	SMU.765	*nox-1*	alkyl hydroperoxidase reductase, subunit F (NADH oxidase)	-1.3	0.2110	-1.2	**-1.6**	0.0070	ns
others									
641	SMU.1348c	*psaA*	ABC transporter, ATP-binding protein	**1.4**	0.0340	ns	1.1	0.3000	1.1
638	SMU.1742c	*fabK*	trans-2-enoyl-ACP reductase II	-1.1	0.6780	-1.0	**-1.3**	0.0430	1.0
748	SMU.1760c		conserved hypothetical protein	**-1.6**	0.0070	-1.6	**1.7**	0.0002	-1.2
400	SMU.961		conserved hypothetical protein	**1.6**	0.0120	2.2	**3.5**	0.0260	-1.3

[*]Fold of changes of proteins under starvation stress (stationary phase of growth) compared to the log phase in wild type (W1/W0) and in the Δ*rpoE* mutant (M1/M0). Values in bold are significant (fold of changes >=1.3, P values < 0.05).

[§] t: transcriptome data. Changes in gene expression were determined under the same conditions as those for the proteome. Data show fold of change of gene expression in the stationary phase compared to gene expression in the log phase of growth. All transcriptome data which were significant (with p<0.005) are shown. Those with p>=0.005 are indicated as ‘‘ns’’ (not significant).

Table T3.3 Differentially expressed proteins under acid stress in comparison to the log phase in the *S. mutans* wild type and the Δ*rpoE* mutant, and the corresponding changes in gene expression.

Spot No.	Gene code	Gene name	Protein name	W2/ W0*	P (anova)	W2/ W0 t§	M2/ M0	P (anova)	M2/ M0 t
acid stress defense									
237	SMU.233	*ilvC*	ketol-acid reductoisomerase	**2.1**	0.0280	1.3	1.1	0.1480	1.2
238	SMU.233	*ilvC*	ketol-acid reductoisomerase	**2.1**	0.0270	1.3	**2.0**	0.0082	1.2
215	SMU.1203	*ilvE*	branched-chain amino acid aminotransferase IlvE	**2.1**	0.0060	3.9	**1.4**	0.0170	2.0
497	SMU.2128	*ilvD*	dihydroxy-acid dehydratase	**1.5**	0.0050	1.8	-1.1	0.3740	1.2
481	SMU.137	*mleS*	malolactic enzyme	1.2	0.2350	1.5	**1.9**	0.0050	-1.0
general stress									
44	SMU.562	*clpE*	ATP-dependent protease ClpE	**-1.4**	0.0490	-1.0	1.3	0.0510	1.2
469	SMU.2036	*pepO*	endopeptidase O (peptidase)	1.4	0.1190	-1.2	**2.2**	0.0027	-1.1
149	SMU.466	*pepC*	cysteine aminopeptidase C	1.1	0.5240	1.3	**2.0**	0.0020	-1.0
682	SMU.1954	*groEL*	chaperonin GroEL	-1.1	0.5070	ns	**1.4**	0.0260	ns
466	SMU.956	*clp*	ATP-dependent Clp protease, ATP-binding subunit	-1.0	0.9730	1.8	**1.6**	0.0160	1.7
467	SMU.956	*clp*	ATP-dependent Clp protease, ATP-binding subunit	-1.2	0.1620	1.8	**1.5**	0.0310	1.7
translation									
92	SMU.2098	*argS*	arginyl-tRNA synthase	-1.4	0.0710	-1.4	**-2.4**	0.0117	-1.1
147	SMU.2102	*hisS*	histidyl-tRNA synthetase (histidine--tRNA ligase)	**-1.3**	0.0330	-1.4	**-2.5**	0.0016	1.0
501	SMU.773c	*lysS*	lysyl-tRNA synthetase	-1.2	0.2590	-1.5	**-2.6**	0.0000	-1.3
53	SMU.1586	*thrS*	threonyl-tRNA synthetase	**1.5**	0.0010	-1.1	**1.9**	0.0001	-1.1
182	SMU.1085	*prfA*	peptide chain release factor 1	-1.3	0.1300	-1.3	**-1.6**	0.0007	-1.5
719	SMU.1847	*elp*	translation elongation factor P	1.0	0.9690	-1.3	**-2.2**	0.0190	-1.0
277	SMU.445	*glyQ*	glycyl-tRNA synthetase alpha subunit	**1.9**	0.0030	-1.4	**-1.4**	0.0140	-1.3
581	SMU.1200	*rpsA*	ribosomal protein S1	-1.3	0.3350	-1.1	**-1.3**	0.0300	ns
628	SMU.2032	*rpsB*	30S ribosomal protein S2	-1.7	0.2950	-1.2	**-1.7**	0.0010	-1.1
63	SMU.2101	*asps*	aspartyl-tRNA synthetase	1.1	0.4790	1.4	**-1.6**	0.0010	1.2
transcription									
48	SMU.751		putative transcriptional accessory protein	**-2.3**	0.0040	-1.9	**-2.3**	0.0090	-1.6
6	SMU.1990	*rpoB*	DNA-dependent RNA polymerase, beta subunit	-1.6	0.2370	ns	**-3.3**	0.0245	1.2
444	SMU.1990	*rpoB*	DNA-dependent RNA polymerase, beta subunit	1.3	0.2080	ns	**6.2**	0.0122	1.2
108	SMU.2157	*guaB*	inosine monophosphate dehydrogenase	**1.6**	0.0110	2.6	1.2	0.4350	1.7
115	SMU.2157	*guaB*	inosine monophosphate dehydrogenase	**1.6**	0.0220	2.6	-1.2	0.2850	1.7

oxidative stress defense									
519	SMU.765	*nox-1*	alkyl hydroperoxidase reductase, subunit F (NADH oxidase)	**2.1**	0.0121	-1.1	**1.8**	0.0170	ns
376	SMU.629	*sodA*	manganese-type superoxide dismutase, Fe/Mn-SOD	1.8	0.1040	-1.2	**2.0**	0.0017	ns
375	SMU.629	*sodA*	manganese-type superoxide dismutase, Fe/Mn-SOD	**2.3**	0.0150	-1.2	**1.8**	0.0390	ns
318	SMU.247	*yurY*	ABC transporter, ATP-binding protein	1.5	0.0560	-1.4	**2.1**	0.0003	ns
carbohydrate metabolism									
321	SMU.1322	*budC*	acetoin reductase (acetoin dehydrogenase)	**2.3**	0.0012	2.9	-1.1	0.7360	2.7
352	SMU.636	*nagB*	glucosamine-6-phosphate isomerase (N-acetylglucosamine-6-phosphate isomerase)	**2.0**	0.0124	1.2	**2.4**	0.0010	1.3
577	SMU.1426c	*glmM*	phosphoglucosamine mutase (phosphoacetylglucosamine mutase)	-1.2	0.0840	1.0	**-2.4**	0.0013	-1.3
272	SMU.1043c	*pta*	phosphotransacetylase (phosphate acetyltransferase)	-1.3	0.1160	1.7	**-2.2**	0.0018	-1.4
15	SMU.670	*citB*	aconitate hydratase, aconitase A	**-1.7**	0.0370	2.7	-1.1	0.7290	-1.9
20	SMU.670	*citB*	aconitate hydratase, aconitase A	**-2.0**	0.0320	2.7	-1.4	0.1240	-1.9
70	SMU.1077	*pgm*	phosphoglucomutase	**1.6**	0.0020	1.9	**-1.3**	0.0120	-1.8
71	SMU.1077	*pgm*	phosphoglucomutase	**-1.4**	0.0200	1.9	**1.3**	0.0270	-1.8
187	SMU.886	*galK*	galactokinase GalK	**1.5**	0.0240	18.6	1.1	0.4380	-1.5
235	SMU.127	*adhA*	acetoin dehydrogenase (TPP-dependent), E1 component alpha subunit	**1.4**	0.0410	-2.5	**4.3**	0.0002	1.7
305	SMU.99	*fbaA*	fructose-1,6-biphosphate aldolase	**1.6**	0.0100	ns	1.1	0.1240	ns
744	SMU.1247	*eno*	enolase	-1.3	0.4760	ns	**1.5**	0.0110	ns
194	SMU.361	*pgk*	phosphoglycerate kinase	1.1	0.6550	ns	**1.8**	0.0030	ns
231	SMU.360	*gapC*	extracellular glyceraldehyde-3-phosphate dehydrogenase, plasmin receptor	-1.1	0.7000	ns	**-1.6**	0.0020	ns
676	SMU.402	*pfl*	pyruvate formate-lyase	1.1	0.5470	1.4	**-1.4**	0.0120	1.3
492	SMU.2038	*pttB*	phosphotransferase system, trehalose-specific IIBC component (EIIBC-tre) (PTS system, trehalose-specific IIABC component)	1.1	0.3070	-1.9	**-1.5**	0.0130	-2.5
533	SMU.1536	*glgA*	starch (bacterial glycogen) synthase	-1.0	0.8280	3.4	**1.7**	0.0390	-1.7
lipid metabolism									
216	SMU.1309c	*gldA-2*	glycerol dehydrogenase	**2.1**	0.0002	1.6	**2.3**	0.0010	1.1

638	SMU.1742c	*fabK*	trans-2-enoyl-ACP reductase II	-1.0	0.6980	1.0	**-2.8**	0.0005	-1.0
198	SMU.1739	*fabF*	3-oxoacyl-(acyl-carrier-protein) synthase	1.1	0.3180	-1.1	**-1.4**	0.0140	-1.1
others									
32	SMU.546	*typA*	putative GTP-binding protein, possible elongation factor	-1.6	0.0520	-1.6	**1.8**	0.0040	-1.2
214	SMU.1653	*serA*	D-3-phosphoglycerate dehydrogenase	**1.5**	0.0230	2.3	-1.3	0.1510	1.2
641	SMU.1348c	*psaA*	ABC transporter, ATP-binding protein	**1.4**	0.0210	ns	**-1.7**	0.0030	1.1
726	SMU.557	*divIVA*	cell division initiation protein DivIVA	**-1.3**	0.0250	-1.1	-1.1	0.4460	-1.0
168	SMU.2085	*recA*	recombination protein RecA	-1.2	0.3240	ns	**-1.5**	0.0260	-1.0
72	SMU.1444c	*yqgA*	metallo-beta-lactamase superfamily proteinhetical protein	-1.2	0.2190	-1.4	**-1.5**	0.0180	-1.2
116	SMU.1691	*dltA*	D-alanine-D-alanyl carrier protein ligase	-1.1	0.2420	-1.1	**1.7**	0.0010	1.1
748	SMU.1760c		conserved hypothetical protein	1.1	0.0740	-1.3	**2.0**	0.0006	-1.0
94	SMU.475		conserved hypothetical protein	1.3	0.2460	-1.8	**2**	0.0190	-1.4
388	SMU.554		conserved hypothetical protein	1.0	0.7330	1.0	**-1.8**	0.0160	1.0

[*] Fold of changes of proteins under acid stress in the log phase of growth compared to the log phase of growth without acid stress in the wild type (W2/W0) and in the Δ*rpoE* mutant (M2/M0). Values in bold are significant ($p < 0.05$).

[§] t: transcriptome data. Changes in gene expression were determined under the same conditions as those for the proteome. Data show fold of change of gene expression under acid stress (log phase of growth) compared to gene expression in the log phase of growth without acid stress. All transcriptome data which were significant (with $p<0.005$) are shown. Those with $p>=0.005$ are indicated as ‘‘ns’’ (not significant).

Table T3.4 Differentially expressed proteins under acid and oxidative combined stress in comparison to the log phase in the *S. mutans* wild type and the Δ*rpoE* mutant, and the corresponding changes in gene expression.

Spot No.	Gene code	Gene name	Protein name	W4/ W0*	P (anova)	W4/ W0 t§	M4/ M0	P (anova)	M4/ M0 t
oxidative stress defense									
375	SMU.629	*sodA*	manganese-type superoxide dismutase, Fe/Mn-SOD	**9.6**	0.0001	1.1	**5.6**	0.0100	ns
376	SMU.629	*sodA*	manganese-type superoxide dismutase, Fe/Mn-SOD	**1.5**	0.0130	1.1	1.7	0.0570	ns
146	SMU.838	*gshR*	glutathione reductase	**2.5**	0.0310	1.5	1.8	0.0520	1.5
317	SMU.247	*yurY*	ABC transporter, ATP-binding protein	2.0	0.1080	1.3	**2.7**	0.0270	ns
general stress									
466	SMU.956	*clp*	ATP-dependent Clp protease, ATP-binding subunit	**2.4**	0.0102	7.6	**2.1**	0.0460	5.5
467	SMU.956	*clp*	ATP-dependent Clp protease, ATP-binding subunit	**1.5**	0.0280	7.6	1.5	0.1620	5.5
44	SMU.562	*clpE*	ATP-dependent protease ClpE	**1.6**	0.0001	1.3	**1.5**	0.0170	2.0
389	SMU.1672	*clpP*	ATP-dependent Clp protease, proteolytic subunit	-1.4	0.1930	ns	**1.9**	0.0310	ns
682	SMU.1954	*groEL*	chaperonin GroEL	1.1	0.5540	ns	**1.6**	0.0440	ns
149	SMU.466	*pepC*	cysteine aminopeptidase C	**3.1**	0.0090	-1.0	**3.9**	0.0040	1.1
558	SMU.466	*pepC*	cysteine aminopeptidase C	**-3.6**	0.0010	-1.0	**-2.6**	0.0002	1.1
carbohydrate metabolism									
622	SMU.1191	*pfkA*	6-phosphofructokinase	**1.8**	0.0002	ns	**1.5**	0.0040	ns
305	SMU.99	*fbaA*	fructose-1,6-biphosphate aldolase	**2.9**	0.0098	ns	**1.6**	0.0250	ns
231	SMU.360	*gapC*	extracellular glyceraldehyde-3-phosphate dehydrogenase, plasmin receptor	**4.8**	0.0003	ns	**1.5**	0.0440	ns
750	SMU.360	*gapC*	extracellular glyceraldehyde-3-phosphate dehydrogenase, plasmin receptor	**7.6**	0.0000	ns	**2.9**	0.0004	ns
440	SMU.360	*gapC*	extracellular glyceraldehyde-3-phosphate dehydrogenase, plasmin receptor	**-1.6**	0.0460	ns	**-2.9**	0.0030	ns
665	SMU.676	*gapN*	NADP-dependent non-phosphorylating glyceraldehyde-3-phosphate dehydrogenase	**1.9**	0.0180	ns	1.7	0.0510	ns
744	SMU.1247	*eno*	enolase	2.1	0.0600	ns	**2.9**	0.0003	ns
118	SMU.1190	*pykF*	pyruvate kinase	**1.9**	0.0220	ns	1.5	0.1070	ns
70	SMU.1077	*pgm*	phosphoglucomutase	**-1.5**	0.0005	1.7	**-1.9**	0.0002	-1.1
458	SMU.402	*pfl*	pyruvate formate-lyase	**3.1**	0.0010	1.5	1.3	0.1640	1.4
459	SMU.402	*pfl*	pyruvate formate-lyase	**2.1**	0.0092	1.5	1.3	0.2040	1.4
461	SMU.402	*pfl*	pyruvate formate-lyase	**2.1**	0.0078	1.5	1.1	0.7840	1.4
676	SMU.402	*pfl*	pyruvate formate-lyase	1.0	0.9500	1.5	**-1.5**	0.0050	1.4

252	SMU.1115	*ldh*	lactate dehydrogenase	**2.6**	0.0290	ns	1.5	0.0960	ns
235	SMU.127	*adhA*	acetoin dehydrogenase (TPP-dependent), E1 component alpha subunit	1.7	0.0710	1.1	**2.6**	0.0163	2.5
577	SMU.1426c	*glmM*	phosphoglucosamine mutase (phosphoacetylglucosamine mutase)	**-2.3**	0.0090	-1.0	-1.9	0.1140	1.2
492	SMU.2038	*pttB*	phosphotransferase system, trehalose-specific IIBC component (EIIBC-tre) (PTS system, trehalose-specific IIABC component)	-1.0	0.9640	-4.5	**-2.3**	0.0075	-2.0
71	SMU.1077	*pgm*	phosphoglucomutase	**1.6**	0.0060	1.7	**1.4**	0.0370	-1.1
183	SMU.1233	*deoB*	phosphopentomutase	**-1.4**	0.0040	1.5	**-1.4**	0.0420	1.3
17	SMU.148	*adhE*	alcohol-acetaldehyde dehydrogenase	**1.6**	0.0490	7.0	-1.3	0.4930	2.8
125	SMU.881	*gtfA*	sucrose phosphorylase GtfA	1.1	0.6390	7.8	**2.4**	0.0120	1.1
187	SMU.886	*galK*	galactokinase GalK	-1.1	0.3110	8.5	**-1.3**	0.0480	-1.6
194	SMU.361	*pgk*	phosphoglycerate kinase	-1.3	0.5220	ns	**2**	0.0040	ns
fatty acid biosynthesis									
198	SMU.1739	*fabF*	3-oxoacyl-(acyl-carrier-protein) synthase	1.3	0.0900	-1.4	**-2.0**	0.0002	-1.4
638	SMU.1742c	*fabK*	trans-2-enoyl-ACP reductase II	1.0	0.8930	-1.3	**-3.7**	0.0010	-1.4
translation									
719	SMU.1847	*elp*	translation elongation factor P	**-2.1**	0.0099	-1.5	**-2.2**	0.0190	-1.9
63	SMU.2101	*asps*	aspartyl-tRNA synthetase	-1.1	0.5720	-1.2	**-2.8**	0.0060	-1.5
147	SMU.2102	*hisS*	histidyl-tRNA synthetase (histidine--tRNA ligase)	-1.6	0.0700	-1.1	**-2.3**	0.0267	1.0
501	SMU.773c	*lysS*	lysyl-tRNA synthetase	-1.2	0.1730	-2.1	**-4.1**	0.0002	-1.6
217	SMU.1512	*pheS*	phenylalanyl-tRNA synthetase alpha subunit	**-2.0**	0.0290	-1.9	-1.1	0.8580	-1.6
182	SMU.1085	*prfA*	peptide chain release factor 1	-1.5	0.0730	-1.3	**-1.5**	0.0260	-1.6
53	SMU.1586	*thrS*	threonyl-tRNA synthetase	**1.9**	0.0001	-1.1	**1.6**	0.0110	1.1
628	SMU.2032	*rpsB*	30S ribosomal protein S2	-1.4	0.4380	-1.7	**-1.6**	0.0140	-1.3
transcription									
6	SMU.1990	*rpoB*	DNA-dependent RNA polymerase, beta subunit	-1.3	0.5330	ns	**-4.2**	0.0230	-2.0
444	SMU.1990	*rpoB*	DNA-dependent RNA polymerase, beta subunit	1.7	0.2560	ns	**5.8**	0.0220	-2.0
115	SMU.2157	*guaB*	inosine monophosphate dehydrogenase	-1.2	0.1210	-1.2	**-2.4**	0.0107	-1.5
108	SMU.2157	*guaB*	inosine monophosphate dehydrogenase	**1.6**	0.0060	-1.2	-1.3	0.0850	-1.5
208	SMU.2001	*rpoA*	DNA-directed RNA polymerase, alpha subunit	1.2	0.5040	ns	**1.9**	0.0050	-1.5
48	SMU.751		putative transcriptional accessory protein	**-2.0**	0.0166	-2.3	**-2.5**	0.0280	-2.8
two-component response regulator									
330	SMU.1517	*vicR*	two-component response regulator	**-1.4**	0.0030	1.1	-1.5	0.0950	1.1

			CovR, VicR-like protein						
acid defense									
237	SMU.233	*ilvC*	ketol-acid reductoisomerase	**2.8**	0.0210	1.0	1.4	0.0690	1.1
497	SMU.2128	*ilvD*	dihydroxy-acid dehydratase	**2.1**	0.0001	1.1	-1.1	0.6790	-1.3
481	SMU.137	*mleS*	malolactic enzyme	1.1	0.6950	1.6	**3.0**	0.0250	-1.0
DNA replication									
168	SMU.2085	*recA*	recombination protein RecA	1.0	0.9290	ns	**-2.2**	0.0228	-1.1
others									
32	SMU.546	*typA*	putative GTP-binding protein, possible elongation factor	**1.6**	0.0350	-1.4	**2.6**	0.0175	-1.5
214	SMU.1653	*serA*	D-3-phosphoglycerate dehydrogenase	1.1	0.3860	-1.1	**-1.9**	0.0160	-1.2
72	SMU.1444c	*yqgA*	metallo-beta-lactamase superfamily proteinhetical protein	**-2.3**	0.0059	-1.4	1.0	0.7700	-1.3
641	SMU.1348c	*psaA*	ABC transporter, ATP-binding protein	1.0	0.6840	ns	**-2.1**	0.0053	-1.1
728	SMU.557	*divIVA*	cell division initiation protein DivIVA	1.2	0.1450	-1.4	**2.1**	0.0270	-1.3
116	SMU.1691	*dltA*	D-alanine-D-alanyl carrier protein ligase	1.1	0.2180	-1.9	**1.6**	0.0250	-1.9
400	SMU.961		conserved hypothetical protein	**-1.4**	0.0470	9.3	1.7	0.1630	2.3
624	SMU.1760c		conserved hypothetical protein	2.0	0.0860	1.6	**2.4**	0.0350	1.5
748	SMU.1760c		conserved hypothetical protein	1.1	0.0060	1.6	**1.7**	0.0070	1.5

[*] Protein fold of changes under acid and oxidative combined stress in the log phase of growth compared to the log phase of growth without stress in the wild type (W4/W0) and in the Δ*rpoE* mutant (M4/M0). Values in bold are significant ($p < 0.05$).

[§] t: transcriptome data. Changes in gene expression were determined under the same conditions as those for the proteome. Data show fold of change of gene expression under acid and oxidative combined stress (log phase of growth) compared to gene expression in the log phase of growth without stress. All transcriptome data which were significant (with $p<0.005$) are shown. Those with $p>=0.005$ are indicated as ‘‘ns’’ (not significant).

Chaper 4

Lack of RpoE increases virulence related traits of *Streptococcus mutans*

Xiaoli Xue[1], Helena Sztajer[1], Nora Buddruhs[2], Jörn Petersen[2], Manfred Rohde[3], Susanne R. Talay[3], Irene Wagner-Döbler[1]

[1]Research Group Microbial Communication, Division of Cell Biology, Helmholtz Centre for Infection Research, Inhoffenstr. 7, D-38124 Braunschweig, Germany

[2]Research Group Roseobacter Molecular Systematics, German Collection of Microorganisms and Cell Cultures GmbH, Inhoffenstr. 7B, 38124 Braunschweig, Germany

[3]Department of Medical Microbiology, Helmholtz Centre for Infection Research, Inhoffenstr. 7, D-38124 Braunschweig, Germany

4 Chaper 4 - Lack of RpoE increases virulence related traits of *Streptococcus mutans*

4.1 Abstract

The delta subunit of the RNA polymerase, RpoE, maintains the transcriptional specificity in Gram-positive bacteria. Lack of RpoE results in massive changes in the transcriptome of the human dental caries pathogen *Streptococcus mutans*. In this study, we analyzed traits of the Δ*rpoE* mutant which are important for biofilm formation and interaction with oral microorganisms and human cells and performed a global phenotypic analysis of its physiological functions. The Δ*rpoE* mutant showed higher self-aggregation compared to the wild type and coaggregated with other oral bacteria and *Candida albicans*. It formed a biofilm with a different matrix structure and an altered surface attachment. The amount of the cell surface antigens I/II SpaP and the glucosyltransferase GtfB was reduced. The Δ*rpoE* mutant displayed significantly stronger adhesion to human extracellular matrix components, especially to fibronectin, than the wild type. Its adhesion to human epithelial cells HEp-2 was reduced, probably due to the highly aggregated cell mass. The analysis of 1920 physiological traits using phenotype microarrays showed that the Δ*rpoE* mutant metabolized a wider spectrum of carbon sources than the wild type and had acquired resistance to antibiotics and inhibitory compounds with various modes of action. The reduced antigenicity, increased aggregation, adherence to fibronection, broader substrate spectrum and increased resistance to antibiotics of the Δ*rpoE* mutant reveal the physiological potential of *S. mutans* and show that some of its virulence related traits are increased.

4.2 Introduction

Streptococcus mutans is the main causative agent of human dental caries, which is one of the most prevailing infectious diseases in the world (Ajdic *et al.*, 2002). Since *S. mutans* causes damage to the tooth surface of the host, it is considered a cariogenic pathogen (Mitchell, 2003). The key factors contributing to the pathogenesis are its strong acidogenicity and aciduricity. *S.*

mutans produces acid through metabolism of a wide variety of carbohydrates, which can lower the pH down to pH 4 and causes demineralization of tooth enamel (Ajdic & Pham, 2007;Garcia-Godoy & Hicks, 2008). Moreover, *S. mutans* has a well equipped acid defense system (Lemos & Burne, 2008), thus it has growth advantages compared to other non-aciduric bacteria and becomes dominant in the acidic stage of the caries process (Takahashi & Nyvad, 2010). Furthermore, to avoid being cleared by saliva and to survive in the highly fluctuating conditions of the oral cavity, it needs to adhere to surfaces, and the best way is the formation of biofilms. *S. mutans* produces extracellular polysaccharides and surface adhesins that mediate its adherence and interaction with other microorganisms in the oral cavity (Kreth *et al.*, 2008;Zhu *et al.*, 2009). The polymicrobial community within the biofilms profits from metabolic and genetic communication and is protected against external stress factors (Hojo *et al.*, 2009). Sophisticated communication mechanisms have been discovered, e.g. *S. mutans* produces, secretes, and senses the peptide pheromone competence-stimulating peptide (CSP) which controls its genetic competence (Li *et al.*, 2001), biofilm formation (Senadheera & Cvitkovitch, 2008), and bacteriocin production (Perry *et al.*, 2009). *S. mutans* also interacts with the pathogenic fungus *Candida albicans*, whose hyphae formation is suppressed by CSP (Jarosz *et al.*, 2009), as well as by a secreted fatty acid signal, trans-decenoic acid (Vilchez *et al.*, 2010).

Another aspect of *S. mutans* pathogenesis is its ability to infect host cells. Compared to other streptococci, *S. mutans* is not highly invasive, but it is frequently detected in heart valve and atheromatous plaque specimens (Nakano *et al.*, 2006a), and has been isolated from infective endocarditis (Nomura *et al.*, 2006), suggesting that it is a possible causative agent. The pathogenesis of streptococci (Mitchell, 2003) includes: (1) adherence to the tissue surface, mainly through binding to the human extracellular matrix (ECM) components, e.g. fibronectin, via surface antigens and other surface structures. Several ECM binding proteins have been identified in *S. mutans* (Nobbs *et al.*, 2009). (2) Survival in the host. For example, a newly isolated *S. mutans* strain was shown to have lower cariogenicity but higher virulence in the blood due to loss of important antigens that allow to escape host phagocytosis (Nakano *et al.*, 2010). (3) Invasion into and survival within host cells. A serotype f *S. mutans* OMZ175 was capable to invade into and survive in the human coronary artery endothelial cells (HEAEC) (Abranches *et al.*, 2009). (4) Causing damage to the host by modulating host inflammatory response. *S. mutans*

can effectively stimulate inflammatory cytokine production of mononuclear cells (Jiang & Schilder, 2002) and endothelial cells (Shun *et al.*, 2005).

The delta subunit of the RNA polymerase, RpoE, is conserved in low G+C Gram positive bacteria (Firmicutes). Biochemical studies proved that RpoE reduces unspecific binding of DNA to RNA polymerase and accelerates the core enzyme recycling, thus it is required for transcriptional specificity (Achberger & Whiteley, 1981;Juang & Helmann, 1994). RpoE has been shown to be associated with virulence in *S. agalactiae* (Jones *et al.*, 2003;Seepersaud *et al.*, 2006). In our previous studies, we characterized the function of RpoE for the first time in *S. mutans*, and showed that loss of RpoE caused massive changes in the transcriptome (Xue *et al.*, 2010) and proteome (Xue et al. submitted). Here, we studied the functional changes in virulence related traits of the Δ*rpoE* mutant. We analysed the effect of RpoE on self- and co-aggregation, biofilm formation and structure, adherence to ECM, and attachment to and invasion of human epithelial cells. Furthermore, a global phenotypic characterization of the metabolic capabilities of the Δ*rpoE* mutant was performed.

4.3 Results

4.3.1 Increased self- and co-aggregation in the Δ*rpoE* mutant

The *S. mutans* cells from the stationary growth phase were used for the self-aggregation analysis. The Δ*rpoE* mutant showed higher self-aggregation than the wild type in PBS buffer (Fig. 4.1). The reduction in optical density (OD_{600}) in the Δ*rpoE* mutant reached 38% after 2 hours, while the wild type obtained only 11% reduction. Proteinase K treatment had no obvious effect on the wild type under these conditions. By contrast, proteinase K treatment strongly reduced the self-aggregation of the Δ*rpoE* mutant, suggesting that surface proteins contribute to its self-aggregation. However, the self-aggregation of the Proteinase K treated Δ*rpoE* mutant was still higher than that of the wild type, thus a different surface structure would be expected in the mutant.

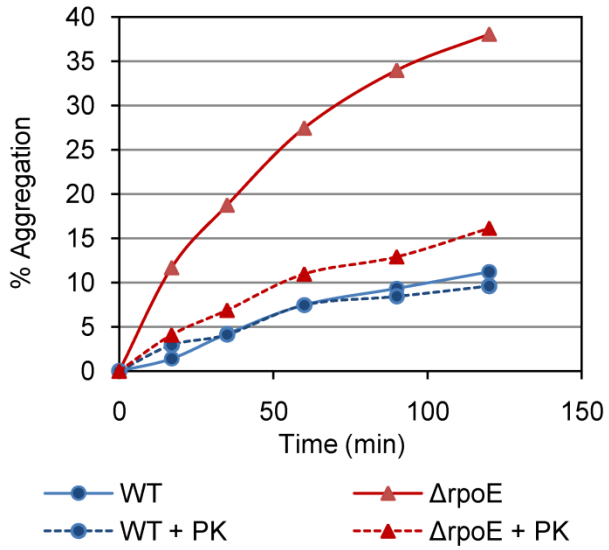

Fig. 4.1 Self-aggregation of *S. mutans* wild type (■) and the Δ*rpoE* mutant (□). Bacterial cells were in PBS buffer without (solid lines) and with Proteinase K treatment (dashed lines). Percent of aggregation was calculated as (OD_{600} at time zero - OD_{600} at time x min) / (OD_{600} at time zero) × 100%. The representative results from three independent experiments are shown. The Δ*rpoE* mutant showed higher self-aggregation compared to the wild type. Pre-treatment with Proteinase K diminished the self-aggregation of the Δ*rpoE* mutant.

Dental biofilms start with the adherence of the initial colonizers, e.g. Streptococci, and *Actinomyces* (Zijnge *et al.*, 2010), to the exposed salivary pellicle. Then genetically distinct species of microorganisms coaggregate with these pioneer colonizers through specific receptors (Kolenbrander *et al.*, 2006). The ability of *S. mutans* to coaggregate with other oral microorganisms, e.g. the initial colonizers *S. oralis*, *S. sanguinis*, and *A. naeslundii* was therefore investigated, as well as the coaggregation with the yeast *C. albicans.* Following the procedure described by Periasamy et al. (Periasamy *et al.*, 2009), cells grown in THBY medium until the exponential phase were collected and transferred into the coaggregation buffer to give a similar cell density (OD_{600} about 0.4) before each pair of two strains was mixed together. The result was recorded after 90 min of coaggregation, and the self-aggregation of each strain was used as a control. As shown in table 4.1A, the wild type had weak self- and co-aggregation, and no visible flocs were formed. By contrast, the Δ*rpoE* mutant formed flocs in the self-aggregation test and coaggregated with *S. sanguinis*, *A. naeslundii*, and *C. albicans.* This is in line with previous findings that *S. mutans* had weak coaggregation with *A. naeslundii* (Crowley *et al.*,

1987;Riihinen *et al.*, 2010), and with *C. albicans* (Jenkinson *et al.*, 1990). The secreted or surface associated proteins in *S. mutans* strains contribute to the bacterial cell-cell interaction, e.g. the surface antigen SpaP (Jakubovics *et al.*, 2005), have been reported. As shown in table 1B, treatment of Proteinase K reduced the coaggregation capability of both strains, which was indicated by the increased optical density (OD_{600}) in the supernatant of Proteinase K treated samples. In addition, the flocs formation of the Δ*rpoE* mutant was eliminated by Proteinase K (table 4.1B). Expression of the aggregation-mediating proteins depends on the growth phase and the extent of aggregation is also influenced by the buffer, since Proteinase K treatment had no obvious effect on the self-aggregation of the wild type for stationary phase cells suspended in PBS buffer (Fig. 4.1).

S. mutans is known to metabolize sucrose and to produce polysaccharides (glucans and fructans) to promote adherence and aggregation (Kreth *et al.*, 2008). In agreement with this, supplementation of the THBY growth medium with sucrose resulted in very effective coaggregation for both the wild type and the Δ*rpoE* mutant with all other microorganisms (table 4.2A), and Proteinase K only partially diminished the coaggregation effect (table 4.2B), suggesting not only proteins, but also polysaccharides are involved in the coaggregation reaction, which is in line with previous findings (Kolenbrander *et al.*, 2006).

4.3.2 Biofilm structure and biofilm matrix assay

Differences in the structure of the biofilm surrounding matrix were revealed under the scanning electron microscope. The wild type biofilm matrix appeared to be more compact (Fig. 4.2A) than that of the Δ*rpoE* mutant (Fig. 4.2B). Moreover, unlike the smooth surface formed by the wild type (Fig. 4.2C), the Δ*rpoE* mutant produced dendrite-like extracellular components to attach on the surface (Fig. 4.2D, arrow). This is consistent with our previous reports that the Δ*rpoE* mutant formed a clumping inhomogeneous biofilm compared to the wild type (Xue *et al.*, 2010).

Table 4.1 Coaggregation of *S. mutans* wild type (WT) and Δ*rpoE* mutant with oral microorganisms without (A) / with (B) Proteinase K treatment.

A

	S. mutans WT		*S. mutans* Δ*rpoE*		*C. albicans*		*S. sanguis*		*S. oralis*		*A. neaslundii*	
S. mutans WT	-[a]	0.23	+	0.14	-	0.10	-	0.24	-	0.24	-	0.23
S. mutans Δ*rpoE*			++	0.08	+	0.07	+	0.17	nd	nd	+	0.12
C. albicans					-	0.08	-	0.20	-	0.24	-	0.14
S. sanguis							-	0.29	-	0.30	-	0.22
S. oralis									-	0.30	-	0.22
A. neaslundii											-	0.20

B

	S. mutans WT		*S. mutans* Δ*rpoE*		*C. albicans*		*S. sanguis*		*S. oralis*		*A. neaslundii*	
S. mutans WT	-	0.39	-	0.39	-	0.27	-	0.37	-	0.41	-	0.34
S. mutans Δ*rpoE*			-	0.39	-	0.37	-	0.40	-	0.41	-	0.32
C. albicans					-	0.14	-	0.27	-	0.28	-	0.20
S. sanguis							-	0.37	-	0.41	-	0.30
S. oralis									-	0.42	-	0.34
A. neaslundii											-	0.24

[a]The settlement of flocs is record after 90 minutes as shown in the first column, the number of '+' indicates the strength of floc settlement, while '-' indicates no visible coaggregation flocs. The optical density (OD_{600}) of the supernatant is also recorded as shown in the second column. Since each strain had a similar optical density before mixing, the turbidity changes helped to judge coaggregation strength.

Table 4.2 Coaggregation of sucrose grown *S. mutans* wild type (WT) and Δ*rpoE* mutant with oral microorganisms without (A) / with (B) Proteinase K treatment.

A

	S. mutans WT		*S. mutans* Δ*rpoE*		*C. albicans*		*S. sanguis*		*S. oralis*		*A. neaslundii*	
S. mutans WT	++++	0.01	++++	0.01	+++	0.05	++	0.13	+++	0.09	++	0.15
S. mutans Δ*rpoE*			++++	0.01	+++	0.08	++	0.13	+++	0.11	+	0.19
C. albicans					-	0.23	+	0.19	+	0.15	-	0.15
S. sanguis							-	0.32	+	0.20	+/-	0.27
S. oralis									+	0.18	+	0.24
A. neaslundii											+/-	0.28

B

	S. mutans WT		*S. mutans* Δ*rpoE*		*C. albicans*		*S. sanguis*		*S. oralis*		*A. neaslundii*	
S. mutans WT	+++	0.04	++	0.06	-	0.13	++	0.22	++	0.11	++	0.22
S. mutans Δ*rpoE*			++	0.08	-	0.17	++	0.29	++	0.13	+	0.49
C. albicans					-	0.28	-	0.32	+	0.23	-	0.31
S. sanguis							+	0.39	++	0.18	+/-	0.38
S. oralis									++	0.28	+	0.28
A. neaslundii											-	0.39

[a]Same as in table 1.

The biofilm matrix is comprised of polysaccharides, proteins, and DNA together with other substances (Flemming & Wingender, 2010), thus the total amount of these three major components was quantified. The amount of extracellular insoluble polysaccharides and DNA was slightly less in the Δ*rpoE* mutant than in the wild type when normalized to dry weight (Fig. 4.3A and C). Lower yield of extracellular proteins was obtained in the Δ*rpoE* mutant using the NaOH/EDTA extraction method, however, a similar amount of proteins was found in both strains by mild detergent triton extraction. Thus the Δ*rpoE* mutant probably had a different extracellular protein composition compared to the wild type (Fig. 4.3B). To investigate the effect of these components on biofilm formation, sodium *meta*-periodate ($NaIO_4$), Proteinase K, and DNase I were used as inhibitors for polysaccharides, proteins, and DNA, respectively. Treatment with Proteinase K caused partial detachment of 16 hour old biofilms of both strains, and moreover, adding the Proteinase K directly to the medium from the beginning of bacterial

growth, strongly inhibited the adherence of both strains, thus no biofilm was formed (supplementary figure S4.1). Thus, the extracellular proteins are necessary for initial adhesion of *S. mutans* to the surface.

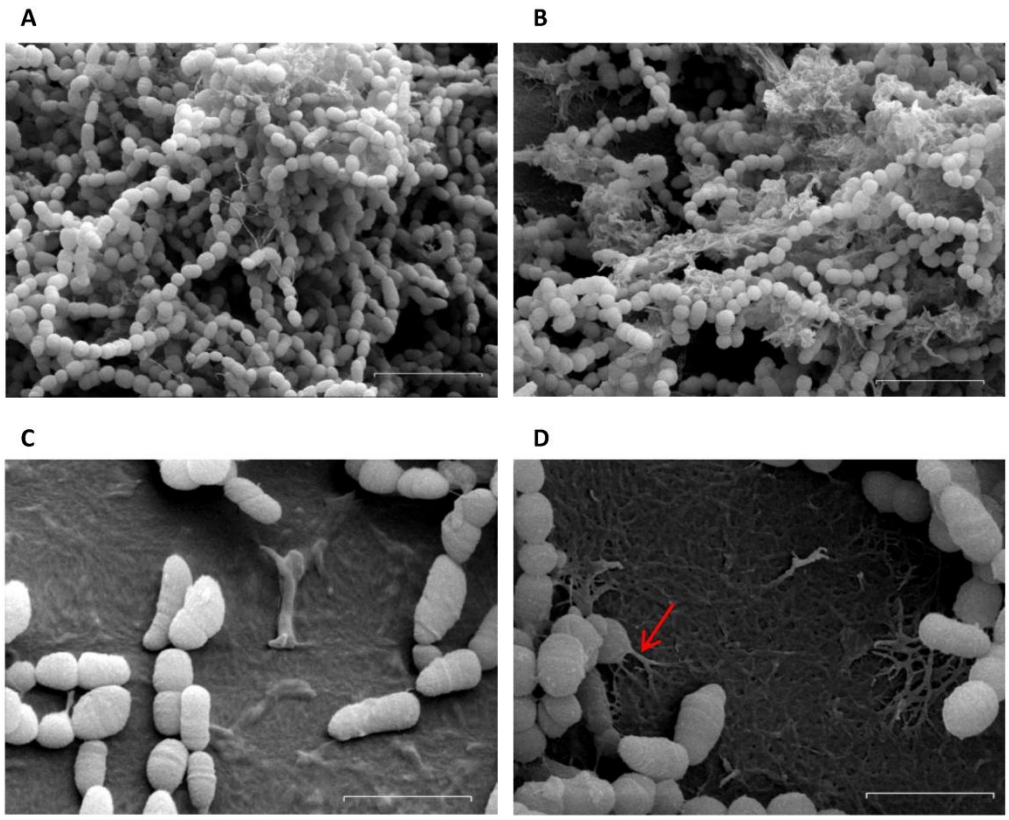

Fig. 4.2 Scanning electron microscopy of 16 h old biofilms of *S. mutans* strains. Wild type (A, C); Δ*rpoE* mutant (B, D). The Δ*rpoE* mutant had a different structure of the biofilm matrix compared to the wild type. The red arrow shows the dendrite-like structure of the Δ*rpoE* mutant biofilm that attached to the polystyrene surface. The bars in image A, B indicate 5 µm, while in image C, D they indicate 2 µm.

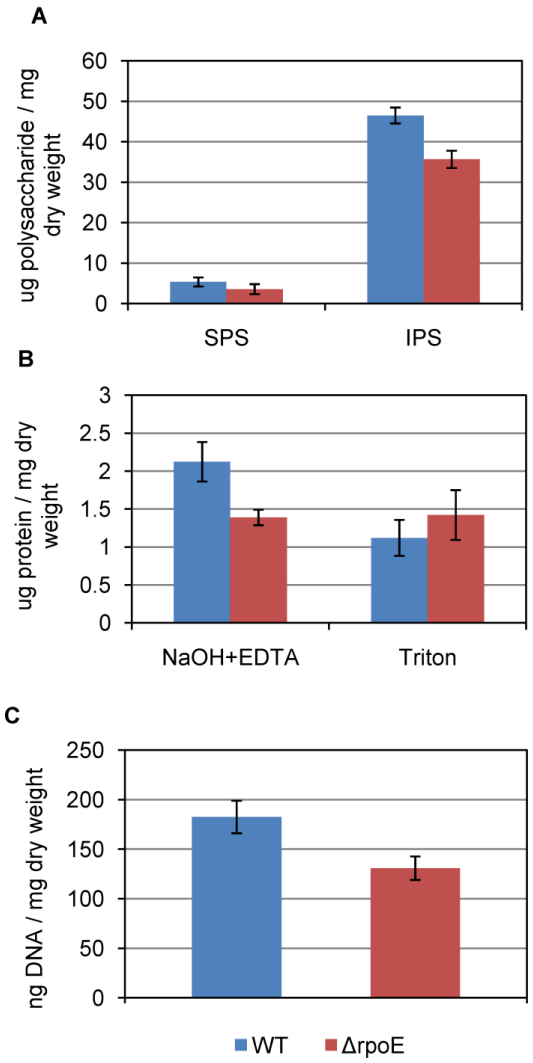

Fig. 4.3 Quantification of extracellular polysaccharides (A), proteins (B), and DNA (C) in *S. mutans* biofilms. Blue columns: wild type; red columns: Δ*rpoE* mutant. Two different methods were used for the extraction of proteins, including EDTA/NaOH and triton extraction. Mean value and standard deviation were calculated from three biological replicates.

The proteins of the extracellular matrix were extracted and subjected to SDS-PAGE and the differentially expressed proteins were excised, digested with trypsin, and identified by MALDI-TOF (PMF and MS/MS) (supplementary table T4.1). As shown in Fig. 4.4, the Δ*rpoE* mutant had a reduced expression of the cell surface antigen I/II SpaP, glucosyltransferases GtfB, and alcohol-acetaldehyde dehydrogenase AdhE; while increased expression of fructan hydrolase FruA was observed, all of which were consistent with our previous microarray data (Xue *et al.*,

2010). AdhE is a bifunctional enzyme that is involved in carbon utilization and alcohol metabolism and its reduced expression has also been detected in our previous proteome study (Xue et al., submitted). The increased amount of fructan hydrolase FruA in the Δ*rpoE* mutant could lead to quicker degradation of fructans, which are suggested as extracellular storage polysaccharides of *S. mutans*. Moreover, since the glucosyltransferases GtfB is responsible for synthesis of water insoluble glucans (Koo *et al.*, 2010), the reduced amount of GtfB in the mutant strain explains its decreased extracellular insoluble polysaccharides as shown above (Fig 4.3A). The surface antigen SpaP in *S. mutans* has been reported to contribute to biofilm formation in a glucan-binding independent way (Zhu *et al.*, 2009). Since both SpaP and GtfB displayed reduced expression in the Δ*rpoE* mutant, the altered biofilm matrix structure and surface attachment shown above indicate a biofilm formation mechanism that is independent of SpaP and glucans. Two protein bands were clearly identified as GtfD, however, according to the molecular weight (about 160 kD), the second band could be truncated proteins. Since GtfD synthesizes water soluble glucans (Honda *et al.*, 1990), the switch of GtfB to GtfD in the Δ*rpoE* mutant could alter the glucan structure in a way that changes the biofilm matrix structure. Similar observations have been reported previously. The mutation of trigger factor (*ropA*) caused reduced expression of the GtfB and GtfD enzymes, but the Δ*ropA* mutant had an increased biofilm formation compared to the wild type (Wen *et al.*, 2005).

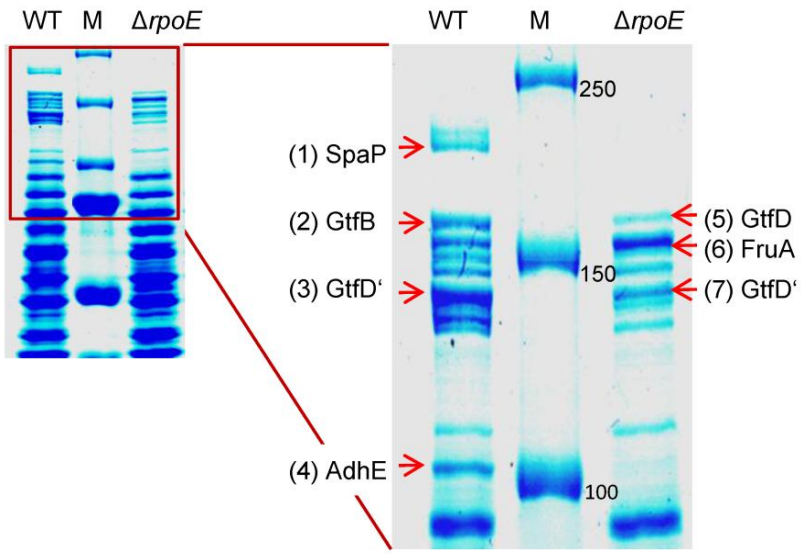

Fig. 4.4 Extracellular matrix proteins of *S. mutans* biofilms. Similar protein amounts extracted from 16 h old biofilms of the wild type (WT) and the Δ*rpoE* mutant were subjected to the 7.5% SDS-PAGE gel electrophoresis, and stained by Coomassie blue. Prestained protein marker (M) was used, with the first three reference bands having a molecular weight of 250, 150, and 100 kD. Proteins were excised and identified by MALDI-TOF. The Δ*rpoE* mutant had a reduced expression of surface antigen I/II SpaP and glucosyltransferase GtfB, while increased expression of fructan hydrolase FruA can be seen. The lower band was probably truncated glucosyltransferase GtfD, thus marked as GtfD'.

4.3.3 The Δ*rpoE* mutant strongly bound to the human extracellular matrix (ECM) components

The ability to bind ECM is one of the major mechanisms for streptococcal pathogenesis (Paterson & Orihuela, 2010). As shown in Fig. 4.5, the wild type bound poorly to all of the ECM molecules under our experimental conditions. The weak binding of the wild type strain to the ECM components could be due to differences in *S. mutans* strains. Although *S. mutans* has been reported to bind to ECM components, e.g. fibronectin through surface antigen I/II SpaP (Beg *et al.*, 2002;Kelemen *et al.*, 2004), to the cell wall associated protein WapA (Han *et al.*, 2006;Zhu *et al.*, 2006), the PavA-like protein (SMU. 1449) (Mitchell, 2003), and AtlA (Jung *et al.*, 2009), none of these experiments was carried out using the UA159 strain. Moreover, the expression and activity of these receptors is highly regulated by environmental factors (Nobbs *et al.*, 2009), thus our experimental conditions could have been not suitable for induction of the high binding

activity. By contrast, the Δ*rpoE* mutant effectively bound to the ECM components collagen I, collagen II, tenascin, laminin, and most strongly, to fibronectin. However, the Δ*rpoE* mutant had decreased expression of genes encoding the known ECM binding proteins as reported in *S. mutans*, e.g. surface antigen I/II SpaP, AtlA, and no changed transcription level of WapA and PavA-like protein according to our transcriptome data (microarray GEO record GSE22333). The strong adherence of the Δ*rpoE* mutant to the ECM components, especially fibronectin, must therefore be due to some other differentially expressed surface receptor or modified surface structures.

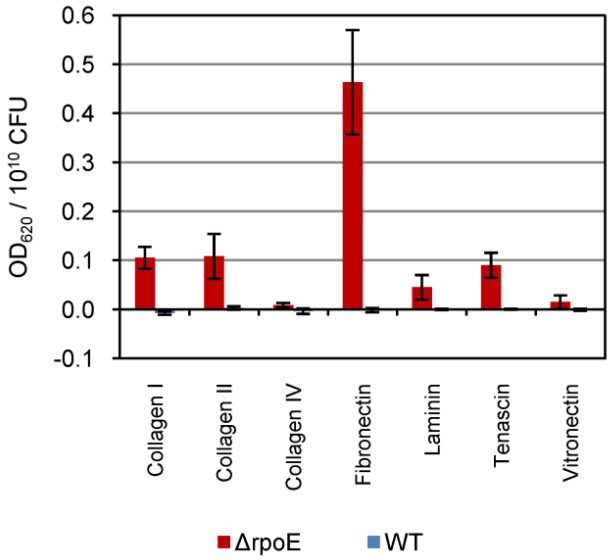

Fig. 4.5 Adherence of *S. mutans* strains to human extracellular matrix (ECM) components. Blue columns: wild type; red columns: Δ*rpoE* mutant. The mean value and standard deviation were calculated from five biological replicates.

4.3.4 The Δ*rpoE* mutant had a reduced adherence to HEp-2 cells

Because of the strong adherence of the Δ*rpoE* mutant to the ECM components, its adherence to and invasion of host cells was tested using human epithelial cells HEp-2 and primary human large vascular endothelial cells HUVEC. Both the wild type and the Δ*rpoE* mutant showed low adhesion to the endothelial cells HUVEC (data not shown). In comparison, they had much higher adhesion to the epithelial cell line HEp-2 (Fig. 4.6A). This is consistent with previous reports

that *S. mutans* was found to adhere to oral epithelial cells (Sklavounou & Germaine, 1980), and its biofilm triggered complex host immune responses (Eberhard *et al.*, 2009).
Although weakly bound to the ECM matrix, the wild type effectively bound to HEp-2 cells, suggesting that *S. mutans* adhesion can be triggered by the presence of specific host cells, or there is an alternative adhesion mechanism independent of ECM binding. By contrast, the Δ*rpoE* mutant had reduced adherence compared to the wild type, especially at the later time points (after 3 hours of incubation) when both strains started fast multiplication. The scanning electron microscope images show the adhesion of the wild type (Fig. 4.6B) and the Δ*rpoE* mutant (Fig. 4.6C) to HEp-2 cells. The Δ*rpoE* mutant tended to clump together when attached to the surface of HEp-2 cells. Thus, the attachment area was relatively small compared to the big mass of the aggregates, and this might have caused easier detachment. Indeed, according to the observation during the experiment, at the later time points, the Δ*rpoE* mutant started to form detached flocs which were easily washed away at the washing step (data not shown).

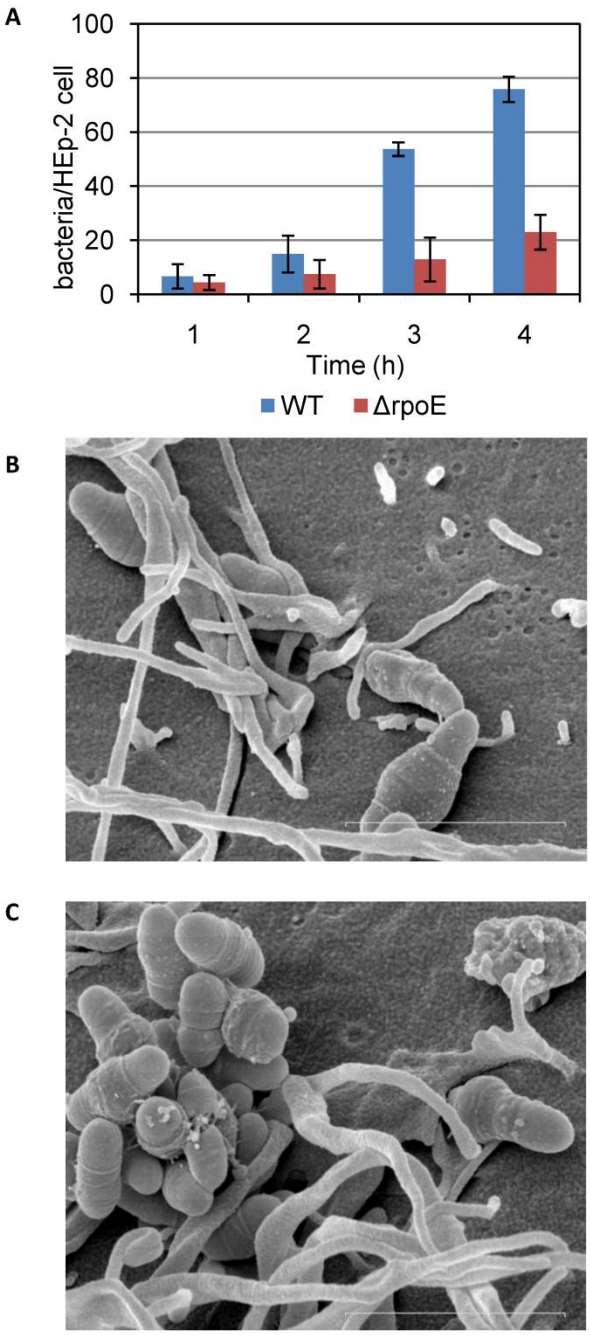

Fig. 4.6 Adherence of *S. mutans* wild type and the Δ*rpoE* mutant to human epithelial cells HEp-2. (A) Quantification of adherent bacteria on the HEp-2 cells. The mean value and standard deviation of the ratio of bacteria/HEp-2 cells was calculated from six biological replicates obtained from three independent experiments. The scanning electron microscope images show the attachment of wild type (B) and the Δ*rpoE* mutant (C) to the surface of human epithelial cells HEp-2. The Δ*rpoE* mutant cells were clumping together. The bars indicate 2 µm.

S. mutans wild type and the Δ*rpoE* mutant had a low frequency of invasion to both epithelial and endothelial cells (data not shown), indicating that *S. mutans* UA159 derived strains are not strongly invasive. In addition, the lactate dehydrogenase (LDH) enzyme released upon HEp-2 cell lysis was quantified to determine the cytotoxicity upon bacterial adhesion. No obvious differences in the released LDH amount between autolyzed cells and cells to which bacteria adhered were found (data not shown). This suggests that there were no holes in the cell membrane upon *S. mutans* adherence, consistent with the previous finding that serotype *c S. mutans* strains (including strain UA159), although they are the most prevalent strains in dental plaque, are not invasive (Abranches *et al.*, 2009). However, rare examples of *S. mutans* invading epithelial (Fig. 4.7) and endothelial cells (supplementary figure S4.2) could occasionally be observed.

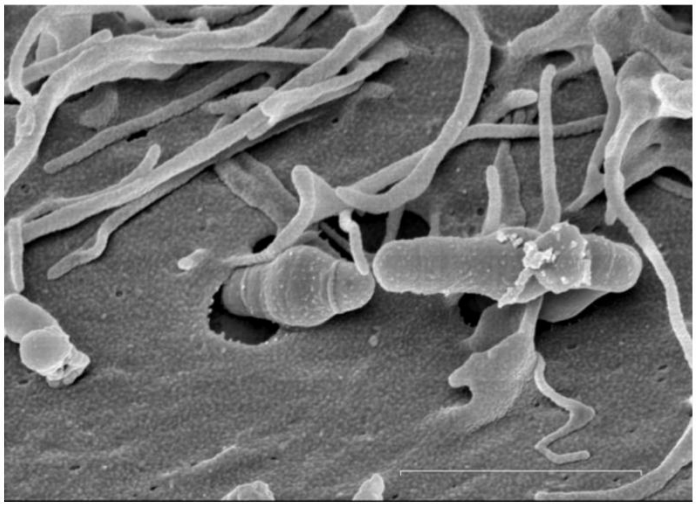

Fig. 4.7 Invasion of human epithelial HEp-2 cells by *S. mutans* wild type cells. The scanning electron microscope image was recorded after 4 hours of incubation of the bacterial culture with HEp-2 cells. The bar indicates 2 µm.

4.3.5 Chacterization of the Δ*rpoE* mutant by phenotypic microarray (PM) assays

The PM technology is with 1,920 testable traits the most comprehensive approach for high throughput phenotyping (Bochner *et al.*, 2001). The system detects the conversion of carbon, nitrogen, phosphate and sulfate sources, but it also monitors the sensitivity for osmotic stress,

various heavy metal ions, the pH and inhibitory chemicals. PM assays are performed in microtiter plate format and record the respiration of living cells by the NADH-dependent reduction of a tetrazolium redox dye. The formation of the purple color reflects both the import as well as the metabolic conversion of a specific substrate. The absence of enzymes, e.g. induced by gene knock-outs, results in lack of color formation. Measurement intervals of 15 minutes of the CCD camera are the prerequisite for the generation of PM-kinetics, which provide information about timing and strength of the cell ́s metabolic activity. The assay is more sensitive than traditional phenotypic growth tests on minimal medium because it also allows to monitor the usage of substrates that are not sufficient for growth (Bochner, 2009).

Freshly grown *S. mutans* wild type and mutant cells were inoculated within the complete set of all twenty PM plates (PM 1- PM 20). We established PM data from two biological replicates, e.g. two independent experiments, of both strains in order to investigate the reproducibility of these experiments. Among all twenty plates, the reproducibility was generally high for PM 1, PM 2, and PM 9 to PM 20, as shown in the comprehensive overview in supplementary figure S4.3. The respiration curves of PM 10 are shown as examples of good reproducibility for both the wild type and the Δ*rpoE* mutant (supplementary figure S4.3).

The results from PM 3 to PM 8 exhibited a very low reproducibility. The poor metabolic response of *S. mutans* in PM 3 to PM 8 assays has previously been reported (Biswas & Biswas, 2005;Zhang & Biswas, 2009b). We improved it by modifying the pH of tricarballylic acid (see methods section), but the results were still not satisfactory, thus, the results from PM 3 to PM 8 will not be discussed in this study. Although Biolog PM plates and protocols were conceived to be applicable to diverse bacterial lineages, a further improvement of specific assay conditions, including the provision of supplementary ingredients, is required to obtain optimal results for *S. mutans*.

The PM data from PM 1, 2 and PM 9 to PM 20 were further analyzed by comparing the Δ*rpoE* mutant with the wild type, and a general overview of both biological replicates is shown in the supplementary figure S4.4. The Δ*rpoE* mutant and the wild type kinetics are colored in green and red, respectively. The predominant occurrence of green signals reflect a conspicuous gain of functions to metabolize sugars (PM 1 & PM 2) and an enhanced resistance against various antibiotics and toxic compounds (PM 9 to PM 20). A complete list of deviating phenotypes of

the Δ*rpoE* mutant including the plate type, the well position of each chemical compound and its mode of action is given in the supplementary table T4.2.

The comparison of the Δ*rpoE* mutant with the wild type respiratory activity indicates that the mutant strain can metabolize 20 additional carbon sources (Fig. 4.8). The 20 sugars that are exclusively metabolized by the Δ*rpoE* mutant are highlighted with black boxes, they include mono- (e.g. D-galactose, PM 01, A06), di- (e.g. sucrose, PM 01, D11), tri- (e.g. D-raffinose, PM 01, D 01), and tetra-saccharides (e.g. stachyose, PM 02, D 05) and the sugar derivates (e.g. D-mannitol, PM 01, B 11).

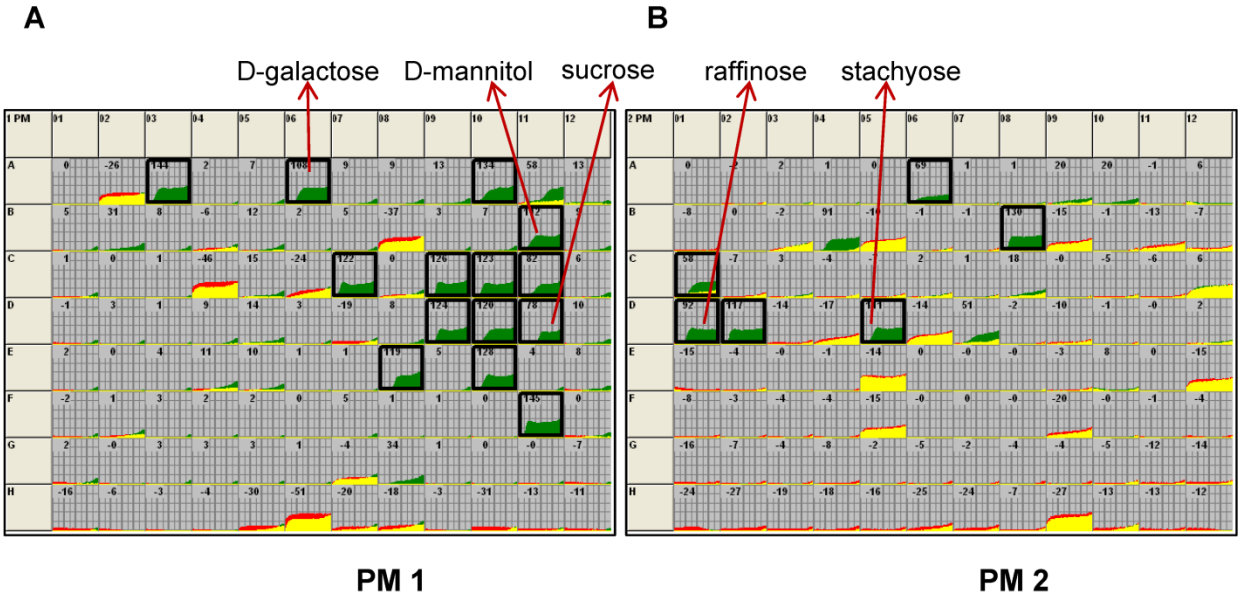

Fig. 4.8 Phenotype Microarray comparison of carbon source utilization by the Δ*rpoE* mutant to the wild type. 190 different substrates were tested in PM 1 and PM 2 plates. The metabolic responses of the mutant and the wild type are presented in green and red, respectively, and shared signals are shown in yellow. Black boxes indicate the 20 carbon sources that are exclusively utilized by the mutant, which are reproducible in both experiments. The arrows represent different sugar types that can be metabolized by the Δ*rpoE* mutant, e.g. D-galactose (monosaccharide), sucrose (disaccharide), raffinose (trisaccharide), stachyose (tetrasaccharide), and D-mannitol (sugar alcohol).

The major involved pathways are the galactose and sucrose metabolism (Table 4.3). These results confirm our previous transcriptome data (Xue *et al.*, 2010), which suggested an alternative carbon metabolism in the Δ*rpoE* mutant. We showed that the multiple sugar metabolism (MSM) system, which transports and metabolizes various sugars (e.g. raffinose, sucrose, and melibiose) and plays a major role in galactose and sucrose metabolism (Ajdic &

Pham, 2007;Tao *et al.*, 1993), was highly induced in the Δ*rpoE* mutant (Xue *et al.*, 2010). In addition, the upregulation of other genes in the sucrose metabolism pathway, e.g. the sucrose specific transporter (*scrA*) and the sucrose-6-phosphate hydrolase (*scrB*) was also found in our microarray data (microarray GEO data GSE22333). A weaker metabolic activity was observed for four aldopentoses (PM 1: A 02, B 08, C 04, H 06; see table 3) that are involved in the pentose phosphate pathway. The inefficient pentose phosphate metabolism of the Δ*rpoE* mutant is in agreement with our previous proteome data showing that the mutant had reduced expression of phosphopentomutase DeoB, which catalyzes the intramolecular transfer of the phosphate group between Ribose-1P and Ribose-5P, an important step in the pentose phosphate pathway (Xue et al., submitted).

The metabolic advantage of the Δ*rpoE* mutant in such a large number of assays for chemical sensitivity (PM 9 to PM 20) was unexpected (supplementary figure S4.4). The mutant showed an enhanced resistance against 142 different antibiotics or toxic compounds (table 4.4, see also supplementary S4.5). For example, metabolic activity of the Δ*rpoE* mutant was observed in the presence of chemicals which affect DNA synthesis, unwinding, and replication. Many inhibitors that block protein synthesis generated positive results for the Δ*rpoE* mutant. The Δ*rpoE* mutant was resistant to many toxic anions and cations, and chemicals that interfere with the tRNA synthetase, cell wall and membrane synthesis. Similar findings were also reported for the mutation of the histidine kinase gene *liaS* in *S. mutans*, which was found to be resistant to antibiotics that are targeting cell-wall biosynthesis, as well as antibiotics inhibiting protein and DNA synthesis (Zhang & Biswas, 2009b). Since antibiotic resistance mechanisms are normally very specific, we speculate that the increased resistance to such a large number of antibiotics could result from general changes in the Δ*rpoE* mutant. The modified surface structure may block the entry of antibiotics and the loosened transcriptional specificity might generate a larger variety of proteins allowing the cell to be readily prepared for facing toxic compounds.

Table 4.3 Gained and lost metabolic activity in carbon sources utilization in the *S. mutans* Δ*rpoE* mutant compared to the wild type.

Phenotypes Gained - better metabolic activity				
Plate	Wells[a]	Test	Type of sugar	Pathway involved
PM01	A03	N-Acetyl-D-Glucosamine	Monosaccharide derivative of glucose	Amino sugar and nucleotide sugar metabolism
PM01	A06	D-Galactose	Monosaccharide	Galactose metabolism
PM01	A10	D-Trehalose	Disaccharide	Starch and sucrose metabolism
PM01	B11	D-Mannitol	Sugar alcohol	Fructose and mannose metabolism
PM01	C07	D-Fructose	Monosaccharide	Fructose and mannose metabolism
PM01	C09	α-D-Glucose	Monosaccharide	Glycolysis / Gluconeogenesis
PM01	C10	Maltose	Disaccharide	Starch and sucrose metabolism
PM01	C11	D-Melibiose	Disaccharide	Galactose metabolism
PM01	D09	α-D-Lactose	Disaccharide	Galactose metabolism
PM01	D10	Lactulose	Disaccharide	-
PM01	D11	Sucrose	Disaccharide	Galactose metabolism; Starch and sucrose metabolism
PM01	E08	β-Methyl-D-Glucoside	Monosaccharide derivative of glucose	-
PM01	E10	Maltotriose	Trisaccharide	Starch and sucrose metabolism
PM01	F11	D-Cellobiose	Disaccharide	Starch and sucrose metabolism
PM02	A06	Dextrin	Mixtures of polymers of D-glucose units	Starch and sucrose metabolism
PM02	B08	Arbutin	Glycosylated hydroquinone	Glycolysis / Gluconeogenesis
PM02	C01	Gentiobiose	Disaccharide	-
PM02	D01	D-Raffinose	Trisaccharide	Galactose metabolism
PM02	D02	Salicin	Alcoholic β-glycoside that contains D-glucose	Glycolysis / Gluconeogenesis
PM02	D05	Stachyose	Tetrasaccharide	Galactose metabolism
Phenotypes Lost - less metabolic activity				
Plate Type	Wells	Test	Type of sugar	pathway involved
PM01	A02	L-Arabinose	Aldopentose	Pentose phosphate pathway
PM01	B08	D-Xylose	Aldopentose	Pentose and glucuronate interconversions
PM01	C04	D-Ribose	Aldopentose	Pentose phosphate pathway
PM01	H06	L-Lyxose	Aldopentose	Pentose and glucuronate interconversions

[a] The wells with reproducible results from both experiments are listed.

Table 4.4 Gained resistance to antibiotics and toxic compounds in the *S. mutans* Δ*rpoE* mutant compared to the wild type.

Mode of Action	Compounds
DNA synthesis	Hexaminecobalt (III) Chloride, Nitrofurantoin, Bleomycin, Trifluoperazine, Myricetin, 5-Fluoro-5'-deoxyuridine, Semicarbazide hydrochloride, Trifluoperazine
DNA intercalator	9-Aminoacridine, 2- Phenylphenol, Coumarin, Umbelliferone
DNA methyltransferase	5-Azacytidine
DNA topoisomerase	Norfloxacin, Ciprofloxacin
DNA unwinding	Oxolinic acid, Pipemidic Acid, Lomefloxacin, Enoxacin, Ofloxacin, Nalidixic acid
folate antagonist	Sulfadiazine, Sulfamethazine, Sulfamethoxazole, Sulfathiazole, Sulfanilamide, Sulfachloropyridazine, Sulfamonomethoxine, Trimethoprim, Sulfisoxazole
Nucleic acid analogs	Azathioprine, 5-Fluorouracil, Cytosine arabinoside
thymidylate synthetase	Trifluorothymidine
ribonucleotide DP reductase	3,5- Diamino-1,2,4-triazole (Guanazole)
protein synthesis	Phenyl-Methyl-Sulfonyl-Fluoride (PMSF), Capreomycin, Spectinomycin, Chloramphenicol, Cinoxacin, Blasticidin S, Rolitetracycline, Tylosin, Oleandomycin, Paromomycin, Tobramycin, Geneticin (G418), Streptomycin, Hygromycin B, Spiramycin, Josamycin, Tetracycline, Amikacin, Gentamicin, Kanamycin, Neomycin, Erythromycin[a], Lincomycin, Sisomicin, Minocycline
tRNA synthetase	D,L-Serine Hydroxamate, L-Aspartic-b-Hydroxamate, L-Glutamic-g-Hydroxamate
Cell wall synthesis	Glycine, Phosphomycin, Cefoxitin, Cetoperazone, Ampicillin, Moxalactam, Piperacillin, Aztreonam, D-Cycloserine, Cefazolin, Ceftriaxone
toxic anions	Sodium bromated, Sodium periodate, Potassium chromate, Sodium Cyanate, Sodium Arsenate, Sodium Dichromate, Sodium metasilicate, Cobalt chloride, Zinc chloride, Chromium Chloride
toxic cations	Cesium chloride, Nickel chloride, Thallium (I) acetate, Aluminum Sulfate
toxicity	5-Fluoroorotic Acid, Sodium Nitrate, Sodium Phosphate

membrane	Cetylpyridinium Chloride, Polymyxin B, Colistin
Chelating agents	Sodium pyrophosphate decahydrate, 2,2`-Dipyridyl, 1-Hydroxy-Pyridine-2-thione, Fusaric Acid, 1,10-Phenanthroline
fungicide	Chloroxylenol, Dodine, Nordihydroguaiaretic acid
oxidation	1-Chloro-2,4-Dinitrobenzene, Diamide, Methyl viologen, 3, 4-Dimethoxybenzyl alcohol, Phleomycin
respiration	18-Crown-6-Ether, Sorbic Acid, Pentachlorophenol (PCP), Menadione, Sodium azide, Ruthenium red
others	X-α-D-Galactoside, X-β-D-Glucoside, X-β-D-Glucuronide, Atropine, Thiosalicylate, Apramycin, Ethionamide, X-PO4, X-SO4, Triclosan, D,L-Propranolol, Caffeine, Aminotriazole, Harmane, D-Serine, Dequalinium, Lidocaine, Tinidazole, 20% Ethylene Glycol, pH 8, Phenylarsine Oxide, b-Chloro-L-Alanine, Trifluoperazine

[a] *S. mutans* Δ*rpoE* mutant contains an erythromycin resistance gene.
[b] mode of action includes: α-D-galactosidase, β-D-glucosidase, β-D-glucuronidase, acetylcholine receptor, anti-capsule, antimicrobial, anti-tuberculosic, aryl phosphatase, aryl sulfatase, bacterial fatty acid synthesis, beta-adrenergic blocker, cyclic AMP phosphodiesterase, histidine biosynthesis, imidazoline binding sites, 3PGA dehydrogenase inhibitor, ion channel inhibitor, mutagen, osmotic sensitivity, pH sensitivity, tyrosine phosphatase, aminotransferase inhibitor.

Our previous data showed that the Δ*rpoE* mutant was more sensitive to antibiotics that target protein synthesis, such as tetracycline and kanamycin (Xue *et al.*, 2010). However, the PM assays showed that the mutant strain had metabolic advantages in the presence of different concentrations of kanamycin (PM 11, H 05 - H 08) and tetracycline (PM 12, A 05, 06) (supplementary figure S4.5). We therefore conducted independent growth tests which showed that the growth conditions strongly influenced the growth and antibiotic resistance of *S. mutans*, and caused these variations. As shown in supplementary figure S4.6, when grown in 96-well microtiter plates at 37 ℃ without enriched CO_2 (similar growth condition as in the PM assays), the Δ*rpoE* mutant had growth advantages compared to the wild type in the presence of 100 μg/ml kanamycin, while both strains could overcome the inhibitory effect of 1 μg/ml tetracycline after 48 hours of growth. However, when grown in 96-well microtiter plates at 37 ℃ enriched with 5% CO_2 , the wild type could overcome the inhibitory effect of kanamycin; by contrast, the

growth of both strains was inhibited by tetracycline (supplementary figure S4.6). Our previous antibiotic sensitivity test was carried out at 37 ℃ enriched with 5% CO_2, but growth was in falcon tubes rather than microtiter plates. As shown in supplementary table S3, under this condition the wild type strain had no difficulty to grow in the presence of both antibiotics, while the Δ*rpoE* mutant failed to grow after the first 20 h, confirming our previous results. Better growth was also found in the closed system with a larger volume of cultures, which left less free space for air than that of smaller volume and thus less oxygen stress occurred. These different cultivation conditions, e.g. the extent of oxygen stress and CO_2 supplementation, affect the growth and metabolism of both strains in different ways, and thus indirectly result in altered antibiotic sensitivity. In contrast to the drastic effect of growth conditions, the effects of growth media were less pronounced (data not shown).

4.4 Discussion

The results from this study show the multi-dimensional influence of RpoE on virulence related traits of *S. mutans.* The investigated traits are related to plaque formation potentially resulting in damage to host teeth (caries) as well as traits related to adherence, invasion, and survival in host cells and tissues. Both aspects are important for its pathogenesis.

Being not an initial colonizer, *S. mutans* needs to coaggregate with the pioneer species to adhere and build a spatially organized community in dental biofilms (Kolenbrander *et al.*, 2010). Moreover, the ability to self-aggregate also allows the quicker accumulation of bacterial cells to become dominant in the bacterial population. Thus, the higher self- and co-aggregation of the Δ*rpoE* mutant suggests that it could be more competitive in the oral bacterial community. The oral environment is characterized by quick fluctuations of all parameters, including carbohydrate sources and concentrations (Bowden & Hamilton, 1998). The acquired functions in the usage of a broader spectrum of carbon sources suggest a growth advantage of the Δ*rpoE* mutant under aerobic growth conditions. More importantly, since antibiotic treatment is still the most important means of disease control (Kinney, 2010), the acquired functions of the Δ*rpoE* mutant in resistance to such a large spectrum of antibiotics make it potentially more difficult to be removed by conventional antibiotic treatment.

Biofilm formation is important for *S. mutans* to survive inside the host oral cavity and on other tissues, e.g. heart valves. The Δ*rpoE* mutant produced a reduced amount of the extracellular proteins SpaP and GtfB and formed biofilms with a looser extracellular matrix. However, the dendrite-like structure of the Δ*rpoE* mutant biofilm extracellular matrix might allow firm attachment to surfaces. This could benefit its colonization inside the human organism or tissue, where the concentration of sucrose is low compared to the oral cavity and the expression of Gtfs and SpaP should be low to avoid inducing host immune defense mechanisms. Indeed, the *S. mutans* strains isolated from infective endocarditis patients were lacking the intact Gtfs enzymes and had lower sucrose-dependent adhesion (Nomura *et al.*, 2006). Moreover, mutant strains defective for the surface antigen SpaP resulted in less phagocytosis by human polymorphonuclear leukocytes, thus had a higher survival rate and caused more severe systemic inflammation (Nakano *et al.*, 2006b).

Binding to extracellular matrix components is important for virulent streptococci, e.g. *S. pneumonia*, *S. pyogenes* (Group A streptococcus), and *S. algalactiae* (Group B streptococcus) in the adhesion and invasion of host cells, and many ECM binding proteins have been identified (Mitchell, 2003;Nobbs *et al.*, 2009). The strong adherence of the Δ*rpoE* mutant to the ECM components, especially fibronectin, suggests that it might have a higher potential to bind to host cells. However, probably due to the clumping effect, the Δ*rpoE* mutant could not adhere as well as the wild type on the epithelial HEp-2 cells. Nevertheless, the invasion of human cells could be seen in both the wild type and the Δ*rpoE* mutant occasionally. With its reduced expression of Gtfs and SpaP, the Δ*rpoE* mutant could have low antigenicity and escape the host immune system, thus it might survive longer once it invades the host, and it could be more virulent than its parent strain under certain conditions.

We previously showed that loss of RpoE resulted in massive changes in the transcriptome, and that these changes caused impaired growth, reduced stress tolerance, inhomogeneous biofilm structure, and decreased resistance to tetracycline and kanamycin (Xue *et al.*, 2010). In contrast to these, we find in this study that the mutant has increased virulence related traits and broader metabolic functions, which however depend strongly on the cultivation conditions. The data show that the transcriptional specificity provided by RpoE apparently restrains the physiology of *S. mutans* to a specific ecological niche in the oral cavity. Loss of RpoE results in lack of regulation of these traits, reducing the fitness of *S. mutans* in the ecological niche to which it has

evolved. However, at the same time a wide range of hidden physiological capabilities of *S. mutans* become visible upon loss of RpoE. The more or less uncoordinated transcription of a large number of genes results in the synthesis of diverse functional proteins which can be important in different ecological niches in nature. From this point of view, loss of RpoE must not automatically be considered as a disadvantage for survival. The work presented here shows that some of the newly expressed traits might increase the virulence of the Δ*rpoE* mutant, e.g. by enhancing its resistance to antibiotics and toxic compounds, reducing its immunogenic surface properties, and altering its carbon metabolism, all of which could result in better survival in the host. Our data also show that many of the virulence related traits essentially depend on cultivation conditions, and thus extrapolation from laboratory data to *in vivo* processes requires extreme caution.

From a genetic perspective, the overall observed differences of the phenotypes between the *S. mutans* wild type and Δ*rpoE* mutant are striking, especially since their genome composition and organization is identical, with the sole exception of the *rpoE* gene replaced by an erythromycin antibiotic resistance gene. The acquired metabolic capacities of the Δ*rpoE* mutant indicate the physiological potential of *S. mutans* UA159 strain. However, these traits may just reflect the tip of the iceberg because they simply occurred due to the release of regulative restraints. As shown in this and our previous work, the transcriptional control was loosened by lack of RpoE, thus causing global changes in transcriptome and physiological functions. It is conceivable that processes occurring in nature, such as genetic mutations, horizontal gene transfer or environmental changes, could similarly trigger a modification or release of control, thus resulting in comparable phenotypic or functional changes in natural isolates. Our data show that a microbe has at least a hundred different faces, of which we generally see only a fraction by the standard conditions in the laboratory.

4.5 Acknowledegments

We gratefully acknowledge Dr. Manfred Nimtz for the support in MALDI-TOF-MS and related data analysis. We thank Ina Schleicher for technical support for the scanning electron microscope. Xiaoli Xue was supported by a CSC-Helmholtz Joint Fellowship. IWD

acknowledges the support of the BMBF (FK 0315411A) and the DFG (TRR 51). The research leading to the Phenotype Microarray (PM) results has received funding from the European Community ś Seventh Framework Programme (FP7/2007-2013) under grant agreement number 222886-2 (Microme project).

4.6 Supplementary materials

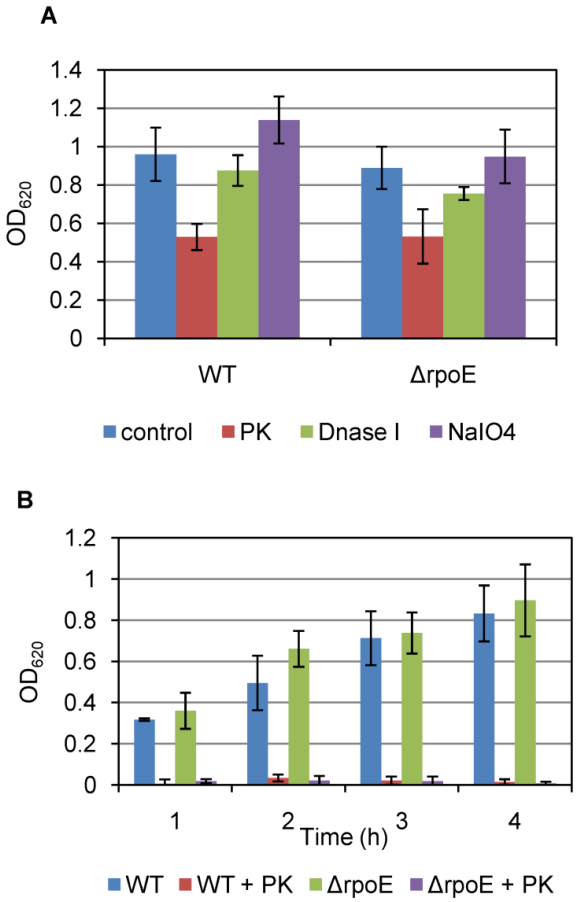

Figure S4.1 Detachment and inhibition of 16 h old biofilms of *S. mutans* strains. (A) Detachment of wild type (WT) and the Δ*rpoE* mutant biofilm by Proteinase K (PK, degrades proteins), DNase I (digests DNA) and $NaIO_4$ (oxidizes carbohydrates). (B) Inhibition of *S. mutans* wild type and the Δ*rpoE* mutant biofilm formation by Proteinase K added directly to BMS medium from the beginning of biofilm growth. The biofilms from A and B were quantified by crystal violet staining, and the extracted dye was measured at 620 nm. The representative results from four independent experiments are shown. Mean value and standard deviation were calculated from eight biological replicates from one experiment.

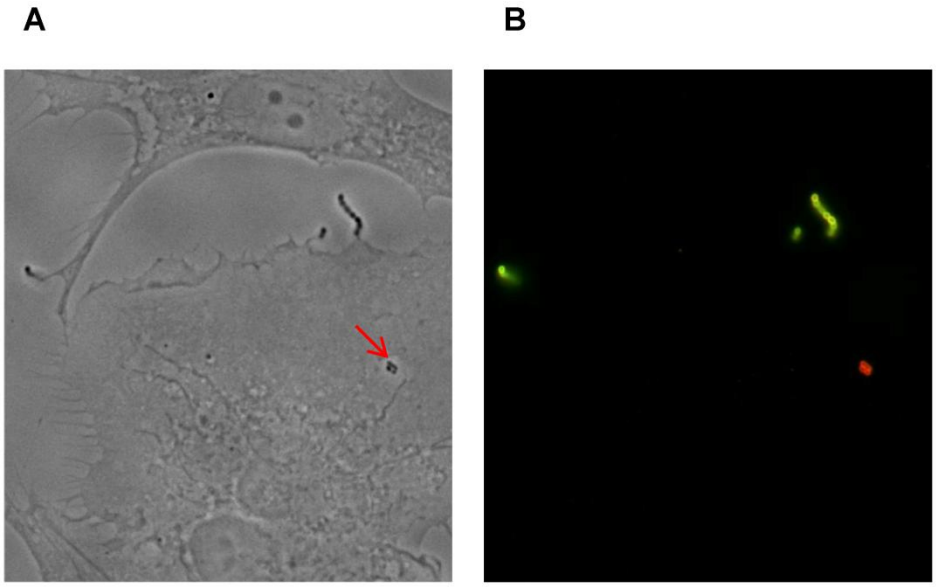

Figure S4.2 The rare example of invasion of the *S. mutans* Δ*rpoE* mutant into human endothelial HUVEC cells. Samples were fixed after 1 hour of incubation. Images were taken (A) under white light; and (B) using green and red excitation filters to see fluorescent light from antibody marked *S. mutans*, then these two images were merged. Extracellular adherent bacteria were visualized using rabbit polyclonal *S. mutans* antibody (Abcam, USA) and Alexa Fluor 488-conjugated goat anti-rabbit IgG (green). Following permeabilization with 0.01% Triton X-100, extra- and intracellular bacteria were detected by incubation with *S. mutans* antibody followed by an Alexa Fluor 568-conjugated goat anti-rabbit IgG (red). According to their respective label, intracellular bacteria appear red, while extracellular bacteria appear yellow (combined color of green and red). The arrow indicates the intracellular bacteria.

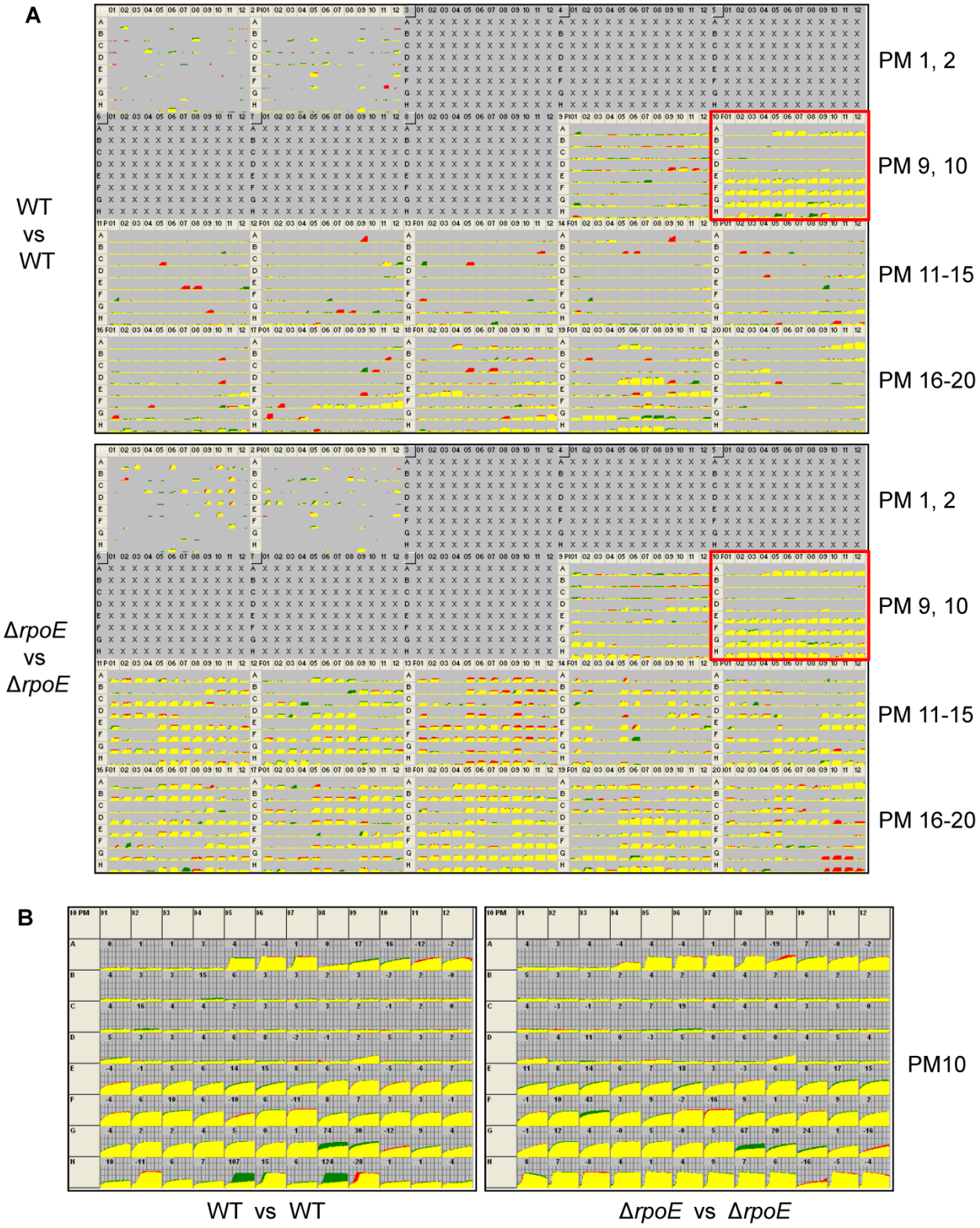
A
WT
vs
WT
PM 1, 2
PM 9, 10
PM 11-15
PM 16-20
ΔrpoE
vs
ΔrpoE
PM 1, 2
PM 9, 10
PM 11-15
PM 16-20
B
PM10
WT vs WT
ΔrpoE vs ΔrpoE

Figure S4.3 Comparison of Phenotype Microarray (PM) data from two independent experiments. (A) The overview of PM data from PM 1, 2 and PM 9 to PM 20 (format row left to lowest row right). The curves show the rate of respiration. The data for the first experiment are shown red, while those for the second experiment are shown green. Thus, perfect reproducibility is indicated by a yellow curve. The upper panel shows the *S. mutans* wild type (WT) and the lower panel shows the Δ*rpoE* mutant in two experiments, respectively. The variations in two experiments are indicated by red or green colours. The results from PM 1, PM 2, and PM 9 to PM 20 assays are generally fine, some discrepancies could however be observed in PM 9 to 20 for the wild type, the respiration for some inhibitor compounds which was not observed a second time, indicated by red or green curves. The data for the Δ*rpoE* mutant, which had a better reproducibility, show that growth was possible for *S. mutans* under these conditions. Thus, the variations in the wild type seen in the two sets of PM experiments could be due to turning on or off certain functional genes by accidentally releasing regulatory restraints. The red boxes show the example of good reproducibility in PM 10 for both the wild type and the Δ*rpoE* mutant, which is enlarged in (B). Most results were reproducible, indicated by yellow curves. Slight changes of the signal strength in the two biological replicates are indicated by red or green margins.

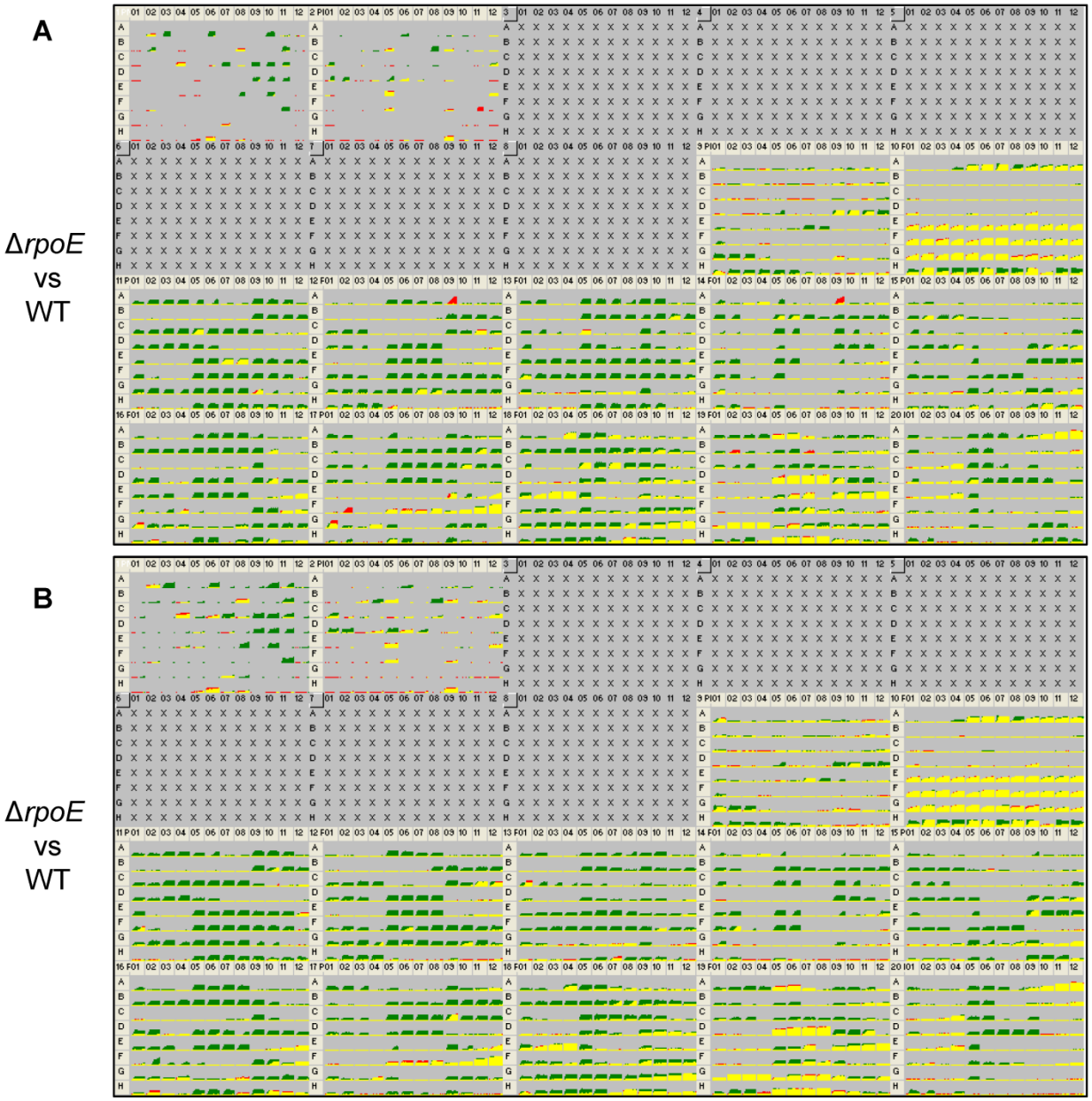

Figure S4.4 Phenotype Microarray (PM) comparison of the *S. mutans* Δ*rpoE* mutant with the wild type. The results from the first and the second experiments are shown in the upper and lower panels, respectively. Yellow indicates the similar metabolic activity in both the wild type and the mutant strain. Higher metabolic response of the wild type is indicated in red; while the response of the Δ*rpoE* mutant is indicated in green.

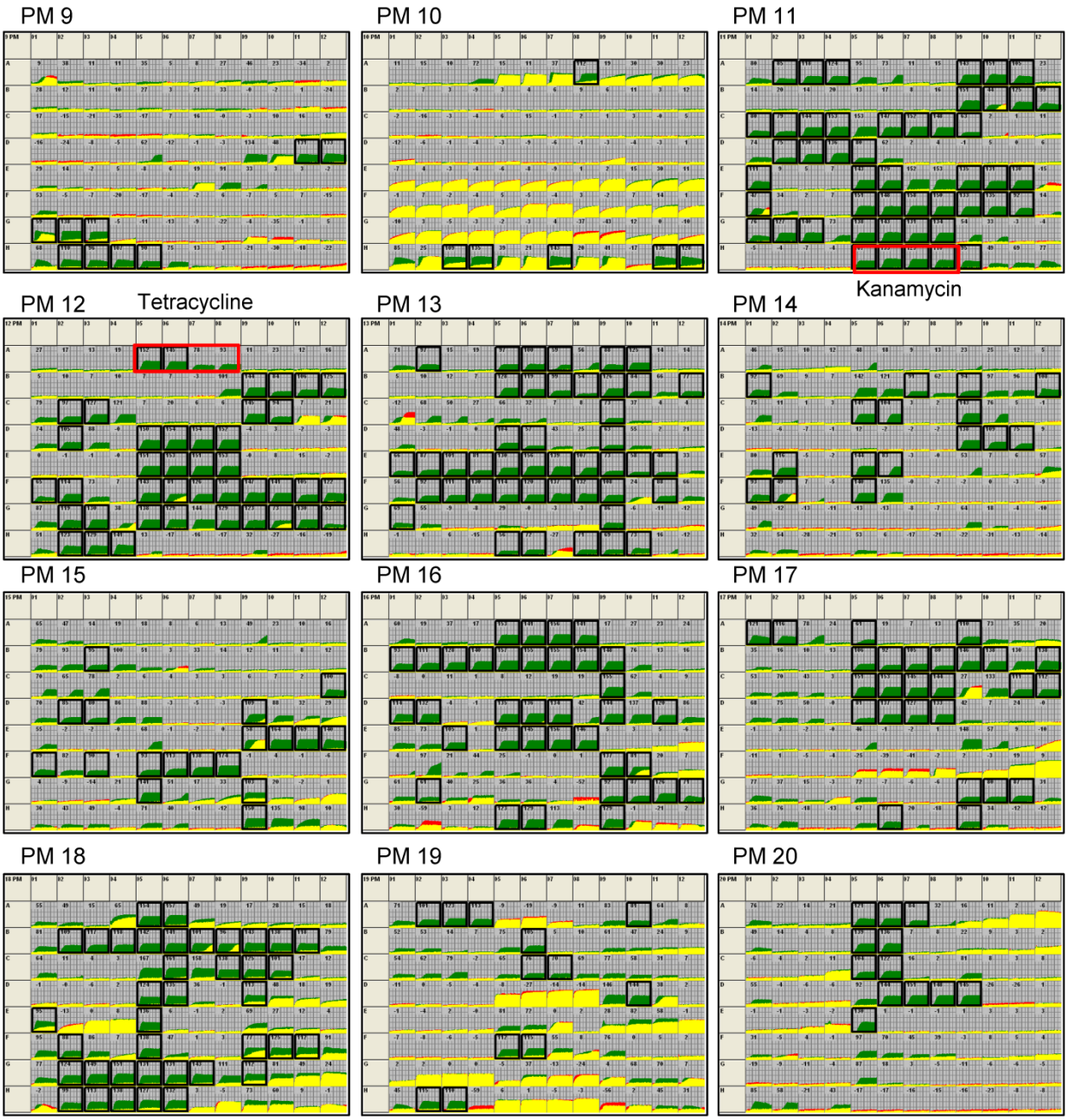

Figure S4.5 Comparison of the *S. mutans* Δ*rpoE* mutant to the wild type in sensitivity assays. The PM 9 to PM 20 assays were performed in rich medium in presence of antibiotics or toxic compounds. Yellow indicates the similar metabolism activity in both the wild type and the mutant strains. A metabolic advantage by the wild type is indicated in red; while a metabolic advantage by the Δ*rpoE* mutant is indicated in green. The wells with reproducible results in both experiments, and height differences over the threshold in at least one experiment, are highlighted with black boxes. The Δ*rpoE* mutant was more resistant to a large spectrum of or toxic compounds as indicated by many green kinetics curves. The red boxes highlight the resistance of the Δ*rpoE* mutant to 4 different concentrations of kanamycin (PM 11, H 05 - H 08) and 2 of the 4 concentrations of tetracycline (PM 12, A 05, A 06).

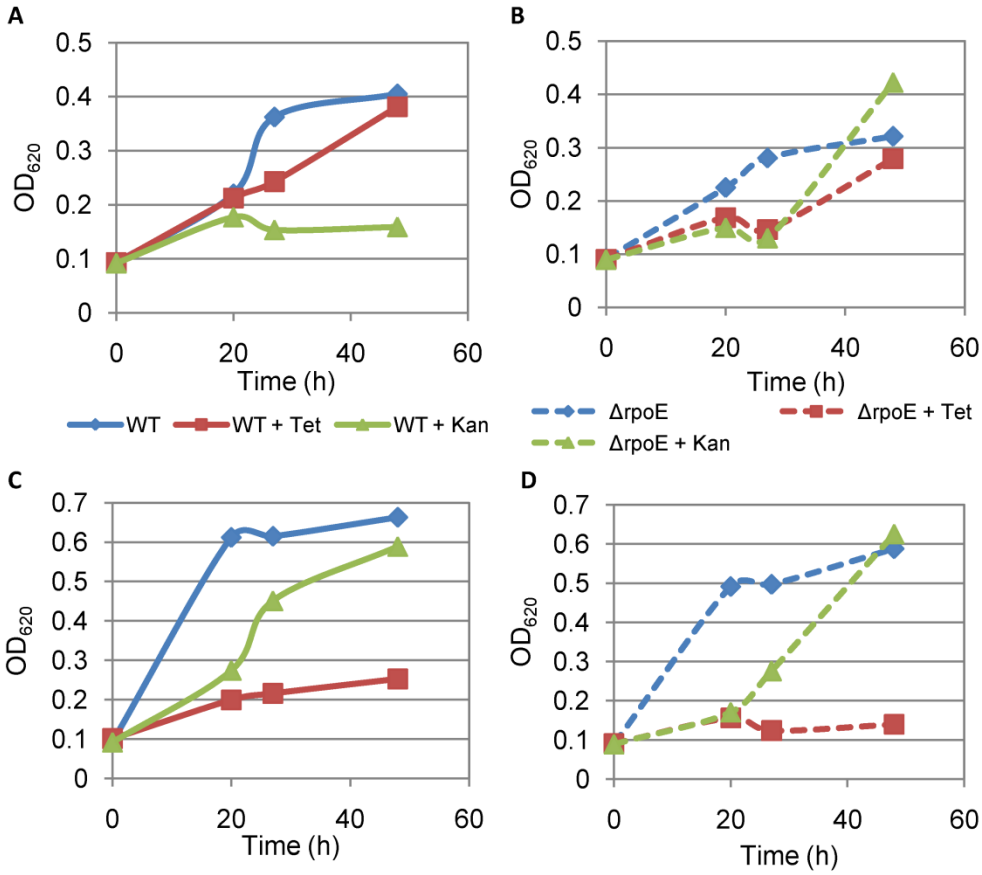

Figure S4.6 Growth of the *S. mutans* wild type and the Δ*rpoE* mutant under different conditions. Bacterial cells were grown in the 96-well microtiter plate at 37 ℃ (A, B) and at 37 ℃ enriched with 5% CO_2 (C, D). A, C: wild type (WT, solid lines); B, D: Δ*rpoE* mutant (dashed lines). +Tet, +Kan: growth in THBY medium supplied with 1 μg/ml tetracycline (red lines), or 100 μg/ml kanamycin (green lines). The growth of both strains in medium without antibiotics are shown in blue lines.

Table T4.1. Identification of the extracellular proteins in the biofilms matrix of *S. mutans*.

Protein identification by MALDI-TOF (PMF)[a]									
No. band	Protein symbol	Gene code	GI No.	Protein name	Protein MW, Da	Matched peptides	sequence coverage (%)	Protein score	P value
3	GtfD'	smu.910	153645	glucosyltransferase	159667	23	18	154	2.70E-09
4	AdhE	smu.148	24378663	alcohol-acetaldehyde dehydrogenase	97331	17	27	142	4.30E-08
5	GtfD	smu.910	153645	glucosyltransferase	159667	20	16	122	4.30E-06
6	FruA	smu.78	24378602	fructan hydrolase	158848	31	28	239	8.60E-18
7	GtfD'	smu.910	153645	glucosyltransferase	159667	15	12	114	2.70E-05

Protein identified by MALDI-TOF/TOF (PMF+ MS/MS)[b]										
No. band	Protein symbol	Gene code	GI No.	Protein name	Protein MW, Da	Peptide for MS/MS	Peptide mass error, Da	Ion Score	P value	Protein score
1	SpaP	smu.610	47267	cell surface antigen I/II	170014	ATAATLATFNADLTK	-0.0755	79	9.20 E-05	79
2	GtfB	smu.1004	153640	glucosyltransferase-I	165594	NAQGQWFYFDNNGYAVTGAR	-0.1604	102	1.40 E-07	99
2	GtfB	smu.1004	153640	glucosyltransferase-I	165594	TINGQHLYFR	-0.1124	64	3.20 E-03	99

[a]Proteins were digested with trypsin and analyzed by a matrix-assisted laser desorption / ionization time of flight mass spectrometry (MALDI-TOF MS) to produce a peptide mass fingerprint (PMF). The obtained peptide masses were used for protein identification using the program MASCOT. Protein score is -10*Log(P), while P is the probability of a random event. Protein scores >81 are significant ($P<0.05$).
[b]Proteins were digested and analyzed by in the same manner as above to produce a peptide mass fingerprint (PMF). The most abundant peptide ions are then subjected to MALDI-TOF/TOF analysis to determine the sequence. The results from both types of analyses were combined and searched for protein identification using the program MASCOT. Ions score is -10*Log(P), while P is the probability of a random event. Ions scores >51 indicate identical peptide identity or extensive homology ($P<0.05$). Protein scores are derived from ions scores as a non-probabilistic basis.

Table T4.2. Gained and lost functions in the *S. mutans* Δ*rpoE* mutant compared to the wild type.

Phenotypes Gained - better metabolic activity			
Plate Type	Wells[a]	Test	mode of action
PM01	A03	N-Acetyl-D-Glucosamine	C-source
PM01	A06	D-Galactose	C-source
PM01	A10	D-Trehalose	C-source
PM01	B11	D-Mannitol	C-source
PM01	C07	D-Fructose	C-source
PM01	C09	a-D-Glucose	C-source
PM01	C10	Maltose	C-source
PM01	C11	D-Melibiose	C-source
PM01	D09	a-D-Lactose	C-source
PM01	D10	Lactulose	C-source
PM01	D11	Sucrose	C-source
PM01	E08	b-Methyl-D-Glucoside	C-source
PM01	E10	Maltotriose	C-source
PM01	F11	D-Cellobiose	C-source
PM02	A06	Dextrin	C-source
PM02	B08	Arbutin	C-source
PM02	C01	Gentiobiose	C-source
PM02	D01	D-Raffinose	C-source
PM02	D02	Salicin	C-source
PM02	D05	Stachyose	C-source
PM09	D11	15% Ethylene Glycol	osmotic sensitivity, ethylene glycol
PM09	D12	20% Ethylene Glycol	osmotic sensitivity, ethylene glycol
PM09	H02	20mM Sodium Nitrate	toxicity, nitrate
PM09	H03	40mM Sodium Nitrate	toxicity, nitrate
PM09	H04	60mM Sodium Nitrate	toxicity, nitrate
PM09	H05	80mM Sodium Nitrate	toxicity, nitrate
PM09	G01	20mM Sodium Phosphate pH 7	toxicity, phosphate
PM09	G02	50mM Sodium Phosphate pH 7	toxicity, phosphate
PM09	G03	100mM Sodium Phosphate pH 7	toxicity, phosphate
PM10	H04	X-α-D-Galactoside	α-D-galactosidase
PM10	H03	X-β-D-Glucoside	β-D-glucosidase
PM10	H07	X-β-D-Glucuronide	β-D-glucuronidase
PM10	H11	X-PO4	aryl phosphatase
PM10	H12	X-SO4	aryl sulfatase

PM10	A08	pH 8	pH, growth at 8
PM11	C01, C02, C03, C04	Bleomycin	DNA synthesis; polymerase inhibitor
PM11	B09, B10, B11, B12	Lomefloxacin	DNA unwinding; gyrase (GN); topoisomerase (GP); fluoroquinolone
PM11	E05, E06	Enoxacin	DNA unwinding; gyrase (GN); topoisomerase (GP); fluoroquinolone
PM11	H09	Ofloxacin	DNA unwinding; gyrase (GN); topoisomerase (GP); fluoroquinolone
PM11	E09, E10, E11	Nalidixic acid	DNA unwinding; gyrase (GN); topoisomerase (GP); quinolone
PM11	C06, C07, C08	Colistin	membrane; transport
PM11	D02, D03, D04	Capreomycin	protein synthesis
PM11	F01	Chloramphenicol	protein synthesis
PM11	A02, A03, A04	Amikacin	protein synthesis; 30S ribosomal subunit; aminoglycoside
PM11	F09, F10, F11	Neomycin	protein synthesis; 30S ribosomal subunit; aminoglycoside
PM11	G05, G06, G07, G08	Gentamicin	protein synthesis; 30S ribosomal subunit; aminoglycoside
PM11	H05, H06, H07, H08	Kanamycin	protein synthesis; 30S ribosomal subunit; aminoglycoside
PM11	C09	Minocycline	protein synthesis; 30S ribosomal subunit; tetracycline
PM11	D05	Demeclocyline	protein synthesis; 30S ribosomal subunit; tetracycline
PM11	F05, F06, F07, F08	Erythromycin	protein synthesis; 50S ribosomal subunit; macrolide
PM11	A09, A10, A11	Lincomycin	protein synthesis; lincosamide
PM11	E01	Cefazolin	wall; cephalosporin first generation
PM11	G01, G02, G03	Ceftriaxone	wall; cephalosporin third generation
PM12	F09, F10, F11, F12	5-Fluoroorotic Acid	
PM12	D05, D06, D07, D08	Sulfamethazine	folate antagonist
PM12	E05, E06, E07, E08	Sulfadiazine	folate antagonist
PM12	F05, F06, F07, F08	Sulfathiazole	folate antagonist
PM12	G05, G06, G08	Sulfamethoxazole	folate antagonist
PM12	B09, B10, B11, B12	Polymyxin B	membrane, outer
PM12	G02, G03	Spectinomycin	protein synthesis
PM12	C02, C03	Paromomycin	protein synthesis, aminoglycoside

PM12	D02	Sisomicin	protein synthesis, aminoglycoside
PM12	F01, F02	Tobramycin	protein synthesis, aminoglycoside
PM12	H02, H03, H04	Spiramycin	protein synthesis, macrolide
PM12	A05, A06	Tetracycline	protein synthesis, tetracycline
PM12	C09, C10	D,L-Serine Hydroxamate	tRNA synthetase
PM12	G09, G10, G11, G12	L-Aspartic-b-Hydroxamate	tRNA synthetase
PM13	G09	Trifluoperazine	cell cycle modulation, DNA synthesis, Ca(2+)/calmodulin dependent protein phosphorylation and lipid
PM13	B05, B06, B07, B08	2,2`-Dipyridyl	chelator, Fe++
PM13	B09, B10, B12	Oxolinic acid	DNA unwinding, gyrase (GN), topoisomerase (GP), quinolone
PM13	A05, A06, A07	Dequalinium	ion channal inhibitor, K+ (m)
PM13	D05, D06	5-Fluorouracil	nucleic acid analog, pyrimidine
PM13	E01, E02, E03, E04	Cytosine arabinoside	nucleic acid analog, pyrimidine
PM13	D09	Rolitetracycline	protein synthesis, 30S ribosomal subunit, tetracycline
PM13	H09, H10	Tylosin	protein synthesis, 50S ribosomal subunit, macrolide
PM13	E05, E06, E07, E08	Geneticin (G418)	protein synthesis, aminoglycoside
PM13	E09, E10, E11	Ruthenium red	respiration, mitochondrial Ca++ porter
PM13	C09	Potassium chromate	toxic anion
PM13	A09, A10	Nickel chloride	toxic cation
PM13	F02, F03, F04	Cesium chloride	toxic cation
PM13	F09, F11	Thallium (I) acetate	toxic cation
PM13	G01	Cobalt chloride	toxic cation
PM13	F05, F06, F07, F08	Glycine	wall
PM13	A02	Ampicillin	wall, lactam
PM13	H05, H06, H08	Moxalactam	wall, lactam
PM14	B07	Fusaric Acid	chelator, lipophilic
PM14	C05, C06	1-Hydroxy-Pyridine-2-thione	chelator, lipophilic
PM14	B01	9-Aminoacridine	DNA intercalator
PM14	E05, E06	Nitrofurantoin	DNA synthesis, nitro-compound, multiple sites
PM14	F01, F02	Chloramphenicol	protein synthesis

PM14	C09	Sodium Cyanate	transport, toxic anion
PM14	B09, B12	Sodium Arsenate	transport, toxic anion, PO4 analog
PM14	D09, D10, D11	Sodium Dichromate	transport, toxic anion, SO4 analog
PM14	E02	Cefoxitin	wall, cephalosporin
PM14	F05	Piperacillin	wall, lactam
PM15	C12	1,10-Phenanthroline	chelator, Fe++, Zn++, divalent metal ions
PM15	D02, D03	Phleomycin	DNA damage, oxidative, ionizing ratiation
PM15	D09	Nordihydroguaiaretic acid	lipoxygenase, fungicide
PM15	E09, E10, E11, E12	Methyl viologen	oxidizing agent
PM15	F01, F03	3, 4-Dimethoxybenzyl alcohol	oxidizing agent, free radical-peroxidase substrate
PM15	F05, F06, F07, F08	Oleandomycin	protein synthesis, 50S ribosomal subunit, macrolide
PM15	G05	Sodium azide	respiration, uncoupler
PM15	G09	Menadione	respiration, uncoupler
PM15	H09	Zinc chloride	toxic cation
PM15	B03	D-Cycloserine	wall, sphingolipid synthesis
PM16	E05, E06, E07, E08	5-Azacytidine	DNA methyltransferase
PM16	B01, B02, B03, B04	Norfloxacin	DNA topoisomerase, quinolone
PM16	B05, B06, B07, B08	Sulfanilamide	folate antagonist
PM16	B09	Trimethoprim	folate antagonist, dihyldrofolate reductase
PM16	H05, H06	Chloroxylenol	fungicide
PM16	C09	Cetylpyridinium Chloride	membrane, detergent, cationic
PM16	D01, D02	1-Chloro-2,4-Dinitrobenzene	oxidation, glutathione
PM16	D05, D06, D07	Diamide	oxidation, glutathione
PM16	D09, D11	Cinoxacin	protein synthesis
PM16	E03	Streptomycin	protein synthesis, aminoglycoside
PM16	H09	Sorbic Acid	respiration, ionophore, H+
PM16	F09, F10	Aluminum Sulfate	transport, toxic cation
PM16	G02	Chromium Chloride	transport, toxic cation
PM16	G09, G10, G11, G12	L-Glutamic-g-Hydroxamate	tRNA synthetase
PM16	A05, A06, A07, A08	Phosphomycin	wall
PM17	A05	b-Chloro-L-Alanine	aa analog, alanine, aminotransferase inhibitor
PM17	A09	Thiosalicylate	anti-capsule, thiol

PM17	B09, B10, B12	Ethionamide	anti-tuberculosic
PM17	H06	Caffeine	cyclic AMP phosphodiesterase
PM17	C05, C06, C07, C08	Sulfachloropyridazine	folate antagonist
PM17	C11, C12	Sulfamonomethoxine	folate antagonist
PM17	D05, D06, D07, D08	Aminotriazole	histidine biosynthesis, catalase
PM17	A01, A02	D-Serine	inhibits 3PGA dehydrogenase (L-serine and pantothenate synthesis)
PM17	B05, B06, B07, B08	Hygromycin B	protein synthesis, aminoglycoside
PM17	H09	Phenylarsine Oxide	tyrosine phosphatase
PM17	G09, G10, G11	Cetoperazone	wall, cephalosporin
PM18	G02, G03, G04	Triclosan	bacterial fatty acid synthesis, enoyl-acyl carrier protein reductase
PM18	F02	Semicarbazide hydrochloride	carbonyl agent, semicarbazide-sensitive amine oxidase, DNA damage
PM18	A05, A06	Sodium pyrophosphate decahydrate	chelating agent
PM18	G09	Myricetin	DNA & RNA synthesis, polymerase inhibitor (e. coli)
PM18	H05, H06	2- Phenylphenol	DNA intercalator
PM18	B05, B06, B07, B08	Pipemidic Acid	DNA unwinding, gyrase (GN), topoisomerase (GP), quinolone
PM18	C06, C08	Sulfisoxazole	folate synthesis, PABA analog
PM18	D09	Lidocaine	ion channal inhibitor, Na+
PM18	F05	Tinidazole	Mutagen, nitroimidazole (GP, GN)
PM18	B09, B10, B11	Azathioprine	nucleic acid analog, purine
PM18	H02, H03, H04	5-Fluoro-5'-deoxyuridine	pyrimidine antimetabolite: inhibits nucleic acid replication
PM18	C09, C10	Pentachlorophenol (PCP)	respiration, ionophore, H+
PM18	G05, G06, G07	3,5- Diamino-1,2,4-triazole (Guanazole)	ribonucleotide DP reductase
PM18	B02, B03, B04	Trifluorothymidine	thymidylate synthetase, DNA polymerase
PM18	D05, D06	Sodium bromate	toxic anion
PM18	E01	Sodium metasilicate	toxic anion
PM18	E05	Sodium periodate	toxic anion, oxidizing agent
PM18	F09, F10, F11	Aztreonam	wall, lactam
PM19	A10	Coumarin	DNA intercalator
PM19	C06, C07	Umbelliferone	DNA intercalator
PM19	H02, H03	Hexaminecobalt (III)	DNA synthesis

		Chloride	
PM19	B06	Harmane	imidazoline binding sites, agonist
PM19	D10	Phenyl-Methyl-Sulfonyl-Fluoride (PMSF)	protease inhibitor, serine
PM19	F05, F06	Blasticidin S	protein synthesis
PM19	A02, A03, A04	Josamycin	protein synthesis, macrolide
PM20	C05, C06	Atropine	acetylcholine receptor, antagonist
PM20	A05, A06, A07	Apramycin	antimicrobial, aminocyclitol
PM20	B05, B06	D,L-Propranolol	beta-adrenergic blocker
PM20	D06, D07, D08	Ciprofloxacin	DNA topoisomerase, quinolone
PM20	E05	Dodine	fungicide, guanidine, membrane permeability
PM20	D09	18-Crown-6-Ether	respiration, ionophore
Phenotypes Lost - less metabolic activity			
Plate Type	Wells	Test	mode of action
PM01	H06	L-Lyxose	C-source

[a] Wells were scored positive if the difference in the height of the respiration curve was above the threshold value in one experiment and a similar result occurred in the second experiment, albeit sometimes below the threshold value are listed.

Table T4.3 Growth of the *S. mutans* wild type and the Δ*rpoE* mutant in the falcon tubes.

		20 h		48 h	
		2 ml[b]	7 ml	2 ml	7 ml
WT[a]	supernatant	+++	+++	++	+++
	pellet	+	+	++	++
WT + Tet[c]	supernatant	+	+	-[d]	-
	pellet	+++	++++	+++	++++
WT + Kan[c]	supernatant	+++	+++	++	+++
	pellet	+	+	++	++
Δ*rpoE*	supernatant	++	+++	+	+++
	pellet	+	+	++	++
Δ*rpoE* + Tet	supernatant	-	-	-	-
	pellet	-	-	++++	++
ΔrpoE + Kan	supernatant	-	-	+	+++
	pellet	-	-	++	++

[a] Both wild type (WT) and the Δ*rpoE* mutant initial inoculums were taken from liquid culture at the log growth phase. Bacterial cells were grown at 37 ℃ enriched with 5% CO_2.
[b] The volume of inoculums in the 15 ml falcon tubes.
[c]+T, +K: growth in medium supplied with 1 μg/ml tetracycline, or 100 μg/ml kanamycin;
[d] '-' means no obvious growth, while '+' means slightly growth, and with the increase of number in '+' shows increase in growth or formation of pellet.

Supplementary PM procedures

PM Procedures for *E. faecalis* and other Lactic Acid Bacteria

SECTION I: MATERIALS

Section A. List of Equipment, Chemicals and Materials

Table 1. Equipment

Equipment	Source	Catalog #
OmniLog PM System	Biolog	93171, 93182, 93184
Turbidimeter	Biolog	3531, 3532, 3585
Multichannel Pipetter	Biolog	3501A, 3505A and B

Table 2. Chemicals and Materials for Inoculation Procedure

Chemicals and Materials	Source	Catalog #
PM panels 1-20	Biolog	12111, 12112, 12121, 12131, 12141, 12181, 12182, 12183, 12161, 12162, 12211-12220
IF-0a GN/GP Base inoculating fluid (1.2x)	Biolog	72268
IF-10b GN/GP Base inoculating fluid (1.2x)	Biolog	72266
Biolog Redox Dye Mix F (100x)	Biolog	74226
Biolog Redox Dye Mix G (100x)	Biolog	74227
Biolog Redox Dye Mix H (100x)	Biolog	74228
BUG+B agar plates	Biolog	71102
turbidity standard, 85% T	Biolog	3431
sterile cotton swabs	Biolog	3021
sterile pipet tips	Biolog	3001
sterile reservoirs	Biolog	3102
sterile 20 x 150 test tubes	E+K Scientific	266B
sterile 120 ml plastic vial	Capitol Vial Corp.	1-24-786
sealing tape for microplates (optional)	Phenix Research Products	LMT-SEAL-EX
tricarballylic acid	Sigma	T9251
magnesium chloride ($MgCl_2$, $6H_2O$)	Sigma	M0250
calcium chloride ($CaCl_2$, $2H_2O$)	Sigma	C3881
L-arginine, HCl	Sigma	A5131
L-glutamate, Na	Sigma	G1626
L-cystine	Sigma	C8755
uridine-5'-monophosphate (5'-UMP), 2Na	Sigma	U6375
hypoxanthine	Sigma	H9377
β-NAD, hydrate	Sigma	N7004
riboflavin	Sigma	R4500
yeast extract	Oxoid	L21
tween 40	Sigma	P1504
tween 80	Sigma	P1754
D-glucose	Sigma	G8270
pyruvate, Na	Sigma	P2256

Table 3. Composition and Preparation of 12x PM Additive Solutions

Prepare all 120x stock solutions, filter sterilize, and store at 4° C. Combine ingredients and Q.S. to 100 ml. Store at 4° C.

Ingredient	1x Conc.	40-120x Conc.	Formula Weight	Grams/ 100 ml	PM 1,2	PM 3,6,7,8	PM 4	PM 5	PM 9+
tricarballylic acid, pH 5.5 [a]	20mM	800mM	176.1	14.088	-	30ml	30ml	30ml	-
$MgCl_2$, $6H_2O$ $CaCl_2$, $2H_2O$	2mM 1mM	240mM 120mM	203.3 147.0	4.88 1.76	10ml	10ml	10ml	10ml	10ml
L-glutamate, Na	50uM	6mM	169.1	0.101	10ml	-	10ml	-	-
L-cystine pH8.5 [b] 5'-UMP, 2Na	12.5uM 25uM	0.5mM 1mM	240.3 368.1	0.012 0.037	30ml	30ml	-	-	-
L-arginine, HCl hypoxanthine β-NAD, hydrate riboflavin yeast extract tween 80 [c]	25uM 25uM 5uM 0.25uM 0.005% 0.005%	3mM 3mM 0.6mM 30uM 0.6% 0.6%	210.7 136.1 663.4 376.4 - -	0.063 0.041 0.040 0.0011 0.6 0.6	10ml	10ml	10ml	-	10ml
D-glucose pyruvate, Na [d]	2.5mM 5mM	300mM 600mM	180.2 110.0	5.40 6.6	-	10ml	10ml	10ml	10ml
sterile water					40ml	10ml	30ml	50ml	70ml
Total					100ml	100ml	100ml	100ml	100ml

[a]Prepare by adding 14.088g to 55ml of water and then adjust pH to 5.5 with NaOH. Dissolve with stirring and check the pH on the meter and with pH paper. Then Q.S. the final volume to 100ml.

[b]Adjust pH to 8.5 with NaOH and check with pH paper. Check the pH on the meter and with pH paper. Then add the 5'UMP and Q.S. the final volume to 100ml.

[c]Tween 80 is recommended Enterococcus faecalis. Some other species may prefer tween 40.

[d]If the A-1 well in PM3-8 is too false positive, the concentration of the glucose/pyruvate can be decreased to one half or one quarter of this concentration. Alternatively, the pH of the tricarballylic acid buffer can be lowered a little, for example to pH 5.0. If there are no reactions in PM3-8, the pH of the tricarballylic acid buffer can be raised, for example to 6.0, 6.5, or 7.0.

Table 4. Recipe for 1x PM Inoculating Fluids from Stock Solutions

PM Stock Solution	PM1,2 (ml)	PM3,6,7, 8 (ml)	PM4 (ml)	PM5 (ml)	PM9+ (ml)
IF-0a GN/GP (1.2x)	20.0	40.0	10.0	10.0	-
IF-10b GP/GP (1.2x)	-	-	-	-	110.0
Dye mix F, G or H [e] (100x)	0.24	0.48	0.12	0.12	1.32
PM additive (12x)	2.0	4.0	1.0	1.0	11.0
Sterile water	-	-	-	-	-
cells (13.64x)	1.76	3.52	0.88	0.88	9.68
Total	24.0	48.0	12.0	12.0	132.0

[e]Dye mix H is recommended for Enterococcus faecalis. In general, Dye mix F or H is used for fast growing GP genera (Listeria, Enterococcus) and Dye Mix G is used for slow growing GP genera (Streptococcus, Lactococcus, Lactobacillus).

SECTION II: PROCEDURES for PM Inoculation

Section A. Cell Suspension Preparation and PM Inoculation

Preparation of PM Inoculating Fluids

1. Prepare a test tube containing 20 ml of 1x IF-0a.
2. Prepare inoculating fluids as specified in Tables 3 and 4.
3. Dispense inoculating fluids into tubes as diagrammed in Figure 1.

Inoculation of PM Panels (see procedure diagrammed in Figure 1)

Step 1: Prepare Cell Suspension

Grow the bacterium on a BUG+B agar plate by streaking for isolated colonies and allow it to grow overnight at 33 °C. Subculture a second time.
Remove cells from the BUG+B plate using a sterile swab and transfer into a sterile capped tube containing 20 ml of 1x IF-0a. Stir the cell suspension with the swab to obtain a uniform suspension. Do not vortex or mix turbulently.
Check the turbidity of the suspension; add cells to achieve 81% T (transmittance).

Step 2: Inoculate PM 1,2

Add 1.76 ml of cell suspension to 22.24 ml of PM1,2 inoculating fluid.
Inoculate PM 1 and PM 2 with this cell suspension, 100 ul / well.

Step 3: For PM 3, 6, 7 and 8

Add 3.52 ml of cell suspension to 44.48 ml of PM3,6,7,8 inoculating fluid.
Inoculate PM 3, 6, 7 and 8 with this cell suspension, 100 ul / well.

Step 4: For PM 4

Add 0.88 ml of cell suspension to 11.12 ml of PM4 inoculating fluid.
Inoculate PM 4 with this cell suspension, 100 ul / well.

Step 5: For PM 5

Add 0.88 ml of cell suspension to 11.12 ml of PM5 inoculating fluid.
Inoculate PM 5 with this cell suspension, 100 ul / well.

Step 6: For PM 9+

Add 9.68 ml of cell suspension to 122.32 ml of PM9+ inoculating fluid.
Inoculate PM 9-20 with this cell suspension, 100 ul / well.

Figure 1. PM Procedures for *B. subtilis* and other GP Bacteria

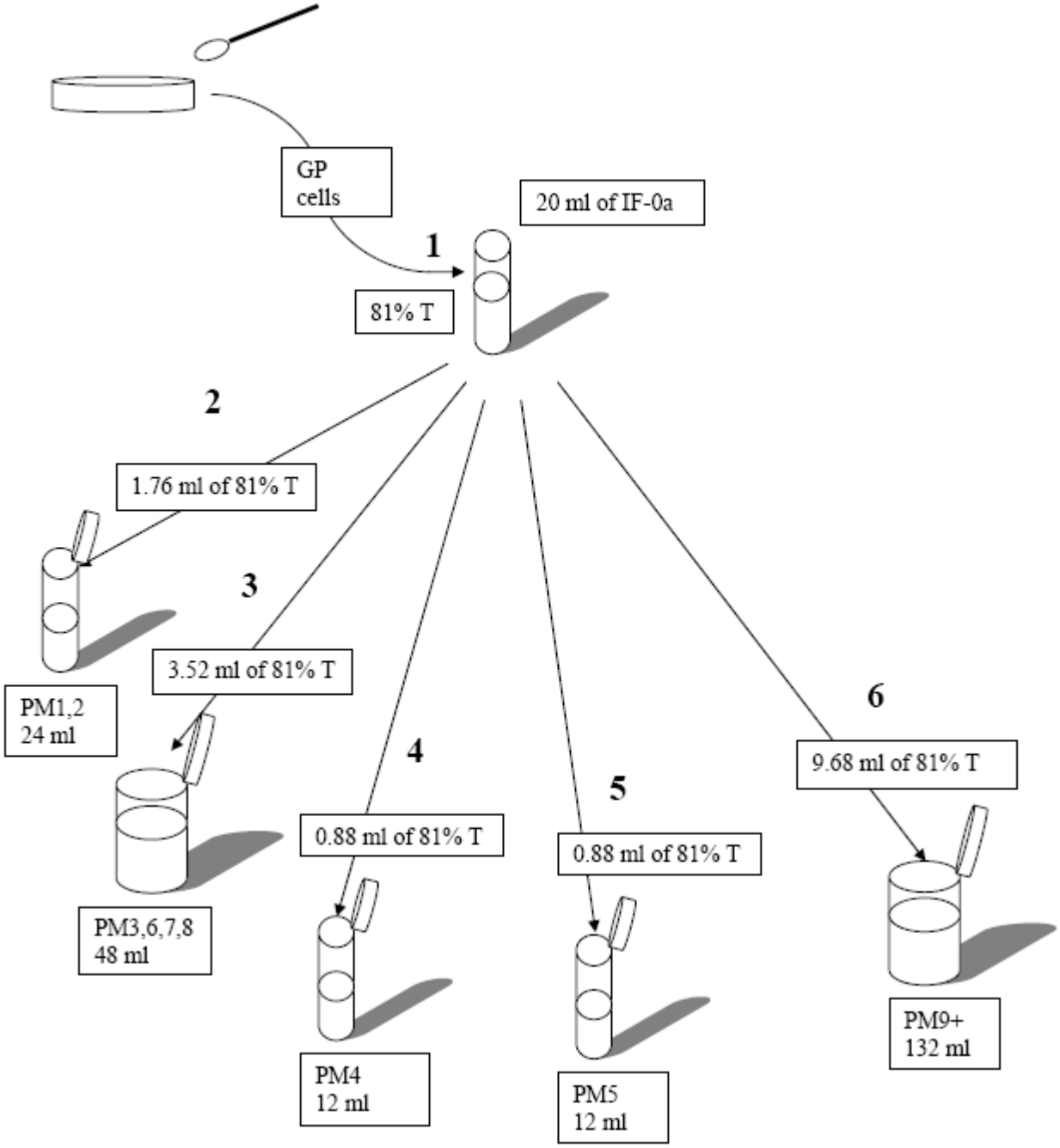

Section B. Incubation and Data Collection

1. Enter worksheet data into OmniLog Software.
2. Load the OmniLog.
3. Incubate all PMs in OmniLog at 30-37°C for 24-48 hours (e.g. 33°C, 36 hr).
4. Remove plates from OmniLog and store at 4°C.
5. Collect the data for analysis.

5 Chapter 5 - Material and methods

5.1 Bacterial strains, plasmids and growth conditions

Bacterial strains and plasmids used in this study are listed in Table 5.1. *Escherichia coli* strains were grown in Luria-Bertani medium (LB) (Carl-Roth, Germany) at 37 ℃. *Streptococcus mutans* UA159 strains were grown in Todd Hewitt broth (Becton Dickinson, USA) supplemented with 1% yeast extract (THBY) at 37 ℃ aerobically (5% CO_2 enriched) or in BM medium (39) containing 0.5% (w/v) glucose or sucrose under anaerobic conditions (80% N_2, 10% H_2, 10% CO_2). For stress tolerance assays, *S. mutans* strains were grown in THBY supplied with 75 mM phosphate buffer. Erythromycin was included where indicated at a final concentration of 200 μg/ml for *E. coli* and 10 μg/ml for *S. mutans*, Spectinomycin with 50 μg/ml for *E. coli* and 300 μg/ml for *S. mutans*. For coaggregation, strains *Streptococcus oralis* 7, *S. sanguinis* 22, and *Actinomyces naeslundii* (gifts from Dr. G. Conrads, Germany), and *Candida albicans* DSM 11225 were grown in THBY medium with or without supplementation of 0.5% (w/v) sucrose (THBYS).

5.2 Genetic modification of bacteria

5.2.1 Construction of a *S. mutans* Δ*rpoE* strain

PCR ligation mutagenesis (Lau *et al.*, 2002) was used for gene knockout in the *S. mutans* wild type chromosome. However, the *rpoE* knockout mutant was not obtained, presumably due to the importance of this gene. To increase the efficiency of recombination with a higher concentration of the whole DNA construct, the *rpoE* up-stream fragment, the erm^r gene, and the *rpoE* down-stream fragment, were amplified separately using primer pairs RP1F/ PR2R-AscI, ErmF-AscI/ ErmR-FseI, and RP3F-FseI/ RP4R (table 5.2), and then these 3 fragments were cloned step by step into the vector pCR2.1-TOPO to construct pCR2.1-Δ*rpoE*. The resulting plasmid was transformed into *E. coli* Top10F' cells. Positive clones were confirmed by PCR, sequencing and restriction enzyme digestion. The insertion with the complete *rpoE* up- erm^r -*rpoE* down sequence was released from pCR2.1-Δ*rpoE* by HindIII (NEB, England) and XhoI (NEB)

digestion, and then was transformed into *S. mutans* to generate Δ*rpoE* mutants through double homologous recombination. The deletion of *rpoE* was confirmed by PCR and sequencing.

Table 5.1 Bacterial strains and plasmids used in this study.

Strain/plasmid	Relevant characteristics[a]	Source /reference
***E. coli* strain**		
Top10F'	Strain for routine cloning work	Invitrogen
***S. mutans* strains**		
UA159	Wild type, Erm^s, Sp^s	ATCC 700610
Δ*rpoE*	UA159 with deletion of *rpoE* gene, Erm^r	This study
Δ*rpoE* comp	Complementation of the *rpoE* mutation, Erm^r, Sp^r	This study
WT-luc	*rpoE* reporter strain carrying pFW-P_{rpoE}-luc in wild type background, Sp^r	This study
Plasmids		
pCR2.1-TOPO	*E. coli* cloning vector	Invitrogen
pCR2.1- Δ*rpoE*	*E. coli* cloning vector containing the *rpoE* up-stream fragment, *erm*^{r} gene, and *rpoE* down-stream fragment	This study
pDL278	*E. coli*-streptococcal shuttle vector; Sp^r	20
pDL-*rpoE*	pDL278 harboring the promoter region and coding sequence of *rpoE*; Sp^r	This study
pFW5-luc	Streptococcal suicide vector containing promoterless firefly luciferase gene; derivate pFW5, Sp^r	36
pFW- P_{rpoE} -luc	pFW5-luc harbouring the promoter region of *rpoE* fused with luciferase gene; Sp^r	This study

[a] Erm^r, erythromycin resistance; Sp^r, spectinomycin resistance; luc, luciferase.

Table 5.2 Primers used in this study.

Primers	Sequence (5'→3') [a]	Description
RP1F	CGAGCTCTTCGGTAGAATCGG	*rpoE* upstream
PR2R-AscI	GGCGCGCCTTCACGAATGTCTGCATCTG	*rpoE* upstream
RP3F-FseI	GGCCGGCCATTCCAGATGAAGATTTAGAC	*rpoE* downstream
RP4R	GCTTCTGGAGCAACATCACA	*rpoE* downstream
ErmF-AscI	GGCGCGCCCCGGGCCCAAAATTTGTTTGAT	erm^r gene
ErmR-FseI	GGCCGGCCAGTCGGCAGCGACTCATAGAAT	erm^r gene
CPF-BamHI	TTCAGGATCCGATAAAAAGCAGCGTTCATA	*rpoE* complementation
CPR-HindIII	AGTCAAGCTTTTATTCTCCTTCTTCATCTTCC	*rpoE* complementation
RL5F-NcoI	TAGGCCATGGATAAAAAGCAGCGTTCATAT	*rpoE* reporter
RL5R-NcoI	CGTTCCATGGTGGTTCTCCTTATCATAATC	*rpoE* reporter
hisCF	CCCCTACTGGCATTTACAAG	QPCR, *hisC*
hisCR	CGATTGACCGCCAAAACTGA	QPCR, *hisC*
fruCF	TTGTTGCTGGTGGTGTTTTGG	QPCR, *fruC*
fruCR	GAGTCATAACGCCCATCGCA	QPCR, *fruC*
levDF	CAGTAGATGATTTTGCGGAAAC	QPCR, *levD*
levDR	GCTGTTGTCAAAGGGCTTCC	QPCR, *levD*
msmEF	GTTTGCTTTAGCGGGAACAG	QPCR, *msmE*
msmER	AATCGAATTTGGTTGGGAAAAG	QPCR, *msmE*
smu322F	TGCCTGTTAAGGTGATTATTGG	QPCR, SMU.322
smu322R	ATAAAGAAGCCTAGACTTGTCC	QPCR, SMU.322

[a] Restrictions sites underlined.

5.2.2 Complementation of the *rpoE* mutation *in trans*

To complement the *rpoE* mutation, a fragment of 1.2 kb containing the entire *rpoE* coding sequence plus the promoter region was amplified by PCR using primers CPF-BamHI and CPR-HindIII (table 5.2) from the chromosomal DNA of *S. mutans*, and inserted into the shuttle vector pDL278. The resulting plasmid pDL-*rpoE* was then transformed into the Δ*rpoE* mutant strain to generate the complementing strain Δ*rpoE*comp. The complementation of *rpoE* was confirmed by PCR and sequencing.

5.2.3 Construction of *rpoE*-luc reporter gene fusion.

To construct a luciferase transcriptional reporter fusion to the *rpoE* promoter, the promoter region of *rpoE* (0.6 kb) was amplified by PCR using primers RL5F-NcoI and RL5R-NcoI from the chromosomal DNA of strain UA159. The promoter region was then cloned into pFW5-luc to generate the plasmid pFW-P*rpoE*. The resulting construct was confirmed by restriction analysis, PCR, and sequencing. The confirmed plasmid was integrated into the chromosome of *S. mutans* via single-crossover homologous recombination, to generate the reporter strain WT-luc with the promoter region followed by the luciferase gene and the rest of the plasmid inserted before the intact *rpoE* promoter and coding sequence. The positive clones were confirmed by PCR, sequencing and luciferase assay. For the luciferase reporter assay, samples from each time point were collected and treated with chloramphenicol to reduce the intracellular enzymatic activity, and the OD_{600} was measured. Following treatment with chloramphenicol (50 μg/ml) and short cooling on ice, the samples were washed and resuspended in the same volume of 20 mM tricine buffer (pH 7.8). 100 μl of each sample was mixed with 3 × assay buffer (75 mM Tricine, 15 mM $MgSO_4$, 1.5 mM DTT, 900 μM ATP, 3 mg/ml BSA, 2% w/v D-glucose, pH7.8) and incubated at room temperature for 20 minutes before injection of 100 μl D-luciferin (120 μM solved in 20 mM tricine, pH 7.8). D-luciferin (Carl-Roth, Germany) stock solution (1 mg/ml) was solved in 20 mM tricine, aliquoted and stored at -70 ℃. Luminescence was recorded by Wallac Victor^2 and normalized against the OD_{600} to calculate the relative light units (RLU). All measurements were done in duplicate in at least two independent experiments.

5.3 Transcriptome analysis

5.3.1 Microarray design

A customized whole genome microarray containing all ORFs as well as all noncoding regions of *Streptococcus mutans* UA159 (gb|AE014133.1) has been used in this study. For microarray-design the earray-platform by Agilent has been utilized (https://earray.chem.agilent.com/earray/). For each open reading frame (ORF) and intergenic region, three antisense probes (60 bp in length) were designed and each probe was in duplicate on the array. The positive and negative controls from Agilent, and the spike-in control for GFPmut2 and RFPExpress, were included.

5.3.2 Sample preparation for microarray analysis

Overnight culture of *S. mutans* wild type and Δ*rpoE* were 1:20 diluted in fresh THBY medium buffered with 75 mM phosphate at pH 7.5 and grown at 37 ℃ aerobically until OD_{600} ~ 0.5. An aliquot of each log-phase cell culture was withdrawn as a control. At the same time point, the other part of the log-phase cells was collected (12000 × g, 30 sec) and incubated in buffered THBY as follows: (a) pH 7.5; (b) pH 5.0; (c) pH 7.5 + 2 mM H_2O_2; (d) pH 5.0 + 2 mM H_2O_2. After 2 hours of treatment, samples were collected (12000 × g, 30 sec). For each sample, two biological replicas were collected. 2 volumes of RNA protect (Qiagen) were immediately added to 1 volume of each sample, then mixed by vortexing for 5 seconds, and incubated at room temperature for 5 minutes. Pellets were collected by centrifugation (5000 × g, 5 min) and were stored at -70 ℃. For RNA isolation, the cell pellets were resuspended and lysed by incubation in tris buffer (10 mM Tris and 1 mM EDTA, pH 8.0) containing 2.5 mg/ml lysozyme (Sigma, Germany) and 50 U/ml mutanolysin (Sigma) at room temperature for 45 min, followed by vortexing 3 minutes in the presence of 50 µg sterile, acid washed glass beads (diameter 106 µm, Sigma) (60). RNA extraction was performed using the RNeasy mini kit (Qiagen). The integrity and quality of RNA was assessed by electrophoresis on a denaturing formaldehyde agarose gel. Traces of genomic DNA were removed by RNase-free DNase I (Qiagen) digestion (13.5 U, room temperature 45 min), and the RNA was purified using RNeasy mini kit (Qiagen). The

concentration of RNA was measured by the Nanodrop 1000 spectrophotometer (Peqlab, Germany). The genomic DNA contamination was checked by using RNA directly as template for PCR. Furthermore, the RNA quality was checked by Bioanalyzer (Agilent, Germany) before labelling.

5.3.3 Microarray analysis

For wild type and mutant strains, two biological replicas and two technical replicas for dye swabs were used in microarray study. RNA samples were labelled either with Cy3 or Cy5 using the ULS fluorescent labelling kit (Kreatech, Germany). The degree of labelling was calculated by the following formula: % Labelling = (340 × pmol dye × 100%) / (ng nucleic acid ×1000). 900 ng of each Cy3- and Cy5-labeled RNA was fragmented, and hybridized to the microarray at 65 ℃ for 17 hours using the Agilent Hybridization Chamber according to the manufacturer's instructions. The arrays were scanned using the Agilent DNA Microarray Scanner, and the raw data were extracted using Agilent Feature Extraction software (v9.5). The data were processed by Bioconductor packages written in R language (http://www.r-project.org/). The Linear Models for Microarray analysis (LIMMA) package (Wettenhall & Smyth, 2004) was used for background correction, Lowess-normalization of the two channels of one array, quantile-normalization between different arrays and identification of differentially expressed genes. Genes with log2 fold change >1.0 and p value <0.05 were selected for gene expression pattern discovery using clustering analysis from Genesis (Sturn *et al.*, 2002). KegArray (Kanehisa Laboratories, http://www.genome.jp/download/) was used for integrated analysis of gene expression profiles together with KEGG pathways. The function of genes was categorized into functional groups according to *S. mutans* Clusters of Orthologous Groups of proteins (COGs) functional categories file NC_004350.ptt, which was downloaded from (ftp://ftp.ncbi.nih.gov/genomes/Bacteria/Streptococcus_mutans).

5.3.4 Microarray data accession number

Microarray data have been deposited at NCBI-GEO (GSE22333).

5.3.5 Quantitative PCR

The reverse transcription reaction, performed on the same RNA samples which were used for microarray experiments, was carried out using 1.5 µg random hexamers and 200 U SuperScript III reverse transcriptase for 2 µg RNA samples in total volume of 30 µl (Invitrogen). The genomic DNA contamination was checked by a control without SuperScript III reverse transcriptase. Oligonucleotides primers for quantitative PCR were designed using Primer3 (http://frodo.wi.mit.edu/primer3/). For each set of primer pairs (table 5.2), a standard amplification curve was plotted (critical threshold cycle against log of concentration), and only those primer pairs with slopes about -3 were considered as reliable. Quantitative PCR was performed using the LightCycler 480 system (Roche, Germany) and the reaction mixtures were prepared using Quantitect SYBR Green PCR kit (Qiagen), including a non-template control. The expression of the hypothetical protein (SMU.322) was constant in the wild type and Δ*rpoE* mutant under all tested conditions in the microarray results, thus this gene was chosen as a reference gene for quantification. Changes in the level of gene expression were calculated using the $\Delta\Delta C_T$ method (Pfaffl, 2001). All steps were performed according to the manufacturer's protocols. All measurements were done in triplicate reactions.

5.4 Two-dimensional gel electrophoresis (2-DE)

5.4.1 Chemicals and enzymes

Amberlite, amidosulfobetaine-14 (ASB-14), 3[(3-Cholamidopropyl)dimethylammonio]-propanesulfonic acid (CHAPS), chloramphenicol, Coomassie Blue G-Colloidal Concentrate, diethanolamine, dithiothreitol (DTT), ethylenediaminetetraacetic acid (EDTA), phenylmethylsulfonyl fluoride (PMSF), thiourea, Triton X-100, trizma base, trypsin, and urea were obtained from Sigma-Aldrich. Roti-Aqua-Phenol was obtained from Roth. Ammonium persulfate was obtained from MERCK. Immobiline DryStrips (pH 4-7, 24 cm), IPG buffer (pH 4-7, pH 3-10) were purchased from GE Healthcare. Sypro-RuBPS (Ruthenium (II) tris bathophenantroline disulfonate) was self prepared according to the method described by Rabilloud et al (Rabilloud *et al.*, 2001).

5.4.2 Preparation of whole-cell protein lysates

Overnight cultures of the *S. mutans* wild type and the Δ*rpoE* mutant were 1:20 diluted in fresh THBY medium buffered with 75 mM phosphate buffer at pH 7.5 and grown at 37 ℃ aerobically until OD_{600} reaching about 0.5. An aliquot of each culture at log phase was withdrawn and used as a control for comparative proteome analysis. The rest log phase cells were collected by centrifugation (12,000 rpm, 30 sec) and incubated in buffered THBY medium for 2 hours as follows: (a) at pH 7.5; (b) at pH 5.0; (c) at pH 7.5 + 2 mM H_2O_2; (d) at pH 5.0 + 2 mM H_2O_2. Chloramphenicol at concentration of 50μg/mL and 1 mM PMSF were added immediately to the cultures before centrifugation at 5,000 rpm and 4 ℃ for 10 min. The pellets were washed twice in cold PBS (pH7.4) containing 1 mM EDTA, 50μg/ml chloramphenicol and 1 mM PMSF. After centrifugation, pellets were stored at -70 ℃ till use. For each sample, two biological replicates were analyzed.

Whole-cell protein lysate preparation was carried out according to methods described before (Wang *et al.*, 2005;Wang *et al.*, 2006) with some modifications. Briefly, cell pellets were resuspended in 1.5 ml lysis buffer (OD_{600} about 30) containing 7 M urea, 2 M thiourea, , 2% (w/v) CHAPS, 40 mM DTT, 0.5% (w/v) ASB-14, 0.5% (w/v) Triton X-100, and 1mM Pefabloc. Cells were disrupted using a FastPrep-24 high-speed homogenizer (MP Biomedicals) with the Lysis Matrix C tubes containing 0.1 mm silica spheres. Disruption was performed for 8 cycles of 1 min at a speed of 6.0 m/sec with 5 min interval between each cycle. Following centrifugation at 13,000 rpm for 10 min, the supernatant of the samples were collected and purified by phenol precipitation (Carpentier *et al.*, 2005;Saravanan & Rose, 2004). After resuspended the pellet in the lysis buffer, the protein concentrations were determined by the 2-D Quant Kit according to the manufacturer's instruction (GE Healthcare).

5.4.3 2-DE

For each sample, 250 μg of each whole-cell protein lysate in the rehydration buffer containing 7 M urea, 2 M thiourea, 2% (w/v) CHAPS, 40 mM DTT, 0.5% (w/v) amidosulfobetaine-14 (ASB-14), 0.5% (w/v) Triton X-100, and 0.5% v/v IPG buffer pH 4-7, was loaded onto a Immobiline DryStrip gel (24 cm, pH 4-7). The first dimension isoelectric focusing was run on an IPGPhor

Isoelectric Focusing System (GE Healthcare) at 20 ℃ for a total of 100.5 kVh (30 V for 6 h, followed by 60 V for 6 h, 200 V for 1 h, 500 V for 1 h, 1000 V for 1 h, gradient to 8000 V within 30 min and 8000 V for 12 h). After focusing, the proteins were reduced by incubating the IPG strips with 1% w/v DTT for 15 min and then alkylated with 2.5% w/v iodoacetamide for 15 min in 15 ml equilibration buffer (50mM Tris-HCl, pH8.8, 6M urea, 30% w/v glycerol, 2% w/v SDS). The strips were then transferred to 12.5% SDS-PAGE gels for second dimension using a vertical slab separation unit Ettan Dalt II System (GE Healthcare) with running conditions 2 W/gel for 1 h and then 15 W/gel until the the bromophenol blue dye reached the bottom of the gel. Gels were fixing overnight in a fixing solution (10% v/v glacial acetic acid, 30% v/v ethanol, 60% v/v MilliQ water), washed 3 times (30 min each time) in washing solution (20% v/v ethanol, 80% v/v MilliQ water). Gels were transferred to (250 ml/gel) Sypro-RuBPS staining solution (2 µM Sypro-RuBPS fluorescent dye in washing solution) and stained in the dark overnight. After equilibrated in MilliQ water 2 times (10 min each time), the gels were destained (40% v/v ethanol, 10% v/v acetic acid) for 15 hours.

5.4.4 Image acquisitions and analysis

Destained gels were scanned with a CCD based Fujifilm LAS-1000 image analyzer using the parameters described before (Wang *et al.*, 2006). The images from 24 gels (2 biological replicates and 0-2 technical replicates for both wild type and the mutant strains in each of five conditions) were analyzed by using Progenesis SameSpots (Non-linear dynamic, UK) software (version 3.3). Image alignment was based on automatic default analysis and manual editing of matched vectors. The spot detection was performed simultaneously across all of the images, obtaining a master list of detected spots and corresponding spot boundaries for quantification of protein spot volume. For calibration of gel-gel variation and for spot volume normalization, an improved method, instead of the traditional Total Spot Volume approach, was used (http://www.nonlinear.com/support/progenesis/samespots/faq/normalisation.aspx). Normalized spot volumes were used for comparison. P values of differentially expressed proteins were calculated according to the one way Anova test. The whole dataset of each group was used for principle component analysis to have a general overview of data variation, by using the Bioconductor packages written in R language (http://www.r-project.org/).

5.4.5 Protein identification

2-DE gels were further stained using Brilliant Blue G-Colloidal Concentrate according to the manufacturer's instruction. Protein spots of interest (fold of changes >= 2 and P<0.05 in at least one comparison) were excised from gels and subjected to tryptic digestion according to a method described previously (Wang *et al.*, 2003;Wang *et al.*, 2005) with some modifications. Briefly, protein spots were excised to 96-well microtiter plates and rinsed with acetonitrile, washed twice with MilliQ water and 50 mM NH_4HCO_3 in turn, destained by washing in 50 mM NH_4HCO_3 and acetonitrile alternatively for several times until Coomassie dye became nearly invisible. Then gel pieces were dehydrated with acetonitrile and dried completely by lyophilisation. After in-gel tryptic digestion and extraction by 5% formic acid and actonitrile sequentially, the pooled peptide extracts were concentrated by lyophilisation and spotted on Prespotted Anchorchip (PAC 384/96 CHCA, Bruker, Germany) according to the manufacturer's instruction.
Subsequently, the tryptic peptides were analyzed by MALDI-TOF MS with a Bruker Ultraflex time-of-flight mass spectrometer (Bruker Daltonics GmbH). Peptide masses obtained from MALDI-TOF MS analysis were used for protein identification by peptide mass fingerprinting (PMF) using the MASCOT program licensed in-house to search the strain-specific protein database "smu" which was downloaded from NCBI (URL: ftp://ftp.ncbi.nih.gov/genomes/Bacteria/Streptococcus_mutans/NC_004350.faa) and installed on our local Mascot server. Parameters for protein identification included a mass tolerance of 100 p.p.m. and allowed up to one missed cleavages per peptide while taking into consideration carboxymethyl (fix modification) and methionine oxidation modifications (variable modification). Protein score is -10*Log(P), where P is the probability that the observed match is a random event. Protein scores greater than 45 are considered as positive results ($p<0.05$).

5.5 Phenotypic characterization

5.5.1 Antibiotic resistance

Overnight cultures of *S. mutans* strains were 1:10 diluted in fresh THBY, and grown until OD_{600} ~ 0.5. 0.2% of the log-phase cells were added to fresh THBY medium which contained antibiotics at different concentrations. After 16 hr of incubation at 37 ℃ aerobically, visible growth of bacteria was determined by the turbidity by eyes.The antibiotics included kanamycin (100 mg/ml in H_2O), tetracycline (25 mg/ml in 70% ethanol), ampicillin (100 mg/ml in H_2O), rifampicin (25 mg/ml in methanol), at final concentrations 0.1, 1, 10, 100, 500 μg/ml. A second experiment was carried out at a smaller concentration range to determine the exact inhibitory concentration of growth.

5.5.2 Acid and H_2O_2 stress killing assays

The ability of *S. mutans* strains to survive acidic and oxidative stress challenge was determined according to Wen et al. with some modifications (Wen *et al.*, 2006). Briefly, overnight cultures of wild-type, Δ*rpoE* and Δ*rpoE*comp were diluted 20-fold in fresh THBY and grown to mid-exponential phase (OD_{600} ~ 0.5) in THBY at pH7.5, and two aliquots (1 ml) of each cell suspension were pelleted by centrifugation (12000 × g, 30 sec). One aliquot of the culture was used to assay the survival of 'unadapted' cells by directly resuspending them in THBY at the challenge stresses pH 3.0 or pH 7.5 + 20 mM H_2O_2. Another aliquot of each culture was resuspended in the same volume of THBY buffered at pH 5.0 or pH 7.5 + 2 mM H_2O_2 and incubated for 2 h to induce an adaptation response. The resulting 'adapted' cells were then exposed to the challenging stresses pH 3.0 or pH 7.5 + 20 mM H_2O_2. After incubation for 30 min, cells were collected by centrifugation (12000 × g, 30 sec) and serially diluted with fresh THBY. Aliquots of 100 μl of appropriate dilutions of each strain were spread in 4-8 replicates onto THBY agar plates. The survival rate was expressed as the percentage of cells surviving the challenge for 30 minutes compare to the total viable cells before treatment.

5.5.3 Self-aggregation assay

Self-aggregation assays were carried out as previously described with minor changes (Ahn *et al.*, 2009). Briefly, cultures of *S. mutans* strains at stationary growth phase were collected by centrifugation (12,000 rpm, 30 sec), washed twice and resuspended in PBS (pH 7.4) to reach an optical density (OD_{600}) of about 0.6 and transferred to cuvettes. Samples were incubated at 37 ℃ for 2 h and the OD_{600} was recorded at different time intervals. Before measurement, samples were equilibrated at room temperature for 5 min. Percent of aggregation was calculated as (OD_{600} at time zero - OD_{600} at time x min) / (OD_{600} at time zero) × 100%.

5.5.4 Coaggregation with oral microorganisms

The coaggregation assay was carried out as described before (Cisar *et al.*, 1979;Periasamy *et al.*, 2009). The interactions of *S. mutans* wild type and the Δ*rpoE* mutant with the oral microorganisms *S. sanguis*, *S. oralis*, *A. naeslundii*, and *C. albicans* were investigated. The overnight cultures of these strains were 1: 10 diluted in fresh THBY or THBYS (supplied with 0.5% w/v sucrose) media and cultivated until an OD_{600} of about 0.4 had been reached, corresponding to the logarithmic growth phase. The cells were harvested by centrifugation (5000 rpm, 5 min), washed twice and resuspended in coaggregation buffer (0.1 mM $CaCl_2$, 0.1 mM $MgCl_2$, 0.15 M NaCl dissolved in 1 mM Tris adjusted to pH 8) to give an OD_{600} of about 0.4. 1 ml of each microbial suspension was combined in a falcon tube and vortexed for 10 sec. Individual bacterial suspensions were used as a control. Coaggregation was scored after 90 min according to Cisar et al. (Cisar *et al.*, 1979) to evaluate the degree of coaggregation flocs by viewing the tubes with the naked eye. The scores ranged from - to ++++, as follows: -, no evidence of coaggregates in the mixed suspensions; +, finely dispersed coaggregates which did not precipitate immediately; ++, definite coaggregates easily seen, but there was no immediate settling of coaggregates; +++, formation of large precipitating coaggregates; and ++++, large coaggregates that precipitated immediately. Additionally, after 90 min of coaggregation, the turbidity (OD_{600}) of the supernatant above the flocs was measured to confirm the strength of aggregation quantitatively.

5.5.5 Biofilm formation and confocal laser scanning microscope (CLSM)

The ability of *S. mutans* strains to form stable biofilms was assessed by growing the cells in 96-well black microtiter plates with flat-bottom (Corning, Germany) containing THBY or BM medium supplemented with either 0.5% (w/v) sucrose under anaerobic conditions and grown for 16 hours. Precultures were grown at 37 ℃ aerobically for 13-15 hr to reach stationary phase. Then the precultures were 1:10 diluted in fresh THBY, and grown until log-phase (OD_{600} ~ 0.5). The cells were collected by centrifugation (12000 × g, 30 sec) and resuspended in fresh medium to reach an OD_{600} ~ 0.01. Aliquots of 200 µl of the cell suspension were inoculated into 12 parallel wells of the microtiter plates and grown under anaerobic condition. Several plates were prepared to quantify the biofilms at different time points. After growth, the culture medium was withdrawn, and the plates were rinsed with 0.85% NaCl to remove the planktonic and loosely bound cells. The biofilms were stained with 50 µl Live/Dead BacLight stain (L7012, Invitrogen) working solution and the biofilm architecture was recorded using the FluoView FV1000 CLSM (Olympus, Germany). In each experiment, exciting laser intensity, background level, and contrast were maintained at the same level. For each sample, two replicas and at least three random fields per replica were analyzed. Using a 40 × objective lens, a series of optical cross-section images were acquired at 2 µm depth intervals from the surface, through the vertical axis of the specimen. Three dimensional confocal images were reconstituted by the software Imaris (BitPlane AG, Switzerland). For biofilm quantification, the plates with biofilms were rinsed three times with deionised water. The biofilms were stained with 50 µL of 0.1% crystal violet and incubated at room temperature for 15 minutes. After rinsing 2 times with deionised water, the bound dye was extracted from the stained cells by adding 200 µL of 99% ethanol, shaking overnight at room temperature to facilitate full release of the dye. The biomass was quantified by measuring the absorbance of the dye solution at 620 nm in Wallac Victor (Perkin Elmer, Germany). Each experiment was carried out at least three times.

5.5.6 Biofilm detachment

Bacterial cells from the early stationary phase (OD_{600} ~2) were collected by centrifugation (12,000 rpm, 30 sec), washed once and then diluted 1:100 in BMS medium to an initial OD_{600} ~0.02. 48-well polystyrene plates (Nunc, Roskilde, Denmark) were inoculated with 400 µl cell suspension and biofilms were cultured anaerobically for 16 h . The planktonic phase was removed, biofilms were washed once with water, and treated with (1) 1 mg/ml Proteinase K (>30 U/mg dry weight) (Sigma, Germany); (2) 0.2 mg/ml DNase I (>60,000 Dornase unit/mg dry weight) (Calbiochem, Germany); (3) 10 mM sodium *meta*-periodate (Thermo Science, Germany). Control wells were treated with water alone. Plates were incubated at 37 ℃ for 1 h, after then the biofilms were quantified by crystal violet staining as described before (Xue *et al.*, 2010). For each experiment, eight biological replicates were performed; the mean value and standard deviation were calculated accordingly. The experiment was repeated four times. The results from one representative experiment are shown.

5.5.7 Inhibition of biofilm growth

S. mutans strains at late exponential phase (OD_{600} ~ 1) were collected by centrifugation (12,000 rpm, 30 sec), washed once and resuspended in BMS medium supplied with 1 mg/ml Proteinase K, while control cells were grown in BMS medium alone. Biofilms were cultured in 48-well polystyrene plates for 1, 2, 3, 4 h, and after then the biofilms were quantified by crystal violet staining as described above. For each experiment, eight biological replicates were performed; the mean value and standard deviation were calculated accordingly. The experiment was repeated four times. The results from one representative experiment are shown.

5.5.8 Analysis of the extracellular biofilm matrix

Bacterial cells of *S. mutans* strains from the early stationary phase (OD_{600} ~2) were collected by centrifugation (12,000 rpm, 30 sec), washed once and then diluted 1:100 in BMS medium to an initial OD_{600} ~0.02. Biofilms were grown in polystyrene petri dishes (Nunc Lab-Tek™, Roskilde,

Denmark) in 5 ml BMS medium for 16 h anaerobically. The planktonic phase was removed, and the biofilms were washed three times with sterile water to remove loosely bound material. The biofilm cells were collected by scraping and resuspended in sterilized water supplemented with a protease inhibitor cocktail (Cat. No. 04693124001, Roche, Germany) and chloramphenicol (50 µg/ml). For each strain, eight biofilm samples were pooled (final volume of 5 ml) and digested with 75 U/ml N-glycanase (NEB, England) at 37 ℃ for 1 h to disrupt the biofilm flocs. The digested samples were used for biomass, polysaccharide, extracellular DNA and protein determinations. For biomass (dry weight) determination, three volumes of cold ethanol (-20 ℃) were added to 1 volume of biofilm suspension, and centrifuged at 10,000 g for 5 min at 4 ℃. The pellets were washed two times with cold ethanol, vacuum dried (Eppendorf Concentrator 5301, Germany) and weighed. The extracellular polysaccharides (soluble and insoluble)–were extracted as described before (Aires *et al.*, 2008). The amount of total carbohydrates was determined by the phenol-sulfuric acid method (Masuko *et al.*, 2005). Extracellular DNA was extracted using the cetyltrimethylammonium bromide (CTAB)-DNA precipitation method (Corinaldesi *et al.*, 2005;Wu & Xi, 2009). For extracellular protein extraction, 500 µl of (1) 0.5 M NaOH containing 5 mM EDTA (Cury *et al.*, 2000); or (2) 0.5% Triton X-100 were added to 2 ml biofilm samples and incubated at 4 ℃ for 1 h with agitation. The extracts were centrifuged at 10,000 g for 10 min at 4 ℃. One volume of a solution containing 20% trichloracetic acid (TCA), 80% acetone and 0.14% 2-mercaptoethanol (2ME) was added to the supernatant and proteins wereprecipitated at -20 ℃ for at least 1 h. Pellets were collected by centrifugation (10,000 g for 10 min), washed with acetone supplemented with 0.07% 2ME, and kept at -20 ℃ for at least 1 h. Pellets were collected by centrifugation (10,000 g for 15 min) and vacuum dried (Eppendorf Concentrator 5301, Germany). Pellets were resuspended in 150 µl 50 mM Tris buffer (pH 6.8). The protein concentration was determined using the Coomassie (Bradford) protein assay kit (Thermo Science, Germany). The extracellular proteins extracted from about 5 mg biomass of the wild type and the Δ*rpoE* mutant were subjected to SDS-PAGE using 7.5% and 12% separating gels. The gels were stained using EZBlue Gel staining reagent (Sigma, Germany) according to the manufacturer's instruction. Prestained protein standard marker (BioRad, Germany) was used. The interesting protein bands were excised, digested with trypsin, and analyzed by MALDI-TOF MS (Matrix-Assisted-Laser-Desorption/Ionization-Time-Of-Flight Mass Spectrometry) as described before (Wang *et al.*, 2003). The obtained peptide masses were

used for protein identification by peptide mass fingerprinting (PMF) using the MASCOT program. Protein score is -10*Log(P), where P is the probability of a random event; scores higher than 81 are considered as significant ($P<0.05$). For proteins not identified by MALDI-TOF/PMF, the most abundant peptide ions are then subjected to MS/MS analysis to determine the sequence. The results from both analyses were combined and searched for protein identification using the program MASCOT. Ions score is -10*Log(P), while P is the probability of a random event. Ions scores >51 indicate identical peptide identity or extensive homology ($P<0.05$). Protein scores are then derived from ions scores as a non-probabilistic basis.

5.6 Binding to human extracellular matrix (ECM) components

ECM microtiter plates precoated with collagen I, collagen II, collagen IV, fibronectin, laminin, tenascin and vitronectin and BSA (as a negative control) were purchased from Chemicon (Millipore, Germany). The ECM assay was performed as described before with minor modifications (Vollmer *et al.*, 2010). Briefly, the overnight cultures of *S. mutans* wild type and the Δ*rpoE* mutant were 1:10 diluted with fresh THBY medium and cultivated until late exponential phase (OD_{600} ~ 1.0). 100 µL of cultures were inoculated into precoated wells and incubated for 2 h at 37 ℃ without agitation. In parallel, bacterial cultures were serially diluted and plated on THBY agar plates in three replicates for colony forming unit (CFU) counting. After 2 h incubation, the ECM plate was washed two times with PBS (pH 7.4) and dried for 20 min under the cleanbench. The attached bacteria were stained with 100 µl of 0.4% crystal violet at room temperature for 45 min. After washing five times with PBS and drying under the cleanbench, the crystal violet dye was extracted by adding 100 µL of absolute ethanol and incubating for 2 h at room temperature with agitation. The supernatant (50 µl) was transferred to a microtitre plate and absorbance was measured at 620 nm with the Wallac Victor multi-label counter (Perkin-Elmer, Germany). For each ECM component, both strains were tested in five replicates, while the THBY medium without cells was measured in two replicates as a negative control. Mean and standard deviation were calculated from the replicate samples.

5.7 Adherence and infection of human cells

5.7.1 Cultivation of epithelial and endothelial cells

The human epithelial cell line HEp-2 (ATCC CCL23) (Hela derivative) was cultured in Dulbecco's modified Eagle's medium (DMEM; GibcoBRL, Karlsruhe, Germany) supplemented with 10% fetal calf serum (FCS; GibcoBRL), 5 mM glutamine, penicillin (100 U/ml), and streptomycin (100 mg/ml) as described (Molinari *et al.*, 1997). Primary human large vascular endothelial cells (HUVEC) isolated from umbilical cord were purchased from PromoCell (Cat. No. 12200, Heidelberg, Germany). Endothelial cells were cultured and propagated with a maximum of eight passages in EGM-2 medium (PromoCell) with 5 mM glutamine, penicillin (100 U/ml), and streptomycin (100 mg/ml) according to the supplier's protocol. For adherence and invasion assays, cells were resuspended and seeded onto coverslips in multiwell plates (Nunc, Roskilde, Denmark) at a concentration of 1×10^5 cells/ml (500 µl/well) and cultivated for 24 hours to reach confluent monolayers. Cultured cells were maintained in a cell incubator at 37 ℃ in an atmosphere containing enriched 5% CO_2.

5.7.2 Bacterial adherence and invasion assays

Monolayers of epithelial or endothelial cell were cultivated as described above. The media were exchanged to fresh media (without antibiotics), and the cells were incubated for 1 hour. *S. mutans* wild type and the Δ*rpoE* mutant from the stationary growth phase (OD_{600} ~ 2) were harvested by centrifugation (5000 rpm, 20 min), washed once with PBS and adjusted to an OD_{600} ~ 1, and diluted 1:20 in DMEM (HEp-2 medium) or EGM (HUVEC medium) supplied with 5% fetal calf serum. Bacterial density was determined by CFU counting. 250 µl bacterial inoculum (5×10^7 CFU/ml) were added to the epithelial or endothelial cells at a multiplicity of infection (MOI) of 125:1 (1.25×10^7 CFU bacteria at 1×10^5 cells per well), and incubated for 1-4 hours. The supernatant was taken for quantification of the lactate dehydrogenase (LDH) enzyme that is released upon cell lysis using the CytoTox 96 non-radioactive cytotoxicity assay (Promega, Germany) according to the manufacturer ́s instruction.

5.7.3 Immunofluorescence microscopy

Epithelial or endothelial cells infected with *S. mutans* strains were washed twice with fresh medium, fixed with PBS containing 4% paraformaldehyde, and stained for extra- and intracellular bacteria using a polyclonal rabbit anti-*S. mutans* antibody (Abcam, USA) and Alexa Fluor 488-(green) and 568-(red) conjugated goat anti-rabbit IgG as described before (Kaur *et al.*, 2010). Immunofluorescence was visualized under the Axiophot microscope (Zeiss) and eight to ten random images of each coverslip were recorded using the AxioCam HRc camera and AxioVision software (version 4.7). The number of cells and adherent bacteria were counted. For each image, the mean value and standard deviation of the ratio of bacteria/cell were calculated from six coverslips obtained from three independent experiments.

5.8 Field emission scanning electron microscopy (FESEM)

HEp-2 cells infected with *S. mutans* strains were fixed with 5% formaldehyde and 2% glutaraldehyde in cacodylate buffer (0.1 M cacodylate, 0.01 M $CaCl_2$, 0.01 M $MgCl_2$, 0.09 M sucrose, pH 6.9). For morphological analysis of the biofilm structure, biofilms of *S. mutans* wild type and the Δ*rpoE* mutant were grown on plastic coverslips as described above for the determination of extracellular biofilm matrix components. Biofilms were washed and fixed with 5% formaldehyde and 2% glutaraldehyde in cacodylate buffer, dehydrated, critical-point dried and sputter coated with gold as described before (Kockritz-Blickwede *et al.*, 2008). The images were taken by a field emission scanning electron microscope (Zeiss DSM 982 Gemini) using the Everhart Thornley SE detector and the inlens detector in a 50:50 ratio at an acceleration voltage of 5 kV.

5.9 Phenotype microarray (PM) tests

PM tests were performed using Biolog's PM facility of the DSMZ, essentially as described elsewhere (Bochner *et al.*, 2001;Zhou *et al.*, 2003). The PM experiments included eight metabolic arrays supplied with different carbon sources, nitrogen sources, phosphorus sources,

and sulphur sources (PM 1-8) and 12 sensitivity arrays that contained inhibitory compounds (PM 9-20). Both the wild type and the Δ*rpoE* mutant were subjected to full 20-panel PM analysis according to the Biolog's procedures for ''*Enterococcus faecalis* and other lactic acid bacteria'' (Supplementary materials in chaper 4, PM procedures). To improve the response of *S. mutans* for PM 3 – PM 8, four different pH values (5.5 to 7.0) for tricarballylic acid pH were tested in a pilot experiment with PM 3. The best results could be obtained at pH 6.5, and this pH was used in the subsequent experiments for PM 3 – PM8.The PM tests were repeated in two independent experiments. The formation of the tetrazolium redox dye was recorded every 15 min for 96 hours, and data were analyzed with the OmniLog-File Management and Parametric Management softwares (version 1.20.02). A height difference threshold of 50 for metabolic arrays (PM 1 – PM 8) and a threshold of 100 for sensitivity assays (PM 9 – PM 20) was used to determine metabolic activity differences. Detailed information about the PM technique is available at http://www.biolog.com.

6 - Summary

The results from this study show the multi-dimensional influence of the delta subunit of RNA polymerase, RpoE, in the human dental caries pathogen *Streptococcus mutans* on transcriptome, proteome and phenome levels.

Transcriptome analysis

Construction of *rpoE* knockout mutant and its genetic complementation strain

1. Inactivation of *rpoE* caused impaired growth, altered biofilm formation, reduced resistance to certain antibiotics, acid and oxidative stresses.
2. Complementation of the mutant with *rpoE* expressed in *trans* restored its phenotype to wild type.

Characterization of *rpoE* gene expression

3. The luciferase fusion reporter showed that *rpoE* was highly transcribed throughout growth.
4. The *rpoE* expression was repressed by acid and hydrogen peroxide stresses.

Transcriptome profiling of the Δ*rpoE* mutant

5. Transcriptome comparison of wild type and Δ*rpoE* cells under five conditions revealed differential expression of 550 genes, among them a core-set of 24 genes involved in histidine synthesis, malolactic fermentation, biofilm formation, and antibiotic resistance, which were always down-regulated in the Δ*rpoE* mutant.
6. Moreover, the loss of RpoE resulted in dramatic changes in transcription of genes required for transport and metabolism of carbohydrates and amino acids.
7. Interestingly, 330 intergenic regions had altered expression, most of which were upregulated in the Δ*rpoE* mutant.

Proteome analysis

Proteome response of *S. mutans* wild type under stresses

8. The transition to the stationary growth phase (nutrient starvation) resulted in a shift to proteins required for an alternative carbohydrate metabolism.
9. Oxidative stress (2 mM H_2O_2) induced a very strong response, including changes in proteins for oxidative stress defense, general stress, glycolysis, translation and transcription.
10. Weak acid stress (pH 5) induced proteins for malolactic fermentation (MLF) and branched chain amino acids (BCAAs) biosynthesis, two known acid defense systems of *S. mutans*, as well as proteins required for protection against oxidative stress.
11. The response to oxidative stress was reduced when it was combined with acid stress, indicating that *S. mutans* cells which are adapted to low pH are prepared for the stronger stress caused by H_2O_2.

Effect of the *rpoE* mutation on *S. mutans* proteome

12. Loss of RpoE caused changes in proteins responsible for the acid defense and carbohydrate metabolism, downregulation of general stress proteins and upregulation of several tRNA synthetases.
13. Compared to the wild type, the Δ*rpoE* mutant was not able to respond discriminately to adaptive stresses. This was observed for the attenuated responses at entry into the stationary growth phase, and for the oxidative stress.
14. Acid stress had stronger effect on the Δ*rpoE* mutant, indicated by induction of general stress proteins and repression of translation related proteins.
15. The acid and oxidative cross-protection was reduced in the Δ*rpoE* mutant due to the weaker changes of the mutant under the oxidative stress.

Phenome analysis

Virulence related traits of the Δ*rpoE* mutant

16. The Δ*rpoE* mutant showed higher self-aggregation compared to the wild type and coaggregated with other oral bacteria and *Candida albicans*.
17. It formed a biofilm with a different matrix structure and an altered surface attachment. The amount of the cell surface antigens I/II SpaP and the glucosyltransferase GtfB was reduced.
18. The Δ*rpoE* mutant displayed significantly stronger adhesion to human extracellular matrix components, especially to fibronectin, than the wild type.
19. Its adhesion to human epithelial cells HEp-2 was reduced, probably due to the highly aggregated cell mass.

Phenotype microarray (PM) comparison

20. The analysis of 1920 physiological traits using phenotype microarrays showed that the Δ*rpoE* mutant metabolized a wider spectrum of carbon sources than the wild type and had acquired resistance to antibiotics and inhibitory compounds with various modes of action.
21. Independent growth experiments showed that in *S. mutans* the resistance to certain antibiotics is dependent on the growth conditions.

The function of RpoE in *S. mutans* is summarized in Fig. 6.1. Loss of RpoE resulted in dramatic changes in expression of genes and proteins required for transport and metabolism of carbohydrates (see yellow blocks in Fig. 6.1), which was confirmed by the increased spectrum of carbon sources utilized in PM assays. The alternative carbohydrate metabolism of the Δ*rpoE* mutant can be part of the reason for its altered surface structure, which is indicated by its increased self-aggregation as well as increased co-aggregation with other oral microorganisms, and its increased adherence to ECM components. Biofilm formation is an important life-style for *S. mutans*. The reduced expression of genes necessary for biofilm formation in the Δ*rpoE* mutant may be one reason for its decreased amount of extracellular proteins and altered biofilm structure found in the proteome and phenome studies.

Loss of RpoE also affected *S. mutans* stress response (see pink blocks in Fig. 6.1). For example, the Δ*rpoE* mutant had already repressed expression of genes for the acid defense system MLF during its growth without stress, moreover, it failed to induce the high-affinity manganese and iron transporter *sloABC* and the regulator *sloR* (important for oxidative stress defense) under 2 mM H_2O_2 stress. Accordingly, the protein changes in the Δ*rpoE* mutant were reduced under oxidative and starvation stresses. While the pH 5.0, which should be quite mild for the aciduric bacterium *S. mutans*, caused stronger induction of general stress proteins and repression of translation related proteins in the mutant than in the wild type. The cross-protection effect between acid and oxidative stresses was also reduced in the mutant. The inefficient stress adapation in the Δ*rpoE* mutant may lead to the inability of protecting itself from further challenging acid (pH 3.0) and oxidative (20 mM H_2O_2) stresses as confirmed by the phenotypic analysis.

The proteome comparison of the mutant to the wild type without stress revealed already altered expression of proteins for translation, and for acid, oxidative, and general stress defense, suggesting that the mutant could be under internal stress due to loss of RpoE. A total of 550 genes (only a small subset of genes were discussed in this study due to data complexity and time limitation) and 330 of intergenic regions were differentially expressed in the mutant transcriptome, apparently due to the loosened control of gene transcription by lack of RpoE (see blue blocks in Fig. 6.1). The unspecific transcription of such a large number of genes and non-coding regions could cost the valuable sources and energy in the mutant, which would be the reason of its slower growth. However, the products of the unspecific transcription may be associated with the resistance of the mutant to the large spectrum (142) of inhibitory compounds shown by the PM experiments. Taken together, RpoE has global effects on *S. mutans* transcriptome, proteome, and phenome.

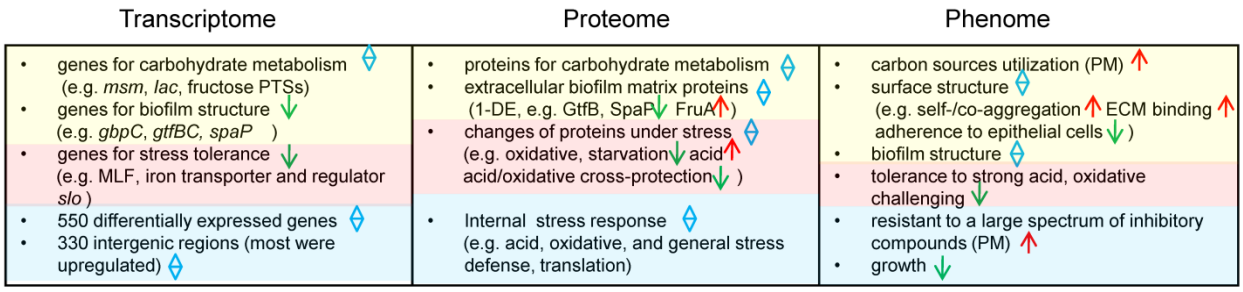

Fig. 6.1 Function of RpoE in *S. mutans* revealed by transcriptome, proteome, and phenome analyses. The extracellular biofilm matrix proteins were analyzed using normal (1-DE: 1 dimension) SDS-PAGE. The phenome study includes conventional phenotypic characterization and phenotype microarray (PM) comparison. The functions of genes, proteins, or phenotypic traits that were induced and reduced in the Δ*rpoE* mutant are shown by red and green arrows, respectively. The ⟠ shows both up- and down-regulation of genes or proteins, or altered phenotypic traits . *msm*: genes for multiple sugar transport and metabolism system; *lac*: lactose transport and metabolism genes; fructose PTSs: phosphoenolpyruvate-phosphotransferase systems for fructose; MLF: operon containing genes for malolactic fermentation. In phenotypic characterization, pH 3.0 and 20 mM H_2O_2 were used for acid and oxidative stress challenging experiments, while weaker stresses (pH 5.0 and 2 mM H_2O_2) were used in transcriptome and proteome studies of *S. mutans* stress adaptation responses.

7 - Reference

Aas, J. A., Paster, B. J., Stokes, L. N., Olsen, I. & Dewhirst, F. E. (2005). Defining the normal bacterial flora of the oral cavity. *J Clin Microbiol* **43**, 5721-5732.

Abranches, J., Chen, Y. Y. & Burne, R. A. (2004). Galactose metabolism by *Streptococcus mutans*. *Appl Environ Microbiol* **70**, 6047-6052.

Abranches, J., Lemos, J. A. & Burne, R. A. (2006). Osmotic stress responses of *Streptococcus mutans* UA159. *FEMS Microbiol Lett* **255**, 240-246.

Abranches, J., Zeng, L., Belanger, M., Rodrigues, P. H., Simpson-Haidaris, P. J., Akin, D., Dunn, W. A., Jr., Progulske-Fox, A. & Burne, R. A. (2009). Invasion of human coronary artery endothelial cells by *Streptococcus mutans* OMZ175. *Oral Microbiol Immunol* **24**, 141-145.

Achberger, E. C., Hilton, M. D. & Whiteley, H. R. (1982). The effect of the delta subunit on the interaction of *Bacillus subtilis* RNA polymerase with bases in a SP82 early gene promoter. *Nucleic Acids Res* **10**, 2893-2910.

Achberger, E. C. & Whiteley, H. R. (1981). The role of the delta peptide of the *Bacillus subtilis* RNA polymerase in promoter selection. *J Biol Chem* **256**, 7424-7432.

Ahn, S. J., Ahn, S. J., Browngardt, C. M. & Burne, R. A. (2009). Changes in biochemical and phenotypic properties of *Streptococcus mutans* during growth with aeration. *Appl Environ Microbiol* **75**, 2517-2527.

Ahn, S. J., Ahn, S. J., Wen, Z. T., Brady, L. J. & Burne, R. A. (2008). Characteristics of biofilm formation by *Streptococcus mutans* in the presence of saliva. *Infect Immun* **76**, 4259-4268.

Ahn, S. J. & Burne, R. A. (2007). Effects of oxygen on biofilm formation and the AtlA autolysin of *Streptococcus mutans*. *J Bacteriol* **189**, 6293-6302.

Ahn, S. J., Wen, Z. T. & Burne, R. A. (2007). Effects of oxygen on virulence traits of *Streptococcus mutans*. *J Bacteriol* **189**, 8519-8527.

Aires, C. P., Bel Cury, A. A., Tenuta, L. M., Klein, M. I., Koo, H., Duarte, S. & Cury, J. A. (2008). Effect of starch and sucrose on dental biofilm formation and on root dentine demineralization. *Caries Res* **42**, 380-386.

Ajdic, D., McShan, W. M., McLaughlin, R. E., Savic, G., Chang, J., Carson, M. B., Primeaux, C., Tian, R., Kenton, S. & other authors (2002). Genome sequence of *Streptococcus mutans* UA159, a cariogenic dental pathogen. *Proc Natl Acad Sci U S A* **99**, 14434-14439.

Ajdic, D. & Pham, V. T. (2007). Global transcriptional analysis of *Streptococcus mutans* sugar transporters using microarrays. *J Bacteriol* **189**, 5049-5059.

Albrecht, A. G., Netz, D. J., Miethke, M., Pierik, A. J., Burghaus, O., Peuckert, F., Lill, R. & Marahiel, M. A. (2010). SufU is an essential iron-sulfur cluster scaffold protein in *Bacillus subtilis*. *J Bacteriol* **192**, 1643-1651.

Altabe, S., Lopez, P. & de Mendoza, D. (2007). Isolation and characterization of unsaturated fatty acid auxotrophs of *Streptococcus pneumoniae* and *Streptococcus mutans*. *J Bacteriol* **189**, 8139-8144.

Arirachakaran, P., Benjavongkulchai, E., Luengpailin, S., Ajdic, D. & Banas, J. A. (2007). Manganese affects *Streptococcus mutans* virulence gene expression. *Caries Res* **41**, 503-511.

Aziz, R. K., Breitbart, M. & Edwards, R. A. (2010). Transposases are the most abundant, most ubiquitous genes in nature. *Nucleic Acids Res*.

Backofen, R. & Hess, W. R. (2010). Computational prediction of sRNAs and their targets in bacteria. *RNA Biol* **7**.

Baker-Austin, C. & Dopson, M. (2007). Life in acid: pH homeostasis in acidophiles. *Trends Microbiol* **15**, 165-171.

Baldeck, J. D. & Marquis, R. E. (2008). Targets for hydrogen-peroxide-induced damage to suspension and biofilm cells of *Streptococcus mutans*. *Can J Microbiol* **54**, 868-875.

Beg, A. M., Jones, M. N., Miller-Torbert, T. & Holt, R. G. (2002). Binding of *Streptococcus mutans* to extracellular matrix molecules and fibrinogen. *Biochem Biophys Res Commun* **298**, 75-79.

Beighton, D. (2009). Can the ecology of the dental biofilm be beneficially altered? *Adv Dent Res* **21**, 69-73.

Biswas, I., Drake, L., Erkina, D. & Biswas, S. (2008). Involvement of sensor kinases in the stress tolerance response of *Streptococcus mutans*. *J Bacteriol* **190**, 68-77.

Biswas, S. & Biswas, I. (2005). Role of HtrA in surface protein expression and biofilm formation by *Streptococcus mutans*. *Infect Immun* **73**, 6923-6934.

Bochner, B. R. (2009). Global phenotypic characterization of bacteria. *FEMS Microbiol Rev* **33**, 191-205.

Bochner, B. R., Gadzinski, P. & Panomitros, E. (2001). Phenotype microarrays for high-throughput phenotypic testing and assay of gene function. *Genome Res* **11**, 1246-1255.

Borukhov, S. & Nudler, E. (2003).RNA polymerase holoenzyme: structure, function and biological implications. *Curr Opin Microbiol* **6**, 93-100.

Bowden, G. H. & Hamilton, I. R. (1998). Survival of oral bacteria. *Crit Rev Oral Biol Med* **9**, 54-85.

Bruno-Barcena, J. M., Azcarate-Peril, M. A. & Hassan, H. M. (2010). Role of antioxidant enzymes in bacterial resistance to organic acids. *Appl Environ Microbiol* **76**, 2747-2753.

Campbell, E. A., Muzzin, O., Chlenov, M., Sun, J. L., Olson, C. A., Weinman, O., Trester-Zedlitz, M. L. & Darst, S. A. (2002). Structure of the bacterial RNA polymerase promoter specificity sigma subunit. *Mol Cell* **9**, 527-539.

Campbell, E. A., Westblade, L. F. & Darst, S. A. (2008). Regulation of bacterial RNA polymerase sigma factor activity: a structural perspective. *Curr Opin Microbiol* **11**, 121-127.

Carlsson, J., Kujala, U. & Edlund, M. B. (1985). Pyruvate dehydrogenase activity in *Streptococcus mutans*. *Infect Immun* **49**, 674-678.

Carmel-Harel, O. & Storz, G. (2000). Roles of the glutathione- and thioredoxin-dependent reduction systems in the *Escherichia coli* and *saccharomyces cerevisiae* responses to oxidative stress. *Annu Rev Microbiol* **54**, 439-461.

Carpentier, S. C., Witters, E., Laukens, K., Deckers, P., Swennen, R. & Panis, B. (2005). Preparation of protein extracts from recalcitrant plant tissues: an evaluation of different methods for two-dimensional gel electrophoresis analysis. *Proteomics* **5**, 2497-2507.

Chamberlin, M. J. (1974). The selectivity of transcription. *Annu Rev Biochem* **43**, 721-775.

Chaussee, M. A., Dmitriev, A. V., Callegari, E. A. & Chaussee, M. S. (2008). Growth phase-associated changes in the transcriptome and proteome of *Streptococcus pyogenes*. *Arch Microbiol* **189**, 27-41.

Chen, P. M., Chen, H. C., Ho, C. T., Jung, C. J., Lien, H. T., Chen, J. Y. & Chia, J. S. (2008). The two-component system ScnRK of *Streptococcus mutans* affects hydrogen peroxide resistance and murine macrophage killing. *Microbes Infect* **10**, 293-301.

Cisar, J. O., Kolenbrander, P. E. & McIntire, F. C. (1979). Specificity of coaggregation reactions between human oral streptococci and strains of *Actinomyces viscosus* or *Actinomyces naeslundii*. *Infect Immun* **24**, 742-752.

Clancy, A., Loar, J. W., Speziali, C. D., Oberg, M., Heinrichs, D. E. & Rubens, C. E. (2006). Evidence for siderophore-dependent iron acquisition in group B streptococcus. *Mol Microbiol* **59**, 707-721.

Corinaldesi, C., Danovaro, R. & Dell'anno, A. (2005). Simultaneous recovery of extracellular and intracellular DNA suitable for molecular studies from marine sediments. *Appl Environ Microbiol* **71**, 46-50.

Coykendall, A. L. (1989). Classification and identification of the viridans streptococci. *Clin Microbiol Rev* **2**, 315-328.

Crowley, P. J., Fischlschweiger, W., Coleman, S. E. & Bleiweis, A. S. (1987). Intergeneric bacterial coaggregations involving mutans streptococci and oral actinomyces. *Infect Immun* **55**, 2695-2700.

Cury, J. A., Rebelo, M. A., Bel Cury, A. A., Derbyshire, M. T. & Tabchoury, C. P. (2000). Biochemical composition and cariogenicity of dental plaque formed in the presence of sucrose or glucose and fructose. *Caries Res* **34**, 491-497.

Dawes, C. (2003). What is the critical pH and why does a tooth dissolve in acid? *J Can Dent Assoc* **69**, 722-724.

Dawes, C. & Dibdin, G. H. (1986).A theoretical analysis of the effects of plaque thickness and initial salivary sucrose concentration on diffusion of sucrose into dental plaque and its conversion to acid during salivary clearance. *J Dent Res* **65**, 89-94.

De Angelis, M. & Gobbetti, M. (2004). Environmental stress responses in *Lactobacillus*: a review. *Proteomics* **4**, 106-122.

Deng, D. M., Liu, M. J., Ten Cate, J. M. & Crielaard, W. (2007a). The VicRK system of *Streptococcus mutans* responds to oxidative stress. *J Dent Res* **86**, 606-610.

Deng, D. M., Ten Cate, J. M. & Crielaard, W. (2007b). The adaptive response of *Streptococcus mutans* towards oral care products: involvement of the ClpP serine protease. *Eur J Oral Sci* **115**, 363-370.

Diaz, P. I., Slakeski, N., Reynolds, E. C., Morona, R., Rogers, A. H. & Kolenbrander, P. E. (2006). Role of oxyR in the oral anaerobe *Porphyromonas gingivalis*. *J Bacteriol* **188**, 2454-2462.

Drevinek, P., Baldwin, A., Lindenburg, L., Joshi, L. T., Marchbank, A., Vosahlikova, S., Dowson, C. G. & Mahenthiralingam, E. (2010). Oxidative stress of *Burkholderia cenocepacia* induces insertion sequence-mediated genomic rearrangements that interfere with macrorestriction-based genotyping. *J Clin Microbiol* **48**, 34-40.

Eberhard, J., Pietschmann, R., Falk, W., Jepsen, S. & Dommisch, H. (2009). The immune response of oral epithelial cells induced by single-species and complex naturally formed biofilms. *Oral Microbiol Immunol* **24**, 325-330.

Ebright, R. H. (2000).RNA polymerase: structural similarities between bacterial RNA polymerase and eukaryotic RNA polymerase II. *J Mol Biol* **304**, 687-698.

Facklam, R. (2002). What happened to the streptococci: overview of taxonomic and nomenclature changes. *Clin Microbiol Rev* **15**, 613-630.

Facklam, R. R. (1977). Physiological differentiation of viridans streptococci. *J Clin Microbiol* **5**, 184-201.

Ferretti, J. J., Ajdic, D. & McShan, W. M. (2004). Comparative genomics of streptococcal species. *Indian J Med Res* **119 Suppl**, 1-6.

Fischer, H. P. (2005). Towards quantitative biology: integration of biological information to elucidate disease pathways and to guide drug discovery. *Biotechnol Annu Rev* **11**, 1-68.

Flemming, H. C. & Wingender, J. (2010). The biofilm matrix. *Nat Rev Microbiol* **8**, 623-633.

Floss, H. G. & Yu, T. W. (2005). Rifamycin-mode of action, resistance, and biosynthesis. *Chem Rev* **105**, 621-632.

Fozo, E. M. & Quivey, R. G., Jr. (2004). The *fabM* gene product of *Streptococcus mutans* is responsible for the synthesis of monounsaturated fatty acids and is necessary for survival at low pH. *J Bacteriol* **186**, 4152-4158.

Garcia-Godoy, F. & Hicks, M. J. (2008). Maintaining the integrity of the enamel surface: the role of dental biofilm, saliva and preventive agents in enamel demineralization and remineralization. *J Am Dent Assoc* **139 Suppl**, 25S-34S.

Gong, Y., Tian, X. L., Sutherland, T., Sisson, G., Mai, J., Ling, J. & Li, Y. H. (2009). Global transcriptional analysis of acid-inducible genes in *Streptococcus mutans*: multiple two-component systems involved in acid adaptation. *Microbiology* **155**, 3322-3332.

Gorke, B. & Stulke, J. (2008). Carbon catabolite repression in bacteria: many ways to make the most out of nutrients. *Nat Rev Microbiol* **6**, 613-624.

Griswold, A. R., Jameson-Lee, M. & Burne, R. A. (2006). Regulation and physiologic significance of the agmatine deiminase system of *Streptococcus mutans* UA159. *J Bacteriol* **188**, 834-841.

Gruber, A. R., Lorenz, R., Bernhart, S. H., Neubock, R. & Hofacker, I. L. (2008). The Vienna RNA websuite. *Nucleic Acids Res* **36**, W70-W74.

Gruber, T. M. & Gross, C. A. (2003). Multiple sigma subunits and the partitioning of bacterial transcription space. *Annu Rev Microbiol* **57**, 441-466.

Halfmann, A., Kovacs, M., Hakenbeck, R. & Bruckner, R. (2007). Identification of the genes directly controlled by the response regulator CiaR in *Streptococcus pneumoniae*: five out of 15 promoters drive expression of small non-coding RNAs. *Mol Microbiol* **66**, 110-126.

Han, T. K., Zhang, C. & Dao, M. L. (2006). Identification and characterization of collagen-binding activity in *Streptococcus mutans* wall-associated protein: a possible implication in dental root caries and endocarditis. *Biochem Biophys Res Commun* **343**, 787-792.

Hecker, M., Pane-Farre, J. & Volker, U. (2007). SigB-dependent general stress response in *Bacillus subtilis* and related gram-positive bacteria. *Annu Rev Microbiol* **61**, 215-236.

Hengge, R. (2009). Proteolysis of sigmaS (RpoS) and the general stress response in *Escherichia coli*. *Res Microbiol* **160**, 667-676.

Hengge-Aronis, R. (2002). Signal transduction and regulatory mechanisms involved in control of the sigma(S) (RpoS) subunit of RNA polymerase. *Microbiol Mol Biol Rev* **66**, 373-95, table.

Hickman, A. B., Chandler, M. & Dyda, F. (2010). Integrating prokaryotes and eukaryotes: DNA transposases in light of structure. *Crit Rev Biochem Mol Biol* **45**, 50-69.

Higuchi, M., Yamamoto, Y. & Kamio, Y. (2000). Molecular biology of oxygen tolerance in lactic acid bacteria: Functions of NADH oxidases and Dpr in oxidative stress. *J Biosci Bioeng* **90**, 484-493.

Hojo, K., Nagaoka, S., Ohshima, T. & Maeda, N. (2009). Bacterial interactions in dental biofilm development. *J Dent Res* **88**, 982-990.

Honda, O., Kato, C. & Kuramitsu, H. K. (1990). Nucleotide sequence of the *Streptococcus mutans gtfD* gene encoding the glucosyltransferase-S enzyme. *J Gen Microbiol* **136**, 2099-2105.

Hooper, S. D., Mavromatis, K. & Kyrpides, N. C. (2009). Microbial co-habitation and lateral gene transfer: what transposases can tell us. *Genome Biol* **10**, R45.

Horn, C., Jenewein, S., Sohn-Bosser, L., Bremer, E. & Schmitt, L. (2005). Biochemical and structural analysis of the *Bacillus subtilis* ABC transporter OpuA and its isolated subunits. *J Mol Microbiol Biotechnol* **10**, 76-91.

Jakubovics, N. S., Stromberg, N., van Dolleweerd, C. J., Kelly, C. G. & Jenkinson, H. F. (2005). Differential binding specificities of oral streptococcal antigen I/II family adhesins for human or bacterial ligands. *Mol Microbiol* **55**, 1591-1605.

Jansch, A., Korakli, M., Vogel, R. F. & Ganzle, M. G. (2007). Glutathione reductase from *Lactobacillus sanfranciscensis* DSM20451T: contribution to oxygen tolerance and thiol exchange reactions in wheat sourdoughs. *Appl Environ Microbiol* **73**, 4469-4476.

Jarosz, L. M., Deng, D. M., van der Mei, H. C., Crielaard, W. & Krom, B. P. (2009).*Streptococcus mutans* competence-stimulating peptide inhibits *Candida albicans* hypha formation. *Eukaryot Cell* **8**, 1658-1664.

Jenkinson, H. F., Lala, H. C. & Shepherd, M. G. (1990). Coaggregation of Streptococcus sanguis and other streptococci with Candida albicans. *Infect Immun* **58**, 1429-1436.

Jiang, Y. & Schilder, H. (2002). An optimal host response to a bacterium may require the interaction of leukocytes and resident host cells. *J Endod* **28**, 279-282.

Jones, A. L., Needham, R. H. & Rubens, C. E. (2003). The Delta subunit of RNA polymerase is required for virulence of *Streptococcus agalactiae*. *Infect Immun* **71**, 4011-4017.

Juang, Y. L. & Helmann, J. D. (1994). The delta subunit of *Bacillus subtilis* RNA polymerase. An allosteric effector of the initiation and core-recycling phases of transcription. *J Mol Biol* **239**, 1-14.

Jung, C. J., Zheng, Q. H., Shieh, Y. H., Lin, C. S. & Chia, J. S. (2009).*Streptococcus mutans* autolysin AtlA is a fibronectin-binding protein and contributes to bacterial survival in the bloodstream and virulence for infective endocarditis. *Mol Microbiol* **74**, 888-902.

Kaur, S. J., Nerlich, A., Bergmann, S., Rohde, M., Fulde, M., Zahner, D., Hanski, E., Zinkernagel, A., Nizet, V. & other authors (2010). The CXC chemokine-degrading protease SpyCep of *Streptococcus pyogenes* promotes its uptake into endothelial cells. *J Biol Chem* **285**, 27798-27805.

Kelemen, L., Rizk, S., Debreczeny, M., Ogier, J. & Szalontai, B. (2004). Streptococcal antigen I/II binds to extracellular proteins through intermolecular beta-sheets. *FEBS Lett* **566**, 190-194.

Kim, K. H. & Moon, M. H. (2009). Development of a multilane channel system for nongel-based two-dimensional protein separations using isoelectric focusing and asymmetrical flow field-flow fractionation. *Anal Chem* **81**, 1715-1721.

Kinney, K. K. (2010). Treatment of infections caused by antimicrobial-resistant gram-positive bacteria. *Am J Med Sci* **340**, 209-217.

Kockritz-Blickwede, M., Goldmann, O., Thulin, P., Heinemann, K., Norrby-Teglund, A., Rohde, M. & Medina, E. (2008). Phagocytosis-independent antimicrobial activity of mast cells by means of extracellular trap formation. *Blood* **111**, 3070-3080.

Kolenbrander, P. E., Palmer, R. J., Jr., Periasamy, S. & Jakubovics, N. S. (2010). Oral multispecies biofilm development and the key role of cell-cell distance. *Nat Rev Microbiol* **8**, 471-480.

Kolenbrander, P. E., Palmer, R. J., Jr., Rickard, A. H., Jakubovics, N. S., Chalmers, N. I. & Diaz, P. I. (2006). Bacterial interactions and successions during plaque development. *Periodontol 2000* **42**, 47-79.

Koo, H., Xiao, J., Klein, M. I. & Jeon, J. G. (2010). Exopolysaccharides produced by *Streptococcus mutans* glucosyltransferases modulate the establishment of microcolonies within multispecies biofilms. *J Bacteriol* **192**, 3024-3032.

Korithoski, B., Levesque, C. M. & Cvitkovitch, D. G. (2008). The involvement of the pyruvate dehydrogenase E1alpha subunit, in *Streptococcus mutans* acid tolerance. *FEMS Microbiol Lett* **289**, 13-19.

Kreikemeyer, B., Boyle, M. D., Buttaro, B. A., Heinemann, M. & Podbielski, A. (2001). Group A streptococcal growth phase-associated virulence factor regulation by a novel operon (Fas) with homologies to two-component-type regulators requires a small RNA molecule. *Mol Microbiol* **39**, 392-406.

Kreth, J., Zhu, L., Merritt, J., Shi, W. & Qi, F. (2008). Role of sucrose in the fitness of *Streptococcus mutans*. *Oral Microbiol Immunol* **23**, 213-219.

Lancefield, R. C. (1933).A SEROLOGICAL DIFFERENTIATION OF HUMAN AND OTHER GROUPS OF HEMOLYTIC STREPTOCOCCI. *J Exp Med* **57**, 571-595.

Lau, P. C., Sung, C. K., Lee, J. H., Morrison, D. A. & Cvitkovitch, D. G. (2002).PCR ligation mutagenesis in transformable streptococci: application and efficiency. *J Microbiol Methods* **49**, 193-205.

Lemme, A., Sztajer, H. & Wagner-Dobler, I. (2010). Characterization of *mleR*, a positive regulator of malolactic fermentation and part of the acid tolerance response in *Streptococcus mutans*. *BMC Microbiol* **10**, 58.

Lemos, J. A., Abranches, J. & Burne, R. A. (2005). Responses of cariogenic streptococci to environmental stresses. *Curr Issues Mol Biol* **7**, 95-107.

Lemos, J. A. & Burne, R. A. (2008).A model of efficiency: stress tolerance by *Streptococcus mutans*. *Microbiology* **154**, 3247-3255.

Lemos, J. A., Chen, Y. Y. & Burne, R. A. (2001). Genetic and physiologic analysis of the groE operon and role of the HrcA repressor in stress gene regulation and acid tolerance in *Streptococcus mutans*. *J Bacteriol* **183**, 6074-6084.

Lemos, J. A., Luzardo, Y. & Burne, R. A. (2007). Physiologic effects of forced down-regulation of *dnaK* and *groEL* expression in *Streptococcus mutans*. *J Bacteriol* **189**, 1582-1588.

Len, A. C., Cordwell, S. J., Harty, D. W. & Jacques, N. A. (2003). Cellular and extracellular proteome analysis of *Streptococcus mutans* grown in a chemostat. *Proteomics* **3**, 627-646.

Len, A. C., Harty, D. W. & Jacques, N. A. (2004a). Proteome analysis of *Streptococcus mutans* metabolic phenotype during acid tolerance. *Microbiology* **150**, 1353-1366.

Len, A. C., Harty, D. W. & Jacques, N. A. (2004b). Stress-responsive proteins are upregulated in *Streptococcus mutans* during acid tolerance. *Microbiology* **150**, 1339-1351.

Li, Y. H., Lau, P. C., Lee, J. H., Ellen, R. P. & Cvitkovitch, D. G. (2001). Natural genetic transformation of *Streptococcus mutans* growing in biofilms. *J Bacteriol* **183**, 897-908.

Ling, J. & Soll, D. (2010). Severe oxidative stress induces protein mistranslation through impairment of an aminoacyl-tRNA synthetase editing site. *Proc Natl Acad Sci U S A* **107**, 4028-4033.

Liu, J. M. & Camilli, A. (2010).A broadening world of bacterial small RNAs. *Curr Opin Microbiol* **13**, 18-23.

Liu, M., Hanks, T. S., Zhang, J., McClure, M. J., Siemsen, D. W., Elser, J. L., Quinn, M. T. & Lei, B. (2006). Defects in ex vivo and in vivo growth and sensitivity to osmotic stress of group A *Streptococcus* caused by interruption of response regulator gene vicR. *Microbiology* **152**, 967-978.

Lopez de Saro, F. J., Woody, A. Y. & Helmann, J. D. (1995). Structural analysis of the *Bacillus subtilis* delta factor: a protein polyanion which displaces RNA from RNA polymerase. *J Mol Biol* **252**, 189-202.

Lopez de Saro, F. J., Yoshikawa, N. & Helmann, J. D. (1999). Expression, abundance, and RNA polymerase binding properties of the delta factor of *Bacillus subtilis*. *J Biol Chem* **274**, 15953-15958.

Luo, P., Li, H. & Morrison, D. A. (2003). ComX is a unique link between multiple quorum sensing outputs and competence in *Streptococcus pneumoniae*. *Mol Microbiol* **50**, 623-633.

Luo, P. & Morrison, D. A. (2003). Transient association of an alternative sigma factor, ComX, with RNA polymerase during the period of competence for genetic transformation in *Streptococcus pneumoniae*. *J Bacteriol* **185**, 349-358.

Lynch, D. J., Fountain, T. L., Mazurkiewicz, J. E. & Banas, J. A. (2007). Glucan-binding proteins are essential for shaping *Streptococcus mutans* biofilm architecture. *FEMS Microbiol Lett* **268**, 158-165.

Macarthur, D. J. & Jacques, N. A. (2003). Proteome analysis of oral pathogens. *J Dent Res* **82**, 870-876.

Mangold, M., Siller, M., Roppenser, B., Vlaminckx, B. J., Penfound, T. A., Klein, R., Novak, R., Novick, R. P. & Charpentier, E. (2004). Synthesis of group A streptococcal virulence factors is controlled by a regulatory RNA molecule. *Mol Microbiol* **53**, 1515-1527.

Marquis, R. E. (2004). Applied and ecological aspects of oxidative-stress damage to bacterial spores and to oral microbes. *Sci Prog* **87**, 153-177.

Marrakchi, H., Choi, K. H. & Rock, C. O. (2002).A new mechanism for anaerobic unsaturated fatty acid formation in *Streptococcus pneumoniae*. *J Biol Chem* **277**, 44809-44816.

Marsh, P. D. (2006). Dental plaque as a biofilm and a microbial community - implications for health and disease. *BMC Oral Health* **6 Suppl 1**, S14.

Marsh, P. D., Moter, A. & Devine, D. A. (2011). Dental plaque biofilms: communities, conflict and control. *Periodontol 2000* **55**, 16-35.

Martin, M. E., Strachan, R. C., Aranha, H., Evans, S. L., Salin, M. L., Welch, B., Arceneaux, J. E. & Byers, B. R. (1984). Oxygen toxicity in *Streptococcus mutans*: manganese, iron, and superoxide dismutase. *J Bacteriol* **159**, 745-749.

Maruyama, F., Kobata, M., Kurokawa, K., Nishida, K., Sakurai, A., Nakano, K., Nomura, R., Kawabata, S., Ooshima, T. & other authors (2009). Comparative genomic analyses of *Streptococcus mutans* provide insights into chromosomal shuffling and species-specific content. *BMC Genomics* **10**, 358.

Masuko, T., Minami, A., Iwasaki, N., Majima, T., Nishimura, S. & Lee, Y. C. (2005). Carbohydrate analysis by a phenol-sulfuric acid method in microplate format. *Anal Biochem* **339**, 69-72.

Matsumoto-Nakano, M., Fujita, K. & Ooshima, T. (2007). Comparison of glucan-binding proteins in cariogenicity of *Streptococcus mutans*. *Oral Microbiol Immunol* **22**, 30-35.

Mitchell, T. J. (2003). The pathogenesis of streptococcal infections: from tooth decay to meningitis. *Nat Rev Microbiol* **1**, 219-230.

Molinari, G., Talay, S. R., Valentin-Weigand, P., Rohde, M. & Chhatwal, G. S. (1997). The fibronectin-binding protein of *Streptococcus pyogenes*, SfbI, is involved in the internalization of group A streptococci by epithelial cells. *Infect Immun* **65**, 1357-1363.

Mooney, R. A., Darst, S. A. & Landick, R. (2005). Sigma and RNA polymerase: an on-again, off-again relationship? *Mol Cell* **20**, 335-345.

Mooney, R. A., Davis, S. E., Peters, J. M., Rowland, J. L., Ansari, A. Z. & Landick, R. (2009). Regulator trafficking on bacterial transcription units in vivo. *Mol Cell* **33**, 97-108.

Motackova, V., Sanderova, H., Zidek, L., Novacek, J., Padrta, P., Svenkova, A., Korelusova, J., Jonak, J., Krasny, L. & other authors (2010). Solution structure of the N-terminal domain of *Bacillus subtilis* delta subunit of RNA polymerase and its classification based on structural homologs. *Proteins* **78**, 1807-1810.

Moynihan, P. & Petersen, P. E. (2004). Diet, nutrition and the prevention of dental diseases. *Public Health Nutr* **7**, 201-226.

Murakami, K. S. & Darst, S. A. (2003). Bacterial RNA polymerases: the wholo story. *Curr Opin Struct Biol* **13**, 31-39.

Nakano, K., Inaba, H., Nomura, R., Nemoto, H., Takeda, M., Yoshioka, H., Matsue, H., Takahashi, T., Taniguchi, K. & other authors (2006a). Detection of cariogenic *Streptococcus mutans* in extirpated heart valve and atheromatous plaque specimens. *J Clin Microbiol* **44**, 3313-3317.

Nakano, K., Nomura, R., Matsumoto, M. & Ooshima, T. (2010). Roles of oral bacteria in cardiovascular diseases--from molecular mechanisms to clinical cases: Cell-surface

structures of novel serotype k *Streptococcus mutans* strains and their correlation to virulence. *J Pharmacol Sci* **113**, 120-125.

Nakano, K. & Ooshima, T. (2009). Serotype classification of *Streptococcus mutans* and its detection outside the oral cavity. *Future Microbiol* **4**, 891-902.

Nakano, K., Tsuji, M., Nishimura, K., Nomura, R. & Ooshima, T. (2006b). Contribution of cell surface protein antigen PAc of *Streptococcus mutans* to bacteremia. *Microbes Infect* **8**, 114-121.

Nakayama, K. (1992). Nucleotide sequence of *Streptococcus mutans* superoxide dismutase gene and isolation of insertion mutants. *J Bacteriol* **174**, 4928-4934.

Nan, J., Brostromer, E., Liu, X. Y., Kristensen, O. & Su, X. D. (2009). Bioinformatics and structural characterization of a hypothetical protein from *Streptococcus mutans*: implication of antibiotic resistance. *PLoS One* **4**, e7245.

Nelson DL, C. M. (2004). Biosynthesis of amino acids, nucleotides, and related molecules. In *Lehninger Principles of Biochemistry*, pp. 851-852. New York: W. H. Freeman & Company.

Nishimura, Y., Adachi, H., Kyo, M., Murakami, S., Hattori, S. & Ajito, K. (2005).A proof of the specificity of kanamycin-ribosomal RNA interaction with designed synthetic analogs and the antibacterial activity. *Bioorg Med Chem Lett* **15**, 2159-2162.

Nobbs, A. H., Lamont, R. J. & Jenkinson, H. F. (2009). Streptococcus adherence and colonization. *Microbiol Mol Biol Rev* **73**, 407-50, Table.

Nomura, R., Nakano, K., Nemoto, H., Fujita, K., Inagaki, S., Takahashi, T., Taniguchi, K., Takeda, M., Yoshioka, H. & other authors (2006). Isolation and characterization of *Streptococcus mutans* in heart valve and dental plaque specimens from a patient with infective endocarditis. *J Med Microbiol* **55**, 1135-1140.

Opdyke, J. A., Scott, J. R. & Moran, C. P., Jr. (2001).A secondary RNA polymerase sigma factor from *Streptococcus pyogenes*. *Mol Microbiol* **42**, 495-502.

Paik, S., Brown, A., Munro, C. L., Cornelissen, C. N. & Kitten, T. (2003). The *sloABCR* operon of *Streptococcus mutans* encodes an Mn and Fe transport system required for endocarditis virulence and its Mn-dependent repressor. *J Bacteriol* **185**, 5967-5975.

Paterson, G. K. & Orihuela, C. J. (2010). Pneumococcal microbial surface components recognizing adhesive matrix molecules targeting of the extracellular matrix. *Mol Microbiol* **77**, 1-5.

Patterson, S. D. & Aebersold, R. H. (2003). Proteomics: the first decade and beyond. *Nat Genet* **33 Suppl**, 311-323.

Perch, B., Kjems, E. & Ravn, T. (1974). Biochemical and serological properties of *Streptococcus mutans* from various human and animal sources. *Acta Pathol Microbiol Scand B Microbiol Immunol* **82**, 357-370.

Periasamy, S., Chalmers, N. I., Du-Thumm, L. & Kolenbrander, P. E. (2009).*Fusobacterium nucleatum* ATCC 10953 requires *Actinomyces naeslundii* ATCC 43146 for growth on saliva in a three-species community that includes *Streptococcus oralis* 34. *Appl Environ Microbiol* **75**, 3250-3257.

Perry, J. A., Jones, M. B., Peterson, S. N., Cvitkovitch, D. G. & Levesque, C. M. (2009). Peptide alarmone signalling triggers an auto-active bacteriocin necessary for genetic competence. *Mol Microbiol* **72**, 905-917.

Perry, J. A., Levesque, C. M., Suntharaligam, P., Mair, R. W., Bu, M., Cline, R. T., Peterson, S. N. & Cvitkovitch, D. G. (2008). Involvement of *Streptococcus mutans* regulator RR11 in oxidative stress response during biofilm growth and in the development of genetic competence. *Lett Appl Microbiol* **47**, 439-444.

Pfaffl, M. W. (2001).A new mathematical model for relative quantification in real-time RT-PCR. *Nucleic Acids Res* **29**, e45.

Poole, L. B., Higuchi, M., Shimada, M., Calzi, M. L. & Kamio, Y. (2000).*Streptococcus mutans* H_2O_2-forming NADH oxidase is an alkyl hydroperoxide reductase protein. *Free Radic Biol Med* **28**, 108-120.

Poyart, C., Pellegrini, E., Gaillot, O., Boumaila, C., Baptista, M. & Trieu-Cuot, P. (2001). Contribution of Mn-cofactored superoxide dismutase (SodA) to the virulence of *Streptococcus agalactiae*. *Infect Immun* **69**, 5098-5106.

Preiss, J. (1984). Bacterial glycogen synthesis and its regulation. *Annu Rev Microbiol* **38**, 419-458.

Py, B. & Barras, F. (2010). Building Fe-S proteins: bacterial strategies. *Nat Rev Microbiol* **8**, 436-446.

Rabilloud, T., Strub, J. M., Luche, S., van Dorsselaer, A. & Lunardi, J. (2001).A comparison between Sypro Ruby and ruthenium II tris (bathophenanthroline disulfonate) as fluorescent stains for protein detection in gels. *Proteomics* **1**, 699-704.

Renzone, G., D'Ambrosio, C., Arena, S., Rullo, R., Ledda, L., Ferrara, L. & Scaloni, A. (2005). Differential proteomic analysis in the study of prokaryotes stress resistance. *Ann Ist Super Sanita* **41**, 459-468.

Reschiglian, P. & Moon, M. H. (2008). Flow field-flow fractionation: a pre-analytical method for proteomics. *J Proteomics* **71**, 265-276.

Riihinen, K., Ryynanen, A., Toivanentoivanen, M., Kononen, E., Torronen, R. & Tikkanen-Kaukanen, C. (2010). Antiaggregation potential of berry fractions against

pairs of *Streptococcus mutans* with *Fusobacterium nucleatum* or *Actinomyces naeslundii*. *Phytother Res*.

Roberts, S. A. & Scott, J. R. (2007). RivR and the small RNA RivX: the missing links between the CovR regulatory cascade and the Mga regulon. *Mol Microbiol* **66**, 1506-1522.

Rolerson, E., Swick, A., Newlon, L., Palmer, C., Pan, Y., Keeshan, B. & Spatafora, G. (2006). The SloR/Dlg metalloregulator modulates *Streptococcus mutans* virulence gene expression. *J Bacteriol* **188**, 5033-5044.

Romby, P. & Charpentier, E. (2010). An overview of RNAs with regulatory functions in gram-positive bacteria. *Cell Mol Life Sci* **67**, 217-237.

Russell, R. R. (2008). How has genomics altered our view of caries microbiology? *Caries Res* **42**, 319-327.

Sanders, J. W., Leenhouts, K. J., Haandrikman, A. J., Venema, G. & Kok, J. (1995). Stress response in *Lactococcus lactis*: cloning, expression analysis, and mutation of the lactococcal superoxide dismutase gene. *J Bacteriol* **177**, 5254-5260.

Saravanan, R. S. & Rose, J. K. (2004).A critical evaluation of sample extraction techniques for enhanced proteomic analysis of recalcitrant plant tissues. *Proteomics* **4**, 2522-2532.

Seepersaud, R., Needham, R. H., Kim, C. S. & Jones, A. L. (2006). Abundance of the delta subunit of RNA polymerase is linked to the virulence of *Streptococcus agalactiae*. *J Bacteriol* **188**, 2096-2105.

Senadheera, D. & Cvitkovitch, D. G. (2008). Quorum sensing and biofilm formation by *Streptococcus mutans*. *Adv Exp Med Biol* **631**, 178-188.

Senadheera, D., Krastel, K., Mair, R., Persadmehr, A., Abranches, J., Burne, R. A. & Cvitkovitch, D. G. (2009). Inactivation of VicK affects acid production and acid survival of *Streptococcus mutans*. *J Bacteriol* **191**, 6415-6424.

Senadheera, M. D., Guggenheim, B., Spatafora, G. A., Huang, Y. C., Choi, J., Hung, D. C., Treglown, J. S., Goodman, S. D., Ellen, R. P. & other authors (2005).A VicRK signal transduction system in *Streptococcus mutans* affects *gtfBCD*, *gbpB*, and *ftf* expression, biofilm formation, and genetic competence development. *J Bacteriol* **187**, 4064-4076.

Severinov, K. (2000).RNA polymerase structure-function: insights into points of transcriptional regulation. *Curr Opin Microbiol* **3**, 118-125.

Sheng, J. & Marquis, R. E. (2007). Malolactic fermentation by *Streptococcus mutans*. *FEMS Microbiol Lett* **272**, 196-201.

Shirtliff, M. E., Peters, B. M. & Jabra-Rizk, M. A. (2009). Cross-kingdom interactions: *Candida albicans* and bacteria. *FEMS Microbiol Lett*.

Shun, C. T., Lu, S. Y., Yeh, C. Y., Chiang, C. P., Chia, J. S. & Chen, J. Y. (2005). Glucosyltransferases of viridans streptococci are modulins of interleukin-6 induction in infective endocarditis. *Infect Immun* **73**, 3261-3270.

Sitkiewicz, I. & Musser, J. M. (2009). Analysis of growth-phase regulated genes in *Streptococcus agalactiae* by global transcript profiling. *BMC Microbiol* **9**, 32.

Sklavounou, A. & Germaine, G. R. (1980). Adherence of oral streptococci to keratinized and nonkeratinized human oral epithelial cells. *Infect Immun* **27**, 686-689.

Sturn, A., Quackenbush, J. & Trajanoski, Z. (2002). Genesis: cluster analysis of microarray data. *Bioinformatics* **18**, 207-208.

Svensater, G., Sjogreen, B. & Hamilton, I. R. (2000). Multiple stress responses in *Streptococcus mutans* and the induction of general and stress-specific proteins. *Microbiology* **146 (Pt 1)**, 107-117.

Takahashi, N. & Nyvad, B. (2010). The Role of Bacteria in the Caries Process: Ecological Perspectives. *J Dent Res*.

Tao, L., Sutcliffe, I. C., Russell, R. R. & Ferretti, J. J. (1993). Transport of sugars, including sucrose, by the *msm* transport system of *Streptococcus mutans*. *J Dent Res* **72**, 1386-1390.

Tao, L., Wu, X. & Sun, B. (2010). Alternative sigma factor sigmaH modulates prophage integration and excision in *Staphylococcus aureus*. *PLoS Pathog* **6**, e1000888.

Terao, Y., Isoda, R., Murakami, J., Hamada, S. & Kawabata, S. (2009). Molecular and biological characterization of gtf regulation-associated genes in *Streptococcus mutans*. *Oral Microbiol Immunol* **24**, 211-217.

Thaker, M., Spanogiannopoulos, P. & Wright, G. D. (2010). The tetracycline resistome. *Cell Mol Life Sci* **67**, 419-431.

Thibessard, A., Borges, F., Fernandez, A., Gintz, B., Decaris, B. & Leblond-Bourget, N. (2004). Identification of *Streptococcus thermophilus* CNRZ368 genes involved in defense against superoxide stress. *Appl Environ Microbiol* **70**, 2220-2229.

Thomas, E. L. & Pera, K. A. (1983). Oxygen metabolism of *Streptococcus mutans*: uptake of oxygen and release of superoxide and hydrogen peroxide. *J Bacteriol* **154**, 1236-1244.

Tipper, D. J. (1985). Mode of action of beta-lactam antibiotics. *Pharmacol Ther* **27**, 1-35.

Tjaden, B. (2008). TargetRNA: a tool for predicting targets of small RNA action in bacteria. *Nucleic Acids Res* **36**, W109-W113.

Tozzi, M. G., Camici, M., Mascia, L., Sgarrella, F. & Ipata, P. L. (2006). Pentose phosphates in nucleoside interconversion and catabolism. *FEBS J* **273**, 1089-1101.

Tremblay, Y. D., Lo, H., Li, Y. H., Halperin, S. A. & Lee, S. F. (2009). Expression of the *Streptococcus mutans* essential two-component regulatory system VicRK is pH and growth-phase dependent and controlled by the LiaFSR three-component regulatory system. *Microbiology* **155**, 2856-2865.

Tsui, H. C., Mukherjee, D., Ray, V. A., Sham, L. T., Feig, A. L. & Winkler, M. E. (2010). Identification and characterization of noncoding small RNAs in *Streptococcus pneumoniae* serotype 2 strain D39. *J Bacteriol* **192**, 264-279.

van Vliet, A. H. (2010). Next generation sequencing of microbial transcriptomes: challenges and opportunities. *FEMS Microbiol Lett* **302**, 1-7.

Vilchez, R., Lemme, A., Ballhausen, B., Thiel, V., Schulz, S., Jansen, R., Sztajer, H. & Wagner-Dobler, I. (2010).*Streptococcus mutans* Inhibits *Candida albicans* hyphal formation by the fatty acid signaling molecule trans-2-decenoic acid (SDSF). *Chembiochem* **11**, 1552-1562.

Vollmer, T., Hinse, D., Kleesiek, K. & Dreier, J. (2010). Interactions between endocarditis-derived *Streptococcus gallolyticus* subsp. gallolyticus isolates and human endothelial cells. *BMC Microbiol* **10**, 78.

Wang, W., Hollmann, R. & Deckwer, W. D. (2006). Comparative proteomic analysis of high cell density cultivations with two recombinant *Bacillus megaterium* strains for the production of a heterologous dextransucrase. *Proteome Sci* **4**, 19.

Wang, W., Hollmann, R., Furch, T., Nimtz, M., Malten, M., Jahn, D. & Deckwer, W. D. (2005). Proteome analysis of a recombinant *Bacillus megaterium* strain during heterologous production of a glucosyltransferase. *Proteome Sci* **3**, 4.

Wang, W., Sun, J., Hartlep, M., Deckwer, W. D. & Zeng, A. P. (2003). Combined use of proteomic analysis and enzyme activity assays for metabolic pathway analysis of glycerol fermentation by *Klebsiella pneumoniae*. *Biotechnol Bioeng* **83**, 525-536.

Waters, L. S. & Storz, G. (2009). Regulatory RNAs in bacteria. *Cell* **136**, 615-628.

Watson, S. P., Antonio, M. & Foster, S. J. (1998). Isolation and characterization of *Staphylococcus aureus* starvation-induced, stationary-phase mutants defective in survival or recovery. *Microbiology* **144 (Pt 11)**, 3159-3169.

Wen, Z. T., Baker, H. V. & Burne, R. A. (2006). Influence of BrpA on critical virulence attributes of *Streptococcus mutans*. *J Bacteriol* **188**, 2983-2992.

Wen, Z. T., Browngardt, C. & Burne, R. A. (2001). Characterization of two operons that encode components of fructose-specific enzyme II of the sugar:phosphotransferase system of *Streptococcus mutans*. *FEMS Microbiol Lett* **205**, 337-342.

Wen, Z. T., Suntharaligham, P., Cvitkovitch, D. G. & Burne, R. A. (2005). Trigger factor in *Streptococcus mutans* is involved in stress tolerance, competence development, and biofilm formation. *Infect Immun* **73**, 219-225.

Werner, F. (2008). Structural evolution of multisubunit RNA polymerases. *Trends Microbiol* **16**, 247-250.

Wettenhall, J. M. & Smyth, G. K. (2004).limmaGUI: a graphical user interface for linear modeling of microarray data. *Bioinformatics* **20**, 3705-3706.

Wilkins, J. C., Homer, K. A. & Beighton, D. (2002). Analysis of *Streptococcus mutans* proteins modulated by culture under acidic conditions. *Appl Environ Microbiol* **68**, 2382-2390.

Wilson, W. A., Roach, P. J., Montero, M., Baroja-Fernandez, E., Munoz, F. J., Eydallin, G., Viale, A. M. & Pozueta-Romero, J. (2010). Regulation of glycogen metabolism in yeast and bacteria. *FEMS Microbiol Rev*.

Wolff, L. & Liljemark, W. F. (1978). Observation of beta-hemolysis among three strains of *Streptococcus mutans*. *Infect Immun* **19**, 745-748.

Wood, D. N., Weinstein, K. E., Podbielski, A., Kreikemeyer, B., Gaughan, J. P., Valentine, S. & Buttaro, B. A. (2009). Generation of metabolically diverse strains of *Streptococcus pyogenes* during survival in stationary phase. *J Bacteriol* **191**, 6242-6252.

Wu, J. & Xi, C. (2009). Evaluation of different methods for extracting extracellular DNA from the biofilm matrix. *Appl Environ Microbiol* **75**, 5390-5395.

Xue, X., Tomasch, J., Sztajer, H. & Wagner-Dobler, I. (2010). The delta subunit of RNA polymerase, RpoE, is a global modulator of *Streptococcus mutans* environmental adaptation. *J Bacteriol* **192**, 5081-5092.

Yamada, T. & Carlsson, J. (1975). Regulation of lactate dehydrogenase and change of fermentation products in streptococci. *J Bacteriol* **124**, 55-61.

Zeng, L. & Burne, R. A. (2008). Multiple sugar: phosphotransferase system permeases participate in catabolite modification of gene expression in *Streptococcus mutans*. *Mol Microbiol* **70**, 197-208.

Zeng, L. & Burne, R. A. (2010). Seryl-phosphorylated HPr Regulates CcpA-Independent Carbon Catabolite Repression in Conjunction with PTS Permeases in *Streptococcus mutans*. *Mol Microbiol*.

Zeng, L., Wen, Z. T. & Burne, R. A. (2006).A novel signal transduction system and feedback loop regulate fructan hydrolase gene expression in *Streptococcus mutans*. *Mol Microbiol* **62**, 187-200.

Zhang, J. & Biswas, I. (2009a).3'-Phosphoadenosine-5'-phosphate phosphatase activity is required for superoxide stress tolerance in *Streptococcus mutans*. *J Bacteriol* **191**, 4330-4340.

Zhang, J. & Biswas, I. (2009b).A phenotypic microarray analysis of a *Streptococcus mutans liaS* mutant. *Microbiology* **155**, 61-68.

Zhao, Y., Li, H., Hou, Y., Cha, L., Cao, Y., Wang, L., Ying, X. & Li, W. (2008). Construction of two mathematical models for prediction of bacterial sRNA targets. *Biochem Biophys Res Commun* **372**, 346-350.

Zheng, M., Doan, B., Schneider, T. D. & Storz, G. (1999). OxyR and SoxRS regulation of fur. *J Bacteriol* **181**, 4639-4643.

Zhou, L., Lei, X. H., Bochner, B. R. & Wanner, B. L. (2003). Phenotype microarray analysis of *Escherichia coli* K-12 mutants with deletions of all two-component systems. *J Bacteriol* **185**, 4956-4972.

Zhu, L., Kreth, J., Cross, S. E., Gimzewski, J. K., Shi, W. & Qi, F. (2006). Functional characterization of cell-wall-associated protein WapA in *Streptococcus mutans*. *Microbiology* **152**, 2395-2404.

Zhu, M., Ajdic, D., Liu, Y., Lynch, D., Merritt, J. & Banas, J. A. (2009). Role of the *Streptococcus mutans irvA* gene in GbpC-independent, dextran-dependent aggregation and biofilm formation. *Appl Environ Microbiol* **75**, 7037-7043.

Zijnge, V., van Leeuwen, M. B., Degener, J. E., Abbas, F., Thurnheer, T., Gmur, R. & Harmsen, H. J. (2010). Oral biofilm architecture on natural teeth. *PLoS One* **5**, e9321.

8 - Acknowledgements

I would like to express my most sincere thanks to my supervisor Professor Dr. Irene Wagner-Döbler for providing me the opportunity to conduct my PhD project in the Microbial Communication (KOM) group at the Helmholtz Center for Infection Research (HZI). Her broad scientific knowledge, her enthusiasm for science and passion for high-quality research work, combined with her very supportive attitude towards students have built an excellent basis for the completion of this thesis. It has been a great honor to learn from her and work in her group.
I am deeply grateful to Dr. Helena Sztajer, my other supervisor, who has taught me a lot of things in scientific work and in life. She always provides me with encouragement, constructive counseling and is a great fountain of knowledge. I am very lucky to have her as my teacher and my close friend.
I wish to thank all members of the KOM group for many helpful discussions and for maintaining an excellent research atmosphere. In particular, to Dr. Wei Wang and Dr. Jinshan Li who helped me to gain expertise in proteomics.
I am thankful to all collaborators from other scientific groups who contributed to the completion of this thesis. I wish to thank Dr. Susanne Talay and Dr. Manfred Rohde (Department of Medical Microbiology, HZI) for cell infection experiments and electron microscope images, and to Dr. Jörn Petersen and Nora Buddruhs (German Collection of Microorganisms and Cell Cultures GmbH) for phenotype microarray experiments.
I am grateful to my PhD thesis committee members in HZI: Professor Dr. Susanne Häußler, Dr. Wolf-Dieter Schubert, and Dr. Susanne Talay, for their valuable and kind comments on my thesis.
I extend my special thanks to Professor Dr. Dieter Jahn, for his reviewing of this thesis.
I would like to express my warmest thanks to my family and my friends for the encouragement and support throughout my studies.
This work was financially supported by the CSC-Helmholtz Joint Fellowship.